Strategies and Process Development for Particle formation from Aquasolv Lignin and innovative Applications into Consumer Goods

Vom Promotionsausschuss der

Technischen Universität Hamburg

zur Erlangung des akademischen Grades

Doktor-Ingenieurin (Dr.-Ing.)

genehmigte Dissertation

von

Gilda Joana Gil Chavez

aus

Mexiko

2022

DOI: https://doi.org/10.15480/882.4754

1. Gutachterin: Prof. Dr.- Ing. Irina Smirnova
2. Gutachter: Prof. Dr.- Ing. Stephan Heinrich

Vorsitzender des Prüfungsausschusses: Prof. Dr. – Ing. Kerstin Kuchta

Datum der mündlichen Prüfung: 21.12.2021

A mi familia

Papá, Mamá, Yoyis, Lupito

Por haberme enseñado todo lo que sé y lo que soy. Gracias a ustedes nunca he tenido miedo de luchar por alcanzar mis sueños y de volar alto, sin miedo a caer pues yo sé que cuando lo haga, estarán ahí para mí con una red de seguridad, amor y motivación.

¡Su apoyo incondicional es mi motor de cada día!

¡¡Los amo!!

Acknowledgements

This work was made during my time as PhD student at the Institute of Thermal Separation Processes at Hamburg University of Technology. My biggest thanks are to my Professor Irina Smirnova, for opening the doors of your institute to me and for offering the amazing opportunity to work with Lignin. Your passion to bring science to reality is incredible and your impetus is truly empowering, not only for us women but for all the members of the institute. It meant a lot to me having you as my supervisor, always supporting my dreams and career path. Thank you, Professor!

To Professor Stefan Heinrich, for welcoming me into your research group, for the good discussions and for your advice. To the members of your team Monika Goslinska and Tom Wytrwat who were always dear to me and to Frank Rimoschat and Ulrich Hartge † for all the technical and scientific advice.

I want to thank Prof. Dr. Claudia Leopold from the Institute of Pharmacy, University of Hamburg, Dr. Ana Matthias from Instituto de Biologia Experimental e Tecnológica, iBET, and Prof. Mohammed Alnajjar from Applied Science University for the great collaboration to reach the goals of my doctoral thesis.

To Carsten Zetzl for being always kind and patient, for encouraging me to speak German and saying I do it great (we know the truth). Your motivation for new scientific topics, work ethics and your ability to stay calm in stormy situations will always stay with me.

To Steffi, you were always able to see through my happy face and identified when I truly needed a hug and loving words. Thank you for being there for me always!

To my dearest friends Robert, Andres, Raman, Alberto, Fynn & Victor with whom I shared incredible moments and challenging conversations in and outside the institute and to all my institute friends Isabella, Wienke, Simon, Baldur, Imke, Anja, Lilia, Xixi, Ralena, Rene & Marc. Thank you for the nice talks during lunch, all the laughs and the good exchange.

To the best students one can wish for, Sidhant, Razan, Erik, Sahand and Christin, thank you for joining the adventure of giving value to lignin, and not being afraid of getting your hands (and clothes, shoes, face…) dirty. I'm proud of what we achieved together and can't wait to see where life takes you!

To Pavel Gurikov. Thank you for sharing your wisdom, time, and excellent wine with me, I won't be knocking on your door that often anymore, but I will always carry your words with me. You have all my respect and admiration as a professional and as a human.

To Miao, Sheila and Tamara with whom I made the most wonderful memories during my PhD time, our friendship and connection is something that happens rarely in life. I miss our cooking nights and deep talks, and I know that we will always be there for each other. I love you!.

To my Lignopure family, for teaching me new things every day and helping me become a better person and professional.

To my Schatzie (*also known as* Jan), for your unconditional love and support, for celebrating my successes and cheering me on through my darkest times. Thank you for always believing in me even when I'm in doubt. You are my rock and I'm blessed to share my life with you.

Abstract

Aquasolv lignin is a high-molecular weight biopolymer obtained after the pre-treatment of lignocellulosic biomass with liquid hot water (LHW) under elevated pressure followed by enzymatic hydrolysis. Due to its *free-of-solvent* nature and vegetal primary source, lignin applicability opens to high value products as the case for cosmetic, food and pharmaceutical industries. However, current process yields a heterogeneous material and does not control characteristics such as particle size and morphology, such features being important due to their direct impact in biological behaviour and technical properties; for instance, bioavailability, flowability and solubility in pharmaceutical excipients.

The selection of an appropriate method to obtain particles with controlled mean size appears crucial to further product development and formulation. In this regard, a whole process line from crude biomass to lignin powders for the food and pharmaceutical industries has been developed. In the present study, the focus was to tailor the final quality of the lignin in terms of particle size and water content by using spray drying technology. A three-factor central composite rotatory design was used, and the independent variables selected for the set of experiments were inlet temperature, nozzle pressure and feeding rate. The effect of these factors and their interaction was studied and used to model the particle formation and properties of lignin.

A thorough evaluation of the bioactive properties and cytotoxicity of the obtained AS lignin particles was assessed in vitro, and for the first time, the non-cytotoxicity and hypocholesterolemic effect of AS lignin was demonstrated in vivo in a rat model. The results of this thesis are the basis for further valorizing lignin from second generation biorefineries and apply the material into valuable product formulation by using the principles of particle engineering design.

Table of contents

1 Introduction **1**
2 Theoretical background **3**

2.1 Definition and structure of novel and technical lignins **3**
2.2 Lignin functionality and proposed mechanisms **7**
2.2.1 Protection against oxidative stress 7
2.2.2 Antimicrobial activity of lignin and lignin derived products 9
2.2.3 Lignin as antidiabetic functional molecule 13
2.2.4 Lignin as drug release agent in pharmaceutical formulations 13

2.3 Current approaches for lignin valorization and potential application in high value added formulations **15**
2.3.1 Lignin as dispersing, binding and emulsifying agent 15
2.3.2 Lignin as anti-hyperlipidemia and anti-obesogenic agent 16
2.3.3 Use of lignin as food ingredient 19

2.4 Role of particle engineering on product formulation and manufacturability **21**
2.4.1 Influence of particle properties on the flow behavior of powders of particulate solids 21
2.4.2 Influence of particle design in drug release, dissolution and bioavailability 24
2.4.3 Compressibility and mechanical interlocking on compaction 25

2.5 General description of the spray drying process **26**
2.5.1 Particle formation during spray drying 27
2.5.2 Development of solid particles during drying 28
2.5.3 Atomization during spray drying 30

2.6 Overview of previous research on the particle formation from technical and novel lignins **31**
2.6.1 Solvent shifting 32
2.6.2 pH shifting or acid precipitation 32
2.6.3 CO_2 antisolvent 34
2.6.4 Challenges of current research on the production of lignin nanoparticles 35

3 Derivation of the objectives based on the state of the art **38**
4 Materials and experimental methods **41**

4.1 Lignin production and preparation **41**
4.2 Novel and technical lignins used **42**
4.3 Reagents and chemicals **43**
4.4 Spray drying process of lignin **44**
4.4.1 Feed composition and preparation 44
4.4.2 Spray drying process and drying conditions 44
4.4.3 Central Composite Rotatory Design (CCRD) of experiments 45

4.5 Evaluation of primary powder properties **47**
4.5.1 Powder moisture 47

4.5.2 Particle size distribution 47
4.5.3 Powder morphology 47
4.5.4 Bulk density and tap density 47
4.5.5 Powder flowability 48

4.6 Assessment of functional and bioactives properties of lignin 49
4.6.1 Antioxidant capacity DPPH 49
4.6.2 Oxygen Radical Antioxidant Capacity measurement 49
4.6.3 Cellular antioxidant capacity (CAA) Assay 50
4.6.4 In vitro oil adsorption capacity by DIN ISO787/5 51
4.6.5 Activity against α-amylase and α-glucosidase enzymes 51
4.6.6 Cytotoxicity of lignin using Caco-2 cell 52

4.7 Simulated gastrointestinal conditions for lignin dietary oil absorption 53
4.7.1 Simulation of gastric and gastrointestinal conditions 53

4.8 In vivo toxicity and lignin hypocholesterolemic effect in Wistar rats 55
4.8.1 *in vivo* studies: Animal model 56
4.8.2 *in vivo* toxicity and antihyperlipidemic effect of AS lignin spray dried 56
4.8.3 Parameters analyzed in the rat model 57
4.8.4 Lipid extraction from feces 58
4.8.5 Body and heart fat weight and sample collection for further analysis 58
4.8.6 Statistical analysis 59

4.9 Formulation of pharmaceutical dosage form from lignin tablets 59
4.9.1 Mixture design for pharmaceutical formulations containing lignin 59
4.9.2 Direct compression/tableting of formulations 60
4.9.3 Wet granulation 61
4.9.4 Tablet hardness, friability and dissolution 61
4.9.5 Effective pore radius 64
4.9.6 Drug release profiles of Ibuprofen 64
4.9.7 Contact angle of solid dosage forms 64

5 Results and discussion 66

5.1 Evaluation of the influence of spray drying process parameters on the quality of lignin particles 66
5.1.1 Analysis of the model 67
5.1.2 Effect of temperature, atomization pressure and feeding rate on responses 70
5.1.3 Optimization of the factors: Temperature, atomization pressure, feeding rate 77
5.1.4 Characterization of aquasolv lignin particles 79
5.1.5 Flowability and cohesion of the powder 79
5.1.6 Morphology 80
5.1.7 Conclusions PART I 82

5.2 Assessment of the bioactive properties of the spray dried powders 83
5.2.1 Antioxidant activity: ORAC and DPPH 83
5.2.2 Cellular Antioxidant Activity (CAA) 86
5.2.3 Antidiabetic capacity by inhibition of α-glucosidase and α-amylase 87
5.2.4 In vitro cytotoxicity activity 90

5.2.5 Oil adsorption capacity 92
5.2.6 Oil adsorption capacity under simulated gastrointestinal conditions 94

5.3. In vivo assessment of toxicity and hypocholesterolemic activity of AS lignin spray dried particles 98
5.3.1 Body & heart fat weight 98
5.3.2 Rate of total cholesterol levels 101
5.3.3 Rate of triglycerides levels 102
5.3.4 Rate of HDL levels 104
5.3.5 Liver toxicity 105
5.3.6 Conclusion Part II 106

5.4 Spray dried lignin particles for the formulation of oral dosage forms 107
5.4.1 Powder characterization of the lignin used for direct compression 107
5.4.2 Compression properties of lignin during direct compression 110
5.4.3 Mixture design to optimize the use of lignin in solid dosage formulations. 112
5.4.4 Effect of the components in the response tensile strength 113
5.4.5 Optimization of proportions for tensile strength and disintegration 117
5.4.6 Wet granulation 118
5.4.7 Formulation of lignin-based tablets using Ibuprofen as model drug 118
5.4.8 Contact angle and wetting properties of pharmaceutical formulations 123
5.4.9 Effect of process parameters on the disintegration of the formulation DBL 124
5.4.10 Dissolution profiles of the different formulations 125
5.4.11 Conclusion part III 127

Conclusions of the doctoral thesis 128
Outlook 132
References 133
List of figures 150
List of tables 153
Symbols and abbreviations 154
Appendix 156
Publication list 177
Student theses 179

1 Introduction

Aquasolv (AS) lignin is a high-molecular weight biopolymer obtained after pretreatment of lignocellulosic biomass with liquid hot water (LHW) under elevated pressure and further enzymatic hydrolysis [1, 2]. Due to its free-of-solvent nature and inherent vegetal primary source, AS Lignin can be utilized in high value products as the case for cosmetic, food and pharmaceutical industries. Nevertheless, this potential applicability highly depends on the quality in which lignin can be produced on a chemical and physical level. Thus, properties such as particle size and particle morphology may have an impact on the mechanical and biological behavior of end product in terms of its flowability, solubility and compressibility. The reaction rates and the rates of dissolution which is affected by the availability of surface area for mass transfer that finally affect the bioavailability of the drug and the speed of dissolution to achieve desired effect when intended for pharmaceutical or biomedical applications. Cement and paint industries are also interested in the fine particle size which provide a stronger structure due to better chemical interaction of the cement particle and the required product appearance that is achieved through desired light scattering effects.

The selection of an appropriate method to obtain particles with controlled mean size and/or morphology appears to be a crucial step for product development and formulation. In this regard, spray drying is a recognized process for the efficient drying and formulation of solids and widely used in food, pharmaceutical and ceramic industries, to name a few [3-5]. Spray drying is the operation in which a feed/liquid stream is pumped into an atomizer and being constantly divided into very fine droplets in a drying chamber [6]. These droplets are immediately in contact with a hot gas which provides the energy to heat and vaporize the liquid (mostly water) contained in the droplets that are subsequently transformed into dried particles. The dried material can be collected via a cyclone. The process of spray drying is advantageous because powders can be obtained in a consistent/controllable quality throughout the drying process; also it´s applicable for both heat-sensitive and heat-resistant feeds and is suitable for different types of

feedstock such as solutions, suspensions, slurries, pastes, to name a few [5, 7, 8]. Although the basic principles of spray drying may appear as simple, the process becomes complex when the operational parameters in relation to a specific feedstock need to be chosen. Studies must be performed for understanding the most critical factors to obtain a product with desired quality (namely particle size, morphology, antioxidant capacity, stability, etc.) during spray drying; formulation and targeting of product properties and particle formation occur simultaneously. In this regard, process optimization can be habitually time-consuming and costly and therefore, statistical design of experiments (DoE) is frequently applied to establish multidimensional relationships between the factors and responses with a reasonable number of experiments.

In the case of lignins, efforts to control and design particle quality are not substantial as lignin has been considered a residue for a long time and it´s been typically burnt for energy production. Lignin valorization is a key success factor for sustainability and economic viability of both conventional (pulp and paper) and new (liquid hot water, steam explosion, organosolv, etc.) biorefineries. Therefore, in this study, the optimization of the spray drying process to produce AS lignin powder with desired quality was optimized via response surface methodology. Very few approaches can be found in the literature for controlling lignin particle properties, mostly via antisolvent precipitation, self-assembly and interfacial crosslinking [9]. Spray drying and lignin particle formation targeting specific particle size has not been reported before in the literature. With this in mind, the aim of this PhD work was to use particle engineering and lignin product tailoring, to contribute to the efforts of lignin valorization, crucial subject to the biobased economy.

2 Theoretical background

2.1 Definition and structure of novel and technical lignins

Technical lignins is the common name used to describe those lignins being produced at industrial scale, typically in the pulp and paper industry. In this regard, sulphite, soda and kraft lignins are the most important due to the considerable amounts in which they are produced and are available in the market [10, 11]. However, a new group technical lignins from processes such as Steam Explosion (SE), Organosolv (OS), Hydrothermal Pretreatment (AS), and Ammonia Fiber Expansion (AFEX) are emerging and expected to grow in the following years [10, 12, 13]. Unsurprisingly, the chemical, physical and technical properties of these lignins strongly depend on their origin, extraction and/or purification processes. Processes for lignin extraction can be divided into two groups: acidic and basic, relating to the media under which delignification reactions take place during biomass biorefining. Free functional groups in each type of lignin will differ according to the type of linkage that every process aims to cleave. For instance, harsh acidic and alkaline conditions will result in scission of C-O bonds that interconnect the monolignols, cleavage of lignin-carbohydrate linkage and sulphonation of the lignin aliphatic chain [11, 13]. Kraft lignin undergoes depolimerization mainly through hydrolysis of >95 % of the β-O-4´structures, and the cleavage of α and β aryl ether bonds propitiates the generation of free phenolic groups, allowing "kraft lignin" to be soluble in the black liquor [14, 15]. In Table 1, molecular properties of lignins obtained by industrial processes and emerging biorefining processes are summarized.

Novel biorefining technologies have emerged in the last decades aiming both the separation and valorization of the three main biomass components: lignin, cellulose and hemicellulose, within this concept the lignin is no longer considered as a residue but a

source of potential added-value [16, 17]. With today´s society's demand for environmentally friendly processes and products, Organosolv pretreatment (OS) and Hydrothermal processing (HP) can be considered as promising alternatives to obtain high value lignin, which ideally should be Sulphur free, solvent free and sustainable [18]. Organosolv is the process in which a highly pure lignin product is separated from the biomass by treatment with an organic solvent (mostly ethanol or methanol) at high temperatures (100-250°C) and pressure [16]. Organosolv lignins are of high purity; contain negligible amounts of carbohydrates and ash, and due to their solubility in organic solvents and low molecular weights presents technical advantages over other technical lignins for its application in polymer chemistry.

Table 1: Major uses and molecular properties of lignins obtained from different biorefining processes

TECHNICAL LIGNINS				
Type of lignin / major source	**Process conditions**	**Molecular properties**	**Major uses**	**Ref.**
Sulfite / Wood	Digestion at 140-170°C with sulphites and bisulphite salts of sodium, ammonium, magnesium or calcium.	Sulphonate groups: 0.4 to 0.7 groups per phenyl propane unit (C_9 unit) Presence of sulphonate groups (0.4 to 0.7 groups per phenyl propane unit phenolic hydroxyl, aliphatic hydroxyl and carbonyl groups.	Vanillin production, spraying pesticides, carbon black, binders, textile dyeing, clay and bricks production.	[11]
Kraft / Wood	Digestion in a mixture of hot water, sodium hydroxide and sodium sulfide, at 170-176°C.	Primary aliphatic OH (171.7 – 170.2 ppm), secondary aliphatic OH (170.2 – 169.1 ppm), Phenolic OH (169.1 – 167.0 ppm).	Dispersing and binding agents. Steam, heat and power. Activated charcoal.	[14, 15]
Soda / Non-wood fibres, annual plants	Pressurized reactor at 140 -170°C with Sodium hydroxide. Anthraquinone can be used as additive.	Sulphur-free lignin. Aliphatic and aromatic hydroxyl content: 4.4 – 5 mmole g^{-1} Carboxylic groups: 2.1 - 2.3 mmole g^{-1}	Phenol-Formaldehyde resins, dispersants, concrete additives. Animal health and nutrition (antibiotics, enteric disturbances).	[19, 20]
LIGNIN FROM EMERGING BIOREFINING PROCESSES				
Type of lignin	**Process**	**Molecular properties**	**Proposed uses**	**Ref.**

Steam explosion /Hardwood, annual plants	Biomass exposed to pressurized steam (180-240°C, 350 bar), followed by rapid reduction in pressure (70 bar).	Total hydroxyl/C_9: 1.1 groups; Phenolic hydroxyl/C_9: 0.6 groups; Carboxyl/C_9: 5.4 groups; Methoxyl/C_9: 1- 1.1 groups.	Reinforcement fiber in composites. Adhesives for wood composites and replacement of phenol-formaldehyde adhesive.	[21]
Organosolv	Digestion with ethanol, methanol, water/ethanol mixtures at 100-250°C	Phenolic hydroxyl groups: from 0.28 to 0.50 groups per phenylpropane unit. Carboxylic groups: from 0.02 to 0.04 per phenylpropane unit. Aliphatic hydroxyl groups: from 0.67 to 0.19 per phenylpropane unit	Component in Phenol-Formaldehyde resins, adhesives, stabilizer and filler in Polyurethane foams, formulations of Epoxy Resins, dispersant with biocidal properties.	[22, 23]
Aquasolv / Annual plants	Compressed water at 180 – 230 °C during 10-40 min and pressures ranging from 30 to 50 bar	Phenolic hydroxyl groups: 1.84 mmoleg-1. Ratio of monolignols H:G:S-type does not differ from native lignin, ratio of C_9-units 12:40:48.	Aerogels for biomedical applications. Antioxidant and filler in adhesives. Human consumption, alternative to activated charcoal.	[18, 24, 25]

Hydrothermal pretreatments use hot water at high pressures to maintain the liquid state during the solvation process. The hot compressed liquid passes through the biomass dissolving 90 - 97 % of hemicelluloses (40 to 60% of total biomass), while most of the lignin remains in the solid residue linked to cellulose [26]. The pretreated material (mainly composed of lignin and cellulose) is then subjected to enzymatic hydrolysis in a mixture of cellulases and β-glucosidases for the hydrolysis of cellulose, and oligomers. Aquasolv lignin can be recovered afterwards; the structure of this type has been described as similar-to-native-lignin and researchers have identify such feature as advantageous for the production of aerogels [17] and biocompatible lignin-alginate aerogels for tissue engineering scaffolds [27]. Additionally, Aquasolv lignin´s sulfur- and solvent-free nature opens a broad spectrum of applicability in areas like cosmetic, food and pharmaceutical products.

2.2 Lignin functionality and proposed mechanisms

Lignin has been recognized by European and international institutions as a key product of the biobased economy and its use for the formulation of high added-value products is a current scientific and political priority. In this sense, understanding the complex structure of the different technical lignins is a key factor when targeting product formulation, thus having a close and controlled scenario of the molecule behavior, solubility and reactivity. Such properties will affect the mechanisms involved in the functionality of lignin as well as the interaction of lignin with biomolecules, food ingredients or human fluids in the gastrointestinal tract. In the following sections, a structure-related functionality of lignin are presented, and its bioactive properties are described on the basis of the molecule arrangement and functional groups, specifically describing relevant properties for biomedical, food and cosmetic applications.

2.2.1 Protection against oxidative stress

Lignin, being the most abundant natural source of phenolic compounds, is known for its ability to prevent oxidation as well as propagation of reactive oxygen specifies and free radical scavenging. In this regard, the hydroxyl groups of the phenolic acids can act as

Hydrogen donors and inactive reactive species which otherwise will create a chain reaction and convert biomolecules into further free radicals. A number of studies have confirmed the correlation between the total phenolic content (which measures hydroxyl groups) and the antioxidant capacities (AOX) of lignins from various biomasses and isolation methods [28, 29]. In general, lower molecular weights of lignins possess higher antioxidant capacities than that of the higher structures, this can be explained by steric hindrances from internal lignin-lignin interactions playing a significant role on the antioxidant capacity [30-35].

Ponomarenko et al. [35] conducted a thorough study with 50 different lignin samples derived from diverse biomasses using alkaline, kraft and pyrolysis isolation methods. They quantitatively analyzed the lignin structures with a pyrolyser coupled with GC/MS and correlated the detected structures with lignin AOX via stable DPPH radical scavenging. The magnitude of influence of different descriptors on AOX were identified as follows in descending order: phenolic OH content > content of G + S monolignol units > content of monolignols with CH_2 groups in α-position of side chain > content of monolignols with O-containing groups in sidechain > size π-conjugated systems. A similar study conducted by Dizhbite et al. [30] researched the antioxidative capacity via DPPH of 4 lignin samples and 10 lignin-related compounds with regard to their chemical structure analyzed by ESR (electron paramagnetic resonance) spectroscopy. It has been identified, that non-etherified phenolic hydroxyl groups, ortho-methoxy groups, aliphatic hydroxyl groups in the side chain and π-conjugated systems increased the AOX, while **α**-carbonyl substitution in the side chain, high molecular weight, heterogeneity and polydispersity decreased the antioxidative capabilities.

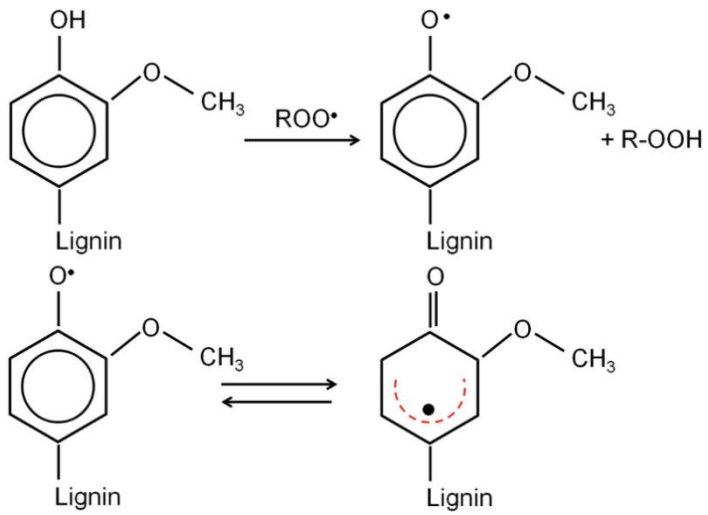

Figure 1: Proposed mechanism of lignin for radical scavenging via electron donation.

The duration of the isolation process has an additional influence, where prolonged processing times cause a decrease in antioxidant capacity due to inaccessibility of phenolic hydroxyl groups caused by lignin-lignin condensation reactions [32, 34]. Apart from the chemical structure of the lignin, the molecular size was also shown to have an impact on the AOX, which might as well be attributed to the accessibility of the phenolic OH groups. The magnitude of AOX were found to be comparable but lower than standard antioxidizing agent Trolox; for DPPH assays the IC50 values range between 36.5±5.5 [36] for alkaline extracted lignins and around 17.8±0.1 to 15.4±0.3 mg/L for solvent fractionated lignins [37] compared to 15.7±0.2 mg/L of Trolox. The antioxidant property of softwood kraft lignins has been proven in films for advanced packaging [38], blends with polyethylene [39] and in cellulose nanofibers [40].

2.2.2 Antimicrobial activity of lignin and lignin derived products

Phenolic compounds, basic monomeric structure of lignins are not only responsible for free radical scavenging but have been also associated to antibacterial capacity potentially via interaction to functional molecules on the bacterial membrane. However, there are different mechanisms by which the antimicrobial activity can be presumably expressed. One proposed mechanism is the release of monomeric or dimeric phenolic compounds

physically adhered to the lignin which can interact with the cell walls or penetrate them [41] and intercepting crucial intracellular compounds [42]. On the other hand, lignin can also interact directly with the microbial cells via phenolic functionalities [43]. Researchers have tested lignins against both gram-positive and gram-negative bacteria, concluding that lignin is not active against gram-negative bacteria which present a secondary cell wall [42-44]. Contrarily, lignins are efficient against gram-positive bacteria where phenolic and polyphenolic compounds can cause lysis of bacteria and thus release of the intracellular content (see Figure 2).

Studies focusing on the biomedical applications have made efforts on the antibacterial properties of lignin and its derived products against plant pathogens [45, 46], or against fungi [31, 43]. Gabov et al. [44] produced lignin containing cellulose beads, which were able to adsorb gram-positive bacteria and consecutively inhibit their growth through leaching of phenolic compounds from the encapsulated lignin.

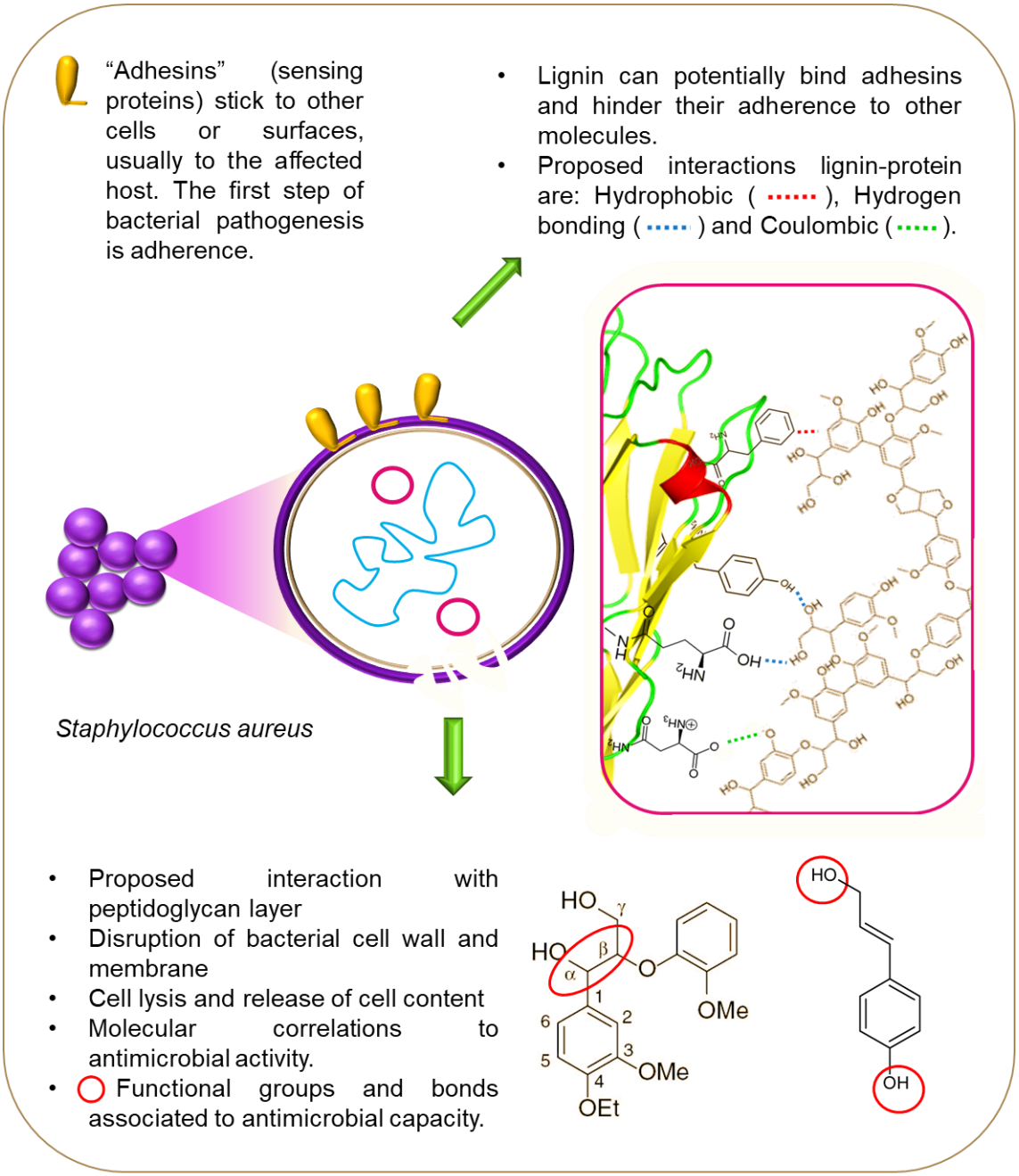

Figure 2: Structure-relationship of lignin as antimicrobial agent. Example is shown for Staphylococcus aureus, spherical gram-positive bacteria causing a wide range of major infections in man and animals.

As it is the case for the antioxidative capacity, the isolation methods of lignin have also shown to have an effect on the antimicrobial characteristics. It is implied, that prolonged pretreatment of biomass or secondary treatment of lignin induces condensation of the lignin molecule, which in turn generates a more inert lignin fraction [34]. The multi-functionality of lignin has been claimed by many of the aforementioned authors, who – in

the majority of studies – tested the antioxidative as well as the antimicrobial characteristics of their materials. Some cases report an inverse correlation between AOX and AMB characteristics by claiming smaller lignin molecules exhibit AOX, whereas larger molecules favor the biocide effect of lignins [32]. Further studies, which quantitatively investigate both of these properties, are needed to prove whether there is a correlation. However, considering the role of molecular size on accessibility of lignin functional groups it is likely that a detailed investigation of distribution of functionalities from different lignin sources will provide an answer.

In a recent study, Gordobil et al. [47] evaluated the antifungal capacity and antibacterial properties against 9 foodborne and human pathogenic bacteria of four lignins from eucalyptus and spruce, and extracted with the organosolv and kraft processes. It was found that Kraft lignins present higher antifungal capacity due to a lower carbohydrate content (2.5-3%) in comparison to organosolv lignins (4-10 %), in addition to the amount of sulfur in kraft lignin. For antimicrobial capacity, kraft lignin from spruce showed inhibition against *E. coli* ATCC 25922 (17.72 ± 1.16 mm), *P. microbilis* ATCC 14153 (19.12 ± 1.22 mm), *P. vulgaris* ATCC13315 (24.68 ± 1.31 mm), *P. aeruginosa* ATCC 27853 (21.89 ± 1.26 mm), *E. aerogenes* ATCC13048 (18.97 ± 1.08 mm), *S. aureus* ATCC 25923 (19.18 ± 0.98 mm) and *B. thuringiensis* (24.76 ± 1.19 mm). On the other hand, Organosolv from spruce showed activity against *E. coli* ATCC 25922 (13.32 ± 1.01 mm), *P. microbilis* ATCC 14153 (18.15 ± 1.04 mm), *P. vulgaris* ATCC13315 (17.91 ± 0.96 mm), *E. aerogenes* ATCC13048 (16.45 ± 0.98 mm) and *B. thuringiensis* (18.36 ± 1.09 mm). Lignins from eucalyptus (kraft and Organosolv) present antimicrobial capacity against *S. typhmurium* SL 1344 (28.92 ± 1.36 mm), *P. aeruginosa* ATCC 27853 (16.10 ± 1.06 mm*), S. aureus* ATCC 25923 (17.88 ± 0.97 mm) and *S. mutans* ATCC 25175 (15.66 ± 0.92 mm). Pseudomonas for example, is the one of the major cause of infections in patients with thermal injury, antineoplastic chemotherapy and patients with chronic pulmonary disease [48]. On the other hand, foodborne diseases are considered a growing public health problem worldwide, such diseases result after ingestion of contaminated foodstuffs. Most common clinical presentation are gastrointestinal ailments, nevertheless; the problem can also be neurological, immunological, and gynecological, as well as causing multi-organ failure (WHO, 2015). In this regard, lignin represents an alternative antimicrobial biomaterial, and its outstanding capacity against food borne and human pathogenic microorganisms

opens new perspectives for application of this biomolecule in food and pharmaceutical industries.

2.2.3 Lignin as antidiabetic functional molecule

Lignin is the most abundant natural source of aromatics and, in its amorphous form is constituted by p-hydroxypenyl (H), guaiacyl (G) and syringyl (S) moieties [49]. The bioactivities attributed to different sources of lignin, such as antioxidant or anti-diabetic are directly linked to the free –OH groups available in the lignin structure, which are able to scavenge free radicals [50, 51]. The potential applications of each material will also depend on their molecular weight, source and method of extraction, therefore, is important to establish structure-bioactivity relationships for specific lignins and join efforts to uphold their way to product formulation and to market insertion. There is a vast information in the literature containing methods and processes of lignin fractionation aiming to improve and/or influence the efficiency of lignin as antioxidants that have been reviewed in Espinoza- Acosta et al., and Arshanitsa et al., [52, 53].

2.2.4 Lignin as drug release agent in pharmaceutical formulations

Lignocellulosic materials are abundant in nature. As a perspective, 54 million tons of the sugarcane bagasse is produced annually throughout the world [54]. Lignin extracted from the bagasse is a ramified polymer in an amorphous state consisting of phenylpropane molecular units [55-57]. Various experiments have been done on pretreated lignin either in industrial scale or lab scale [58]. Most commonly being the acid and base hydrolysis and extraction for small quantities in the lab scale. Industrially, the Kraft process is the most well-founded process [59]. Lignin from the Kraft process is used widely for analyzing the bioactive properties and pharmaceutical experiments. Recently, another pulping technique to produce Organosolv lignin is industrially developing which is a benign alternative to Kraft lignin considering environmentally and the toxicity of the lignin [60, 61]. The analysis and comparison of this two kinds of lignin have been done extensively to understand the bioactive and pharmaceutical properties exhibited by them

in the field of pharmaceutical and recently in lignin recovery methods which were discarded before [62].

Drug release mechanisms of biopolymers are of extreme interest as they can be both biocompatible and biodegradable [63]. Polymer-based controlled drug release mechanisms paved the path to provide useful information and gain better insight about Lignin based CR processes and process mapping of critical process parameters in the tabletting pressing techniques, critical quality attributes of the process and the final tablet characterization [64].

Wetting and hygroscopicity are the two important properties while dealing with polymers, especially biopolymers [65]. It is seen specifically that the hydrophobic or hydrophilic nature of the lignin is dependent on the sources of the origin of lignin and the type of extraction process used for manufacturing the lignin [63]. This nature gives an understanding of the water uptake and the water diffusion and both diffusion and release profiles of the occluded bioactive materials [66]. The water sorption kinetics which is influenced in a biopolymer through the polymer microstructure, polarity of the copolymer segments, glass transition temperature and the flexibility of the polymer backbones, molecular weight of the polymer, crosslink density of the polymer, cross chain interactions and the presence of the bulk co-monomer pendant groups [63, 65].

The experiments of drug loading in the polymer matrix are carried out using Kraft lignin using a melt conditional approach when the lignin was coated with another natural polymeric material and the bioactive release kinetics was studied. The molecular weight and polydispersity of various lignin, along with their multifunctional reactive groups in the lignin structure is posing a lot of problems in the lignin-based CR approach [63, 67].

Apart from Kraft Lignin, different samples of Organosolv lignin were tested as well to compare the processes of direct compression, dry granulation and wet granulation techniques [63, 64, 68]. Lignin, with the hydrophobic matrix, could reach a drug release of 100% with 50% of the water-soluble drug load due to the formation of the interconnecting channels [67]. The lignin depolymerisation and repolymerisation with other monomers can be a useful technique for using water-insoluble drug loading and their release studies [69]. The reduction of polydispersity of the various lignins and the to create a transformed lignin sample that is both uniform and smaller structure can have

a huge potential in future biomedical areas [63, 67, 69]. Organosolv lignin has been compared with the with MCC and lactose to check on various of physical properties of the tablets like compressibility and flowability and evaluate them for the operational limitations and the if lignin can be used as an excipient [70-72]. Lignin was seen to have limited compressibility when compared to MCC and lactose but the behaviour of lignin was seen similar to that of the lactose [64]. On the other hand, lignin has good flowability of and hence can improve the granulation process. The reason for using studying lignin as an excipient is the low cost and ease of availability [64, 70]. The operational limitations in the process were low which gives way to use lignin as an excipient [63, 64, 70].

2.3 Current approaches for lignin valorization and potential application in high value added formulations

2.3.1 Lignin as dispersing, binding and emulsifying agent

Due to its surface-active properties, lignin could enhance the texture of foams and emulsions, besides of being an antioxidant compound and increase the shelf-life of food products. Lignin has already proven efficacy in prolonging the shelf life of food products (in –somehow- indirect contact) when used as polymer in active packaging, for instance; addition of lignin results in controlled water permeability, improved water resistance, and increase antimicrobial activity when combined with chitosan [45, 73]. The active surface molecular surface is given by the functional groups attached to the phenolic ring of lignin; carbonyl, carboxyl and hydroxyl groups [10, 74]. During extraction processes, these functional groups might be oxidized, yielding even more branched structures and different functionalities to the molecule [75]. Therefore, lignins are used as dispersing or emulsifying agent, binder and flow enhancer depending on the origin and separation process (and modification) [74]. Ligninsulfonates, for instance; are used to stabilize emulsions (often one aqueous phase) such as asphalt emulsions, herbicide and pesticide formulations, emulsifier in consumer goods, pigments and dyes [76]. Chemical modifications such as sulfonation, formulation, oxidation graft polymerization just to name a few enhanced in general the performance as bindering or dispersing agent [77].

The binder and agglomeration uses are simple solid–solid dispersions with the lignins aiding by maintaining and affecting fluidity as a result of lignin–lignin, lignin–water interactions [78]. Low-cost binders from ligninsulfonates are commonly used in coal briquettes or ceramics, briquetting of mineral dust (fines, shavings, turnings), and wood-related material such as plywood or particle boards. Lignin binders are used in the development of ecofriendly renewable materials [76, 78]. In addition, with their low toxicity, they can be used as binders in animal feed or soil stabilizers in agriculture. For example, the addition of 2% ligninsulfonate to animal feed improves the feed properties of pellets and helps provide balanced nutrition to livestock [79, 80]. Nevertheless, despite lignin functionalities, no food product or formulation was found after a thorough search in patent databases.

2.3.2 Lignin as anti-hyperlipidemia and anti-obesogenic agent

The metabolism of lignin in humans is not yet well understood, despite the fact that is present in our daily diet (> 1 g/day) as component of grains and cereals, legumes and fruits [81]. Instead, lignin is generally recognized as inert biopolymer in the human intestine, yet recent findings have suggested that some soluble fractions of brewer's spent grain lignin can partially undergo fermentation when exposed to colon microbiota [82, 83]. While lignin in its polymeric form cannot be absorbed in the gastrointestinal tract, it remains in the lumen; where is able to interact with the components of food and affect their further metabolism. For instance, supplementation of lignosulphonates can inhibit intestinal glucose absorption; a decrease in the blood glycemic response when supplementing lignosulphonates to rats diet after sucrose and glucose ingestion was observed [84]. Moreover, lignin has been proven to reduce serum cholesterol by binding to bile in the intestine (see Fig 3) [85, 86]. Both cholesterol and bile acids play an important role in the absorption of dietary oils in the small intestine, and lignin being able to bind/adsorb them might be translated to beneficial effects for the obese and individuals with atherosclerosis.

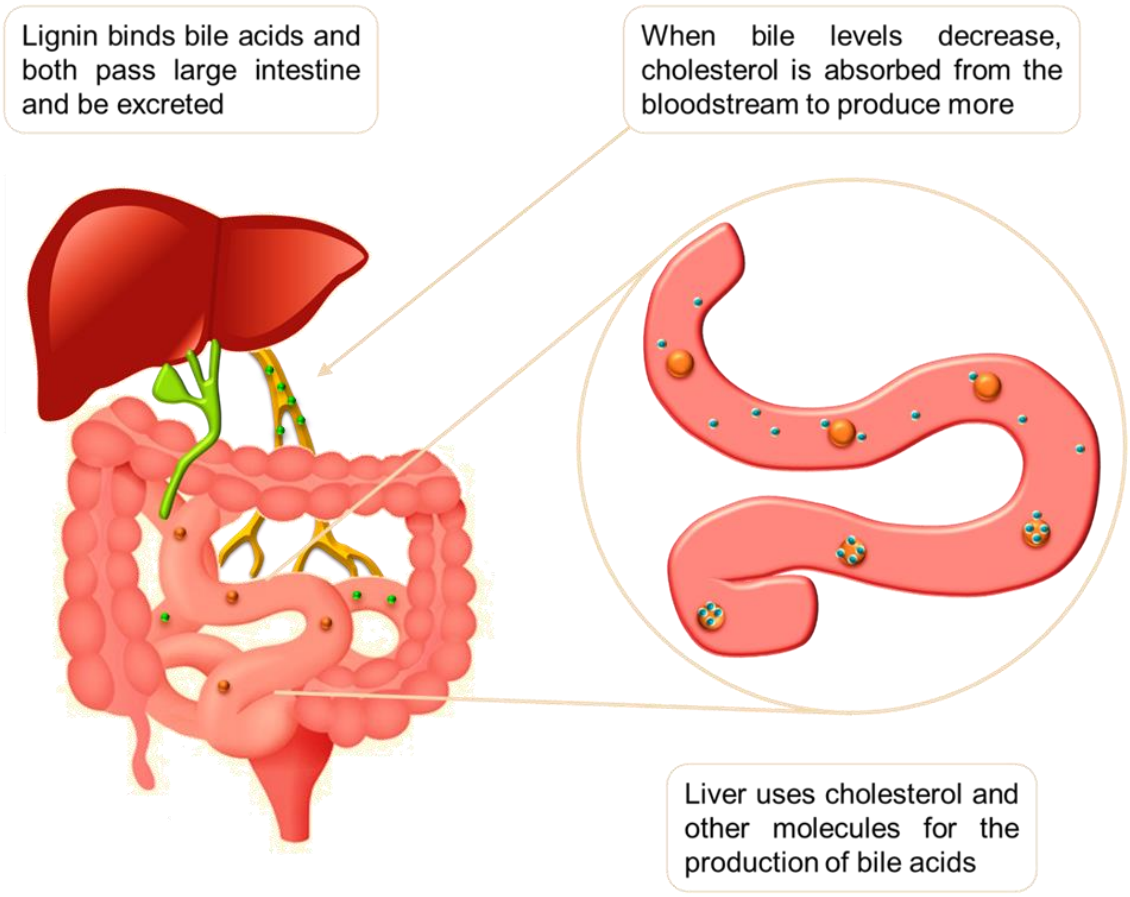

Figure 3: Schematic mechanism proposed for Lignin activity on binding bile acids in the small intestine and lowering cholesterol levels in blood.

Digestion of oils cannot start in the stomach aqueous environment due to their hydrophobicity; lipases are water-soluble and can only interact with big oil globules on the surface [87]. Nevertheless, stomach is the main site for emulsification of dietary oil, being peristalsis a key contributing factor. After that, the oil enters the small intestine in the form of droplets, where these mix with pancreatic juice and bile to form small micelles, phenomena that is possible because of the amphiphilic nature of bile salts present in the bile [87-89]. Pancreatic lipase activity is aided by the increased surface area of the oil micelles (4 – 5 μm), acting on the emulsion-water interface and converting triacylglycerols into monoglycerides and fatty acids, prepared for absorption across the intestinal walls [90-92]. In the absence of bile salts, oil droplets would prone to re-agglomerate, reducing the lipase activity along with the absorption of oil across intestinal walls.

Lignin from bran and *Pinus insignis* sawdust showed adsorption capacity for sodium deoxycholate (bile salt), binding 45 μmol/g and 51 μmol/g, respectively [86]. Similarly, Eastwood & Hamilton [90] reported that lignin produced from wood wool, sawdust and dry grain are able to bind 11 μm sodium cholate/ g. Other studies have shown the binding effect of lignin towards cholate, deoxycholate, chenodeoxycholate, and the conjugated bile acids with taurine and glycine: taurocholic and glycocholic acid [89]. Lignin has been stated to be the strongest bile acid adsorbent of the components in dietary fibers, this capacity is attributed to the presence of methoxyl and β-carbonyl groups in the molecule, and the binding ability differs with molecular weight [93]. As previously described, the lignin-bound bile would be unavailable to form micelles, leading to reduced lipid absorption and decreasing the levels of fat entering the blood stream. Nowadays, several drugs used for the treatment of obesity and hypercholesterolemia target bile binding as is the case for the products Locholest®, Prevalite®, Colestid® and Welchol®.

The bile acid adsorption capacity of lignin increases when higher ionization of the carboxyl groups in lignin takes place, which might turn in influencing the interaction with organic anions. Nevertheless, there is an evidence that at neutral pH, lignin is able to adsorb the less polar, less water soluble dihydroxy bile acids, endorsing the theory that the mechanism involved is hydrophobic bonding [94]. In other study, an increase in the methylation of lignin was related to increase in bile acid adsorption, contrarily; the authors emphasized that adsorption is favored at low pH [90]. In both cases, the acidic or basic environment will block the ionization of the carboxyl and hydroxyl groups present in the phenylpropanoid structure of lignin, which confirms once again the hydrophobic-hydrophobic interactions.

A second mechanism proposes the following; as lignin will pass the gastrointestinal tract with no/or negligible molecular alteration, the bound and/or adsorbed compounds onto lignin are most likely to remain intact and be excreted in the feces. Under normal metabolic conditions, the majority of the bile salts are reabsorbed and reused, nevertheless; if these molecules are trapped (i.e. onto lignin, fiber, etc.) more cholesterol would be catabolized to bile acids [88, 95]. The production of bile is one body's mechanism to dispose the excess of cholesterol, in this regard; the high excretion of bile

leads to a depletion of serum cholesterol levels. In a study carried out in male Golden Syrian hamsters, the effect of diet supplementation with hydrolysis lignin from Aspen wood, and the formulation lignin + lactulose on fecal bile concentration was evaluated [96]. Results on daily bile acid excretion were found to be hydrolysis lignin > lignin + lactulose > control group, furthermore lignin showed the highest preventive activity for the formation of cholesterol gallbladder stones. Similarly, Carter et al. [97] evaluated different diets containing two dosages of four dietary fibers (including steam exploded lignin) in male Sprague Dawley rats. The bile excretion of rats fed with 10% of lignin were significantly higher (16 ± 3.1 mg/day) than that of 10 % cellulose (10.08 ± 0.9), 5% lignin (10.3 ± 0.7), and 10 % pectin (9.5 ± 0.7).

Overall, surface features of lignin, hydrophobicity and charge density might also play an important role in altering the metabolism of fats. Mechanical sorption of the oil droplets in the stomach and small intestine can occur, if the surface area and porosity of the lignin has the ability to trap molecules in its structure. Tolba et al. [98] evaluated the adsorption of six dietary oils on kraft lignin under simulated gastrointestinal conditions. Kraft lignin was found to adsorb up to 6 times its weight in oil and showed great stability at pH 1.7 and pH 8, thus offering competitive advantages in comparison to chitosan, currently used for this purpose. Different lignins exert diverse mechanisms for lowering fat and cholesterol adsorption, being promising natural alternatives for obesity prevention and lowering serum cholesterol levels. Lignins obtained from hydrothermal processes are of particular interest, not only they have been described as non-toxic, biocompatible, biodegradable and non-absorbable biopolymer in the human intestine; but the concept of using water as solvent, adds to the entire concept of a green and natural product.

2.3.3 Use of lignin as food ingredient

Food industry is continuously searching for new ingredients that could be used for improving the quality of food products and promote consumer´s health, by delivering, trapping or impeding the absorption of non-desired molecules in the gastrointestinal tract; the so-called functional foods. The consumer's preferences have evolved in such

way that food products must not only satisfy appetite and provide nutrients, but also help in the prevention of certain diseases and promote well-being [99]. Functional foods are those that when consumed in a regular way, promote a specific beneficial health effect in the human body; such benefit can be an improved physiological function or a decrease in the risk of developing a disease i.e. diabetes, hypercholesterolemia, obesity, etc. [100, 101]. Increasing the consumption of dietary fiber is inversely associated to the risk of chronic diseases, and its use for the formulation of functional foods continues as an emerging trend among food scientists and technologists [102]. In regard to this, multiple functional food products i.e. healthy snacks with added dietary fiber can be found [103, 104] but are non-existing in the case of lignin.

Studies at the VTT technical research center of Finland showed that wood derived products can be used as texture improvers, thickening agent, and emulsion and foams stabilizers in specific products like yoghurt, baked goods and meat products [105]. Lignin was used for baking muffins, resulting in a fluffier texture, and being "surprisingly" able to substitute whole eggs and egg yolks. Since lignin is a calorie-free biopolymer and cannot be absorbed by the human body, the overall caloric content of the food products in which lignin is used can be decreased, and it could even help to lower the cholesterol levels in consumers, as described in a previous section of this review.

Industrial players like DSM have made some first attempts to get approval for lignin as food ingredient, mainly as carrier for vitamins and carotenoids for coloring and nutrient purposes. Nevertheless, the last opinion published by the panel of experts in EFSA declares that more studies are needed (acute toxicity-12 months) in order to determine the safety of the lignin and established its ADI (acceptable daily intake) [106]. Overall, much efforts are being done for the use of lignin in high value added products, however; from 65 Public-Private Partnerships between EU and the Bio-based Industries Consortium, only 1 project (POLYBIOSKIN) covers the use of lignin for biomedical, cosmetic and sanitary purposes [107]. None of these are related to the use of lignin for pharmaceutical or food products. More studies are needed regarding the evaluation of lignin safety, the establishment of ADIs as well as the interactions that lignin could have with other biomolecules when added in to food products.

2.4 Role of particle engineering on product formulation and manufacturability

Regardless of the material source, good quality of any powder is determined by the adjustment of the powder requirements to the application. This section presents an overview of the different powder properties which are important for product formulation, their fundamentals as well as industrial examples of real applicability. Special emphasis is put in flow and compression, considered critical quality points for industries like food, pharmaceutical, ceramics and cosmetic industries.

2.4.1 Influence of particle properties on the flow behavior of powders of particulate solids

Controlling particle properties, especially particle size, size distribution, density, etc. is of high industrial relevance because such properties are proven to have an impact in product formulation, manufacturability, and product performance such as drug release, bio-performance, dissolution and bioavailability of active pharmaceutical ingredients [108]. Nevertheless, these properties need to be controlled earlier on the manufacturing processes in order to maximize efficiency of unit operations and minimize discrepancies and/or inhomogeneities on the final formulation. For example, silos, powder feeders or mass flow hoppers will be designed according to particle´s flowability, which is typically not available and has to be measured experimentally and/or designed accordingly. Powder flow is defined as the displacement of particles in relation to each other, when certain conditions or directional forces are applied (gravity, mixing, agitator, vibrator, entrainment in a fluid stream, etc.). Powder strength is the resistance that the powder effects towards displacement and is given by particle-particle or particle-surfaces adhesive forces. Main types are Van der Waals forces, Liquid bridge (capillary) forces, and electrostatic forces. A way to express can der Waals force, considering two spheres is as follows:

$$F_{vdW} = \frac{C_d}{X^2}$$

d= particle diameter; x = interparticle distance and C is a constant

On the other hand, to express the adhesion forces of two particles (spherical) bound by a liquid bridge, the following equation is used:

$$F_{lb} \approx \pi\gamma d$$

γ= surface tension of the liquid; d= particle diameter

Describing powder flow in terms of adhesion properties is rather difficult, thus; existing methods to analyze flowability of particulate solids consider the bulk powder to be a continuous solid in which particle-particle interactions/forces are treated as friction. If we consider a solid body (powder sample, particulate solid) (Figure 4) resting in a horizontal plane, a constant force *N* acts in the direction of the plane, while T is a force gradually applied to the body parallel to the plane. The body will then move then T is higher than the static friction force F. According to Coulomb´s law of friction (REF) T, and therefore F, is proportional to N.

$$F = \kappa N$$

κ = coefficient of friction

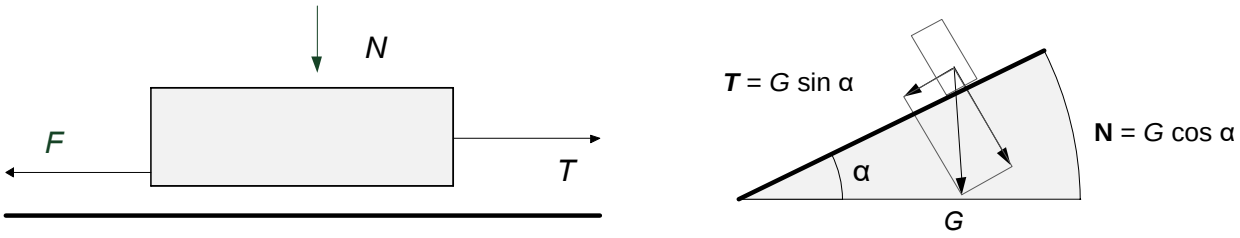

Figure 4: Friction on a horizontal plane (a), and friction on an inclined plane (b).

If we consider a solid body resting on a slope (Figure 4b) and assuming that the angle of the slope α is increasing gradually until the body starts to slide down (applicable to powder flowing down the slope), then; force T equals friction F. For this case, T= G sin α; F= k; N=kG cos α; hence: tan α=k thus:

$$k = tan\ \alpha$$

κ = coefficient of friction, related to the base angle α.

A classification of flowability in powders according to angle of repose principle can be found in the Annex A1. In powder technology, it is common and very simple technique to

use angle of repose to express flowability. However, industrially, it is more common to use stresses (force per unit area) than forces. In this case, if refer to Figure 5 with A as contact area, it is defined:

- Normal stress: $\sigma = N/A$
- Tangential stress: $\tau = T/A$

For this, the Coulomb´s law of friction is written as follows:

$$\tau = k\sigma$$

In an ideal Coulomb system, a straight line with a slope k describes the relationship between T and σ. The slope equals the coefficient of friction. In powder flow, this plot is the yield locus of the powder and it´s the fundament of the Jenike´s Shear Cell, in which the powder is covered with a lid (force N equals weight) and a ring is pushed horizontally. Here, the steady-force T which is required for shear the powder along the plane separating the base of the cell from the ring is recorded.

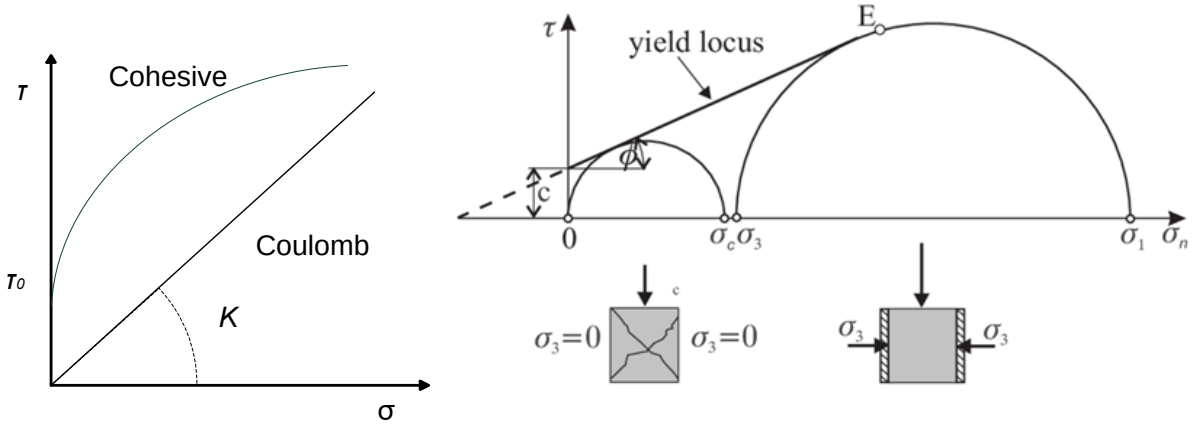

Figure 5: Yield locus of two types of powder a) and illustration of the measurement in the Jenike´s shear cell.

Jenike´s shear test is widely used in academia and industry because the measurement can provide information such as: free-flowing, cohesiveness (which applies for most food powders) and angle of internal friction o the powder. Jenike´s flow function (*ffc*) is used not only to design industrial equipment in production lines handling powders but also for storage bins. Flowability depends upon particle morphology, particle size, particle size distribution, sphericity, density, degree of particle agglomeration and moisture content. The effect of each property on flowability is deeply described in [109-111].

Understanding each effect and how these can be engineered is a great advantage to decrease costs and development times in product development and process optimization.

Particle engineering from the “Research and Development” step of pharmaceuticals is required, there are, however, studies assessing the “typical particle morphologies” used in pharmaceuticals. A study by YU, et al., [108], presented a thorough investigation on the typical particle shape in active pharmaceutical ingredients (study on 1309 API samples). They concluded that the API particles have a typical median aspect ratio between 0.6 and 0.8 and they have low surface roughness, moreover; the API particles are less equant when compared to commonly used excipients. In a study performed with Paracetamol, it was shown that spherical particles show improved flowability (decrease in the angle of repose) when compared to lath-shaped particles [111].

Special emphasis is given by industry to implement online measurements of particle size, particle size distribution and particle morphology to ensure consistent quality during production. Nevertheless, although many alternatives are available for online measurement of particle size and distributions, morphology is not easily controlled and monitored. Flowability is highly impacted by particle size distribution and such effect is well characterized in the literature [112]. Achieving a flowable powder affects manufacturability of pharmaceuticals and must be controlled in each step of the process, a homogeneous powder will result in pharmaceutical dosage forms with constant API distribution and finally in an even disintegration and drug dissolution.

2.4.2 Influence of particle design in drug release, dissolution and bioavailability

Many pharmaceutical products available in the market are solid dosage forms based on microparticles. For instance, microparticles can be filled in capsules for targeted or gastrointestinal drug delivery, or can be tableted for oral applications, additionally; dry powders are inhaled aerosols for lung delivery and can even be applied in transdermal formulations. Conventionally, primary unit operations such as micronization and drying were conducted to obtain the powders. Nevertheless, with pharmaceutical industry developing every day towards more specific medicine, targeted delivery and sophisticated therapeutic approaches, methods that allow control of particle properties

are needed. In this regard, freeze drying, spray drying and supercritical drying have been widely used to control particle properties.

2.4.3 Compressibility and mechanical interlocking on compaction

Compressibility refers to the volume change of a powder as a consequence of an applied force or consolidated stress (Figure 6). When this happens, the initial volume (Xi) of particles is packed into a smaller volume (Xf) thus increasing the bulk density. Compressibility of powders, powder properties and particle engineering are of relevance in i.e. pharmaceutical industry for the process for tablet production [113], in which powder properties have influence on: 1) the mixture of the components, where good flowability is desired to increase efficacy of the mixing process, 2) by feeding the powders into the tableting die, where most industrial processes are based on feeding volume of particles and not weight (potentially causing tablet inhomogeneities) and 3) when compressing the powders into a tablet, where the quality of the pharmaceutical dosage form will depend on how the powders in the formulations stick together and cause the tablet to be resistant to human handling without deformation. Powder systems consist typically of a complex arrangement and population of individual particles, which behavior depends on three general features.

- The intrinsic physical properties such as particle size, density, shape, roughness, and porosity
- The bulk powder properties such as size distribution, bulk density, distribution of forces as well as cohesive and frictional interactions
- The external conditions or processing environment such as temperature and humidity as well as the state of compaction [114].

Achieving a flowable powder affects manufacturability of pharmaceuticals and must be controlled in each step of the process, a homogeneous powder will result in pharmaceutical dosage forms with constant API distribution and finally in an even disintegration and drug dissolution.

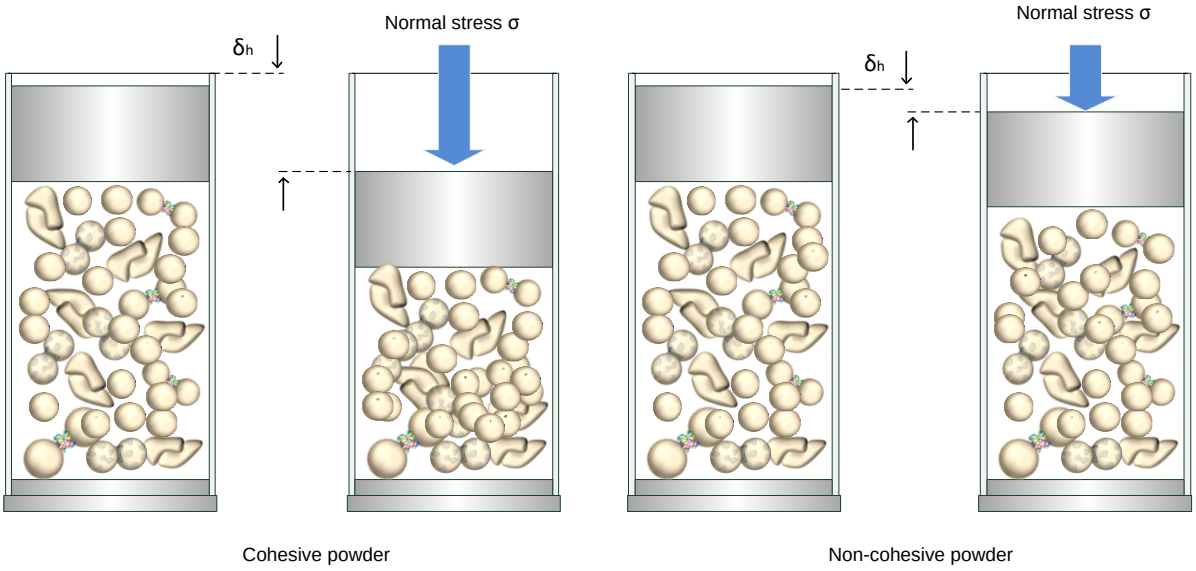

Figure 6: Example of how cohesiveness in the powders affects compression. Non-cohesive powders are less sensitive to changes in the flow/change of volume and the voids between particles almost remain intact unless high stress is applied. For cohesive powders, the particles flow with the stress/change in volume, accomodating within the existing agglomerates [115].

2.5 General description of the spray drying process

Spray drying is the operation in which a feed stream (solution, suspension, slurries, pastes) is atomized into a drying chamber and transformed into a dried particulate form. A general scheme of a spray dryer is shown in Figure 7. First, the feed is pumped into an atomizer and being sprayed into very fine droplets which are typically in the range of 10 µm to 250 µm; these droplets are immediately in contact with a hot gas which enables rapid solvent removal from the droplet and its transformation into dried particles [6]. The size of the droplets will determine the rate of evaporation since increasing the surface area of the atomized feed enables a higher heat and mass transfer. During drying, the temperature of the drying medium will decrease due to an increase on the evaporation and thus increase in the moisture content in the chamber. Afterwards, the dried particles can be collected at the outlet of the dryer and/or a cyclone. In recent years, special attention has been put into controlling the quality of powders/particulate solids via spray drying, particle properties such as morphology, particle size, particle size

distribution are of great interest due to their implication in product formulation, quality and performance, especially in pharmaceutical and food industry. The process of spray drying is advantageous because powders can be obtained in a consistent/controllable quality throughout the drying process; also it´s applicable for both heat-sensitive and heat-resistant feeds and is suitable for different types of feedstock such as solutions, suspensions, slurries, pastes, to name a few [5, 7, 8].

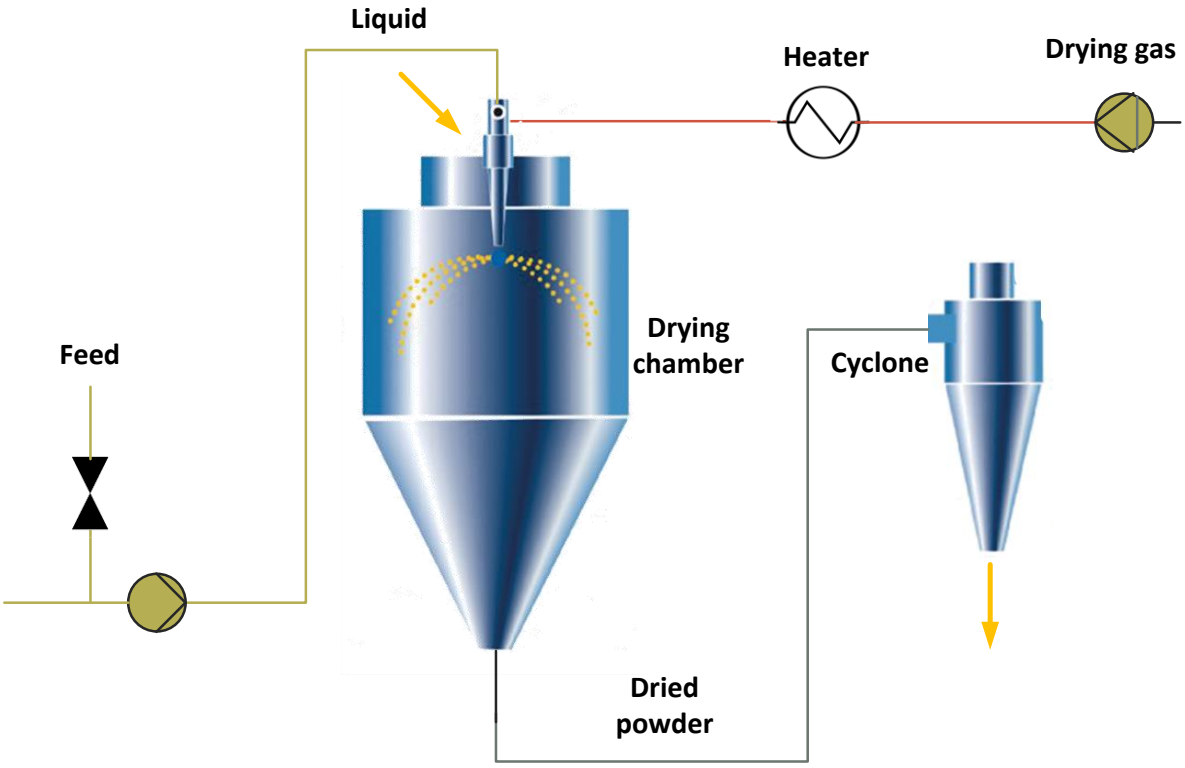

Figure 7. Schematic of a typical spray dryer

2.5.1 Particle formation during spray drying

The theory known nowadays about the particle formation during spray drying has derived from experimental approaches like single droplet [116] and acoustic levitation [117]. Such methods can provide information on the crust formation, shrinking and/or blowing up of the particle as well as the drying rates of droplets with different dimensions and components [5, 118, 119]. A vast number of studies have demonstrated that spray

drying processing conditions have an effect on the particle size, porosity, density, surface roughness and composition, among others. Moreover, process conditions such as temperature and flow rate of the drying gas will govern feedstock properties in the drying chamber like solvent latent heat and solute diffusion coefficient. Complex phenomena take place during liquid evaporation and particle formation and different theoretical models are used to describe the particle formation during drying.

The development of a process for solid particle formation and understanding the mechanisms underlying final powder properties allows for identification of critical process parameters and eases the work of industry in regard to formulation development.

2.5.2 Development of solid particles during drying

Physical models are used to describe the evolution of particle formation during spray drying: 1) In the first stage of the drying, the droplet temperature is increasing to its wet bulb temperature and there is no substantial solvent evaporation taking place, 2) during the constant-rate period, the droplet shrinks due to solvent evaporation and the solutes start arranging themselves within the droplet according to diffusion rates, mostly; accumulating on the surface of the droplet until a solid crust is formed, 3) after this stage, the skin of the particle is formed and no further shrinkage is observed, the solidification causes the remaining solvent evaporation to be diffusion rate-limited. 4) after this point, the temperature of the solid crust increases as the liquid boundary moves inward. Although there is no more shrinkage observed in this falling-rate period, the particle skin can still collapse or deform. Dried particles are collected at the exit of the chamber or via cyclone and where the moisture content does not further decrease. A general illustration of the droplet morphology changes and particle formation during the drying stages can be seen in Figure 8.

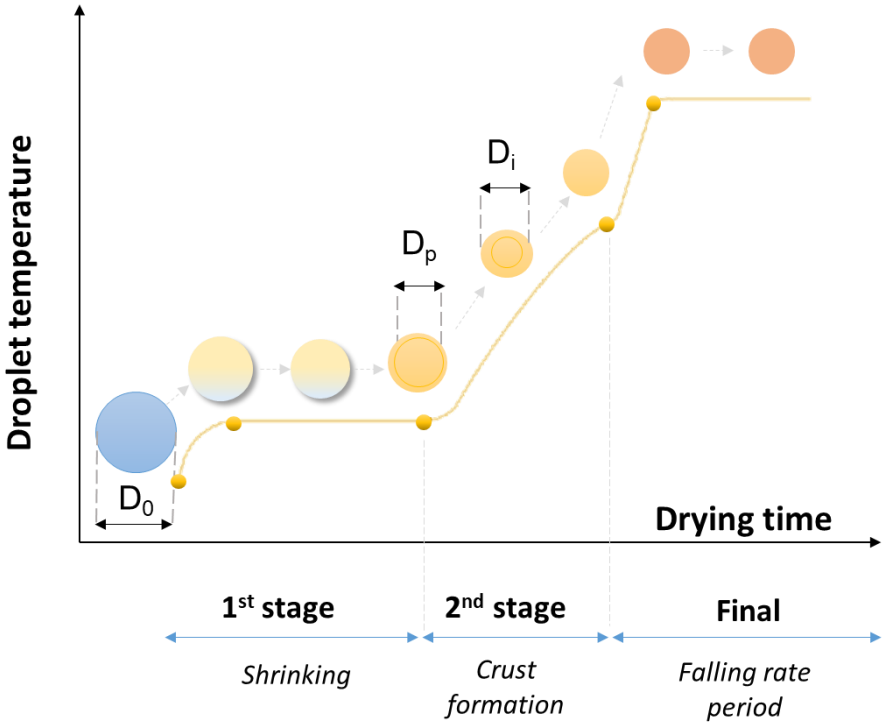

Figure 8: Evolution of particle and crust formation during spray drying.

The droplets atomized in the first stage of the process are mostly liquid which is then immediately in contact with the drying gas. Here, the partial pressure of the liquid on the droplet´s surface is higher than that of the liquid present in the drying gas, being this difference in both phases the main driving force for solvent removal. During this phase, the droplet remains liquid and there is enough solvent for constant evaporation, the droplet radius shrinks, and the solid content of the droplet increases [119-121]. Where there is constant free evaporation of the droplet it is recognized as the first stage of drying, here; the initial mass transfer is similar between pure solvent and atomized feed suspension/solution. As evaporation continues to take place, the solute-feed molecules start to arrange themselves inside the droplet according to the diffusion rates [122]. After that, the crust formation occurs (solidification) and this is the beginning of the falling-rate period. During this period, little to no further shrinkage occurs and the dried droplet/particle solidification causes slows the transport of solvent to the surface for evaporation and the drying becomes diffusion rate limited.

The particle morphology after the drying will depend on the material type, solubility as well as the drying history and the formation of the outer layer of the drop. The different particle forms can be hollow, shuttered or wrinkled particles.

2.5.3 Atomization during spray drying

Atomization is the first and most important stage of spray drying process as it has the capacity to determine both physical and chemical properties of the final particles [123]. The main effect and purpose of atomization is to increase the surface area of the liquid droplets and the increase the heat and mass transfer from the liquid to the drying gas by enhancing the surface exposure [124].

The process of droplet generation is often called liquid atomization and will dictate the path of the droplet drying, time, efficiency as well as the end properties of the dried powder. There are several types of atomizers depending on the composition and quality of the feeds as well as the desired particle properties. Common atomizer types are:

Rotary Nozzles: These atomizers have high centrifugal force that result in the breakdown of liquid feed stream into droplets. In this kind of setup, the diameter of the drying chamber is of paramount importance as material adhesion to the drying chamber pose as the limiting factor for its use in expensive drugs.

Pneumatic nozzles: operate on pressure energy to break up the droplets, the use of kinetic energy of the compressed carrier gas is transferred to the liquid surface causing droplet formation.

Two fluid nozzles (Figure 9): In the two fluid nozzle the relative velocity between the liquid and gas is the main driving force of the atomization process and is controlled by liquid feed and atomization gas flow rates, and nozzle geometry. Produce finer droplets of sizes less than 30 μm. For the production of droplets of less than 10 μm, high gas pressures and high gas to liquid mass flow are required. The energy for atomization is provided by the rapid expansion of air/gas that is mixed with the feed within the nozzle (internal mixing) or at its exit (external mixing).

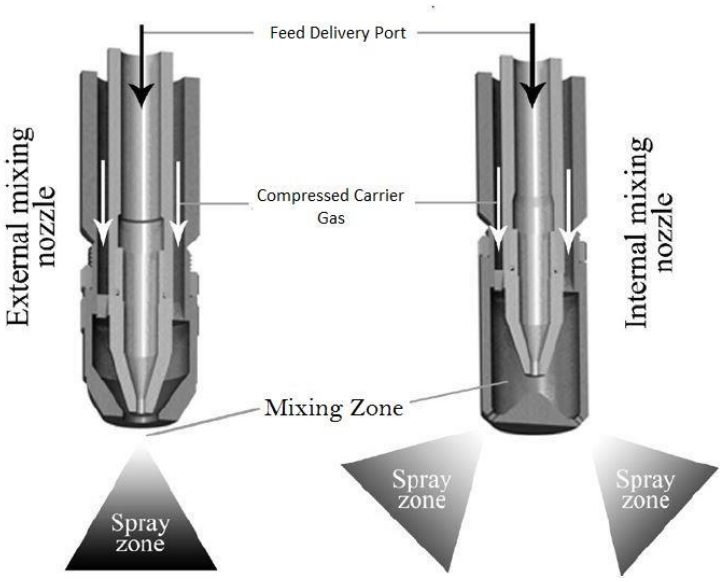

Figure 9: Two fluid nozzles with mechanisms of external (a) and internal (b) mixing. The feed and the atomizing gas are fed into the system in co-current flow and sprayed at the time of contact.

In pharmaceutical industry, the most common type of nozzles are the pressure and two-fluid nozzles due to the flexibility and ability to handle several feeds. The first are mostly used where larger and more uniform spherical particles are desired, whereas two-fluid nozzles are preferred to handle highly viscous feeds and the desired product are very small particles. The type of nozzle used for the spray drying process will have a direct impact in the particle size and particle size distribution of the powders and therefore, on the behavior of the powders when applied into products, regardless of the industry.

2.6 Overview of previous research on the particle formation from technical and novel lignins

A vast number of studies exist in the literature aiming the valorization of technical and novel lignins, and although it has been shown that lignin possesses antioxidant, antimicrobial, and biological relevant activities, only a small percentage of the lignin produced worldwide is being used for value-added products. Controlling particle

properties such as size, morphology, energy and solubility, among others, appears to be an important step between “original lignin” and application potential.

2.6.1 Solvent shifting

Solvent shifting or solvent exchange method has been used for the production of lignin nanoparticles from different technical and novel lignins. This methodology is based on the change of solubility of lignin in a water miscible organic solvent when excess of water is added; in this case, nanoparticles are formed due to a decreasing solubility which causes lignin molecules to associate via hydrophobic interactions [125, 126]. Lignin nanoparticles from hardwood dioxane lignin and softwood alkali lignin were produced via solvent shift and resulting in spherical shape and particles with a size from 80-104 nm [127]. Kraft lignin nanocapsules of 10-100 nm size were also produced by dissolving in ethanol and solvent shift with water (drop by drop method) [128]. Other authors investigated the formation of softwood kraft lignin nanoparticles via dialysis, here, the lignin was dissolved in Tetrahydrofuran (THF) and the final nanoparticles were formed when water was introduced to the system via dialysis. These researchers were able to control particle sizes and stability by changing the process parameters (time, salt concentration and pH) [129]. It was found that the lignin concentration in the pre-dialysis solutions had an influence in the particle size, where the lowest sizes (10 nm) were found at concentrations of 1 mg mL-1 and the biggest (100 nm) at concentrations of 20 mg mL-1, although the authors reported that the lignin dispersion becomes unstable at 20 mg mL-1. Controllable sizes, particle firmness, high surface areas and surface energy can be achieved through this methodology, nevertheless; a major drawback of low solid contents (approx. 1 wt.%) still needs to be overcome in order to scale-up the process and become a feasible alternative for the production of lignin nanoparticles.

2.6.2 pH shifting or acid precipitation

The variations on the stability of lignin upon changing the pH have been used to form, precipitate and produce lignin nanoparticles from diverse biorefining processes and industrially available kraft lignins. For lignins with low-sulfur content as Indulin AT ®

two methods were utilized for the production of nanoparticles: 1) lignin dissolved in ethylene glycol gets precipitated with diluted acid aqueous solutions (i.e. HCl), once the nanoparticles are retrieved they present stability in different pH, and 2) lignin dissolved in high pH aqueous solution can be precipitated via acid addition forming nanoparticles which are stable at low pH [130]. Alkaline lignin nanoparticles were obtained from Sarkanda grass by using acid precipitation [131]. The authors solubilized the lignin with sodium and ammonia hydroxide at up to 95 °C and various pH were tested (7.5-12), finally; lignin/formaldehyde (lignin/aldehyde ratio of 0.5-1.5) nanoparticles were obtained by hydrochloric acid (2 %) precipitation. The previous studies present valid results that show potential for further studying this particle formation processes: 1) via demonstrating the environmental biodegradability of the nanoparticles and non-toxicity against *Chlamydomonas reinhardtii* microalgae and yeast, and 2) by synthesizing lignins that contain high amount of hydroxyl groups and thus being a better phenol substitute in phenol formaldehyde synthesis, composites, etc.

Beisl et al., (2018) tried a more practical and applicable approach when aiming for direct precipitation of lignin nanoparticles from the organosolv liquors in a wheat straw biorefinery process. Nanoparticles from organosolv lignin were obtained by using a combination of pH shifting and acid precipitation with concentrated sulfuric acid. In these research, the authors 1) reduced the solubility of lignin by decreasing the concentration of the solvent and 2) lowered the pH by adding aqueous sulfuric acid. They found out that the pH value of the acid precipitating agent had little to no influence on the particle size (pH 1: 415 nm and pH 2: 385 nm), however; increasing the flow-rates of the antisolvent can decrease particle sizes to 200 nm. Although this methodology still presents some drawbacks, like low productivity and use of hazardous solvents, recently; Fraunhofer CBP patented a process (WO2016062676A1) for the continuous separation of lignin micro and nanoparticles and simultaneous solvent recovery process which was developed a lab scale but already successfully up-scaled to their pilot plant in Leuna [132]. In the future, hazardous solvents used in this process can be replaced by green solvents such as ionic liquids and deep eutectic solvents.

2.6.3 CO_2 antisolvent

In the previous decades, supercritical fluids have gained attention as a green technology for the formation of nanoparticles from different biopolymeric sources and for its applicability to obtain tunable and controllable sizes, morphologies and size distributions, crucial properties for pharmaceutical and drug delivery purposes [133, 134]. Supercritical CO_2 is of special interest because is inexpensive, non-flammable, non-toxic and environmentally friendly. Additionally, CO_2 is miscible in a diversity of organic solvents, and it can be easily recovered and recycled directly after processing. Furthermore, CO_2 near its critical conditions (T_C= 304.3 K and P_C= 7.4 MPa) can be tunable by changing pressure and temperature and it's a poor solvent for polymers, proteins and macromolecules, thus; being an excellent candidate to be used for antisolvent precipitation. The particle formation with CO_2 antisolvent method occurs as follows: first, a solution of the target polymer/macromolecule is sprayed via a co-axial nozzle into the CO_2, subsequently, the CO_2 fluid is diluted into the liquid droplet resulting in a high-volume expansion and reduction of the liquid solvent power. As a result of this, there is a rise in the supersaturation of the polymer and the formation of solid polymer particles occurs.

The production of lignin nanoparticles using CO_2 antisolvent precipitation has been reported in two studies. Myint, et al., (2016) produced nanoparticles from a commercially available Kraft lignin dissolved in N,N – Dimethylformamide (DMF) and using CO_2 as antisolvent [133]. The effect of pressure, temperature, feeding rate and lignin concentration on the nanoparticle size and morphology was assessed. It was observed that at low pressure (7.5 MPa) lignin nanoparticles tend to aggregate/coalesce much more than at high pressures when the same temperature was used. On the other hand, when temperature increases (constant pressure) the particle size and aggregation increases. An important observation was that with low pressure, lignin nanoparticles appear to be "melted" together, this may occur due to the formation of solids bridges between lignin nanoparticles that were in contact with solvent. Moreover, the effect of pressure appeared to be more pronounced than any other processing condition on the particle morphology as well defined, separated, semi-spherical particles were formed. Very promising results arose from this research, highly functional nanoparticles with a

mean size of 38 nm were produced, they showed high UV absorption capacity and did not show cytotoxicity against a bacteria derivative of *Pseudomonas aeruginosa*.

Poplar organosolv lignin nanoparticles were also produced via CO_2 antisolvent precipitation, using acetone as a solvent [134]. Formation of lignin nanoparticles did not result in any degradation and/or modification of the chemical structure, however; the authors studied the impact of the particle size -original against the nanoproduced- and observed a clear enhancement on the radical scavenging capacity and reducing power. Furthermore, a decrease to the nanoscale particle size resulted in a 12.4-fold higher solubility in comparison to the non-nanoparticle, 31 % and 2.5 %, respectively. This feature can be potentially utilized to increase the dissolution rate of poorly soluble drugs or as an active ingredient to increase the dissolution rate of a model compound.

Particles with such properties of biocompatibility and biodegradability may eventually find application in areas such as cosmetics, health and/or drug delivery systems, and the fact that nanoparticles do not exhibit toxic features encourage these processes and applications even more.

As observed, much efforts have been put into the formation of nanoparticles because the utilization of lignin in its “original form” has been related to a decrease on performance of the products where it is applied. For instance, kraft lignin can be obtained industrially in particle sizes from 10-100 μm (Figure 10), however, the application of such lignin into high performance materials hasn’t been successful due to low compatibility and high stiffness in the end product.

2.6.4 Challenges of current research on the production of lignin nanoparticles

The methodologies described in section 2.6.3 , show potential results and are also able to yield micro and nano particles. Nevertheless, it should be noted that the use of these methods may rise industrial drawbacks, for including additional separation processes for achieving dry particles, high residual organic solvents and control of the particle size and size distribution, which are not so desirable in industry. Overall, there is an obvious need for engineering micro and nano material processes that minimize the use of harmful

solvents without compromising the dynamic range of nano and microcarrier fabrication. Especially since lignin will be an intermediary material and will be converted into product only when added to a product formulation and process line.

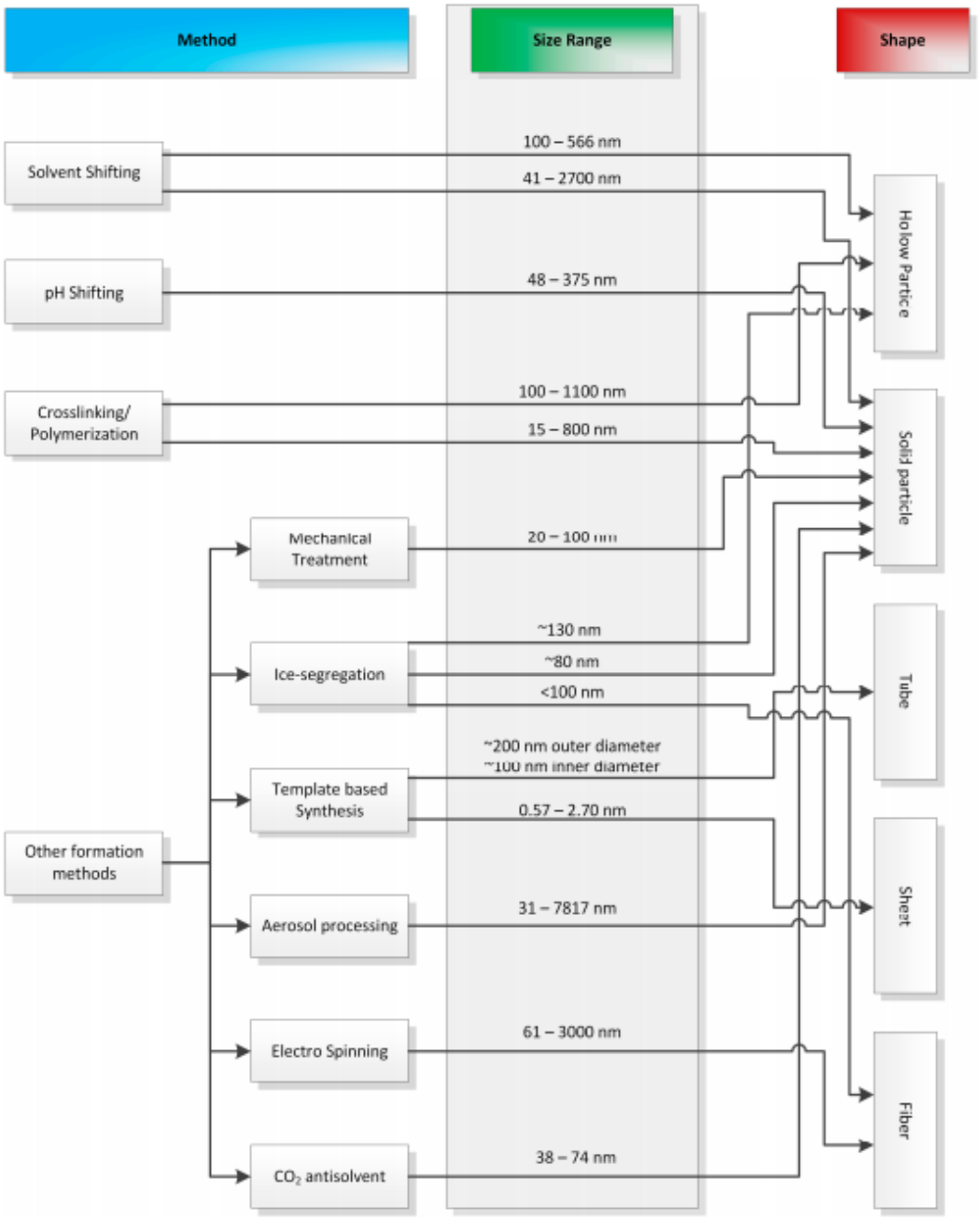

Figure 10: Laboratory scale approaches to produce lignin macro and noparticles for high value applications

The interest for the production of lignin in the nanoscale is well represented in the literature, however, the approaches presented not only have technical challenges but also regulatorily. The European commission and the FDA are making efforts in order to homogenize testing and assessment criteria. In the past, membership to the family of nanomaterials was granted based on physical dimensions; however, modern regulation and guidelines by the FDA and the EC are going away from this strict size dependence and extend the family also to microsized agglomerates. Due to the potential negative effects to the human and environmental health, now, there are several prerequisites' steps for the particle production and optimization steps are required to improve the eco-toxicity of these. This is of high relevance, since nanoparticles present applicability in several sectors like biomedical, personal care and agricultural products, that end up being consumed by the population and end up in the environment after use. The main concern is that the effects in the medium and long term are not yet well understood.

For lignin however, the ecotoxicity is not problem since it's a natural material. Nevertheless, the problematic arises when there is chemical alteration during the production process, transformation, chemical modifications. Crosslinked lignin materials, for instance, can reduce the biodegradability of the end product drastically, which occurs by blocking the -OH groups that are the major site for attack for the enzymatic degradation of lignin in nature. Overall, regardless of the modification ways and production processes of lignin particles, there is still a concern in the particle size, however, materials in which the macromolecular structure of lignin is used have less probability of encountering regulatory hindrances to be used. The latter, being a strong starting point for the further valorization of lignin in its macromolecular state and the use of transforming technologies that can yield tailored particles sized without modifying the chemical structure of the biopolymer.

3 Derivation of the objectives based on the state of the art

The efforts found in literature regarding the valorization of lignin and the process development advancements for the transformation of this biobased material into specific particulate form, makes the importance of a processing approach that can effectively tailor the quality of lignin clear. The experimental experience as well as the reviewed literature led to the conclusion that lignin particles in a spherical and semi-spherical form as well as small particles sizes in the range of 15 µm, 30 µm, 50 µm are needed in order to apply lignin in product formulation and avoid i.e. agglomeration and non-flowability. Approaches to tailor lignin particles deal with the use of organic solvent and expensive process configurations that are in laboratory scale, apart from that, one of the major drawbacks of the processing/drying methods of the lignin found in literature and in industry are the need of multiple unit operations in order to accomplish lignin drying and particle formulation.

Understanding the mechanisms behind particle formation and drying as well as the individual and combined effects of the drying process on the final particles formed was the major scientific goal of this work. Additionally, the effectiveness of the particle tailoring and behavior in product formulation was addressed. In this work, spray drying method was used for the first time in literature for the particle drying and formulation of lignin. Spray drying is a well-known process in industry, especially for the drying of food, pharmaceutical and cosmetic products, and its scalability has been demonstrated at scales up to 30 ton/h, making it a viable process for lignin valorization. However, many process parameters have an effect on the product quality and the implementation is not trivial, therefore, understanding the predominant effects on the lignin quality is highly relevant. The present work is dedicated to this task, covering not only the optimization of the processing conditions to tailor the lignin particle size and morphology but also the application of such particles into product formulation and the evaluation of the relevant bioactive properties in vivo and in vitro, taking the approach even further to the use of lignin into real applications and bringing the valorization of lignin closer to the market.

Thesis structure

The results of this doctoral thesis are structured in three main parts. First the evaluation of feed rate, drying temperature inlet, outlet, as well as the effect of atomization pressure and nozzle size on lignin particles is assessed, furthermore, optimized process parameters were established. A complete evaluation of relevant industrial particle properties is presented in Chapter 5.1. In the second part, the optimized AS lignin powders are evaluated in regard to antioxidant, antidiabetic activity and oil adsorption capacity and compared to other novel lignin (organosolv), technical lignin (alkali) and a commercial lignin used for high value applications (hydrolytic softwood lignin). The spray dried AS lignin particles are also compared to porous AS lignin dried via supercritical CO_2. For a complete understanding of the real potential of the spray dried material, an in vivo toxicity study was conducted in Wistar rats in order to establish the maximum possible consumption dosages. The oil adsorption capacity that the lignin showed in vitro was transferred into the potential use as anti-cholesterolemic ingredient, and a controlled high-fat and conventional diet study in Wistar rats was performed, comparing the effect of AS lignin spray dried particles to the allopathic drug Simvastatin (Chapter 5.3). For the delivery of lignin as oral dosage form, the third part of this work is dedicated to the tablet formulation (mixture design) with relevant commercial excipients, assessment of tableting methods as well as the evaluation of lignin not only as an active pharmaceutical ingredient, but also as a carrier for the controlled delivery of the model drug Ibuprofen (Chapter 5.4).

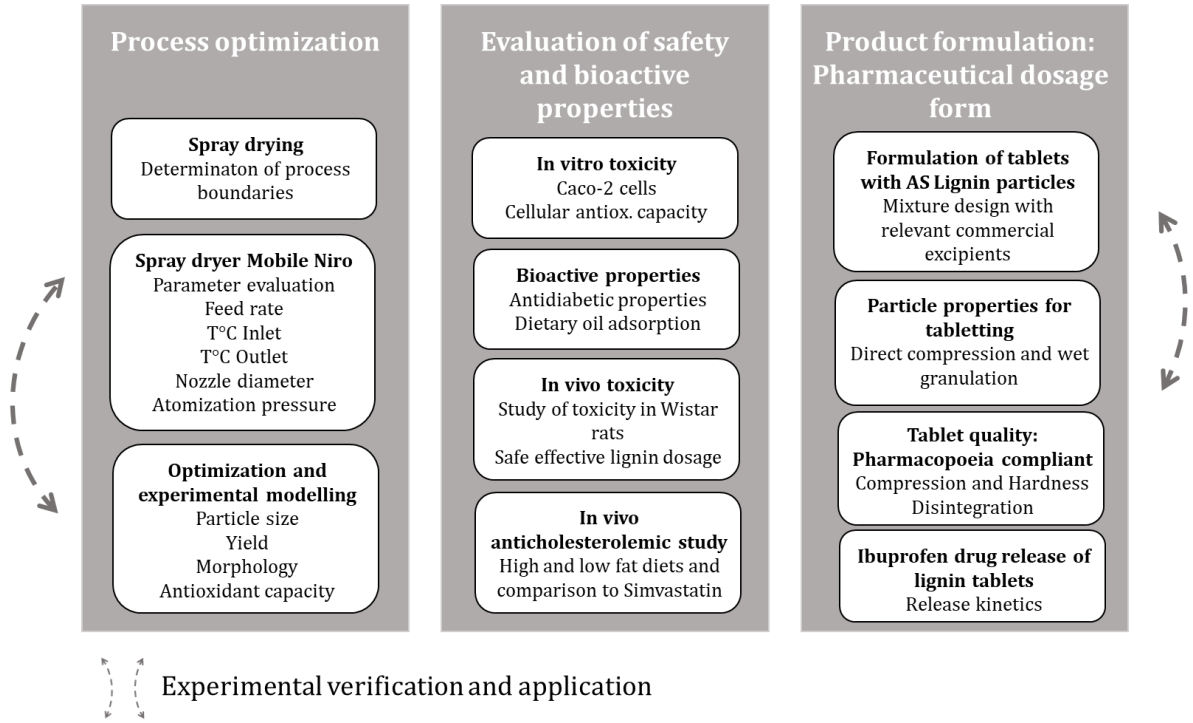

Figure 11: Overview of the experiments, process paramaters and product formulation designed from the AS lignin particles obtained via spray drying.

4 Materials and experimental methods

The following chapter summarizes the analytical methods and experimental procedures applied in this work, including required chemicals and laboratory procedures. It further provides a detailed description of characterization methods used to assess the bioactivity of the AS lignin particles in vitro and in vivo.

4.1 Lignin production and preparation

The AS lignin used in this study was produced in the Biorefinery group of the Institute of Thermal Separation Processes in Hamburg University of Technology. The material was obtained from wheat straw as described in our previous publication [1]. Briefly, wheat straw was fractionated using the Liquid Hot Water (LHW) pretreatment at 50 bar and 200°C for 30 min followed by enzymatic hydrolysis (72 h, 50°C, CTec2 Novozymes) as seen in Figure 12. AS lignin (water insoluble) solids were separated afterwards via decanting and dried as described in the spray drying section of this work.

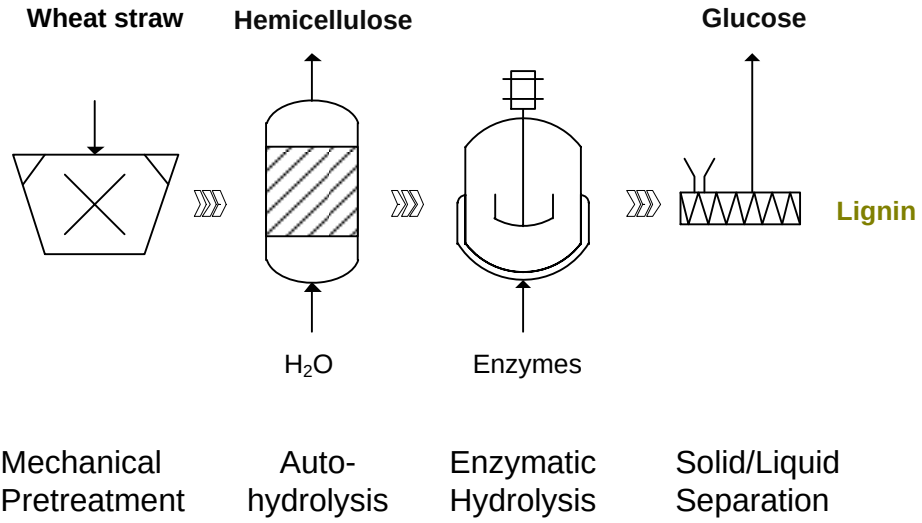

Figure 12: Schematic of the biorefining process existing at TUHH.

In initial experiments, it was observed that the remaining sugar content in the lignin had an effect in the spray drying process. This due to 1) simple sugar attached to the surface of the lignin or 2) complex carbohydrates which couldn't be hydrolyzed during the first enzymatic hydrolysis. For this, a second step enzymatic hydrolsis was performed, and the total hydrolysis residue (reference to lignin content) increased by 4 % and there was a reduction in the carbohydrate content (Table 2). The material which underwent 2 steps of enzymatic hydrolysis could be sprayed withot diffulties and without stickiness in the spray dried walls. For this reason, all the AS lignin used for the whole PhD work was treated in this way.

Table 2: Composition of the AS lignin when submitted to one and two steps enzymatic hydrolysis with CTec2® enzymes

	Hydrolysis residue	**Total carbohydrates**	Xylose	Glucose	Mannose	Galactose	Arabinose	Acid sol. Lignin
	[% abs.]	[% abs.]	[% abs.]	[% abs.]	[% abs.]	[% abs.]	[% abs.]	[% abs.]
Lignin 2 step EH	**85,2**	**6,9**	0,3	6,1	0,3	0,1	0,1	1,4
Lignin 1 step EH	**81,8**	**14,4**	0,1	13,9	0,1	0,1	0,1	0,5

Note: *Particles after drying should not be sticky, since they could permanently attach to the walls and components of the spray drying, clog the ducts or have a negative impact in the particle separtion equipment or cyclones. In industry, spray drier walls ca be manufactured with layers or coated with materials to avoid particle sticking and particle deposition. For AS Lignin, no problem was presented during spray drying after removing excess of sugars. The process canbe transferred to other lignins with similar or higher hydrolysis residue/ lignin content.*

4.2 Novel and technical lignins used

AS-lignin was isolated from wheat straw pellets obtained from Armandus Kahl (Glinde, Germany) and Speers-Hoff (Stelle, Germany) in the process described in section 4.1.

Softwood lignin was purchased from a local shop in Moscow. Alkali Lignin [Mn ca. 28,000. Mw ca. 5,000] was purchased from Sigma Aldrich; Organosolv lignin was obtained from Frauenhofer CBP (München, Germany). Porous AS-lignin and Softwood-lignin, as well as their formulations with alginate were produced at TUHH in collaboration with the aerogel group of the Institute of Thermal Separation Processes. The production process including solvent exchange and supercritical drying can be found in Annex A2.

4.3 Reagents and chemicals

2,2-Diphenyl-1-(2,4,6-trinitrophenyl) hydrazyl DPPH was purchased from Sigma Aldrich (Darmstadt, Germany), Disodium fluorescein from TCI Europe (Antwerp, Belgium), phosphate buffered saline, AAPH, Trolox, NaOH, maleate buffer, sodium carbonate, α – glucosidase enzyme from rat intestinal acetone powder, 4-Nitrophenyl α – D – glucopyranoside, α– amylase (type VI-B: from porcine pancreas), iodine solution from Sigma–Aldrich (St. Quentin Fallavier, France), Dichlorofluorescin diacetate and Quercetin from Sigma–Aldrich (St. Louis, MO, USA), acarbose from Glucobay 50, Bayer, potassium iodide solution and starch (extracted from potatoes) from Honeywell Research Chemicals, cell medium (Roswell Park Memorial Institute medium (RPMI-1640), Fetal bovine serum (FBS), Penicillin and Streptomycin (PS) as cell culture medium from Invitrogen (Gibco, Invitrogen Corporation, Paisley, UK), MTS reagent. In case of *in vitro* cell culture studies, the chemicals used were of analytical reagent or tissue culture grade.

Alginic acid [99.7%] extracted from brown algae, otherwise known as Alginate, was acquired from Aldrich Chemical Company, Inc. (Milwaukee, USA). Pectin was obtained from Carl Roth GmbH + Co.KG (Karlsruhe, Germany). Chitosan was provided as a patented supplement LipoSan Ultra® by Primex (Siglufjordur, Iceland). “Griechisches Natives Olivenöl Extra”, “Monza Maiskernöl”, “Reines Sesamöl”,”Bio Rapsöl” and “Bio Sonnenblumenöl” were purchased at Edeka ®.

Lactose monohydrate (Tablettose ® 100, Granulac ® 70) from Meggle Pharma, Microcrystalline Cellulose (ACCEL 101) from Lehmann and Voss and spray dried

Aquasolv Lignin were used as excipients. Ibuprofen was utilized as a model API and was purchased from Sigma-Aldrich.

4.4 Spray drying process of lignin

4.4.1 Feed composition and preparation

Feed suspensions containing AS lignin were adjusted to 10 wt.% solids and kept constant in all experiments. For every drying charge, 1.5 kg of feed was used and the suspension was stirred by using a Rushton stirrer and heated on a heating plate to 40°C before spraying in the drying chamber. The composition of the feed was set to $10g_{lignin}/100g_{totalsolids}$.

4.4.2 Spray drying process and drying conditions

AS lignin particles were produced in a spray dryer Niro Minor Type Hi-Tec from GEA Technologies (Annex A3). A flow-chart of the spray dryer installation is presented in Figure 13. Drying was performed in a co-current mode using a two-fluid nozzle with external mixture, orifice diameter of 1500 µm (Spray drying Systems, Germany). All drying experiments were conducted under nitrogen atmosphere and the oxygen concentration was maintained below 3 %. Hot nitrogen contacted the sprayed feed at the top of the dryer and the desired powder fraction of fines was separated in a cyclone.

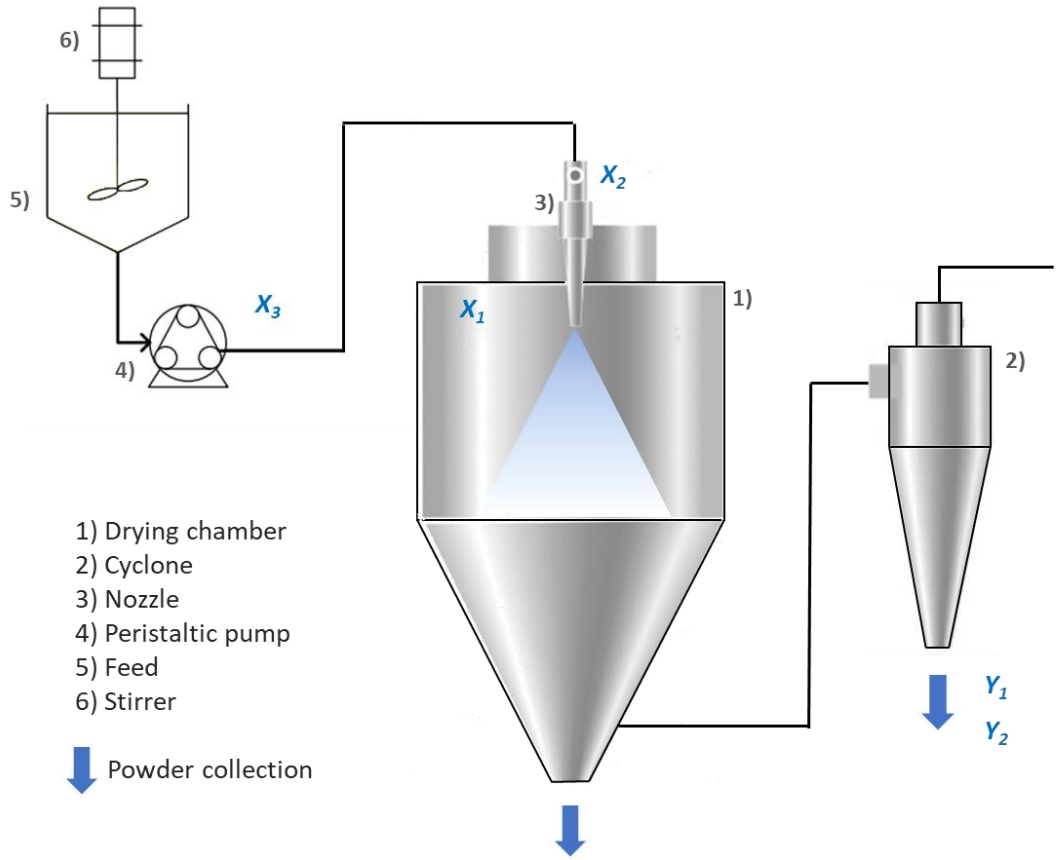

Figure 13: Schematic diagram of the spray drying process. The X_1, X_2, X_3 correspond to the varied process parameters inlet temperature, atomization pressure and feed rate respectively. Y_1 and Y_2 correspond to the process responses of particle size and mass yield of fine powder.

4.4.3 Central Composite Rotatory Design (CCRD) of experiments

A three-factor central composite rotatable design (CCRD) was used. Second order polynomials between factors (process variables) and the particle size of the powders as well as the yield were estimated. The factors studied were drying temperature (X_1: 180-200°C), atomization pressure (X_2:1.3-1.7 bar) and feeding rate (X_3: 65-75 mL min^{-1}); while the response variables were the mass fraction with the desired particle size or "yield fines" (Y_1) and the particle size (D_{50}) of the recovered powder (Y_2). Each factor was coded at three levels -1, 0, +1 (Table 3). Twenty randomized trials, including six replicates as the centre points, were assigned based on structure of the design. The experimental

conditions identified as optimum to obtain lignin desired quality were performed six times.

Table 3: Coded and real levels of the independent variable used in the experimental design to estimate particle size of the aquasolv lignin powders obtained by spray drying.

VARIABLES	UNITS	ACTUAL AND CODED VALUES				
		-1.682	-1	0	+1	+1.682
TEMPERATURE	°C	173	180	190	200	207
ATOMIZATION PRESSURE	BAR	1.2	1.3	1.5	1.7	1.8
FEEDING RATE	ML/MIN	61.6	65	70	75	78.4

First, a second order model was estimated, and its coefficients evaluated. Then, an analysis of variance (ANOVA) was used to establish the significance of the components of the model. Finally, an optimization procedure was used for the adjusted model in order to find the optimal conditions. A second order model was applied to predict the response variables as given below:

$$Y = b_0 + b_1X_1 + b_2X_2 + b_3X_3 + b_{11}X_1^2 + b_{22}X_2^2 + b_{33}X_3^2 + b_{12}X_1X_2 + b_{13}X_1X_3 + b_{23}X_2X_3 \quad (1)$$

Where Y is the predicted dependent variable, b_0 is the constant coefficient; b_1, b_2, b_3, are the linear coefficients; b_{11}, b_{22}, b_{33}, are the quadratic coefficients; b_{12}, b_{13}, b_{23}, are the interaction coefficients, and X_1, X_2 and X_3 were the independent variables. The statistical program Minitab 17 was used to conduct the design of experiments and Design Expert ® was used for the analysis of results.

4.5 Evaluation of primary powder properties

4.5.1 Powder moisture

Moisture content of the obtained powders was measured gravimetrically with a moisture analyzer (Precisa Gravimetrics AG, Switzerland). Briefly, 1 g of powder was placed on an aluminum plate and heated by a halogen lamp to 105 °C. The loss of mass was recorded until the mass loss was less than 1 wt.% within 120 s or maximum of 5 minutes.

4.5.2 Particle size distribution

The particle size distribution and mean size analysis of the powders was performed on laser diffraction particle size analyzer equipped with a Tornado dry powder system (LS 13320, Beckman Coulter, USA). The Fraunhofer theory was used for the determination of the diameters and size distributions [135]. Particle size measurements are reported as size distribution and the average diameter (D_{50}) is reported.

4.5.3 Powder morphology

Investigation of the particle morphology and morphology distribution of the resulting powders were done via scanning electron microscope (SEM) analysis using a Leo 1530 microscope (Carl Zeiss, Germany) at accelerating voltage of 5-10 kV and working distances in the range of 4 to 6 mm.

4.5.4 Bulk density and tap density

The bulk density of the powder was measured by placing a certain amount of AS lignin powder allowed to settle gradually by gravity (no other forces applied) into a calibrated cylinder and weighing the powder occupying specific volume. The tap density was measured using a stomping or tapping volumeter (Tapped Density Assessor; Copley Scientific Ltd.), the volume occupied by a known mass of powder after tapping and when there was no more change in the volume (at least 1250 taps).

4.5.5 Powder flowability

The Carr´s index was derived from bulk and tap density data, according to the following equation:

$$Carr´s\ index\ (\%) = \frac{(Tap\ density - Bulk\ density)}{Tap\ density}\ x\ 100 \qquad (2)$$

The Carr´s index gives an indication of powder flow [110]; a value of >25 % indicates good flow while <25 % suggest cohesive powder with poor flow. Hausner ratio is also used as an indication of flowability [136], where a value less than 1.20 indicates good flow, whereas a value more than 1.30 indicates poor flow. Hausner ratio was calculated according to the following equation:

$$Hausner\ ratio = \frac{Tap\ density}{Bulk\ density} \qquad (3)$$

Flowability and cohesion was measured in a Janike Shear Tester, a detailed description of the methodology can be found in Jaeda et al. [109]. The ratio ffc (flowability factor) of consolidation stress σ_1 to unconfined yield strength σ_c, is used to measure flowability numerically. *ffc* is calculated with the following equation:

$$ffc = \sigma_1 / \sigma_c \qquad (4)$$

Flowability and cohesion according to Jenike´s classification is as follows: ffc < 1 - not flowing, 1 < ffc < 2 - very cohesive, 2 < ffc < 4 - cohesive, 4 < ffc < 10 - easy flowing, 10 < ffc - free flowing.

4.6 Assessment of functional and bioactives properties of lignin

In this section, the experiments related to the assessment of the potential of AS Lignin particles for its use in life science applications are presented. A part of the experiments was conducted in Oeiras, Portugal at IBET (Instituto de Biologia Experimental e Tecnológica) and the results were published in Gil-Chavez et al. 2019.

4.6.1 Antioxidant capacity DPPH

The DPPH free radical scavenging capacity was measured according to the methodology described by Molyneux [137]. DPPH solution of 1 mmol was prepared by dissolving DPPH in ethanol. Briefly, 100 µl of each sample was mixed with 3.9 ml DPPH 1 mmol solution; the mixture was incubated in the dark for 30 min at room temperature and the decrease in the absorbance was determined with a UV-spectrophotometer at 517 nm. Percentage of radical scavenging capacity is presented and it was calculated using the following equation:

$$Radical\ scavenging\ activity(\%) = \frac{Abs_{control} - Abs_{sample}}{Abs_{control}} x\ 100 \quad (5)$$

Different concentrations of DPPH (50 mg/ml, 25 mg/ml, 12.5 mg/ml, 6.25 mg/ml, 3.125 mg/ml) were used for calculating the effective concentration to scavenge 50 % of the free radical in solution (EC_{50}). The EC50 values were processed using the software GraphPad Prism 6.0.1.

4.6.2 Oxygen Radical Antioxidant Capacity measurement

ORAC value was determined according to Cao et al. [138]. AAPH (2,2'-azobis (2-amidino-propane) dihydrochloride) was used as peroxyl radical generator, fluorescein as fluorescent probe, and trolox as standard. The reaction mixture contained 25 µL of extract, 25 µL of 75 mM phosphate buffer (pH 7.4), 75 µL of 0.8 M AAPH, and 200 µL of 0.106 µM fluorescein. Phosphate buffer was used as a blank. Samples, phosphate buffer and fluorescein were pre-incubated at 37 °C for 15 min. AAPH was added to start the

reaction measuring the fluorescence every 2-min using a FLx800 (Bio-Tek Instruments, Winooski, VT, USA) fluorescence microplate reader. The excitation and emission wavelength were set at 484 and 515 nm, respectively. The values were calculated by using a regression equation between the trolox concentration and the net area under the fluorescein decay curve. Results were expressed as μmol TE g^{-1} extract. Each extract was measured by triplicate.

$$y\ (net\ AUC) = 0.4328x\ (concentration\ of\ Trolox) - 0.7811; R^2 = 0.9931 \quad (6)$$

4.6.3 Cellular antioxidant capacity (CAA) Assay

The CAA assay was carried out by the procedure of Wolfe et al. [139]. For the evaluation of the cellular antioxidant activity for the lignin extracts, the Caco-2 cells were seeded at the density of 2×10^4 cells/well in a 96-well plate for 4 days. Intracellular antioxidant activity of the lignin extracts was evaluated by using chemical stress inducer AAPH following the emergence of the reactive oxygen species. These reactive oxygen species were then monitored using a fluorescent probe, Dichlorofluorescin diacetate (DCFA-DA, 50μm in PBS) [140, 141]. Confluent Caco-2 cells were washed twice with PBS and the extracts, previously dissolved in PBS, dispersed into the cells in the 96-well plate and Quercetin was used as standard. Additionally, 50 μL of DCFA-DA were added to the wells and then incubated for 1h at 37°C and 5% CO_2 humidified atmosphere. Following the incubation time, AAPH was added to each well (100 μL/well) with a concentration of 0.6 mM. Fluorescence kinetics was recorded every 5 min in the FLx800 BioTek fluorescence microplate reader ($\lambda_{emission}$ = 538 nm, $\lambda_{excitation}$ = 485 nm) for 60 min. CAA values were calculated using the following equation:

$$CAA\ unit = 1 - (\int SA / \int CA) \quad (7)$$

where ∫SA is the integrated area under the sample fluorescence versus time curve, and ∫CA is the integrated area from the control curve. The results were also expressed in quercetin equivalents per gram of dry extract (μmol Quercetin/g dry extract).

4.6.4 In vitro oil adsorption capacity by DIN ISO787/5

The procedure introduced by international standard DIN-ISO 787-25, named Ölzahl (oil number) was followed. 300 mg of each lignin and biopolymer sample was placed on a Petri dish and weighed. Using a burette, 5 initial drops of the corresponding oil was added. The powders and oil were slowly rubbed together using a spatula until all of the oil was adsorbed. Then, gradually drops of oil were added one at a time and mixed to the pigments. The oil feeding was stopped before evidence of transition to a smooth paste was observed and all the crumbs disappeared. Finally, the Petri dish was weighed again. The oil number tests with corn oil were conducted in three trials and tests including olive oil were conducted in two trials. The oil count was determined as follows:

$$\text{ÖZ} = \frac{V_{oil}}{m_{sample}} \left[{}^{ml}/_{100\ g}\right] \tag{8}$$

$$\text{ÖZ} = \frac{m_{oil}}{m_{sample}} \left[{}^{g}/_{100\ g}\right] \tag{9}$$

4.6.5 Activity against α-amylase and α-glucosidase enzymes

Extracts with known lignin concentration (10 g/ L in ethanol) were used for testing the inhibition of α-glucosidase and α-amylase enzymatic activity. Samples were mixed in a vortex for 5 min, sonicated for 30 min, and finally filtered through a nylon filter and collected for the experiment.

For the α-glucosidase assay, the methodology as described in Mai et al. was used with some modifications; in a 96-well plate 25 µL of the sample and 50 µL of α-glucosidase solution were preincubated for 15 min at 37°C [142]. Then, 50 µL of 4-Nitrophenyl α – D – glucopyranoside were added to the mixture and absorbance at 405 nm was read (t=0 min) in an Epoch Microplate Spectrophotometer (Bio-Tek, Instruments, Winooski, VT, USA). After a further incubation of 30 min at 37°C the reaction was stopped with 175 µL of 1 M Na_2CO_3 and the absorbance at 405 nm read (t=30 min). The experiments were performed in triplicate and IC_{50} values (mg/mL) were calculated from the Inhibition %.

α-amylase inhibitory activity was measured according to the methodology of Al-Dabbas et al. [143]. For this assay, 60 µL of the samples and 200 µL of starch solution were incubated at 37°C for 5 min. Then, 20 µL of α-amylase solution and 20 µL of 0.01 M PBS were added and the mixture was incubated for 7.5 min at 37°C. After the incubation, 200

µL of iodine solution and 1 mL of distilled water were added and the absorbance measured at 660 nm in a spectrophotometer (Genesys10uv, Thermo Spectronic, New York, USA). The experiments were performed in triplicate and IC_{50} values were calculated from the Inhibition %.

$$\%\ Inhibition_{\alpha-amylase} = \left(\frac{\Delta Blank_{660nm} - (\Delta Sample\ without\ enzyme_{660nm} - \Delta Sample\ with\ enzyme_{660nm})}{\Delta Blank_{660nm}}\right) \times 100 \qquad (10)$$

4.6.6 Cytotoxicity of lignin using Caco-2 cell

Caco-2 cell line (human colon adenocarcinoma obtained from DSMZ, Germany) was cultured at 37 °C in humidified air with 5% CO_2. The cells were maintained as monolayers in 75 cm^2 culture flasks containing a RPMI-1640 medium supplemented with 10% (v/v) FBS and 1% (v/v) PS.

Cytotoxicity assay was carried out using the MTS assay in Caco-2 cells. Solubility test were performed specifically for the cytotoxicity test in solvents as DMSO (1% v/v in cell medium) and ethanol (5% v/v) and water (10% v/v) in order to evaluate their performance in the cell medium. Caco-2 cells were seeded at a density of 2×10^4 cells/well in transparent 96-well plates and allowed to grow for 7-8 days in order to perform confluent non-differentiated Caco-2 monolayers [144]. The medium was changed every 2 days. At the day of the experiment, cells were incubated during 4h with the lignin extracts. Afterwards, cells were washed with PBS and viability determined by adding 100 µL MTS reagent (according to manufacturer's guidelines). Absorbance was measure at 490 nm in an Epoch Microplate Spectrophotometer (Bio-Tek, Instruments, Winooski, VT, USA). Data was expressed in cellular viability percentage relative to control (%) and EC_{50} determined. The experiments were performed in triplicate.

4.7 Simulated gastrointestinal conditions for lignin dietary oil absorption

4.7.1 Simulation of gastric and gastrointestinal conditions

Gastric conditions simulation

400 mL of distilled water were poured to a clean beaker and added with 9.0 mL of 1 HCl mol.L-1 to maintain the pH at ~1.65, the solution was kept at 37°C on a heating plate. Then, 1 g of spray dried AS lignin followed (after 5 min) by the dietary oil were added. The mixture was homogenized with a rotary mixer (Phoenix Instrument ®) and stirred during 45 min whilst being heated to maintain the temperature. Afterwards, the saponification value of the non-adsorbed oil was determined. The lignin was separated from the unadsorbed oil via vacuum filtration, the filtrate was then transferred into a conical flask, pipetted with 20 mL of 1 N alcoholic KOH, heated to a 65°C and magnetically stirred for 1 hour to achieve the saponification of the oil. A simple diagram of the experiments can be seen in Figure 14. A condenser was fitted the flask top to impede the evaporation of ethyl alcohol from the solution. In the next step, the flask was detached from the heater/condenser and cooled to room temperature in a water bath. Two drops of phenolphthalein were added to the solution, which was titrated with 1 mol.L-1 HCl until the pink color disappeared. The same procedure was conducted for AS-lignin, SW-lignin, AS-CO2-lignin, SW-CO2-lignin, alkali-lignin, pectin, chitosan and alginate. All the experiments were conducted in triplicates.

Gastrointestinal simulation

For the gastric simulation, 400 mL of distilled water was poured into a clean beaker and added with 9.0 mL of 1 HCl mol.L-1, the solution was kept at a temperature of 37 °C. 1 g of spray dried AS lignin and 3 g of oil sample were added into the beaker. The mixture was steadily agitated for 45 minutes whilst being heated to maintain a constant temperature. Then, 10 mL of 1 mol.L-1 KOH was pipetted to the beaker and the mixture was further agitated for 90 minutes. Afterwards, the beaker was removed from the mixture/heater and the solid phase was filtered out by vacuum filtration. The filtrate was transferred into a conical flask, pipetted with 10 mL of 1 N alcoholic KOH, heated to a 65°C and magnetically stirred for 1 hour for saponification of oils whilst being connected

to a reflux condenser. The flask was detached and cooled to room temperature. Ultimately, two drops of phenolphthalein were added to the solution, which was titrated with 1 mol.L-1 HCl until the pink color disappeared. The same procedure repeated with AS-CO2-lignin, SW-lignin, SW-CO2-lignin, OS-lignin, pectin, chitosan and alginate. All of the aforementioned samples were tested with olive oil and corn oil. Experiment with corn oil and olive were conducted in triplicates.

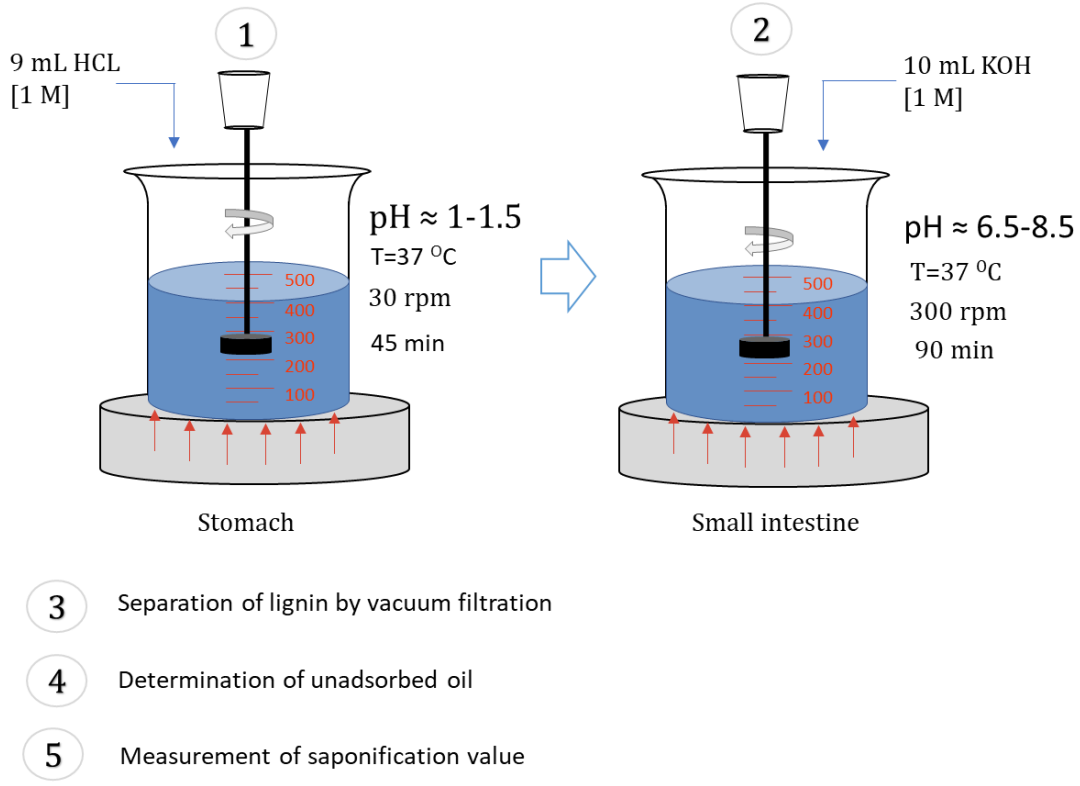

Figure 14: Simplified scheme of the experiments used for the simulated gastrointestinal conditions for the oil adsorption capacity of AS spraz dried particles and lignin-based formulations.

Saponification value of oils under GI conditions

1, 1.5, 2, 2.5, 3 and 3.5 g of corn oil were added to an Erlenmeyer flask and 25 mL of 1 mol.L-1 alcoholic KOH was pipetted in. The flask was attached to the reflux condenser in the same manner as previous experiments and heated to 65°C while being magnetically stirred. After 1 hour, the flask was detached from the condenser and cooled to room temperature. Two drops of phenolphthalein were added to the solution, which was then

titrated with 1 mol.L-1 HCl until the pink color disappeared. The same procedure was repeated for olive oil. All experiments were conducted in duplicates.

Measurement of surface energy

To compare the surface energy on the boundary between biopolymer samples, water and oil, contact angle of droplets on a smooth and non-inclined surface is required. As the biopolymer samples were in powder form, each sample was compressed into a tablet; on which the contact angle was measured. Tablets were produced with with a compression force of 50 kN at the the Institute of 'Technical and Macromolecular Chemistry' in Hamburg University. Contact angle was measured using the optical tensiometry and sensile drop method. In order to perform this analysis 24 samples (3 trials for each biopolymer) were tableted, the samples were placed before on a pedestal before a camera and the focal length was adjusted until the surface was clearly visible. One 0.1 mL drop of water was placed on the surface of the sample. Using the DSA4 program (Krüss), the fitting method used for outline recognition of the droplet was set to T-1 method and the contact angle on both sides of the droplet were recorded. Then the pattern fitting was changed to the circle method and the same procedure was repeated for oil droplets.

4.8 In vivo toxicity and lignin hypocholesterolemic effect in Wistar rats

The toxicity study was divided into two parts: a sighting study aiming at selecting the safest dose for the second part of the toxicity study. In the second part of the study, the animals were exposed to a fixed dose (selected based on the first part of this study) for a longer period of time. For this part of the study, a high fat diet was supplement to the rats in order to assess the hypocholesterolemic effect of lignin and compared to the allophatic drug Simvastatin. Regarding age and weight variations and husbandry conditions during this study, the Organization for Economic Cooperation and Development (OECD) guidelines were followed.

This experimental work was part of a bilateral cooperation of the Institute of Thermal Separation Processes at TUHH with the Applied Sciences University in Jordan.

The following activities were performed by every party: *TUHH, Joana Gil:* Experimental planning, preparation of the spray dried particles, preparation of the porous particles, physico-chemical characterization of the powders (particle size distribution, surface area, porosity, solubility, in vitro dietary oil adsorption, oil adsorption capacity under gastrointestinal simulated conditions, FT-IR), supplementation of material for animal experiments and analysis. *ASU, Mohammad Alnajjar:* Protocol for animal testing, Animals, In vivo assessment of the lignins provided, monitoring and controlling in vivo tests, animal diet planning.

4.8.1 *in vivo* studies: Animal model

This study was performed in accordance with the regulations of Good Laboratory Practices (GLP), and all of the experimental protocols were approved by the Research number (2020-PHA-11) and Ethical Committee at the Faculty of Pharmacy-Applied Science University.

This study was conducted on male Wistar rats (6-8 weeks old) their weight ranged between 130-250 g. The rats of each group were kept individually in plastic cages for ease of observation without disturbing their behavior. Wooden shelves were used as bedding and changed every other day. Rats with ad libitum access to food and water under control conditions of humidity (50%-60%) in the control room 12-hour light 12-hour dark cycles, continuous air ventilation and temperature (22-24 °C).

4.8.2 *in vivo* toxicity and antihyperlipidemic effect of AS lignin spray dried

The lignin powder was assessed to evaluate the toxicity and its hypolipidemic efficacy. The hypolipidemic activity of lignin was compared with commercially available drugs in the market that are used normally to lower improve the lipid profile, through a serious of experiments that were conducted on Wistar rats. Three lignin doses were used (50, 100, and 500 mg/Kg) which were prepared in a 3 ml solution [145] while the drug simvastatin 40 mg/Kg was prepared in 1 ml solution as a control**.** All the doses were given to the rats orally. Two types of diets were used, the normal diet (ND) and a high-fat diet (HFD). The (ND) includes (Fat 5%, carbohydrates 65%, proteins 20.3%, fiber 5%, salt 3.7% and

vitamin 1%) [146]. The HFD was prepared by thoroughly mixing of ND with cholesterol 1% [147] and sheep fat 30% [148]. The rats were divided into eight groups (total n=44) as follows

- C1 (control 1): receive ND only, n=4.
- C2 (control 2): receive HFD only, n=4.
- Group 3: receive ND + lignin 100 mg, n=4.
- Group 4, 5 and 6: HFD + 50, 100 and 500 mg, respectively, n=7 each group.
- Group7: receive HFD +simvastatin 40 mg, n=4.
- Group 8: receive HFD + lignin 100 mg + simvastatin 40 mg, n=7.

After one week of feeding, lignin and simvastatin were started to be given daily for the consecutive 3 weeks.

4.8.3 Parameters analyzed in the rat model

During the experiment, rats' weights were measured once a week to check for weight changes among different groups, using the Digital scale (BEL engineering, Italy). Blood samples of rats were collected weekly from all groups throughout the study (five times). Samples were withdrawn from medial canthus of the eye, via non-heparinized glass capillaries. The serum was separated from the blood by centrifugation at 5000 rpm for 10 minutes and stored at -80°C until further analysis. Lipid profile was measured in the feces in all the treatments to evaluate the effect of lignin on releasing lipids in the feces. Therefore, feces samples were collected weekly from all groups after a one week of feeding (four times), and for gut microbiota evaluation.

Serum and feces analysis for lipid profile –total cholesterol (TC) and triacylglycerides (TG) levels were determined by double-beam UV-VIS spectrophotometer using their respective assay kits. The spectrophotometer was zeroed with distilled water as mentioned in the kit leaflets. Wavelengths were set at 505, 505 and 500 nm to analyze TC and TG levels respectively.

Procedures and instructions were conducted in accordance with kits with catalog numbers: Cholesterol assay kit (Spinreat, Spain) NO.BSIS11-E and Triglycerides-LQ assay kit (Spinreact, Spain) NO.BSIS49-I. Serum of Alanine Transaminase (ALT) levels was

determined by double-beam UV-VIS spectrophotometer using their respective assay kits. Wavelengths were set at 340 nm to analyze ALT levels. Procedures and instructions were conducted in accordance to kits with catalog numbers: ALT assay kit (Cromatest Linear, Spain) NO.B1105-2/0901.

4.8.4 Lipid extraction from feces

Feces samples were collected weekly from all groups. The lipid from the feces sample was extracted by using the Folch method, which depends on the chemical extraction of lipids [149]. This extraction method is composed of several steps. First, homogenizing the feces by using 2:1 chloroform/ methanol mixture (i.e. 1g of the feces in 20 ml of the mixture). Second, after dispersion, the whole mixture is agitated over 20 minutes in a shaking water bath at room temperature. Third, filtration the mixture with filter paper and then washing with distilled water (4 ml for 20 ml). Forth, after washing the mixture was centrifuged to separate the two parts. Five, remove the upper part by siphoning. Finally, the lower chloroform part containing lipids was evaporated under a vacuum. The extracted lipid layer was dissolved with 1 ml of methanol and eventually collected and stored at -80°C for further analysis. Subsequently, using the same kits as for the serum of fecal cholesterol analysis [149] [150].

4.8.5 Body and heart fat weight and sample collection for further analysis

During the experiment, body weight was recorded once a week. Blood samples were withdrawn from medial canthus of the eye via glass capillaries five times throughout the study (n=320). By the end of the experiment, all the rats were sacrificed by cervical dislocation technique. Immediately after sacrifice, hearts weight (fat on heart) were measured from all groups. Additionally, control groups 1 & 6, hearts weight were measured separately without fat.

4.8.6 Statistical analysis

Different parameters were calculated for all groups during the study. Body weight gain was calculated by the average rate, for the heart weight, only the fat weight was measured by taking the average of fat weight for each group. Serum and feces lipid profile for (TC and TG) were calculated through the differences between cholesterol concentration between T14-T21 for serum and feces divided by number of days. Finally, ALT was calculated by the ration of T28/T7.

Data are presented using mean ± SD (Standard Deviation of Mean). The statistical analyses were determined by using IBM SPSS version 21(Statistical Package for the Social Science, Chicago, Illinois). This included one-way analysis of variance (ANOVA) using Dunnett's post-hoc and Tukey HSD test for parameters showing normality using Kolmogorov-Smirnova test. While Mann-Whitney U test were used for the parameters that failed to show normality of initial parameter. A p-value < 0.05 was considered significant.

4.9 Formulation of pharmaceutical dosage form from lignin tablets

All the experimental part of this section was performed at the Institute of Pharmacy, Chemistry Department of the University of Hamburg.

4.9.1 Mixture design for pharmaceutical formulations containing lignin

Mixture design was used for the analysis of the lignin addition on direct compressed tablets and was selected due to the constrained experimental regions associated to pharmaceutical formulations. A three component system Aquasolv Lignin (X1), binder (X2) and disintegrant (X3) was studied. Extreme vertices design was used for the preparation of the experimental run to optimize the concentration of lignin in the formulation as a drug or as an excipient. The observed lower and upper limits of the lactose monohydrate, micro crystalline cellulose and lignin was chosen with a degree of design as three, resulting in 13 design runs of direct compression. For the process of wet

granulation, the final powder blend composition was 20 w/w%. microcrystalline cellulose, 19 w/w% of lactose monohydrate (wet granulation excipient) and 61 w/w%. lignin.

4.9.2 Direct compression/tableting of formulations

The composition of the formulations is shown in Table 4, all the 13 experiments were conducted by extreme vertices mixture design (see section 2.3) and were blended with a Turbula ® T2F mixer (W.A. Bachofen, Basel, Switzerland) for 15 min. The blends were then compacted in a single punch eccentric tablet press (Fette EK-0, Fette Compacting, Schwarzenbek, Germany) using flat-faced plain punches with a diameter of 10 mm. For direct compression and wet granulation, the powder blend was filled in the hopper section of the tablet press and the single punch (diameter of 10 mm) of constant compaction force of 85 kN was used for the tabletting of the powder blends at the designated filling depth of 10 mm.

Table 4: Design of experiments showing the uncoded units for component – DBL.

STD. ORDER	RUN ORDER	D DISINTEGRANT	G GLIDANT	L LIGNIN
4	1	0.15	0.0175	0.8325
1	2	0.1	0.02	0.88
9	3	0.3	0.02	0.68
13	4	0.1	0.015	0.885
12	5	0.3	0.015	0.685
11	6	0.2	0.01	0.79
10	7	0.2	0.02	0.78
2	8	0.3	0.01	0.69
6	9	0.2	0.015	0.785
8	10	0.15	0.0125	0.8375
5	11	0.1	0.01	0.89
3	12	0.25	0.0125	0.7375
7	13	0.25	0.0175	0.7325

4.9.3 Wet granulation

All components were blended using a Morphy Richards Stand Mixer with beater attachment at speed setting 3 (100 RPM approx.) for 15 min. The blend was then dispersed on the drum agglomerator (Maschinenfabrik Gustav Eirich GmbH & Co KG, Hardheim Germany) where the drum inclination, number of revolutions and the period of agglomeration was set at 45°C, 35 rpm and 10 minutes respectively. In the drum agglomerator, the powder mixed with microcrystalline cellulose and lignin was sprayed on by dissolved lactose monohydrate (30 ml of the solution in 30% w/w) after which the agglomerated powders were dried in a tray oven at 80°C for 210 min to remove the surface moisture. The granulated powder was cooled down and subjected to manual sieving for 10 min at with sieves at 1000 microns, 800 microns, 500 microns, 100 microns and base with the schematic diagram of process is seen along with the mass retained in each sieve is mentioned in Figure 41. The granules from the sieve 800, 500 and 100 microns were collected and mixed with ibuprofen in 0.5:0.5 ratio and then compacted in a single punch eccentric press (Fette EK - 0, Fette Compacting, Schwarzenbek, Germany) at the same conditions of the direct compression.

4.9.4 Tablet hardness, friability and dissolution

Hardness

Hardness of the produced tablets was measured by analysing 20 tablets in the tablet hardness tester (ERWEKA TBH 520) to calculate the tensile strength of the cylindrical shaped tablets; given by the formula:

$$Tensile\ strength = \frac{2 \times Hardness}{\pi \times D \times T} \quad (11)$$

where the D, diameter of the tablet (m) and T, thickness of the tablet (m) is also measured in the ERWEKA TBH 520.

The tablet homogeneity was measured by calculating the mass of the 20 tablets which were used in the hardness test in the ERWEKA TBH 520 and the mass deviation of the produced tablets were calculated.

$$Mass\ Deviation\ (\%) = \left(\frac{Mass_{\ tablet} - Mass_{average}}{Mass_{average}}\right) \times 100 \quad (12)$$

Tablet Friability

Ten randomly selected tablets were picked and carefully dusted for any particles stuck to the surface of the tablet prior to weighing them in a weighing balance. The initial mass of the tablets was recorded as M_0 and the tablets were placed in the friability tester where the drum containing the tablets was rotated along a horizontal axis giving the tablets a mechanical shear at 25 rpm for 4 minutes. The tablets were then collected and dusted again to remove off any free surface particles on the tablet followed by the weighing of the tablets to measure M_{final}. The loss in friability was calculated using the formula:

$$Friability\ (\%) = \left(\frac{M_0 - M_{final}}{M_0}\right) \times 100 \quad (13)$$

Tablet disintegration

To measure the disintegration time, ERWEKA ZT 220 Series disintegration tester was used. The assembly is suspended in the deionized water medium of 750 mL volume which is such that when the assembly is in the highest position the wire mesh is at least 15 mm below the surface of the liquid, and when the assembly is in the lowest position the wire mesh is at least 25 mm above the bottom of the beaker and the upper open ends of the tubes remain above the surface of the liquid. A suitable device maintained the temperature of the liquid at 35.5–37.5 °C and a standard test for all the formulations was carried out for a period of 30 min. The analysis was performed according to pharmacopoeial methods and a sample report can be seen in Annex A4.

Measurement of swelling capacity

Swelling studies were done in glass beakers with 1000 mL volume with no rotation speed was applied. Pre-weighted tablets were immersed in the PBS medium with pH 7.4. The tablets were suspended in the medium and the temperature of the medium is kept at 37±0.5°C. The tablets were taken out at predetermined time intervals of 0, 10, 15, 20, 30 min and then every hour till the end of 8h. The swollen tablets were removed from the solution and wiped off with a paper towel to remove surface water and then weighed. The swelling index of the tablets was calculated using the following equation:

$$Swelling\ index\ (SI) = \frac{W_t - W_0}{W_0} \quad (14)$$

where W_0 is the initial weight of the tablet and W_t is the weight of the swollen tablet at time t. Data is then presented as the mean ± standard deviation from the three samples as per formulation.

The tablets were also evaluated on the basis of the volume where the radius and the height of the tablet were measured using a digital Vernier calliper. The swelling capacity is evaluated using the equation:

$$Swelling\ capacity\ (S) = \frac{V_t - V_0}{V_0} \quad (15)$$

where S is the coefficient of swelling, V_0 is the volume before the wetting of the tablet and V_t is the volume after the wetting of the tablet at time "t".

The sample (50 – 100 mg) was filled in micropipette tips (transparent, 1mL, Aldrich) for estimating the water sorption time (WST) and swelling index (SI). The tip of the outlet is blocked with a tiny swab of nylon fiber to avoid leakage of powder during experiment. After placing the solid sample into the tip it was tapped 10 times on a hard surface to obtain a similar packing of the bed within the samples. The plastic tip was weighed initially (W_a) then dipped to 2 – 3 mm layer of phosphate buffer with pH 6.8. The time taken by the liquid to reach to the top of the powder bed was estimated as WST. The wetted bed with liquid, the tip was again weighed (W_b) to find the amount of liquid taken up by the powder.

The swelling index of the powder was calculated from the following equation:

$$SI = \frac{W_b - W_a}{W_a} \times 100 \quad (16)$$

4.9.5 Effective pore radius

The effective pore radius R_{eff} of the powder blend was estimated according to the method reported by Chibowski and Perea-Caprio. The powder sample was filled inside a plastic micropipette tip (transparent, 1mL, Aldrich) and weighed (W_A). The solvent used was n-hexane where the surface tension (γ) value is 18.4 N/m at θ = 0°. The solvent was poured dropwise at the top until the solvent filtered out at the bottom of the tip. The tip was weighed again to find W_B. The effective pore radius was calculated using the formula:

$$R_{eff} = \frac{W_B - W_A}{2\pi\gamma} \quad (17)$$

where π = 3.14. The experiment was repeated three times and the average value was calculated.

4.9.6 Drug release profiles of Ibuprofen

The drug release of the produced tablets was performed using an ERWEKA DT6 manual dissolution testing equipment. For the experiment, 6 tablets were randomly chosen and the mass of each tablet was measured carefully to calculate the amount of medium (PBS pH 6.8, 400 mL of medium/ 100 mg of tablet) for the analysis (example of analysis in Annex A4). The sampling was done at regular intervals and the concertation of the API was measured using UV-Vis spectrophotometer at 221 nm to plot drug release profile, M_t/M_∞ vs. time.

4.9.7 Contact angle of solid dosage forms

Imaging equipment from Krüss was used to observe the dynamic change in contact angle. The software for drop shape analysis (DSA 3) was used to analyze the progression of the droplet while being absorbed into the tablet. Sessile drop method was used for the drop type and evaluation was based on the tangent type of measurement. The edge of the flat surface of the tablet was chosen as the baseline for the measurement on which a single drop of 10µL was positioned on the surface. The measurement is started, and the analyzer takes 5 measurements in 1 second till the drop is completely absorbed into the tablet.

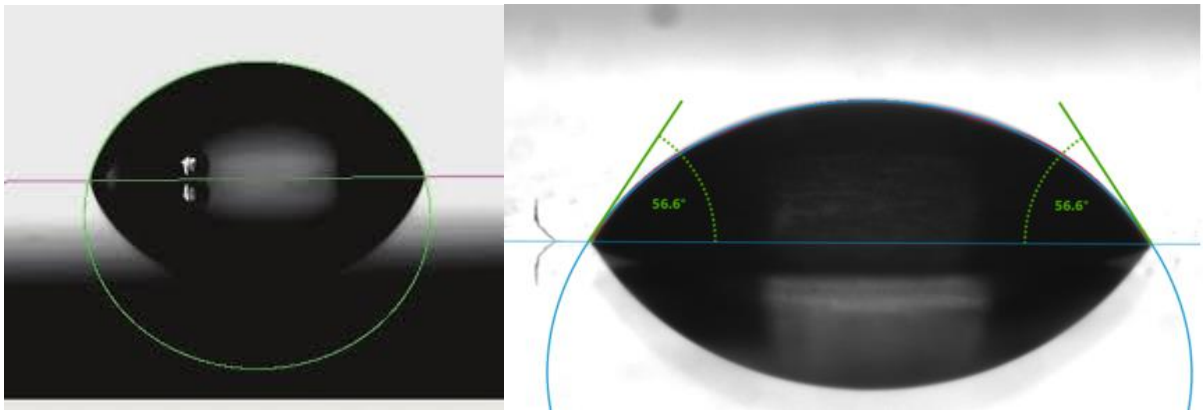

Figure 15: Contact angle measurement through sessile drop measurement technique.

The measurement is stopped and the contact angle vs. time is plotted. The degree of spreading is calculated from the data of the contact angle (Figure 15). It is given by the equation where Θ is the contact angle:

$$degree\ of\ spreading = \frac{1+cos\,\Theta}{2} \qquad (18)$$

where $0 < degree\ of\ spreading < 1$

5 Results and discussion

The results and discussion of this thesis are divided into three main parts. First, the evaluation and optimization of the spray drying processing conditions on the quality of lignin particles is presented. In the second part, the optimized AS lignin powders are evaluated regarding antioxidant, antidiabetic activity and oil adsorption capacity and compared to other novel lignin (organosolv), technical lignin (alkali) and a commercial lignin used for high value applications (hydrolytic softwood lignin). The spray dried AS lignin particles are also compared to porous AS lignin dried via supercritical CO_2. For a complete understanding of the real potential of the spray dried material, an in vivo toxicity study was conducted in Wistar rats in order to establish the maximum possible consumption dosages. The oil adsorption capacity that the lignin showed in vitro was transferred into the potential use as anti-cholesterolemic ingredient, and a controlled high-fat and conventional diet study in Wistar rats was performed, comparing the effect of AS lignin spray dried particles to the allopathic drug Simvastatin. For the delivery of lignin as oral dosage form, the third part of this work is dedicated to the tablet formulation (mixture design) with relevant commercial excipients, assessment of tableting methods as well as the evaluation of lignin not only as an active pharmaceutical ingredient, but also as a carrier for the controlled delivery of the model drug Ibuprofen.

5.1 Evaluation of the influence of spray drying process parameters on the quality of lignin particles

This results chapter first summarizes experimental design for the statistical modeling of the process of spray drying for the production of fine AS lignin particles. Data on the effect of atomization pressure, inlet temperature and feed rate on the particle size and mass yield of fines produced is presented. The preliminary evaluation on the effect of the nozzle size on the particle size distribution can be found in Annex A6. The effect of process parameters on the antioxidant effect of lignin can be found in Annex A7. The results and figures in this chapter have partly been published in Gil-Chavez et al. 2020.

5.1.1 Analysis of the model

There is vast information in the literature, showing that the property of powders obtained by spray drying depends on the feed characteristics such as feeding rate or viscosity, and the drying gas mostly temperature and atomization pressure. For this reason, the goal of this chapter was to evaluate to what extent each of these factors is affecting the desired quality (particle size) of the lignin feed. Through DoE, twenty randomized trials were sprayed for the given conditions (Table 5) and form the mass of the dried material of each run, the yield fines (Y_1, %) was calculated along with the mass loss. The fine fraction was then analyzed for the particle size (Y_2, µm) and the design model was investigated.

Table 5: Central Composite Rotatable Design

Run order	**Actual factors**			**Coded variables**		
	A: Temperature	B: Atomization pressure	C: Feeding rate	A: Temperature	B: Atomization pressure	C: Feeding rate
1	190	1.5	78.4	0	0	1.682
2	207	1.5	70.0	1.682	0	0
3	180	1.3	75.0	-1	-1	1
4	190	1.5	70.0	0	0	0
5	190	1.5	70.0	0	0	0
6	190	1.5	70.0	0	0	0
7	173	1.5	70.0	-1.682	0	0
8	190	1.5	70.0	0	0	0
9	200	1.3	75.0	1	-1	1
10	190	1.2	70.0	0	-1.682	0
11	190	1.5	61.6	0	0	-1.682
12	180	1.3	65.0	-1	-1	-1
13	190	1.8	70.0	0	1.682	0
14	200	1.7	65.0	1	1	-1
15	190	1.5	70.0	0	0	0
16	180	1.7	75.0	-1	1	1
17	180	1.7	65.0	-1	1	-1
18	200	1.7	75.0	1	1	1
19	190	1.5	70.0	0	0	0
20	200	1.3	65.0	1	-1	-1

The experimental design in coded variables for the factors temperature, atomization pressure and feeding rate are given in Table 6.

Table 6: Actual values in the design of experiments and responses

Run order	Actual factors			Responses	
	A: Temperature [°C]	B: Atomization pressure [bar]	C: Feeding rate [ml/min]	R1: Yield fine [%]	R2: Particle size (D50) [µm]
1	190	1.5	78.4	42.3	16.5
2	207	1.5	70.0	50.1	18.2
3	180	1.3	75.0	47.2	19.0
4	190	1.5	70.0	54.8	15.6
5	190	1.5	70.0	60.7	14.7
6	190	1.5	70.0	55.1	16.3
7	173	1.5	70.0	58.4	15.0
8	190	1.5	70.0	59.4	14.5
9	200	1.3	75.0	52.0	16.0
10	190	1.2	70.0	56.0	17.7
11	190	1.5	61.6	64.9	14.0
12	180	1.3	65.0	48.8	15.2
13	190	1.8	70.0	68.5	13.4
14	200	1.7	65.0	64.2	16.3
15	190	1.5	70.0	57.7	15.2
16	180	1.7	75.0	61.9	16.4
17	180	1.7	65.0	70.1	14.0
18	200	1.7	75.0	68.5	14.9
19	190	1.5	70.0	60.7	15.0
20	200	1.3	65.0	54.5	17.6

The ANOVA for the polynomial function of each response can be observed in tables 7 and 8, where it is shown that all components (linear, pure quadratic and interactions) were statistically significant. The model was optimized at 95% confidence interval. The ANOVA table of both the responses showed significant p-values of the regression where X_1 and X_2 were 0.0016 and 0.0007 respectively, additionally, residuals for X_1 and X_2 were non-significant with values of 0.1974 and 0.5557 correspondingly. The model was considered significant with R^2 of 0.9064 for yield fine fraction and 0.8987 for the particle size at D_{50}.

The non-significant residuals of p-value 0.1974 for X_1 and 0.5557 for X_2 along with the F-value of 8.71 for X_1 and 9.86 for X_2 showed that the fitting of the model was appropriate. The probability of occurring noise in the data was 0.16% for X_1 and 0.07% for X_2. The non-significant p-values of the model parameters were removed to attain a better fitting and the regression models for the relationship between dependent variables and coded values of the independent variables: temperature (X_1: 180-200°C), atomization pressure (X_2:1.3-1.7 bar), and feeding rate (X_3: 65-75 mL min^{-1}) are shown in Eq. 5 for Y_1 and Eq. 6 for Y_2.

$$\boldsymbol{Y1 = -3714.64 + 20.46X1 + 6872.33X2 - 38.98X3 - 43.93X1X2 + 0.374X1X3 + 0.0245X2X3 - 1792.33X2^2 + 0.0374X1^2X2 - 0.0009X1^2X3 + 9.696X1X2^2} \quad \textit{(195)}$$

$$\boldsymbol{Y2 = 869.89 - 5.58X1 - 1309.77X2 + 4.76X3 + 6.85X1X2 - 0.02X1X3 - 0.16X2X3 + 0.005X1^2 + 433.12X2^2 - 2.26X1X2^2} \quad \textit{(20)}$$

Table 7: ANOVA data showing the p-value of the model terms and the r2 of the model.

P > F	Yield fine	Particle size (D50)
Model	0.0016	0.0007
A-Temperature	0.1109	0.0067
B- Atomization pressure	0.0261	0.0002
C-Feeding rate	0.0010	0.0120
AB	0.3223	0.4747
AC	0.2484	0.0006
BC	0.9838	0.5132
A^2		0.0098
B^2	0.0414	0.3285
A^2B	0.0540	
A^2C	0.0123	
AB^2	0.0629	0.0323
R2	0.9064	0.8987

Table 8: Regression coefficients for the responses.

Coefficients	Yield fine	Particle size (D50)
Intercept	+56.39	+15.27
A- Temperature	-2.47	+0.9468
B- Atomization pressure	+3.72	-1.00
C- Feeding rate	-6.70	+0.5477
AB	-1.23	+0.1736
AC	+1.45	-1.16
BC	+0.0245	-0.1585
A^2		+0.5517
B^2	+2.07	+0.1780
A^2B	+4.05	
A^2C	+5.71	
AB^2	+3.88	-0.9025

The ANOVA was used to evaluate the significance of the regression coefficients in the model. A larger regression coefficient and a smaller p-value indicate a highest influence on the response variables [151]. The results of the ANOVA indicate a good model fitting. The suitability of the models was evaluated by coefficient of determination R2, which is a measure of the degree of fit [152].

For Y_1: yield fine, the lack of fit was not significant (p= 0.1974) and the second-order polynomial model represents the data in an adequate manner (R^2=0.9064), this suggests that 90 % of the variations can be explained by the fitted model. In a similar manner, lack of fit was not significant for Y_2: particle size (p=0.5577). For a good fit of a model, the R^2 should be at least 0.80; regarding the responses evaluated in this work both Y_1 and Y_2 R^2 were higher than 0.80 with 0.9064 and 0.8987 values respectively.

5.1.2 Effect of temperature, atomization pressure and feeding rate on responses

The effect of processing parameters during spray drying has been investigated in several matrices, i.e. heat sensitive products, food proteins, aerosol formulations, enzymes and bioactive materials in pharmaceuticals [4, 120]. In this regard, drying temperature has shown to control moisture content, bulk density and hygroscopicity in spray dried açai, watermelon and blackberry powders [153-155]. In a similar way, authors reported a more spherical particle shape when lower outlet temperatures are observed during spray

drying of proteins [156]. Other scientific reports also describe the change in non-dimensional numbers such as Peclet and Reynolds numbers with different drying conditions such as feeding rate and atomization nozzle pressure which affects the size of the droplets [157]. Information on wet bulb temperature and drying medium provides the evidence to how change in process conditions change the drying time, finally affecting the distribution of the particle size and the yield of the fines.

In this work, the effect of process conditions on the recovery of fine particles or yield (Y_1) was assessed and results are shown in Table 6. In the model fitting for this response the variables atomization pressure ($p<0.05$) and feeding rate ($p<0.01$) affected the recovery in a linear component through the linear interaction of each factor with the responses. Atomization pressure was the only significant quadratic term in the model ($p<0.05$) and the interaction temperature- feeding rate ($p = 0.0123$). On the other hand, for particle size (Y_2) all individual factors temperature, atomization pressure ($p<0.01$) and feeding rate ($p<0.05$) affected in the liner component, similarly to the quadratic term of temperature ($p<0.01$) and the interaction temperature-atomization pressure ($p<0.05$).

The response surfaces for Y_1 were obtained using Eq. 19, representing the response as function of two factors and keeping the third one at constant level 0 (see Table 5); Eq. 20 was used for obtaining the response surfaces of Y_2. In Figure 16, the surface plot for the effect of the interaction of temperature and atomization pressure on Y_1 and Y_2 can be seen. The interactions of the factors for the responses were also studied to identify the behavior of the feed in different conditions. The response Y_1 was found to be highest at lower temperatures (-1 level) and higher atomization rates (+1 level), same occurs and particle size is the smallest values at (+1, -1) highest level of atomization pressure and lowest level of temperature. The opposite occurs for particle size, in this regard; the higher the atomization pressure and the lower the temperature, particle size will decrease (desired in this work).

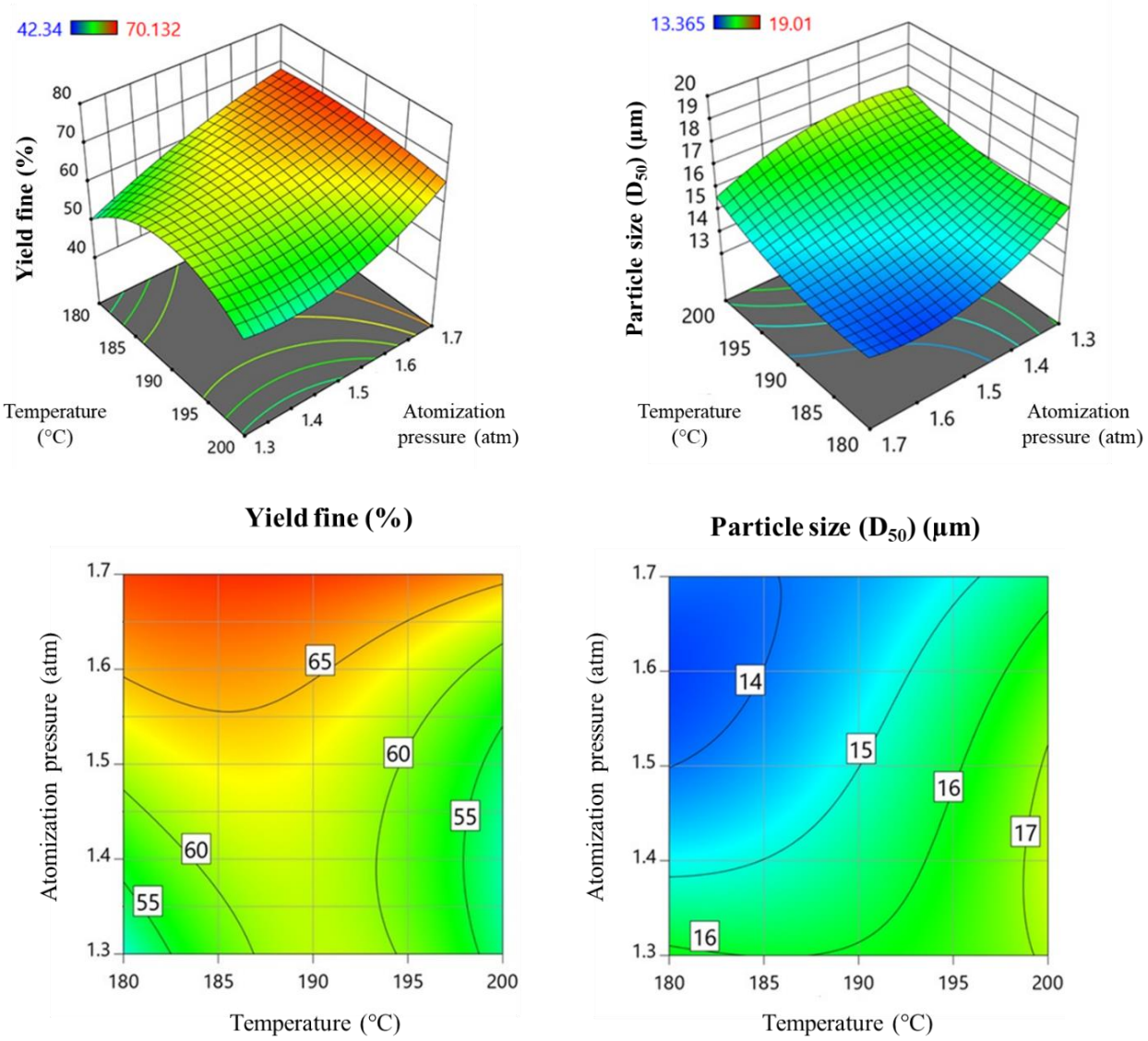

Figure 16: Surface and countour plots presenting the effect of temperature and atomization pressure on the responses “Mass yield of fines” and “Particle size (D50)”

The contour plot of the particles size is also in the agreement of the yield fine in case of obtaining the minimum particle size. The high fine fraction can be explained as the high atomization pressure results in forming smaller droplets and better dispersion, also achieving a final product with smaller particle size. This happens due to the high gas velocity which increases the relative velocity between the suspension and the atomized gas that result in instant atomization [158]. These droplets have higher heat and mass transfer area thus having better drying efficiency. Further higher temperatures increase the drying rate but hinder the shrinkage of particles by delaying the inward movement of

solids while the faster outward movement of water takes place in the droplet during the drying kinetics, hence shortening the drying time [121, 159, 160]. Whereas the temperature of 173°C also satisfies the high convective heat transfer of the feed due to the small droplet size, the diffusion limitations in case of large polymers (in this case lignin) results in higher evaporation rate as compared to the diffusion rate. The high atomization of the droplets and high evaporation rate cause the creation of internal pressure in the droplet and as the temperature is significantly above the boiling point of the solvent, the vapour pressure inside the particles is above that of the outer surface. Such phenomena causes disruption of particle´s integrity and breakage of the dried particles [159].

The formation of fine fraction is affected by the evaporation rate. The formation of smaller and denser particles due to the slow and even evaporation rate that allow a Tetris effect to be seen in the droplets [121]. This might be due to the fact that as the droplet moves in the drying chamber, its viscosity increases and as the solvent continues evaporating, the evaporation rate is solid content dependent [161]. The droplet finally solidifies, and a falling of the drying rate occurs, hindering further evaporation. In cases of higher temperature, the process happens instantaneously due to high evaporation rate and the formation of porous or hollow particles can occur, this will depend mainly on the permeability of the particles [5, 121].

The interaction of feeding rate and temperature for the response Y_1 can be seen in Figure 17 where the maximal response is obtained at lowest feeding rate and lowest temperature (-1, -1 level). This can be explained by the fact that increasing feeding rates will increase the droplet concentration of the particles in the drying chamber [159], thus; increasing the probability of droplet fusion or particle collision and resulting in larger or coarser particles. Additionally, critical moisture content limits the drying efficiency, therefore; an increase in the relative humidity of the chamber will affect both the drying and the particle formation rate [121]. Higher feeding rates typically result in higher water activity thus decreasing drying efficiency. Low feeding rates result in less concentration of material in the drying chamber, higher mass transfer and less chance of fusion of droplets by collisions [162]. Higher temperature affects the particles by increasing the drying rate so the particle structures were formed early thus avoiding shrinkage [163].

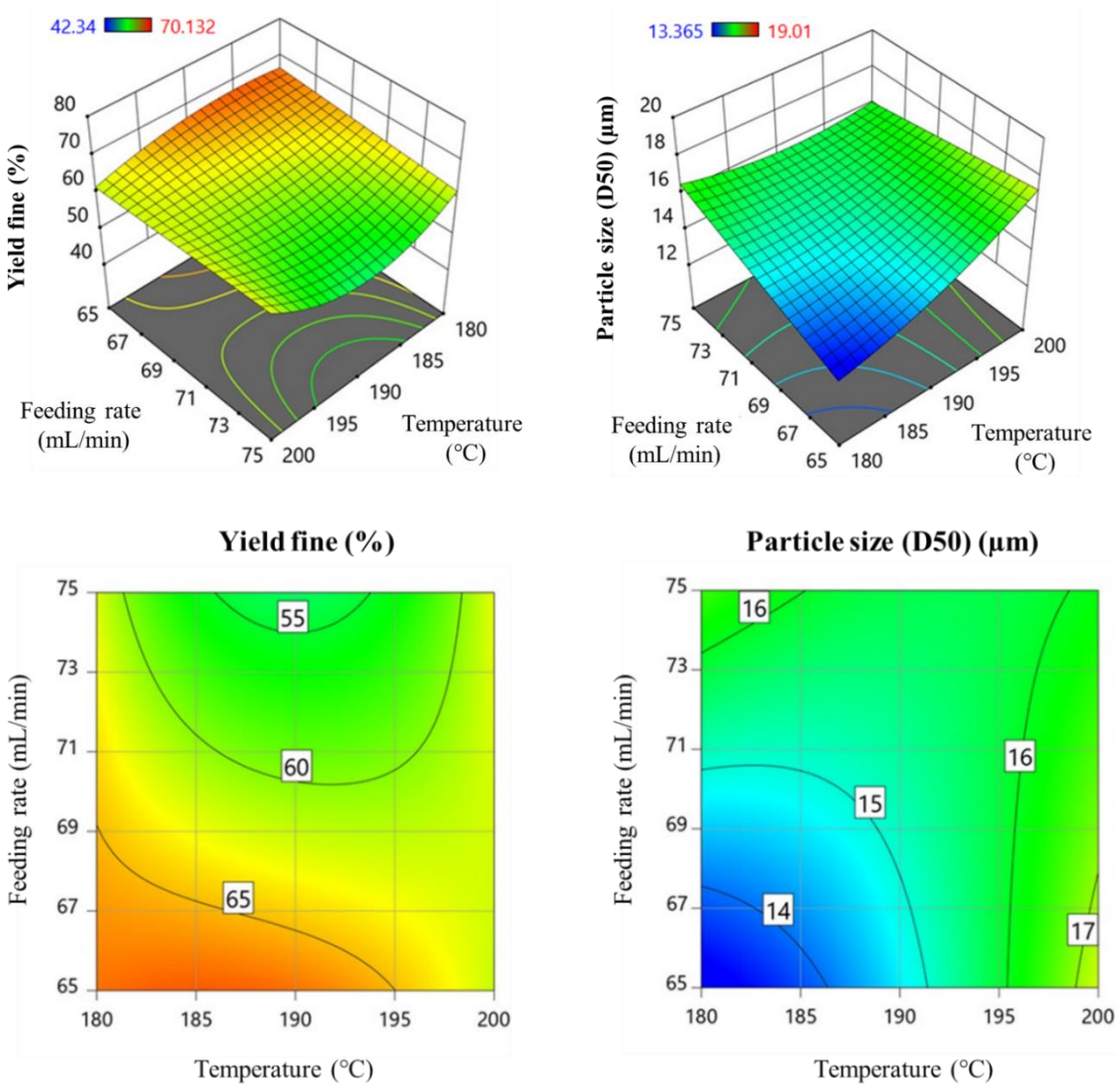

Figure 17: Surface and contour plots presenting the effect of temperature and feeding rate on the responses “Mass Yield fine” and “Particle size (D50)”.

Some authors emphasize the Peclet number as a determining relation for particle formation, in this regard; the ratio of the droplet evaporation rate and the diffusion motion of the solutes give an idea about the particle morphology [164]. High Peclet numbers create hollow particles as the evaporation rate dominates the diffusion rate and the low Peclet number creates the formation of small compact and denser particles [118, 164]. The Peclet number can be reduced by reducing the temperature to allow a slower evaporation rate and smaller feeding rate which creates droplets with low diffusion limitations [3, 164, 165].

The high feeding rate causes the decrease in outlet temperature and increases the moisture level in the final product which creates “humid” particles that can stick to the drying chamber and therefore affect their recovery [118]. The overall humidity of the chamber also increases, reducing the evaporation rate and affecting the particle size of the sample [121]. The most important factors which affect the drying rate are the outlet temperature, droplet diameter, solvent volatility and the relative saturation of the drying gas [165]. All of these factors are affected by the feeding rate of the feed into the drying chamber. Having a low feeding rate maintains the outlet temperature high, a small droplet diameter and high solvent evaporation [118, 121, 166]. The drying kinetics where evaporation is based on the boundary layer theory and the influence of Peclet number justifies the interaction of temperature and feeding rate in case of particle formation and maximizing yield.

For the interaction of atomization pressure and feeding rate (Figure 18) the smaller particle size and the maximum recovery of this fraction was obtained at high atomization pressure and low feeding rates (+1, -1). The high atomizing pressure increases the friction between the fluid and the air, thus disrupting the feed initially into fragments and ultimately into droplets. This results in the formation and production of fine particles and smaller D_{50} values of the resulting powders [119, 162]. Such transition is hindered when very high feeding rates are used or atomization pressures are low [159, 167]. The conversion of the feed to droplets inside the drying chamber is due to the relative velocity difference between the liquid stream of the feed and the surrounding air. Thus, the atomization is a result of the fluid-compressed air collision which generates high shear stress at the tip of the nozzle [3, 168]. Droplet and particle size can be also explained as function of the shrinkage ratio (droplet size/particle size), which also affects the evaporation rate. The shrinkage ratio is higher in case of higher atomization pressure as there is more surface for the drying to take place [4]. The higher atomization allows also higher solid content in the product and avoid diffusion limitations during drying for the small residence time in the spray drying chamber [118, 121, 169].

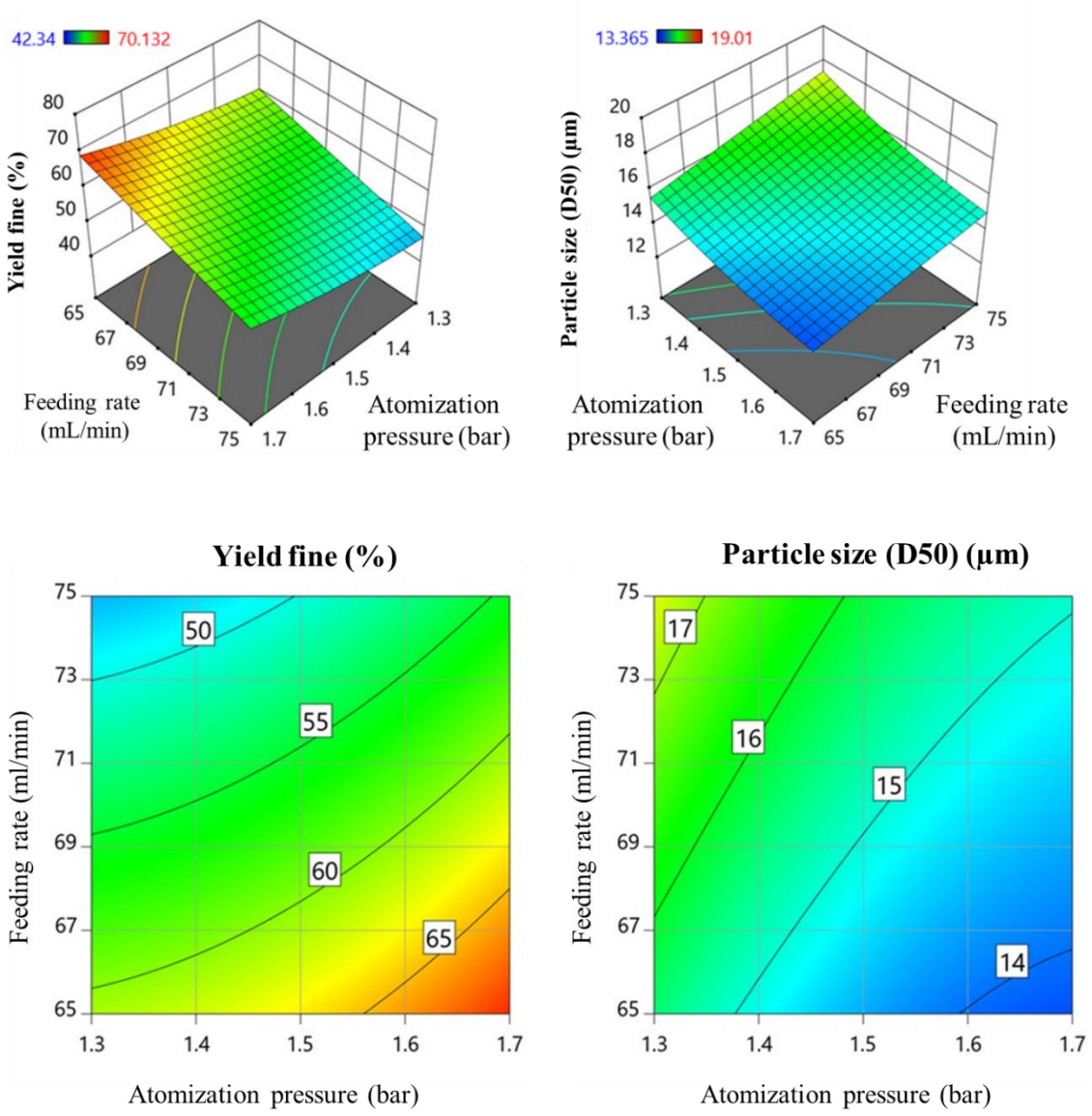

Figure 18: Surface and contour plots on the effect of atomization pressure and feeding rate on the responses “Mass yield fine” and “Particle size (D50)”.

The two-fluid nozzle was used in this work due to its effectiveness to control droplet size and therefore particle sizes of the desired powders. In a two-fluid nozzle with external mixing (atomizing gas and feed), a higher and finer atomization can be achieved, and droplet size can be easily adjusted, thus controlling the particle size of the dried powders. In addition, the use of smaller feeding rate not only creates uniform droplets but also smaller droplets when combined with the high atomization pressure [121, 123, 165]. In this work, this effect was observed experimentally as the smallest particle sizes were

observed when higher atomization pressure was combined with moderate and lower feeding rate.

5.1.3 Optimization of the factors: Temperature, atomization pressure, feeding rate

Due to the solvent-free characteristics of the process to produce AS lignin, this presents potential applicability in high added-value markets, nevertheless; powder properties need to be controlled for specific application, for instance; its use in adhesive masses. For this purpose, lignin needs to be produced on a particle size under 50 µm and fine powders < 30 µm are desired which are able to be homogeneously distributed, dispersed and/or solubilized with the other components in the adhesive's formulation. The main purpose of this chapter was to optimize the production of AS lignin particles with a particle size of <30 µm (Y_2) and maximize the recovery of this fraction (Y_1) in the process of spray drying. The optimum conditions for Y1 and Y2 were found at 173°C, 1.8 bar and 62 mL min^{-1}. The prediction of optimal condition for both responses was performed using desirability function on a scale of 0 to 1, where 0 represents a completely undesirable response and 1 represents the most desirable response. A total desirability of 1 was obtained for both responses (Figure 19), and at this desirability and the optimum conditions, the responses results in optimal Y_1= 69.42 % and Y_2= 13 µm.

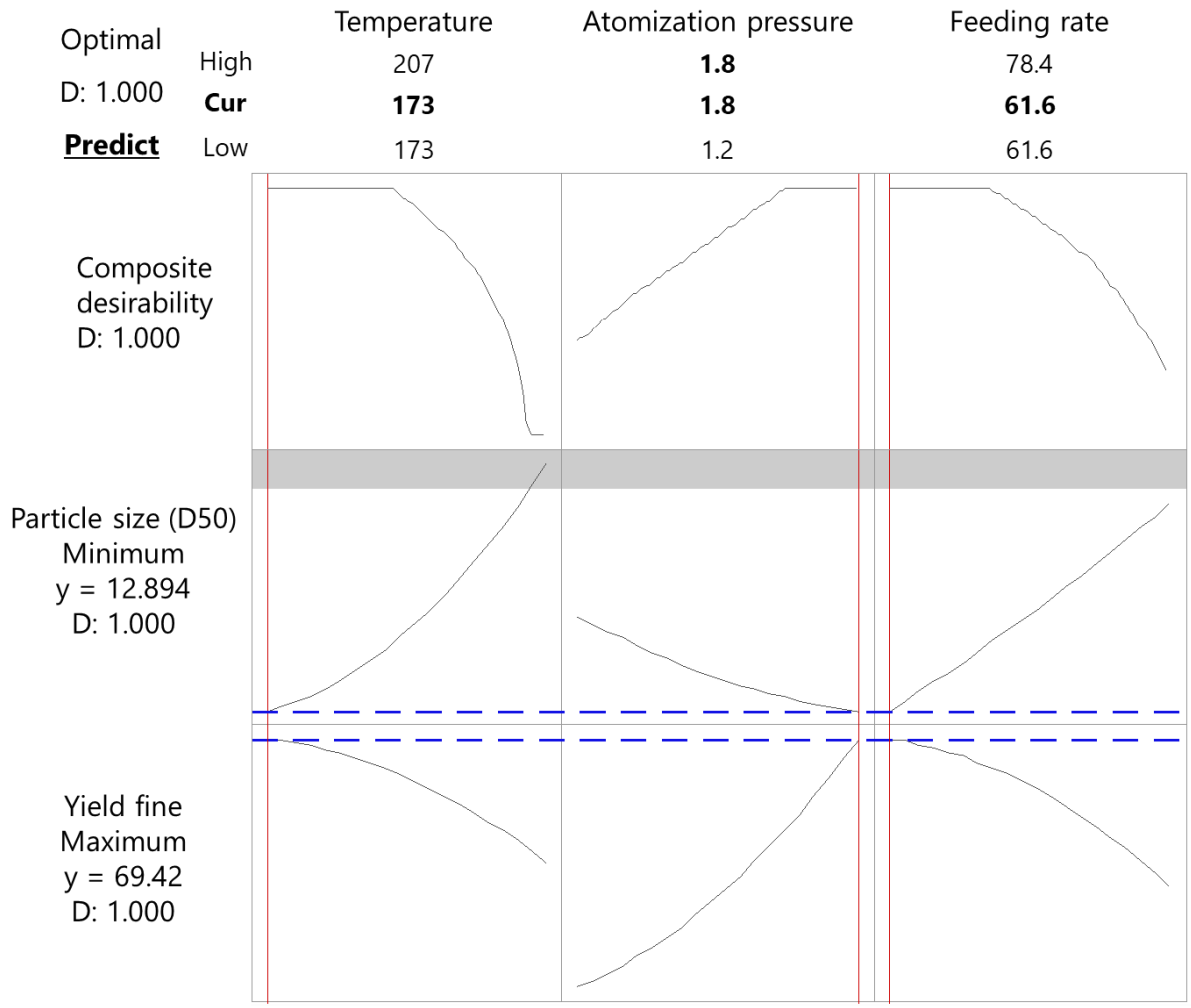

Figure 19: Desirability plots showing the predicted values.

In Table 9, the predicted and experimental values are shown, the values are similar to the predicted responses so the model can be considered as well fitted and desirably optimized.

Table 9: Predicted and experimental value of the responses at optimized conditions.

	Predicted		***Experimental Data***	
	Yield Fine (%)	Particle size (D50) (µm)	Yield Fine (%)	Particle size (D50) (µm)
Optimum Point	69.42	12.8	65.85	11.7

5.1.4 Characterization of aquasolv lignin particles

The AS lignin particles obtained under optimized conditions underwent further characterization for moisture content, flowability, cohesion, among others.

Moisture content

The optimized AS lignin fraction presented a moisture content of 2.9 wt. %. In agreement to the observations in the surface plots and the information present in literature, when higher inlet temperature is used the moisture content decreases. At the same time, when higher atomization pressures are used, small droplets are formed which have a greater surface area for heat and mass transfer. On the other hand, when low feed rate is used in combination when high atomization pressure there is an even distribution of the droplets in the chamber [170, 171]. The temperature being higher than the boiling point of water facilitates uniform drying from the core of the particle to the surface, overall, an increase of inlet temperature led to an increasing rate of water evaporation during spray-drying process. Higher moisture content in powders has an adverse effect on flowability, bulk density and shelf life of the material. Generally, lower moisture content is desired to improve the processability and pouring in industrial processing and to lower the water activity needed for bacteria to grow. This latter is of special importance for natural products which are more prone to bacterial and fungal attack. Other authors have reported moisture contents from 2 to 8 wt% for spray dried biopolymers and natural products [156, 171, 172].

5.1.5 Flowability and cohesion of the powder

The bulk density of the samples was 428 g mL^{-1} and the tap density was found to be 531 g mL^{-1}. The Hausner ratio was 1.24 and Carr´s Index was 19.4 both indicating fair powder flowability. At the same time, AS lignin powder was tested in a Jenike shear tester for the calculation of the flowability or cohesion of the powder. Pre consolidation stress of from range of 8 kPa was used for the measurement of the flowability/cohesion of the samples. With a ffc value of 6.53, spray dried AS lignin is classified as easy flowing powder; in

general, flowability is an important factor that can impact plant efficiency and product quality attributes at an industrial level. Poor flowability will cause the powder to stick to surfaces, making it difficult to handle for further use.

5.1.6 Morphology

The morphological characterization of the optimized AS lignin powder was conducted using scanning electron microscopy (SEM), as presented in Figure 20, for the particles obtained at spray drying conditions of 173 °C, 1.8 bar and 62 mL min^{-1}. The most pronounced morphology within the lignin spray dried particles is spherical, although no typical smooth surface is observed. A general rough surface and hollow structure (Figure 21) can be seen in a significant number of particles, four different morphologies: solid porous, collapsed hollow particle, solid hollow and solid particle, these differences can due to the inherent heterogeneities in the lignin feed, which is composed of insoluble lignin, a small soluble fraction of lignin, cellulose, as well as trace amounts of proteins (from the enzymatic treatment) that can be present. Depending on the composition of the droplet, the fate of the drying will be different. The predominant morphology obtained in the spray dried powders from AS Lignin are the collapsed hollow and solid hollow particles. The morphology with rough surface increases with increasing inlet drying temperature and therefore also outlet temperature. This phenomenon occurs when a solid outer surface is formed but the droplet drying is not complete, in this case, the remaining water in the inner part of the droplet will need to disrupt the surface in order to complete the evaporation/drying process. Other authors have reported that the roughness of the particles increases with increasing T_{out}, in the case of mannitol, smooth spherical surfaces were found with T_{out}= 65°C and rough particle surfaces are found at T_{out}= 114°C and 140°C [173]. In this work, T_{out} varied from 105°C to 115°C depending on the specified T_{inlet}.

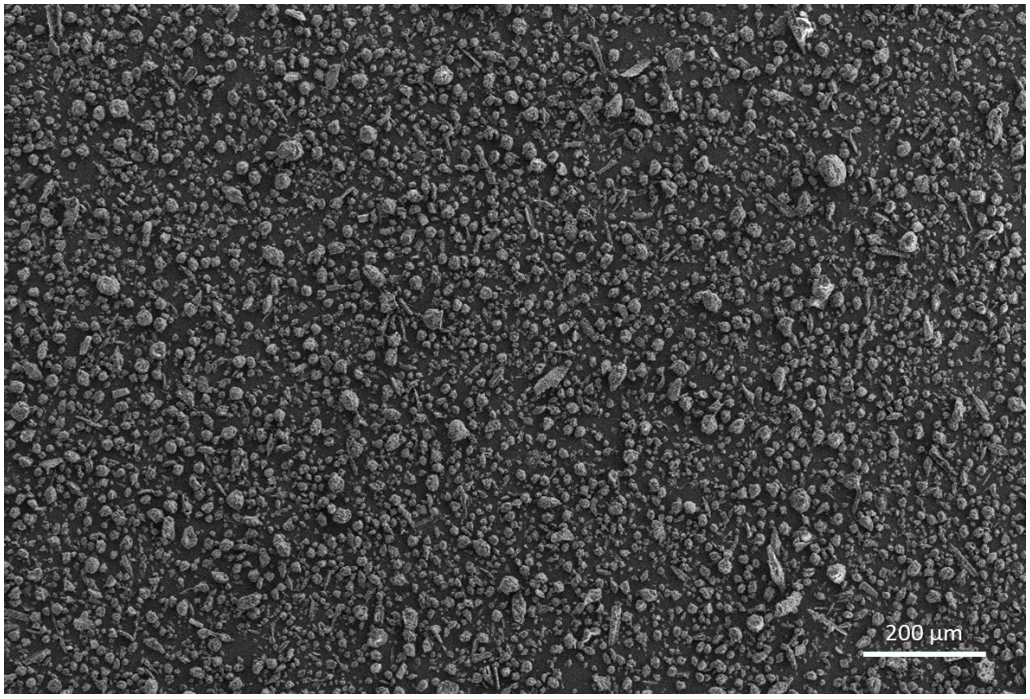

Figure 20: SEM image of AS lignin particles at drying conditions of 173°C, 1.8 bar and 62 mL min-1.

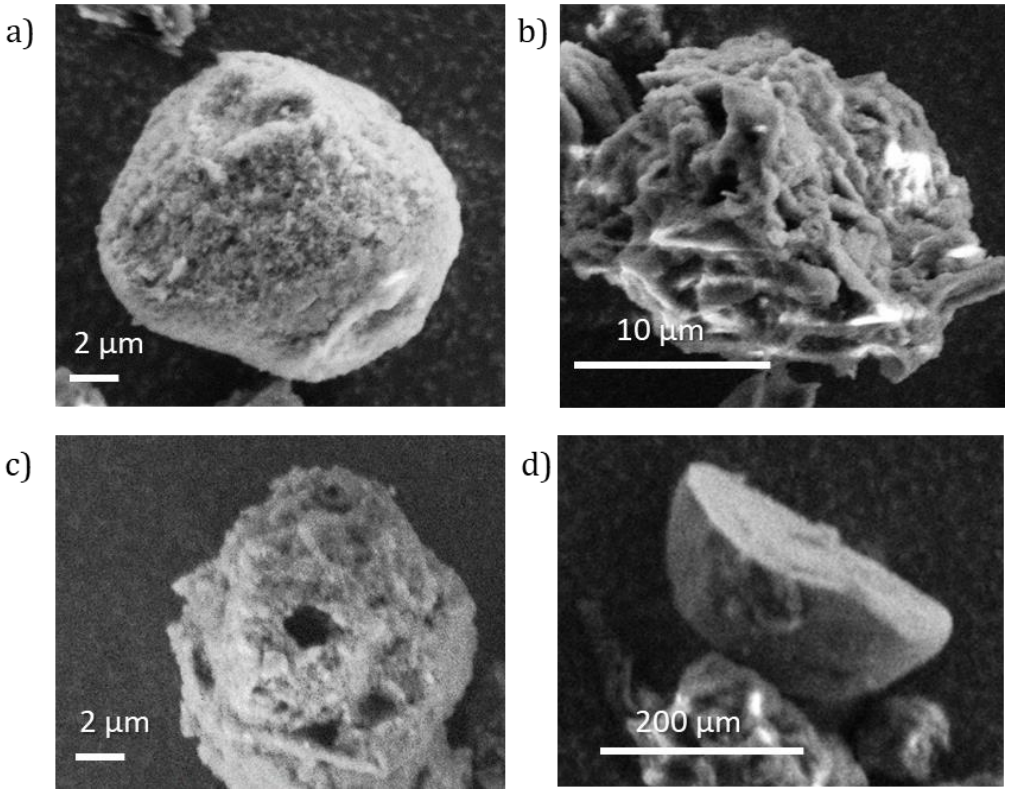

Figure 21: Different morphologies of spray dried AS Lignin a) solid porous, b) collapsed hollow particle, c) solid hollow and d) solid particle.

5.1.7 Conclusions PART I

Aquasolv lignin particles were obtained via spray drying and a design of experiments approach was used to optimize the desired quality of the powder. It was proven that the particle size of the lignin, as well as the yield of powder are strongly dependent of the operating variables temperature, atomization pressure and feeding rate. The atomization pressure resulted to be the most important factor for obtaining small lignin particles (D_{50}: < 30 µm) and temperature showed the smallest effect on this response. The optimization of the spray drying process for AS lignin performed in this work is the basis for product formulation based on AS Lignin but it can also be the basis for valorization and tailoring of powder properties of other types of lignins like soda, kraft and organosolv lignins. In the following two sections, a thorough evaluation of the properties of these particles is presented.

5.2 Assessment of the bioactive properties of the spray dried powders

This section presents the evaluation of the bioactive properties of spray dried AS Lignin in vivo and in vitro. Moreover, a comparison of the performance of AS lignin against novel and technical lignins was assessed to fully understand the potential applicability of the obtained powders in this work. The experimental part of this section was mostly performed at the Institute of Thermal Separation Process at TUHH, but also at Instituto de Biologia Experimental e Tecnológica (IBET) in Portugal and the Applied Sciences University in Jordan.

5.2.1 Antioxidant activity: ORAC and DPPH

Phenolic compounds, which are the monomeric form of the polymer lignin, are known to possess antioxidant capacity due to the high amount -OH groups in their structure. This property is of special interest for cosmetic, food and material industries, where lignin could be applied as functional material, scavenging free radicals and extending the shelf-life and stability of products. In this section, the DPPH radical scavenging and ORAC assays were used to assess the antioxidant capacity of the different lignins, which is generally used to explain and associate biomolecules to their bioactive effects. Several studies report that free phenolic hydroxyl groups are fundamental for antioxidant activity [49, 51, 174], where these can form a phenoxyl radical by hydrogen atom abstraction (and thus stabilization of the free radical), and/or being able to stabilize that phenoxyl radical formed. In Figure 22 and 23, it can be observed that Organosolv lignin showed the highest antioxidant capacity in both ORAC (1463.42 ± 99.11 μm TE/g of extract) and DPPH (84.78 ± 0.55 RSA% and EC_{50}: 3.9 ± 0.87 mg/mL), followed by commercial alkali lignin 1159.82 ± 49.09 μm TE/g of extract and 82.06 ± 0.14 %, respectively.

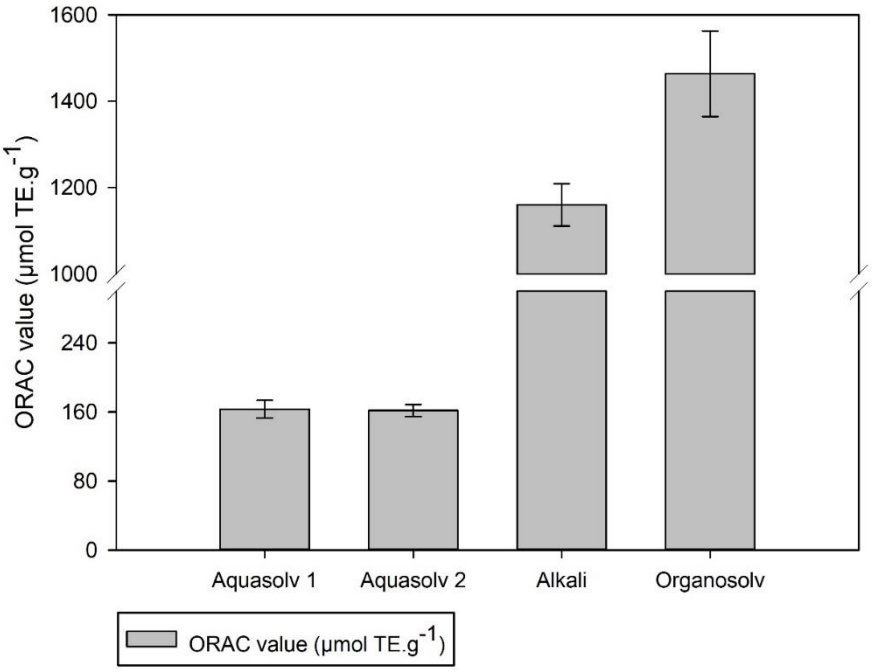

Figure 22: ORAC antioxidant capacity evaluation of four lignin types. Results are expressed as µmol TEg-1.

The efficient concentration EC50 to scavenge half the amount of DPPH free radical can be seen in Figure 24. On the other hand, both ASL1 and ASL2 presented the lowest antioxidant capacity in ORAC (163.33 ± 10.31 µm TE/g of extract and 161.70 ± 7.01 µm TE/g of extract, respectively) and DPPH (83.03 ± 0.49 % and 82.81 ± 0.12 %). This can be attributed to the high molecular weight of AS lignins in addition to their complex branched structure, in which the aliphatic and primarily phenolic –OH groups are most probably interacting with the DPPH free radical. Additionally, Dizhbite et al. reported that the radical scavenging activities of lignins decreased significantly when increasing the conjugation of the carbonyl groups in the polyphenolic chain [174]. Moreover, the ORAC values for Organosolv and Alkali lignins (1100 – 1500 µmol TE/g of extract) in this study were higher than that of vitamin C (530.64 ± 22.37 µmol TE/g of extract), a very well-known powerful antioxidant used in the food industry [50].

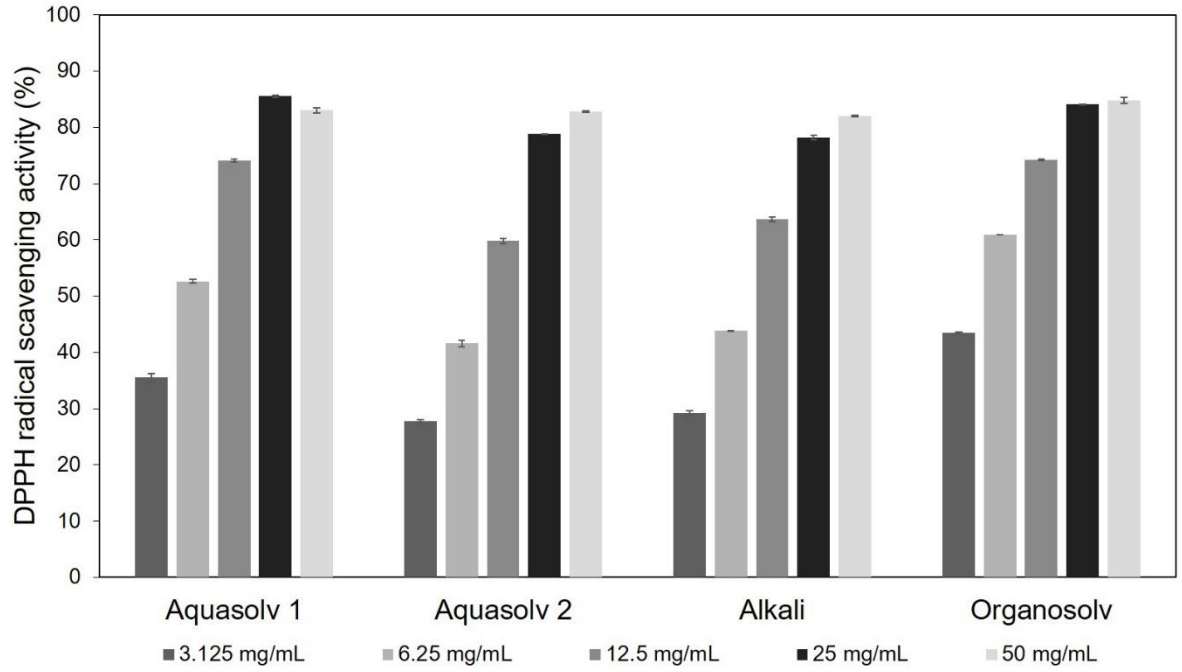

Figure 23: DPPH antioxidant capacity of four different lignins in five free radical concentrations. Results are reported as percentage of DPPH radical scavenging.

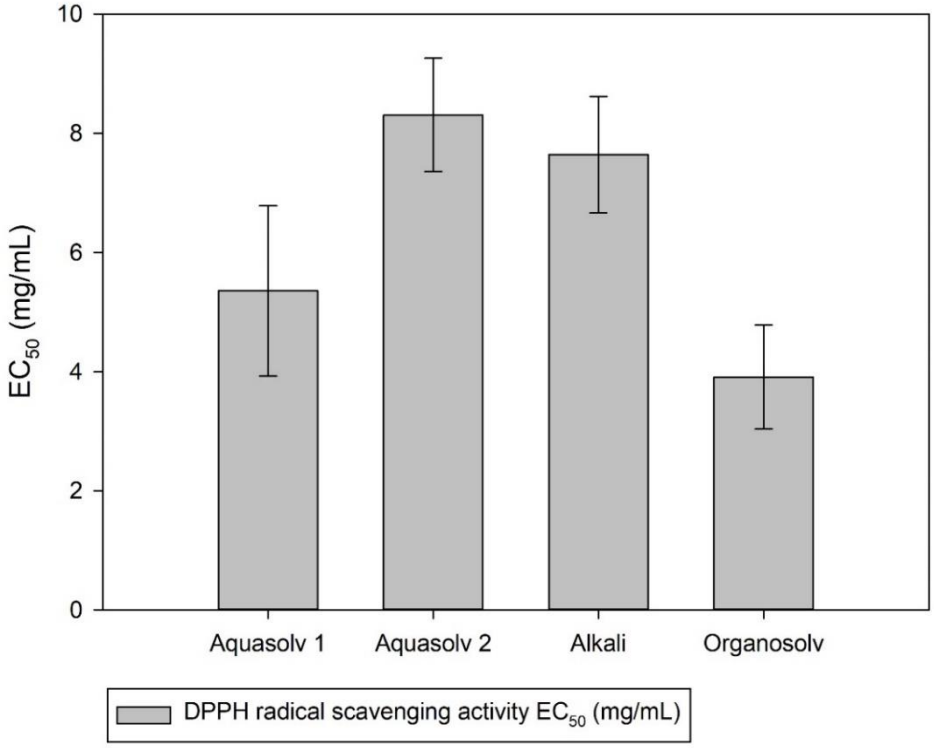

Figure 24: Efficient concentration (EC50) to scavenge half of the amount of DPPH free radical present for four different lignins. Results are presented in EC50 (mg/mL).

The results obtained in these assays demonstrate once more that the extraction process and origin of the lignins have an effect in its bioactive properties. The findings suggest that the molecular weight and thus, free functional groups present in lignin affect not only its antioxidant capacity but also its anti-diabetic properties as described in the next sections.

5.2.2 Cellular Antioxidant Activity (CAA)

Measuring antioxidant capacity *in vitro* does not necessarily correlate and/or demonstrates the antioxidant effect when comparing to the *in vivo* tests and more relevant information like the evaluation of antioxidant capacity in a relevant cellular environment is needed [175]. The cellular antioxidant capacity of a sample is experimentally determined by monitoring the prevention of the oxidation of 2',7' – dichlorofluorescein diacetate to 2',7'-dichlorofluorescein via quenching of the peroxyl radical ($RO_2^{\bullet}$) [176]. In this work, the cellular antioxidant capacity of four different lignins were tested. CAA EC_{50} values of the materials were between 0.356 mg/mL and 0.085 mg/mL and can be seen in Figure 25. ASL1 (0.356 mg/mL) and OSL (0.248 mg/mL) demonstrated the highest CAA EC_{50} therefore showing the least cellular antioxidant capacity. On the other hand, ASL2 and ALK presented the lowest EC_{50} values with 0.158 mg/mL and 0.085 mg/mL, respectively. The lowest values indicated a more effective dose of these lignins for quenching a peroxyl radical and therefore exerting antioxidant capacity in a cellular environment. Some authors suggested that the number of phenolic compounds or phenolic groups have a positive contribution to this assay as well as their ability to cross the cell membrane and survive the metabolism in cells.

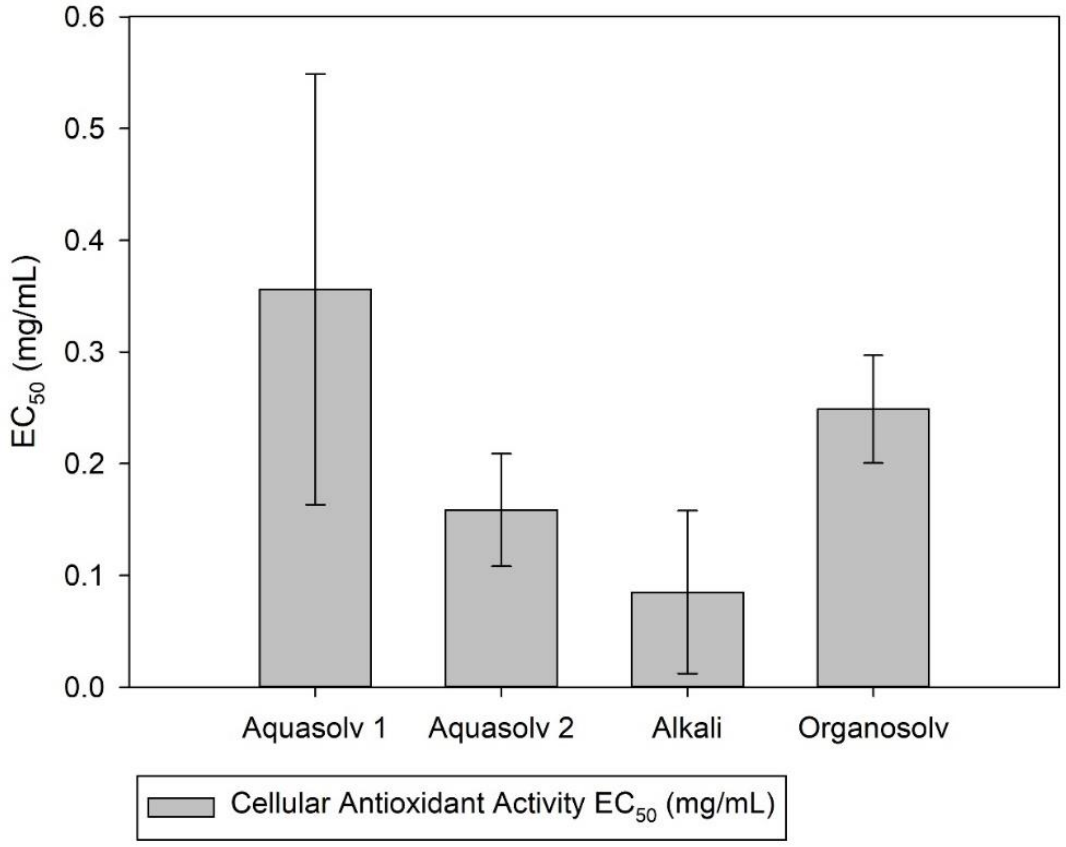

Figure 25: Cellular antioxidant activity (CAA) of four different lignins. Effective concentrations (EC50) are presented in mg/mL.

5.2.3 Antidiabetic capacity by inhibition of α-glucosidase and α-amylase

Reports on ASL and OS lignin cytotoxicity and potential antidiabetic capacity are limited. Isolated α-amylase from porcine pancreas and α-glucosidase from rat intestine were incubated with four different lignins, as described in the Materials and Methods section. Activity data in the presence of lignin was expressed as the effective concentration needed to inhibit 50 % of the α-amylase (Figure 26a) and α-glucosidase (Figure 26b) enzymatic activity (IC_{50}: mg/mL). Additionally, a positive control was used; acarbose, a pharmaceutical inhibitor of amylase and glucosidase (for slow the digestion of carbohydrates and delay glucose absorption). Pancreatic α-amylase is responsible for breaking down complex carbohydrates (starch), in the small intestine, to more simple polysaccharides (dextrins) like maltose. Then, the polysaccharides will be further digested by the α-glucosidases in the brush border to glucose, that is absorbed into the

bloodstream. Thus, the inhibition of the activity of these enzymes is directly related to the decrease in glucose absorption [177]. The α-amylase inhibitory activity of lignin was investigated at an enzyme concentration of 50 µg/ml. As shown in Figure 26a, ASL1, ASL2 and OSL showed similar inhibitory effects with values ranging from 3 – 6 mg/ml of IC_{50}. In this assay, Alkali lignin showed the lowest inhibitory effect (IC_{50} of 23.83 ± 7.53 mg/mL) with four times higher lignin concentration needed to achieve 50% of enzyme inhibition. Some authors reported that an increase in the number of hydrogen atom donor/acceptor in the polyphenolic structure can have a negative effect in decreasing α-amylase effect [178]. Additionally, Xiao et al. reported that methylation of the hydroxyl group greatly enhances the affinity of polyphenols for the enzyme, which clearly does not occur within the Alkali lignin structure [179]. On the other hand, ASL1, ASL2 and OSL showed the best enzyme inhibitory concentrations with 4.317 mg/mL ± 0.71, 5.759 mg/mL ± 0.68 and 3.598 mg/mL ± 0.34, respectively.

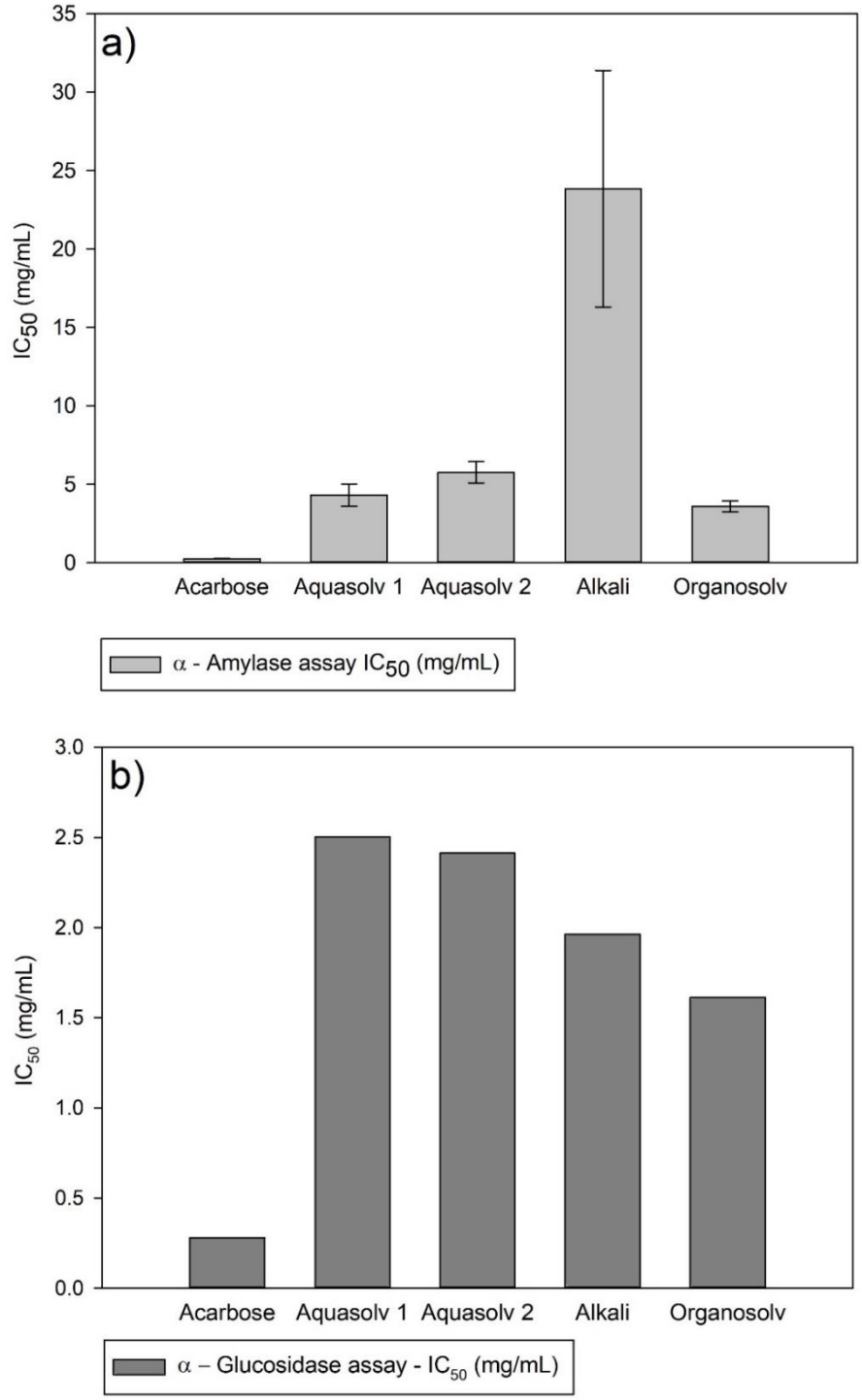

Figure 26: Half maximal inhibitory concentration (IC50) values represent the concentrations that inhibits 50% of enzymatic activity. IC50 values (mg/mL) of four different lignins for (a) α-amylase and b) α-glucosidase assays.

According to Perez-Cantu et al. there was no successful analysis for characterizing the molecular weight of AS Lignin and it was assumed for a value of Mw>30,000 g mol^{-1}, in this work; ASL is described as a hydrophobic lignin with a high molecular weight [24]. Our results suggest that ASL could be forming enzyme-lignin or enzyme-lignin-substrate type complexes which can result in enzyme precipitation. Some authors have described that the main forces involved are hydrophobic-hydrophobic (aromatic ring of lignin and hydrophobic part of the protein) interactions and hydrogen bonding (hydroxyl groups of lignin monolignols and –NH, -OH and –COOH H-acceptor groups of proteins) [178, 180].
One therapeutic approach related to these findings is the decrease in post-prandial plasma glucose through the inhibition of carbohydrate-hydrolysing enzymes such as the α-amylase and α-glucosidase which are present in the digestive tract. Natural inhibitors of these enzymes can be potentially utilized for the treatment and/or prevention of type II diabetes. Nevertheless, regardless of the demonstrated *in vitro* bioactivity, assessment of cytotoxicity must be performed before recommending and/or using any natural product for its use in life sciences.

5.2.4 In vitro cytotoxicity activity

The natural origin of a material does not ensure its safety, in this regard; cytotoxicity is one of the safety indicators. The performance of cytotoxicity assays is needed when cosmetic or pharmaceutical applications are intended, as the materials are required to be harmless. In this work, the Caco-2 cell line was used for the evaluation of cell depletion and compare the cytotoxic effects of the different lignin samples. All the samples were directly dispersed in the cell medium as powders (direct contact), and the cell viability was measured after incubation according to the standard MTS method. The results showed that Alkali lignin (ED_{50}=6.339 mg/mL) exhibited a gradual decrease in the cell viability as the concentrations were increased, and Organosolv Lignin (ED_{50}=3.857 mg/mL) showed a significant increase in cytotoxicity at 5 mg/mL concentration (Figure 27). Both of these lignins are known to have a low molecular weight (3000-5000 g/mol) in comparison to AS Lignin (>30000 g/mol). At the same time the use of organic solvents in the production of the i.e. Organosolv lignin can lead to the formation of lignin by-products and small molecular weight fractions, being one of the factors contributing to the cytotoxicity of the powders. The ED_{50} of the Organosolv lignin upholds the point by

showing the highest cytotoxicity of all the samples. Organosolv lignin from bagasse and Curan-100 showed higher cytotoxicity than Kraft lignin (with sulphur content) when evaluated in HaCat cells and, as expected, Kraft lignin showed a steady decrease in cell viability (higher cytotoxicity) [181]. Alkali lignin contains usually 2-4% of sulfur, which can be associated with the specific inactivation of enzyme functions within the cells [181]. This can be explained by the possible formation of thiol and/or disulphide linkages with the sulphur containing aminoacids (i.e. cysteines) in the enzymes. Another phenomenon can be the sulphur reaction with cellular molecules like nucleic acids, which can cause damage in the DNA leading to cellular apoptosis [182]. The results of the antioxidant activity and cytotoxicity have also been compared and it is seen that the materials with the highest antioxidant activity present highest cytotoxicity. As it was shown in section 5.2.1 and 5.2.2, the Organosolv lignin and Alkali lignin had the highest antioxidant activity and showed the highest cytotoxicity ($AOX_{Organosolv} > AOX_{Alkali}$ and $ED_{50\ (Organosolv)} < ED_{50\ (Alkali)}$) being in accordance with the literature.

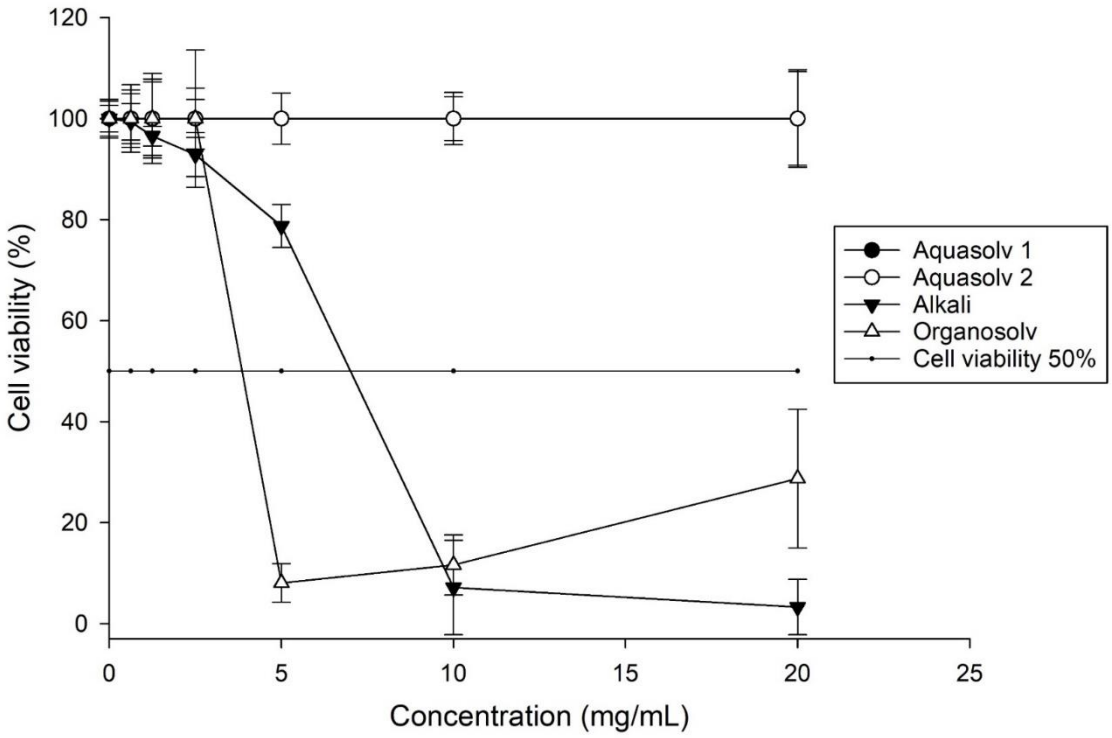

Figure 27: Cytotoxic effect of lignins on Caco-2 cells after 4h of incubation. Results were expressed as mean ± SD of at least three independent experiments performed in triplicate. Aquasolv 1 corresponds to the fine fraction obtained during spray drying and Aquasolv 2 to the coarse fraction.

ASL lignin, on the other hand, is seen to have no cytotoxicity even at concentrations such as 20 mg/mL in the cell medium. The AS Lignin material shows potential for pharmaceutical and/or cosmetic applications, at least in the concentration tested and presented in this section. Other authors have suggested the applicability of lignin as a binding agent to pathogenic bacteria, toxins, alcohol, bile salts and bilirubin, to name a few [183, 184]. Moreover, Alcell lignin was recently used as a carrier of acetylsalicylic acid in tablet formulations and proven efficiency for fast release of the active pharmaceutical ingredient due to the amorphous nature of lignin [185]. In this regard, AS Lignin, which is obtained in a chemical and solvent free biorefining process can be thought of as the alternative to conventional lignins for the mentioned high value applications. The findings of this work open up broad application possibilities for AS Lignin and clearly indicate that it is a better candidate for human consumption products when compared to conventional technical lignins.

5.2.5 Oil adsorption capacity

Lignin is considered to be the hydrophobic component of plants, responsible for the reduction of water permeability in the plant cell walls. Due to this inherent characteristic of the lignin, several attempts have been made to use the lignin as hydrophobic filler and oil adsorbant for oil spillages and soil treatments. Giving that the AS Lignin presented non cytotoxicity at the concentrations tested, it could be used for human consumption and the oil adsorbing property can be also transferred to dietary oil adsorption, which is the main aspect evaluated in this section. When oils are ingested in the human body, this contributes to cholesterol problems and high levels of HDL and LDL cholesterol in blood. In order to assess the potential use of AS lignin in this bioactivity/functionality, the in vitro evaluation based on the ISO787/5 was performed. Different types of lignins, as well as AS lignin prepared with spray drying and via supercritical CO_2 drying were performed. Pectin, alginate and chitosan were evaluated along since these biopolymers are known to possess oil adsorption capacities and specially the chitosan used in this study, is a commercial product sold in Europe with the approved claim of dietary oil adsorption.

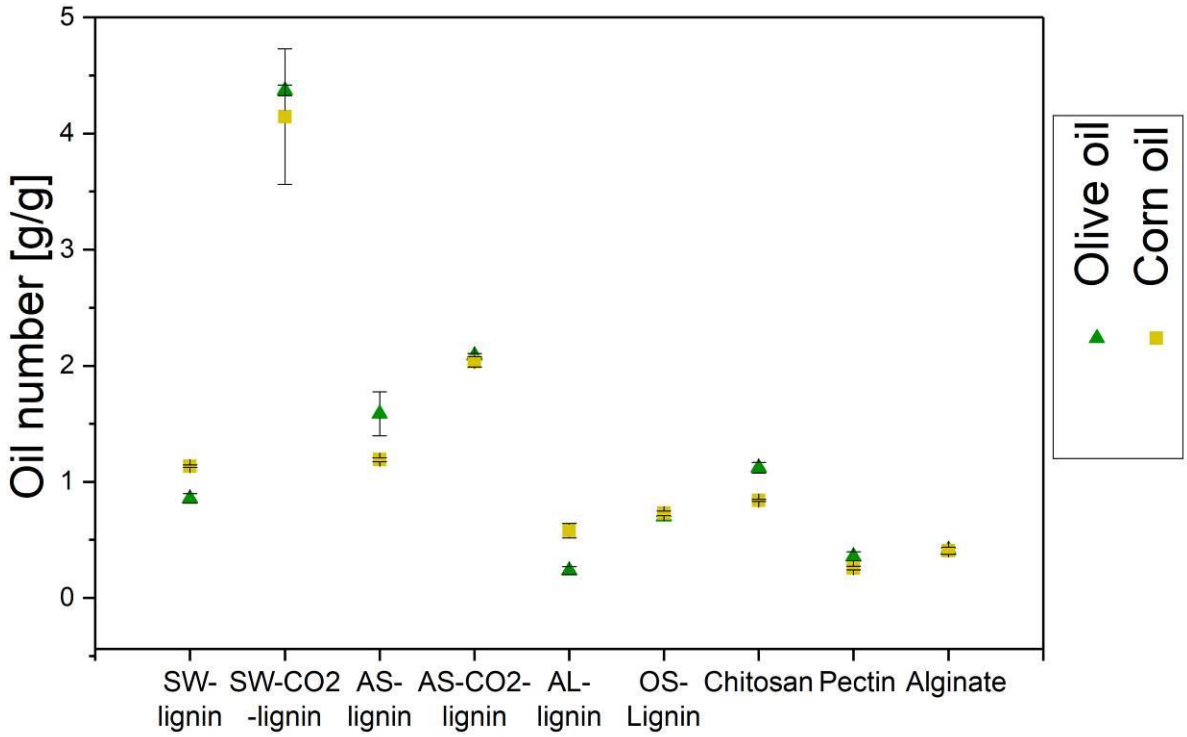

Figure 28: Adsorption capacities of the biopolymer samples according to ISO 787/5. SW lignin (softwood lignin), SW-CO2 lignin (softwood, supercritically dried lignin), AS Lignin (spray dried lignin), AS-CO2 lignin (AS lignin obtained via LHW pretreatment and supercritically dried), AL-Lignin (alkali lignin), OS Lignin (organosolv lignin).

The lignins from SW-CO_2 and AS-CO_2 showed the highest oil adsorption capacity in vitro with 1.97 ± 0.27 g·g^{-1} and 1.60 ± 0.12 g·g^{-1} for corn oil respectively, and 2.42 ± 0.09 g·g^{-1} and 2.98 ± 0.08 g·g^{-1} for olive oil. Both of these were obtained via solvent exchange and supercritical drying, which also presented high surface areas. At an in vitro level, with the ISO787/5 method, only a physical mixture of the lignins and oil are tested and the presence of porosity and surface area may play the biggest role on the oil adsorption. AS lignin powder presented higher oil adsorption capacity than the normally dried powder of SW lignin. Softwood lignins are mostly composed of the Coniferyl alcohol (G) and p-coumaryl alcohol (H), while lignins from annual plants are mostly composed from Coniferyl alcohol (G) and Sinapyl alcohol (s). This latter, with two methoxy groups (hydrophobic) in the phenolic ring, methoxy groups in lignin not only contribute to form

hydrophobic-hydrophobic interactions but it has been reported that the presented of this group ortho to a hydroxyl group can sterically interfere with the formation of hydrogen bonds with the phenolic hydroxyl groups. In this sense, although the lignin is complex and heterogeneous structure, the major composition of the AS Lignin with Sinapyl alcohol can be the reason for this difference in the oil adsorption capacity in vitro. The lowest oil adsorption capacity was shown by the alkali lignin, which is by its characteristics the most hydrophilic lignin of all the lignins tested. Spray dried AS Lignin also presented higher performance (2.67 ± 0.02 $g \cdot g^{-1}$) than the biopolymers alginate (0.41 ± 0.01 $g \cdot g^{-1}$) , pectin (0.36 ± 0.04 $g \cdot g^{-1}$) and chitosan (1.12 ± 0.05 $g \cdot g^{-1}$). However, for a better understanding of how this can be transferred to human consumption products, a following study was performed by assessing the oil adsorption capacity of these material under simulated gastrointestinal conditions. The results are presented in the next section (5.2.6).

5.2.6 Oil adsorption capacity under simulated gastrointestinal conditions

Several studies in literature have shown that lignin is non digestible by mammals, meaning that if we were the ingest lignin, it will be almost intactly discharged in the feces. However, this doesn't exert the lignin from having interactions and effects during the pass in the gastrointestinal tract. In this section, the effect of simulated gastrointestinal conditions on the oil adsorption capacity of lignin was evaluated. Results in Figure 29 show that the positive effect of the high surface area of the powders obtained via supercritical drying is no longer there. The porosity of the powders is then also filled with the testing media, in this case the simulated stomach fluid. The highest oil adsorption capacity was performed by the chitosan (2.80 ± 0.01 $g \cdot g^{-1}$), which is a well-known molecule for this activity, the literature suggests that in the small intestine, with increasing pH, the positively charged amino groups of the chitosan may attract negatively charged fatty acids and bile acids in micelles. In the case of the lignin samples, all presented a similar oil adsorption capacity in the gastrointestinal phase, except for alkali lignin which showed 1.06 ± 0.18 $g \cdot g^{-1}$, the half of the other lignin samples.

In general, all the adsorption capacities under both gastric and GI are higher than their ISO787/5 tested counterparts. This difference leads to the conclusion that pore saturation doesn't occur during the measurement of oil count number. Furthermore, in aqueous solutions, the surfaces of both biopolymer and oil become electrically charged due to polar functional groups. The difference between gastric and intestinal adsorption capacity of the samples is the outcome of either intensified mass transfer to the biopolymer surface, flow of oil inside the porous structure or enhanced triacylglyceride adsorption unto the polymer surface. As rates of adsorption in porous media are dominated by transport phenomena within the pore network, the effect of gastric and GI environment can be neglected in favor of surface diffusion. Although the H_3O^+ ions increase the electric field intensity during gastric (acidic) phase leading to better polarization of the surfaces, they also reduce the hydrophobicity of the molecules in the water phase. This leads to less adsorption sites and in cases when the biopolymer surface acquires adequate negative potential, a layer of water is formed on the pore surface inhibiting the triacylglycerides from adsorbing. This hypothesis is backed up by the fact that AS-lignin, the sample with most C=O/C=C groups, adsorbs much less triacylglyceride than GI phase under gastric condition. Alkali –lignin is the opposite as it forms hydrogen bonds with OH^- ions under GI conditions and begins to dissolve in the aqueous phase; hence, it adsorbs even less oil in basic mediums.

Chitosan exhibited the highest oil adsorption capacity among all samples in the GI tract. In the hypothetical case that acidic food or drinks are to be consumed together with all these samples. Then the efficiency of all the lignins will decrease. However, the efficiency didn't show negative trends in the intestinal phase, in which the lipid absorption by the body occurs. In this sense, all AS lignins and softwoods lignins represent a good option for the purpose of dietary oil adsorption.

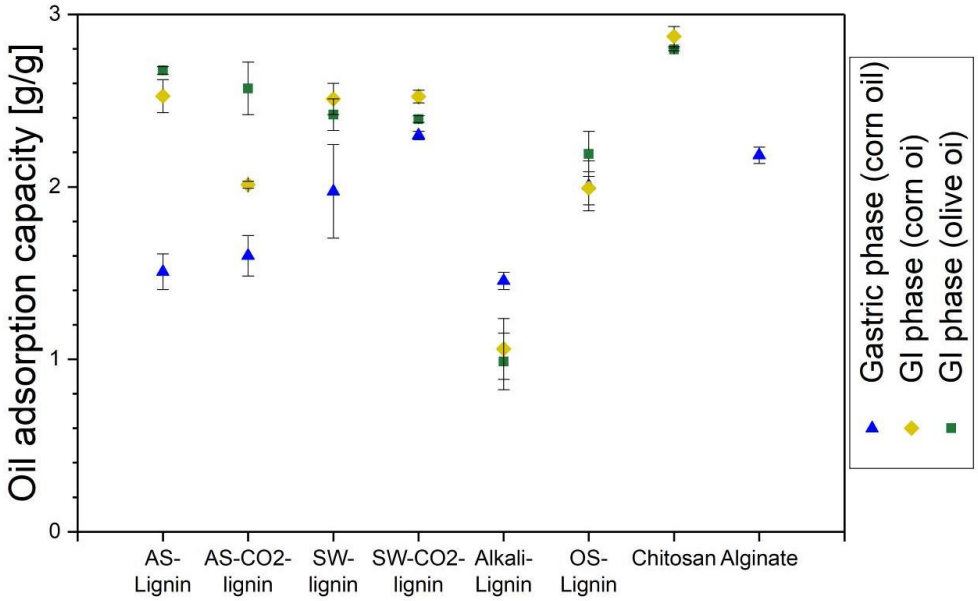

Figure 29: Oil adsorption capacity under simulated gastrointestinal conditions.

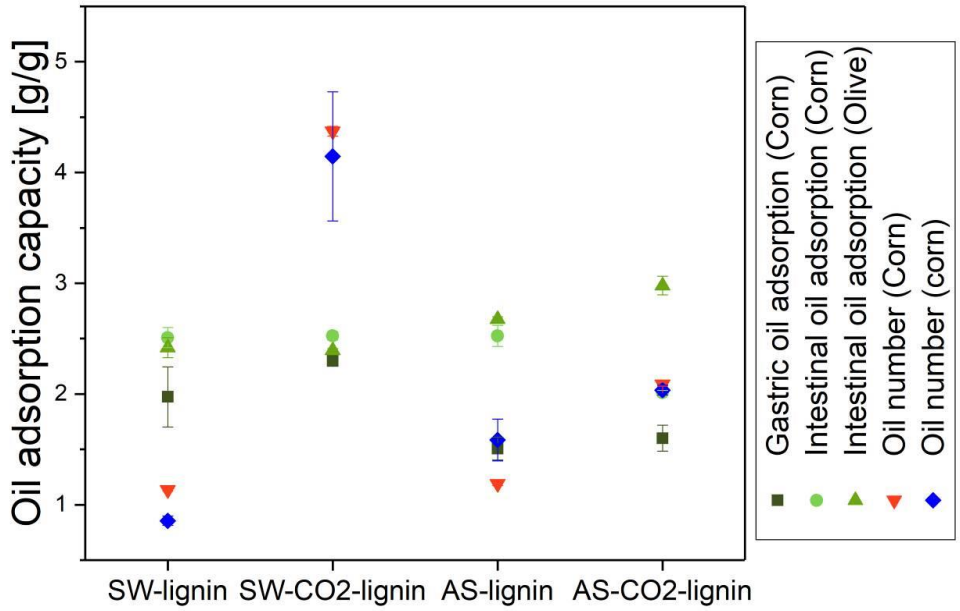

Figure 30: Effect of supercritical CO2/ethanol treatment on adsorption capacity of SW and AL-lignin.

In figure 30, a comparison between wheat straw AS lignin and softwood lignins with and without the supercritical drying is presented. As observed, the positive effect of the supercritical drying is mostly in the softwood lignins and to a lesser extent in the aquasolv

lignin samples. However, the drying method did not have an influence in the oil adsorption when tested under simulated gastrointestinal conditions since the porosity obtained will be as well responsible for the water uptake into the porous network. If these samples are to be taken by humans in the form of tablets or capsules, the time of intake (before or after food) will have an impact on the capacity. The effect of the intake modus: after oil comes into the stomach fluid vs before oil comes into the stomach fluid was evaluated but no differences were observed.

The hydrophilicity/lipophilicity of the samples was assessed by the contact angle measurements (Table 20). And the wetting behavior of all the materials was plotted (Figure 31). In general, all biopolymer samples have higher wettability with oil than water, which is a positive factor contributing to oil adsorption. solid surfaces with water CAs < 10◦ or >150◦ are considered to be superhydrophilic or superhydrophobic surfaces, while surfaces with oil CAs < 10◦ or >150◦ are considered as superoleophilic or superoleophobic surfaces.

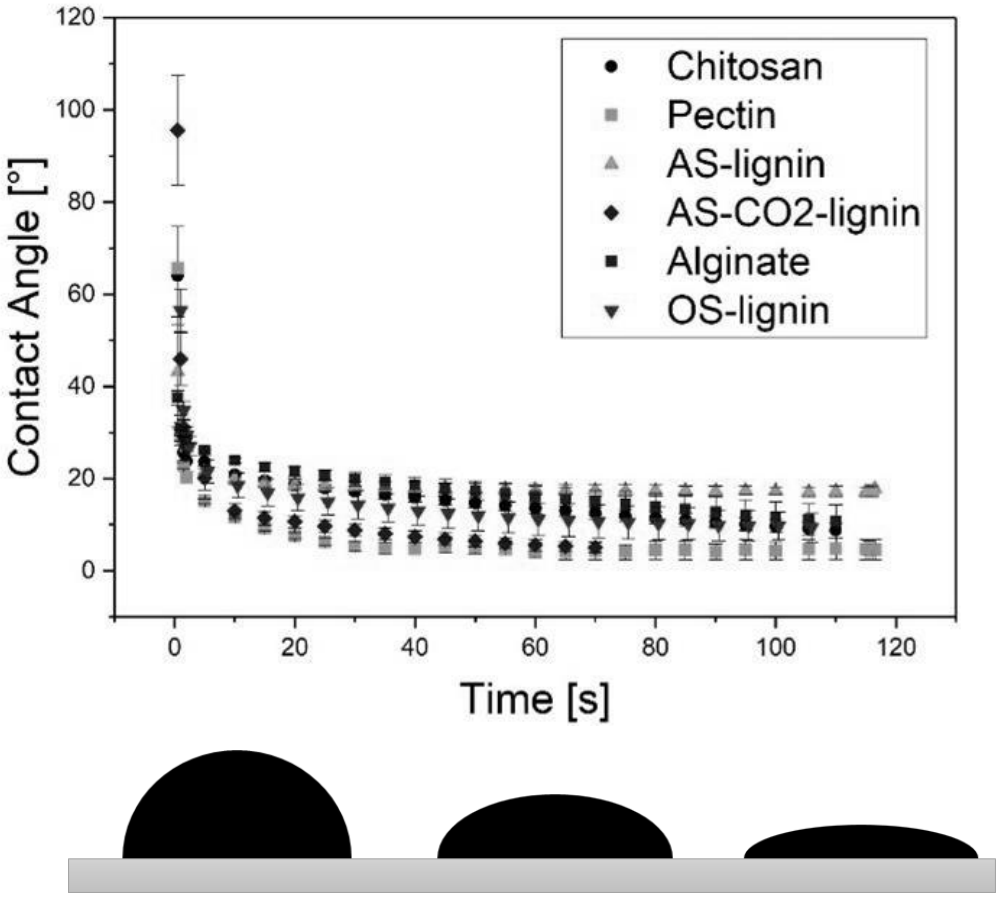

Figure 31: Contact angle (oil) on the different materials used for oil adsorption.

Table 10: Contact angle of all the samples tested for oil adsorption capacity with water and oil (corn oil).

Sample	**Dietary Oil**		**Water**	
	θ_{eq}[°]	$t_{90\%}$ [s]	θ_{eq}[°]	$t_{90\%}$ [s]
SW-lignin	-	<0.25	-	<0.25
SW-CO_2-lignin	-	<0.25	-	<0.25
AS-lignin	18	13	59	12,5
AS-C02-lignin	5	17	1	2
OS-Lignin	9	29	14	15
Chitosan	9	54	75	30
Pectin	5	11	26	56
Alginate	11	74	60	13

5.3. In vivo assessment of toxicity and hypocholesterolemic activity of AS lignin spray dried particles

In the following paragraphs, the spray dried particles from the optimized process parameters were further assessed on their toxicity and hypocholesterolemic effect in vivo, following the in vitro studies already presented.

5.3.1 Body & heart fat weight

Hypercholesterolemia, a disorder of the lipid metabolism, specifically hyperlipidemia, is defined as the presence of abnormally elevated levels of total Cholesterol in the blood stream, also known as serum Cholesterol. The clinical nutrition scientific community asserts that high cholesterol-LDL content in the bloodstream can be strongly linked to the

development of atherosclerosis and cardiovascular diseases, therefore; efforts to lower the blood Cholesterol will preemptively reduce the risk of these diseases. Furthermore, it is demonstrated that excessive high levels of Cholesterol and fatty acid are followed by multiple negative physical manifestation, like fatty liver and fatty heart. In this section, the evaluation of the fatty heart was performed in rats that were fed with high fat diet, with normal diet, as well as with the supplementation of lignin, simvastatin and a combined treatment of lignin/simvastatin as lowering cholesterol levels is presented. Both the heart fat weight and the rats body gain weight were monitored. As shown in Figure 32, no change in the daily increase of the body weight (rate measured as g/day) was noticed among control groups (C1: control 1 receive ND only, n=4; C2: control 2 receive HFD only, n=4), after one month of the experimental period. The average rate of the rats' weights in the two control groups (Control 1 and 2) were calculated to be (2.41 ± 0.08 g/day and 2.41 ± 0.15 g/day) respectively. These results showed that there is an obvious effect of lignin dose on the gained body weight of the rats (see Annex A10). Based on control 2 (fed with HFD), when using 50 mg of lignin, the average rate of body weight gained was markedly decreased to about the half (1.43 ± 0.05 g/day) compared to C2 (2.41 ± 0.15g/day), while it was not affected by lignin 100 mg (2.49 ± 0.32 g/day). Conversely, no notable change was detected in the average rate of body weight gained for the rats given lignin 500 mg (2 ± 0.52 compared to 2.41 ± 0.15 g/day for C2). Based on the results obtained, the group given simvastatin 40 mg showed comparable effect on the average body weight gain as that for the group treated with lignin 50 mg (1.37 ± 0.21 g/day and 1.43 ± 0.05 g/day) respectively. The rats that were given the combination of lignin 100 mg and simvastatin 40 mg also exhibited lower rate of body weight gain (1.88 ± 0.08 g/day compared with 2.41 ± 0.15g/day for C2). Our results showed that there is a significant difference between the different lignin doses on the rate of weight gain. The lignin dose of 50 mg showed much better effect in decreasing the rate of weight gain compared to 100 mg lignin, 500 mg lignin, and to the combination group (p-value=0.001, 0.002 and 0.001, respectively based on Mann Whitney test). As compared with control 1, the group that received lignin 100 mg had no notable change in the rate of body weight gain (2.17 ± 0.07 g/day compared to C1 2.41 ± 0.08 g/day).

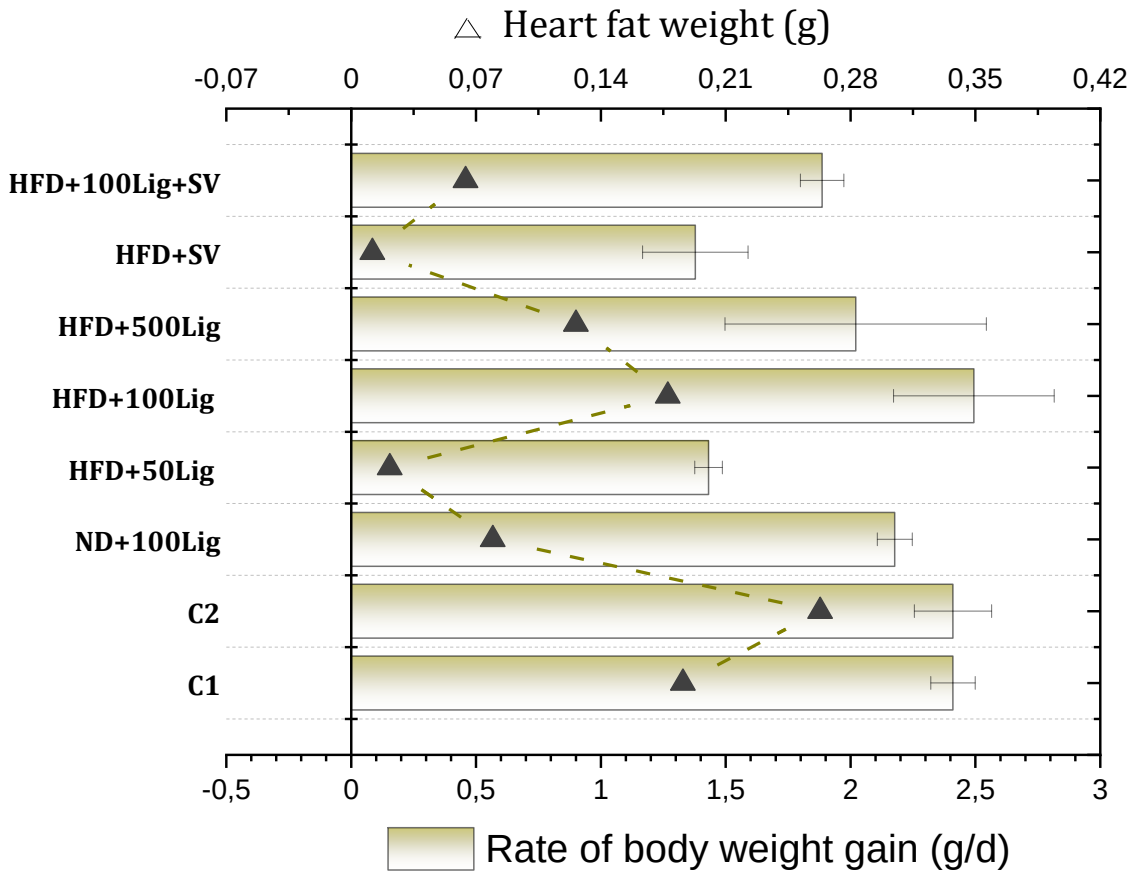

Figure 32: Gained Body weight (bars) and the heart fat weight (circles) of all groups. HFD is the high fat diet, ND is the normal diet. SV is the simvastatin, Lig is lignin.

The average weight of the fat on the heart for the rats in C2 was almost double of that for the rats who ate normal diet (0.186 g compared with 0.263 g). In general, we noticed that the different doses of lignin as well as the drug simvastatin reported significant impact on decreasing the heart fat weight when compared with control 2. However, the average weight of the fat on the heart for the rats given the lowest dose of lignin (50 mg) was significantly reduced, reaching about the tenth only (0.021 g compared to 0.26 g) (p-value=0.01, Mann Whitney test). Furthermore, a significant decrease was reported in the average weight of the heart fat for the rat's treatment with lignin 500 mg (p-value=0.01, Mann Whitney test) when compared to C2. The dose of lignin of 100 mg reached only half (0.177 when compared to 0.26 g). When comparing the effect of the 50 mg lignin with the 100 mg lignin on the heart- fat weight, our statistical analysis using Mann Whitney test showed significant difference (p-value=0.014). Interestingly, the groups treated with simvastatin 40 mg and with lignin 50 mg reported a similar effect, not only on the rate of

the gained body weight but also on the heart fat weight (0.011± 0.023 and 0.021 ± 0.041 g) respectively. The rats were given the combination of lignin 100 mg and simvastatin 40 mg, also showed a clear effect on depleting the weight of the heart fat (0.064g compared to C2 0.26 g).

5.3.2 Rate of total cholesterol levels

The cause of Hypercholesterolemia has been identified to be either hereditary, external stimulants or dietary; with the main prevalent one is the latter. Dietary Hypercholesterolemia is caused by excess of total lipid input into the body through the digestion of aliments. Any carbon-based substance of biological origin soluble in nonpolar solvents can be defined as a lipid and Cholesterol is just one example of the dietary fats, including also saturated and unsaturated fatty acids, triacylglycerides, tocopherols, pigments, phospholipids and other sterols, however, triacylglycerides, fatty acids and cholesterol are the most abundant lipids in the edible oils, being the major markers to look into when evaluating hypocholesterolemic drugs and coadyuvants. Having into consideration all the results presented in the in vitro evaluation of the lignin potential for dietary oil binding with the oil count method, as well as under simulated gastrointestinal conditions, the hypothesis was that lignin, being able to bind cholesterol in the intestines, decreasing its levels in the blood stream and carrying onto the feces. In this section, the evaluation of the total serum cholesterol levels in serum and feces. The results of the serum and feces lipids profile that were measured in rats are shown in Figure 33. The total cholesterol levels in the blood were different between control groups. However, the rats in control 2 group (received HFD only for one month) reported a great reduction in the average of blood cholesterol level, (242.8 mg/dl after one week reach 173 mg/dl) which is approximately 3 times less than that for control 1 (received ND), (9.97 ± 0.90 mg/dl/d and 3.19 ± 0.83 mg/dl/d) respectively. In reference to control 1**,** the rats were given 100 mg of lignin had almost no effects on the serum cholesterol levels but had higher excretion of cholesterol in the feces (2.32 mg/ml. g^{-1} feces. day^{-1}). The groups of rats that had HFD and treated with 50 mg, 500 mg, as well as the combination of lignin and the simvastatin resulted in a similar reduction of the serum cholesterol levels (4.88, 5.2 and 4.87 mg/dl.day^{-1}) respectively. However, the group that had the HFD and treated

with 100 mg lignin had no notable difference in rate of blood cholesterol loss (1.97 ± 1.78 mg/dl.day^{-1} compared to 9.97 ± 0.90 mg/dl.day^{-1}for C2). Although the group that was treated with simvastatin markedly decreased the rate of serum cholesterol levels compared to C2 (6.69 ± 1.63 mg/dl.day^{-1}), it didn't show the highest release of cholesterol in the feces. On the other hand, the rate of fecal cholesterol excretion was the highest for the group treated with 50 mg lignin (3.93 ± 1.96 mg/ml. g^{-1} feces. day^{-1}) followed by simvastatin (2.88 ± 1.03 mg/ml. g^{-1} feces. day^{-1}), because of that, the lowest dose 50 mg of lignin showed a significant difference when compared to C2 and lignin of 100 mg (p-value=0.003 and 0.000 Tukey HDS test,) respectively.

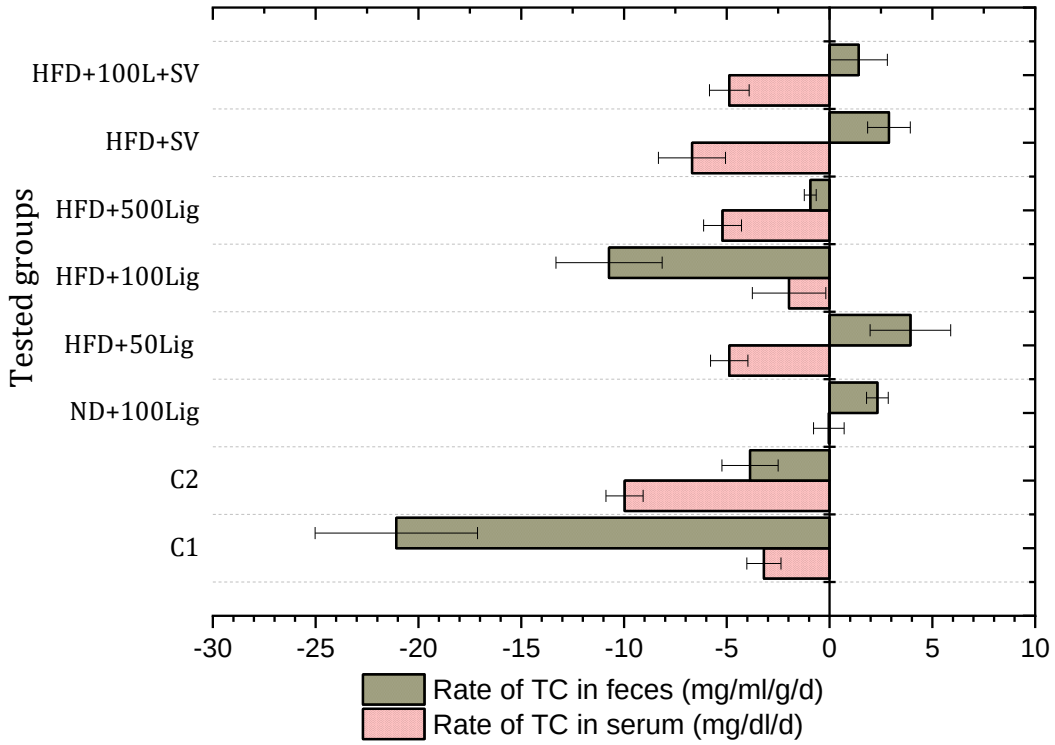

Figure 33: Rate of total cholesterol in the serum (pink) and in the feces (brown) for all groups. The rate was calculated as the differences between cholesterol concentration in day 14 and day 21 for serum and feces divided by number of days.

5.3.3 Rate of triglycerides levels

Both control groups showed an increase in serum triglycerides levels in a similar manner, (Figure 34). Only the rats in control 2 showed increased excretion in total glyceride in

fecal (2.97 ± 2.79 mg/ml. g^{-1} feces. day^{-1}) (p-value=0.004, Dunnett t-test,). Compared with control 1, a group of rats was given ND with 100 mg of lignin observed a significant increase in the rate of TAG fecal excretion (3.46 ± 2.91 mg/ml. g^{-1} feces. day^{-1}) (p-value=0.017, Dunnett t-test, Appendix XIV). However, simvastatin group had the greatest rate of loss of triglycerides levels in the blood (7 ± 3.32 mg/dl.day^{-1}) and the highest rate of fecal excretion (24.6 ± 4.30 mg/ml. g^{-1} feces. day^{-1}), followed by the combination, as the rate of fecal excretion of triglycerides reached (9.74 ± 2.27 mg/ml. g^{-1} feces. day^{-1}). All lignin doses demonstrated a significant increase in the rate of fecal excretion compared to the control groups. For example, lignin 50 mg had a significant rate of excretion of triglycerides when compared to C2 (6.83 to 2.97 mg/ml. g^{-1} feces. day^{-1}). In serum, lignin 500 mg reported a great decrease in the rate of triglycerides levels of about (4.66 ± 3.99 mg/dl.day^{-1}), unlike 50 mg about (1.41 ± 2 mg/dl.day^{-1}). While triglycerides levels were not affected for the rats treated with lignin 100 mg.

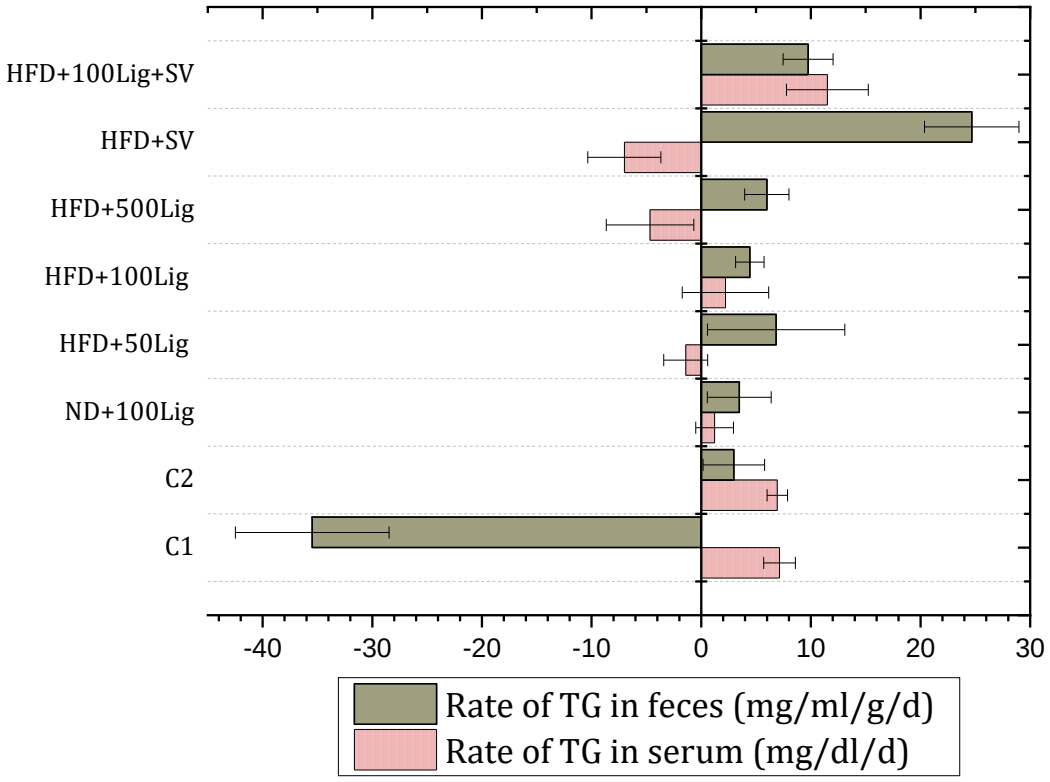

Figure 34: Rate of triglycerides in the serum (pink) and in the feces (brown) for all groups. The rate was calculated as the differences between cholesterol concentration in day 14 and day 21 for serum, and feces divided by number of days.

5.3.4 Rate of HDL levels

The level of HDL concentration was higher in control 1 (received ND) than in control 2 that (received HFD) (0.66 ± 0.21 and 0.34 ± 0.12 mg/dl.day^{-1} respectively) (Dunnett t-test, p-value=0.000). The excretion rate of HDL with the feces was higher in control 1 (0.75 ± 0.17 mg/ml. g^{-1} feces. day^{-1}) than that of control 2 as can be seen in Figure 35. There is a significant difference between control 2 and the group treated with lignin 50 mg (p-value=0.000; Dunnett t-test) calculated as the above. Also, 100 and 500 mg of lignin showed increase in the rate of serum HDL (1 ± 0.30 and 0.73 ± 0.25 mg/dl.day^{-1}) respectively, as well as for the group treated with simvastatin (0.65 ± 0.28 mg/dl.day^{-1}) and combination of lignin and simvastatin (0.54 ± 0.17mg/dl.day^{-1}). Although, the rate of HDL excretion in feces was the highest for the group treated with simvastatin (1.23 ± 0.42 mg/ml. g^{-1} feces. day^{-1}), the combination of lignin and simvastatin (0.37 ± 0.15 mg/ml. g^{-1} feces. day^{-1}) and lignin 50 mg (0.22 ± 0.25 mg/ml. g^{-1} feces. day^{-1}) were significantly less. Additionally, rats were given lignin 100 mg with ND showed higher HDL levels than in control 1.

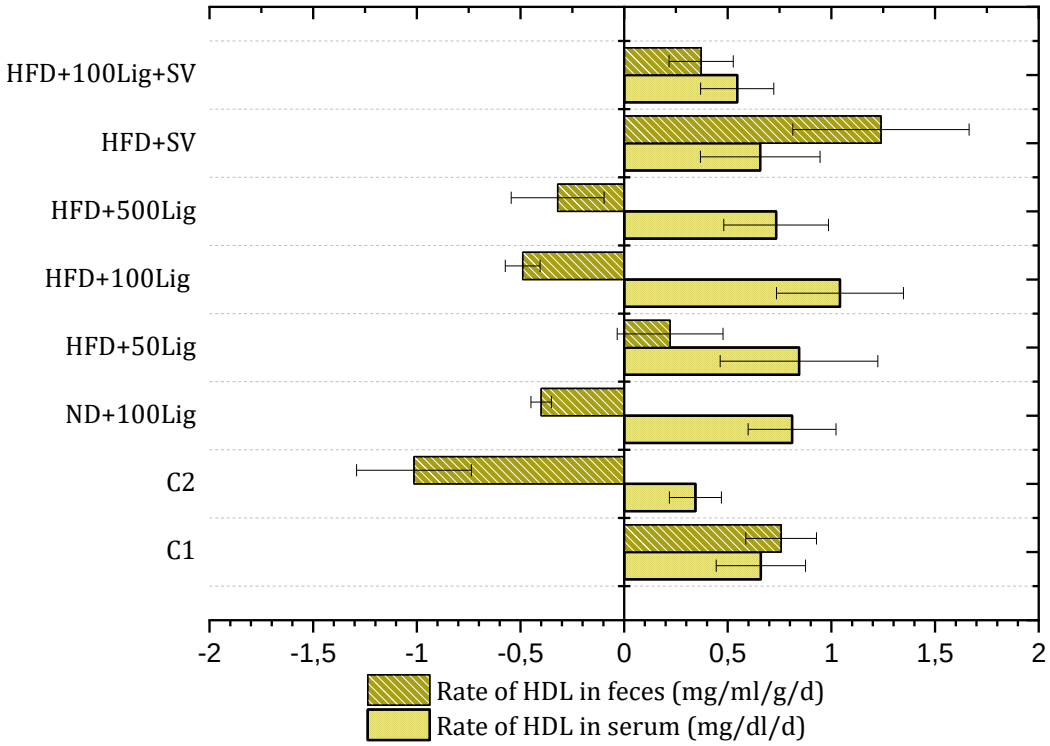

Figure 35: Rate of HDL in the serum (yellow) and in the feces (blue) for all groups. The rate was calculated as the differences between cholesterol concentration in day 14 and day 21 for serum, and feces divided by number of days.

5.3.5 Liver toxicity

Alanine Transaminase (ALT) serum analysis was measured in rats to evaluate liver toxicity of lignin. Figure 36 shows there was significant difference in liver toxicity between control 1 and 2 (1.5 ± 0.4 and 2.56 ± 1.15 U/L) respectively (p-value=0.030, Tukey HDS test). When comparing with control 1, rats were given lignin 100 mg showed reduced ALT measurement (1.24 ± 0.31 U/L), which reflects low toxicity levels in the liver. According to control 2, the lowest dose of lignin 50 mg markedly decreased liver toxicity by 300% (0.71 ± 0.26 U/L compared to 2.56 ± 1.15 U/L for C2), followed by 500 mg of lignin (1 ± 0.46 U/L compared to C2). While the combination and lignin 100 mg had approximately similar results as they raised liver toxicity (1.65 ± 1.01 & 1.81 ± 0.8 U/L) respectively. In comparison with lignin and combination groups, simvastatin raised the level of liver toxicity 200% (2 ± 1.39 U/L), according to that there is a significant difference between lignin 50 mg and simvastatin on liver toxicity (p-value=0.017 Tukey HDS test).

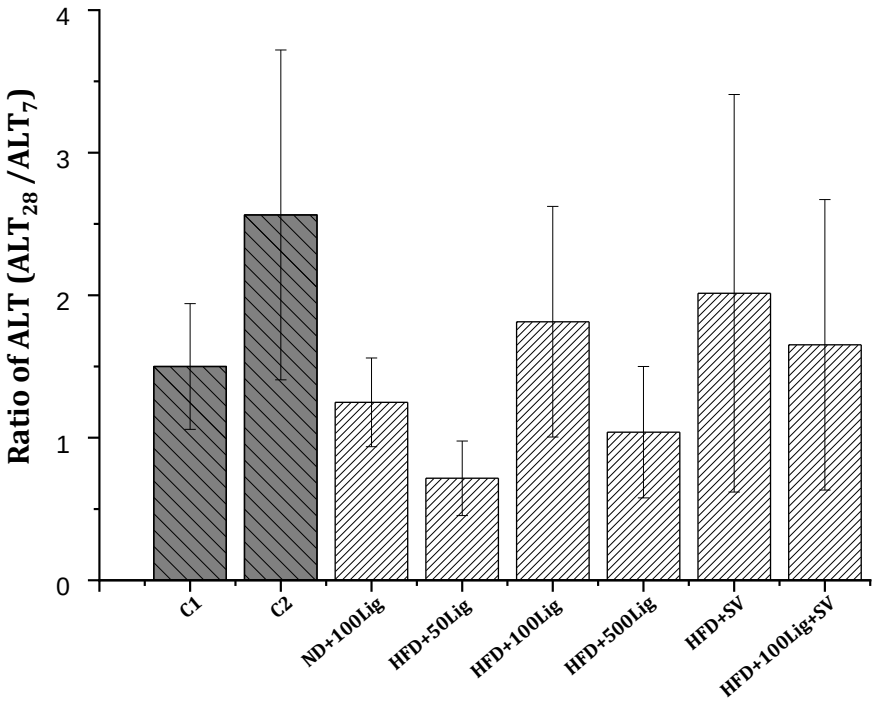

Figure 36: Ratio of Alanine Transaminase measured in serum analysis. ALT concentration in serum U/L., C1: control 1 receive normal diet only, n=4, C2: control 2 receive high fat diet only, n=4, Lig: lignin, SV: simvastatin, ND+100 Lig: Normal Diet + 100 mg lignin, n=4, HFD+50, 100 and 500 Lig: High Fat Diet + 50, 100 & 500 mg lignin, respectively, n=7 each group, HFD+SV: High Fat Deit +simvastatin 40 mg, n=4, HFD+100 Lig+SV: High Fat Diet + 100 lignin + simvastatin 40 mg, n=7.

5.3.6 Conclusion Part II

The non-cytotoxicity of the spray dried AS lignin as well as the bioactive properties was thoroughly assessed in vivo and in vitro. It was proven that the lignin particles obtained in this work can be further evaluated for applications in products for human consumption, moreover, the properties of the AS lignin overperformed other novel and technical lignins like organosolv and alkali. This study provides the properties of AS lignin needed for its further development towards the pharmaceutical applications, for instance as active pharmaceutical ingredient and excipient for the uptake of non-desired molecules in the stomach and/or drug delivery. It was shown that the increase in the antioxidant capacity of lignins also increases their cytotoxicity, which should be taken in to account considering the applicability potentials of each material. Based on these results, the functionality of AS Lignin in targeted product prototypes can be further elaborated aiming high value applications such as cosmetics or pharmaceuticals. The results obtained in the in vitro evaluation were confirmed on the in vivo studies and the lignin shows similar positive effects in serum cholesterol as the ones provided by the allopathic drug simvastatin. However, the AS lignin presented better results in the liver toxicity, which can also be an indication of safety. A potential application will be to use less dosage of simvastatin in patients with hypercholesterolemia and add lignin ingestion as a coadyuvant. This is supported by the fact the treatment of lignin with simvastatin showed a decrease in the heart fat weight. In this study, the supplementation of 50 mg of lignin was the most effective, these results should be further utilized for formulation of food supplements and/or active pharmaceutical ingredients. With this basis, special attention is now to be put on the regulatory framework of biobased materials for such applications.

5.4 Spray dried lignin particles for the formulation of oral dosage forms

The European Pharmacopeia defines tablets as “solid preparations each containing a single dose of one or more active substances”; these are typically produced via direct compression and/or wet granulation. The direct compression of the particles in a specific volume, is a shorter and more cost-effective in process than wet granulation. In general, there is a problem associated with the direct compression process as the excipients should be present with specific properties and powder characteristics able to result in tablet dosage forms with acceptable quality. In this section, the use of lignin biopolymer as direct compression excipient and/or active pharmaceutical ingredient in tablet dosage forms was assessed for the first time. In order to assess the usability of the lignin particles, both direct compression and wet granulation were done and compared in performance.

5.4.1 Powder characterization of the lignin used for direct compression

The lignin fraction utilized to produce tablets via direct compression had a moisture content of 4.6 wt. % while the fraction used for wet granulation had a moisture content of 2.9 wt. %. The low moisture content of these particles is desirable due to avoidance of interparticulate sticking prior to tableting, which has a direct impact in flowability and thus, such moisture content eases the binding process during tablet compression [186, 187]. Particle size distribution is another important property to hinder particle segregation, in this case; lignin for direct compression presented a D_{50} value of 18.49 ± 6.29 μm whereas the fine fraction presented a D_{50} value of 7.89 ± 2.68 μm [188, 189]. Morphology of the particles used was conducted via scanning electron microscopy (SEM) as seen in Figure 37. The most prominent morphology amongst the lignin spray dried particles in both fractions is the presence of semi-spherical particles with rough surfaces, giving a positive quality for mechanical interlocking during compression in the tableting process [190]. Additionally, properties such as flowability, cohesion, bulk density and angle of internal friction were measured.

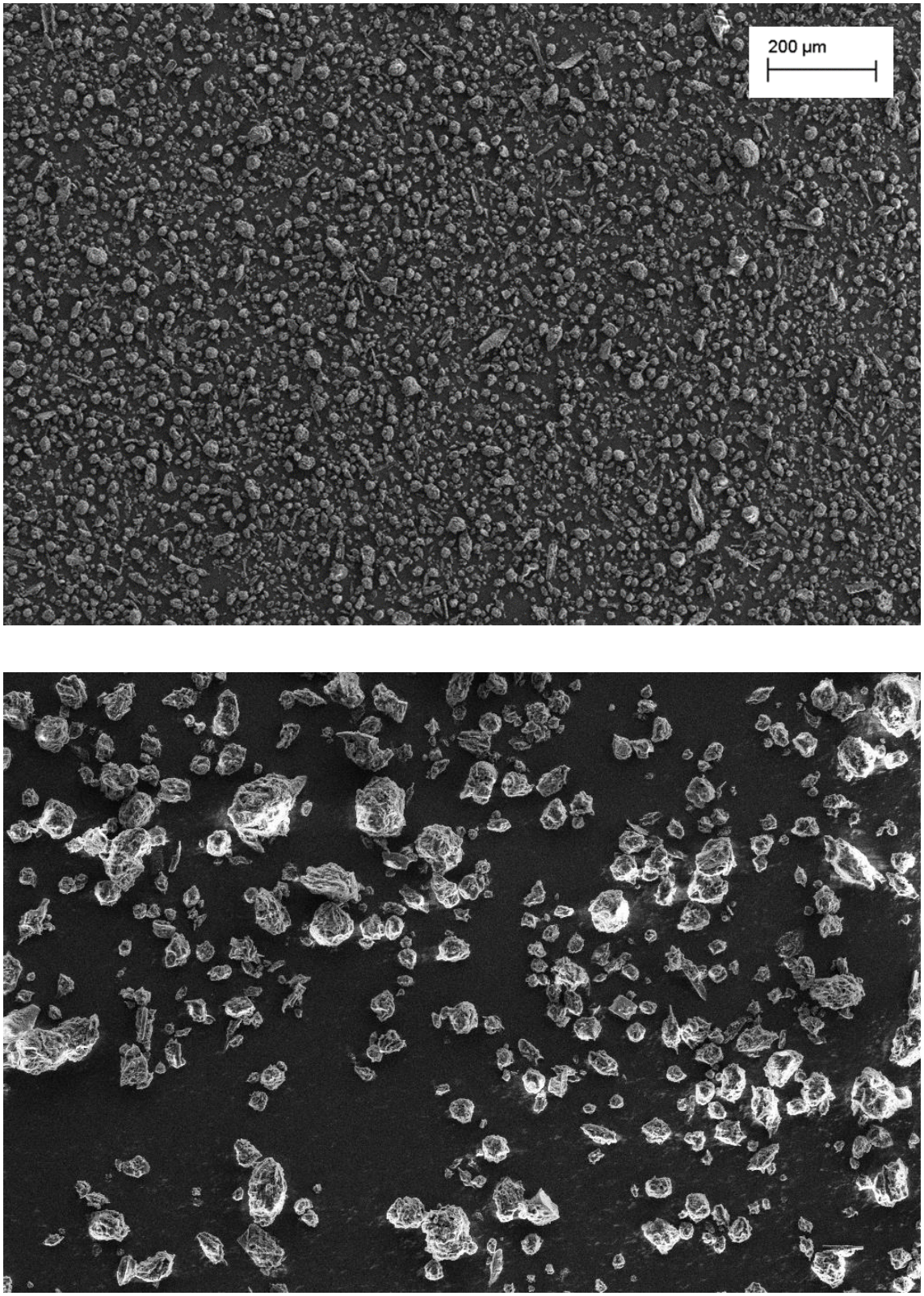

Figure 37: SEM images of AS lignin powder used for tablet formulation

Bulk density of the particles was found to be 450 kg/m^3 and 473 kg/m^3 for the coarse and the fine fraction of the as seen in Table 12 below. The flow index of the powder was calculated to be 16.96 in case of coarse fraction and 9.36 in case of fine fraction. The interparticulate shear in the coarse and fine fraction of the particles was calculated to be 117 Pa and 218 Pa respectively. The values show that the flowability of these particulate bulk solids is good (coarse fraction - free flowing; fine fraction - easy flowing). The unconfined yield strength of the coarse fraction (426 Pa) is low when compared to the fine fraction (763 Pa). The effect of the unconfined yield strength provides information on discharge patterns in the hopper, a lower unconfined yield strength infers that the particles will flow easily and no additional force is needed [191]. Furthermore, as the unconfined yield strength of the fine fraction is 763 Pa, the granulation of this powder is done to increase flowability and reduce cohesion [192]. A summary of the powder properties of the lignin used in this study can be seen in Table 12.

Table 11: Flow property measurement using the Jenike shear cell.

Sample name	Consolidation stress [Pa]	Unconfined yield strength [Pa]	Flow index (ff_c)	Flowability	Shear stress [Pa]	Bulk density [kg/m3]	Angle of internal friction [°]	Tableting process
Coarse	7232	426	16.96	Free flowing	117	450	32.4	Direct compression
Fine	7138	763	9.36	Easy flowing	218	473	30.5	Wet granulation

The tap density of the samples was measured using a Jolting volumeter and was found to be 519 kg/m^3 for coarse fraction and 560 kg/m^3 for fine fraction. The Hausner ratio and Carr's index are industrially followed values of flowability in case of pharmaceutics even though the observations are established empirically. The Hausner ratio for coarse and

fine fraction are calculated as 1.15 and 1.18 respectively and hence has a good flowability [193]. The Carr's index is a measure of the compressibility of the powder and was calculated for coarse and the fine fraction as 13.29 and 15.54 respectively. Carr's index below 15 is an indication is a measure of good flowability and above 25 is poor flowability. The coarse fraction shows good flowability whereas the fine fraction has fair flowability [194]. The fine fraction of lignin was considered for granulation while the coarse fraction was used directly for direct compression due to good compression and flow properties [191, 194].

5.4.2 Compression properties of lignin during direct compression

The use of pure lignin in the compression process highlights the lignin ↔ lignin interaction while the tableting process. The thickness of the tablet is inversely proportional to the increase in the compression force. As the displacement of the punch increased the force increases, and there is a higher compaction force generated that compresses the tablet to the minimum. The diameter of the tablet remains unchanged due the initial size if the die, but minor variations in the radius are seen due to the axial relaxation of the tablets. Furthermore, the breakage force is proportional to the increase in the compression force.

Table 12: Breakage force and tablet disintegration time of pure lignin samples.

COMPRESSION FORCE (KN)	THICKNESS (MM)	DIAMETER (MM)	BREAKAGE FORCE (N)	MASS (MG)	DISINTEGRATION TIME (SEC)
75	5.66 ± 0.01	10 ± 0.01	32.2 ± 3.6	315.2 ± 4.2	30 ± 3
80	5.22 ± 0.02	10 ± 0.03	47.0 ± 3.6	311.7 ± 2.9	39 ± 5
85	4.7 ± 0.01	10 ± 0.02	72.8 ± 4.5	314.2 ± 3.8	103 ± 12
90	4.29 ± 0.01	10 ± 0.04	104.8 ± 3.6	314.6 ± 1.9	293 ± 42
95	3.78 ± 0.01	10 ± 0.02	186 ± 6.7	316.0 ± 2.3	1804 ± 2

The mass of the tablets as seen above in Table 13, it can be observed that the lowest (75 kN) and highest (95 kN) compression forces yield the higher masses in all the tablets and formulations tested. This can be due to the fact that higher particle rearrangement in case of lower forces causes the mass of the tablets to be loosely held to the surface of the tablet whereas, in the case of highest compression forces the highest degree of plastic deformation causes the maximum compaction of the particles in the die. Although this information is important to consider on manufacturability of powders, the mass difference is not significantly different as established in the European Pharmacopoeia 7.0 method 2.9.40. Uniformity of dosage units, which establishes an acceptance limit of 25 mg difference. Very low breakage forces (<60 N) signify the instability of the tablets and high mass loss due to low tensile strength of the tablet, whereas the high breakage forces cause higher disintegration time due to minimized porosity in the tablet. The small porosity of the tablet increases the wicking time, thus decreasing the permeation rate of the solvent into the bulk of the tablet significantly. This effect can be seen in Figure 39 where the tablet hardness is plotted with respect to the compression forces.

Capillary action is considered the first step in tablet disintegration, this occurs when the tablet is placed in the aqueous medium and this penetrates it, the medium will replace the air on the primary particles and weaken the intermolecular bonds. After that, breakage of the tablet starts, and fine particles will be released to the medium, the velocity of the water uptake will depend on the hydrophilicity or hydrophobicity of the drug and excipients as well on the tablet hardness. Due to these facts, it is expected that increasing the mechanical strength of the tablet will delay the disintegration time, the small porosity of the tablets caused by high compression forces will increase the wicking time, thus decreasing the permeation rate of the solvent into the particles. This effect can be seen in Figure 38 where the tablet hardness is plotted with respect to the compression forces.

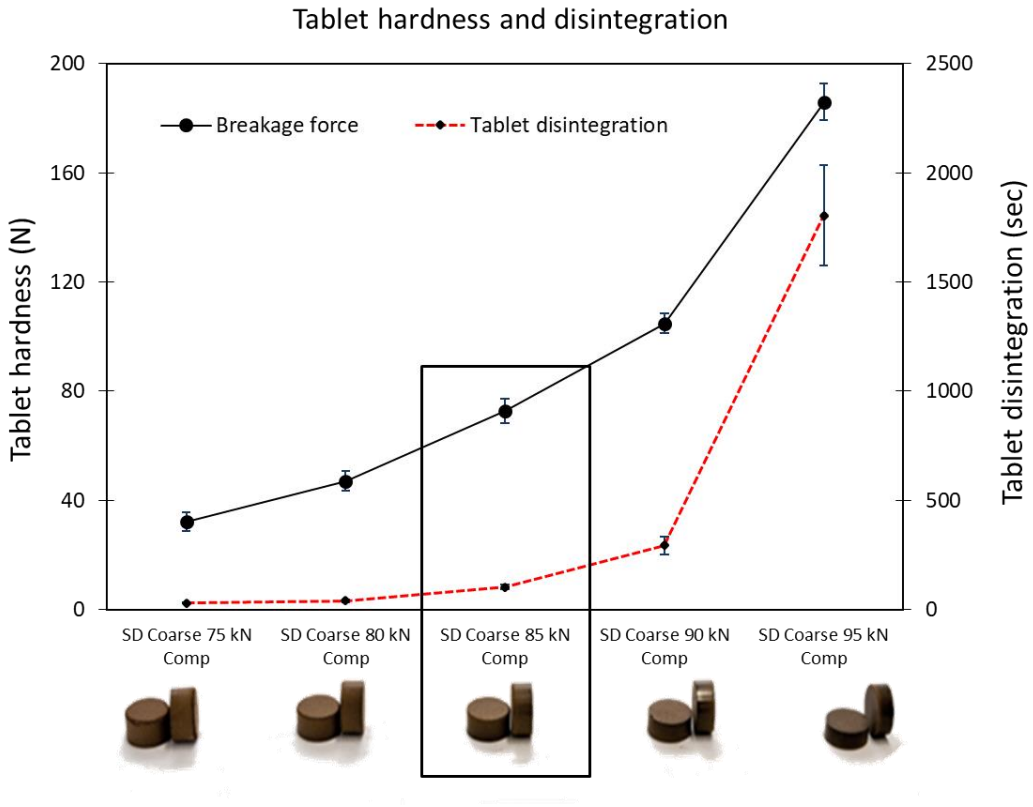

Figure 38: Tablet hardness and disintegration time of pure lignin tablets at different compression forces.

5.4.3 Mixture design to optimize the use of lignin in solid dosage formulations.

Four different designs were considered (data not shown) and the mixture of Disintegrant, Binder and AS Lignin (DBL) was statistically significant. The design was composed of 13 proportions of components. The mixture was modeled for the response of tensile strength using Scheffe's special cubic model and the results of the ANOVA for the polynomial function of the response are seen in Table 14. The regression of the model had 6 degrees of freedom and the residual error of the model had 6 degrees of freedom. The overall model was significant with a P-value 0.01 and R^2 is 89.49%. The linear interactions and the overall quadratic interactions were found to be significant with P-values 0.011 and 0.021 respectively. The response showed the significance of binder and lignin interaction with value 0.034. The model's F-value was 8.52 implying that the model is significant and there is a probability of 0.98% chance that an F-value this large could occur due to noise. Based on the ANOVA (Table 14), the model equation of the response was found out to be:

$$Tensile\ Strength = -18.21D + 16.13B + 0.64L - 15.57DB + 32.6DL - 30.92BL + 102.57DBL$$

Table 13: ANOVA of tensile strength for the formulation of DBL.

SOURCE	**D**	**SEQ SS**	**ADJ SS**	**ADJ MS**	**F-VALUE**	**P-VALUE**
REGRESSION	6	2.4818	2.4818	0.4136	8.52	0.01
LINEAR	2	1.4329	1.0061	0.5030	10.36	0.011
QUADRATIC	3	0.8549	1.0418	0.3472	7.15	0.021
DISINTEGRANT*BINDER	1	0.0045	0.0106	0.0106	0.22	0.656
DISINTEGRANT*LIGNIN	1	0.6078	0.1532	0.1532	3.16	0.126
BINDER*LIGNIN	1	0.2424	0.3654	0.3654	7.53	0.034
SPECIAL CUBIC	1	0.1939	0.1939	0.1939	4	0.093
DISINTEGRANT*BINDER* LIGNIN	1	0.1939	0.1939	0.1939	4	0.093
RESIDUAL ERROR	6	0.2913	0.2913	0.0485		
TOTAL	1	2.7732				
R_2	**89.49%**					

5.4.4 Effect of the components in the response tensile strength

The results of the effect of each individual/liner component (Disintegrant, Binder and AS Lignin) on the tensile strength of the tablets can be observed in Figure 39. The design space is marked as a grey square in the figure and shows the component having a tensile strength in the region of 1 – 2 MPa (requirement of the tableting process is 1.7 MPa). The binder plays an important role in the processability of tablets, directly relating its content

with higher tablet stability and higher tensile strength. The particle size appears to play a role in the compression process, since the plastic and elastic behavior alters the final tensile strength. For instance, the binder used in this study (lactose monohydrate) has the highest particle size among the other ingredients with particle size D_{90} of 250 µm, whereas the microcrystalline cellulose and AS lignin had particle size of D_{90} 116 µm and 83 µm respectively. The variation and the wide particle size distribution in the formulation creates a tablet with denser packing and increases the overall weight of the tablet largely due to the effect of particle rearrangement within the die during tablet compression.

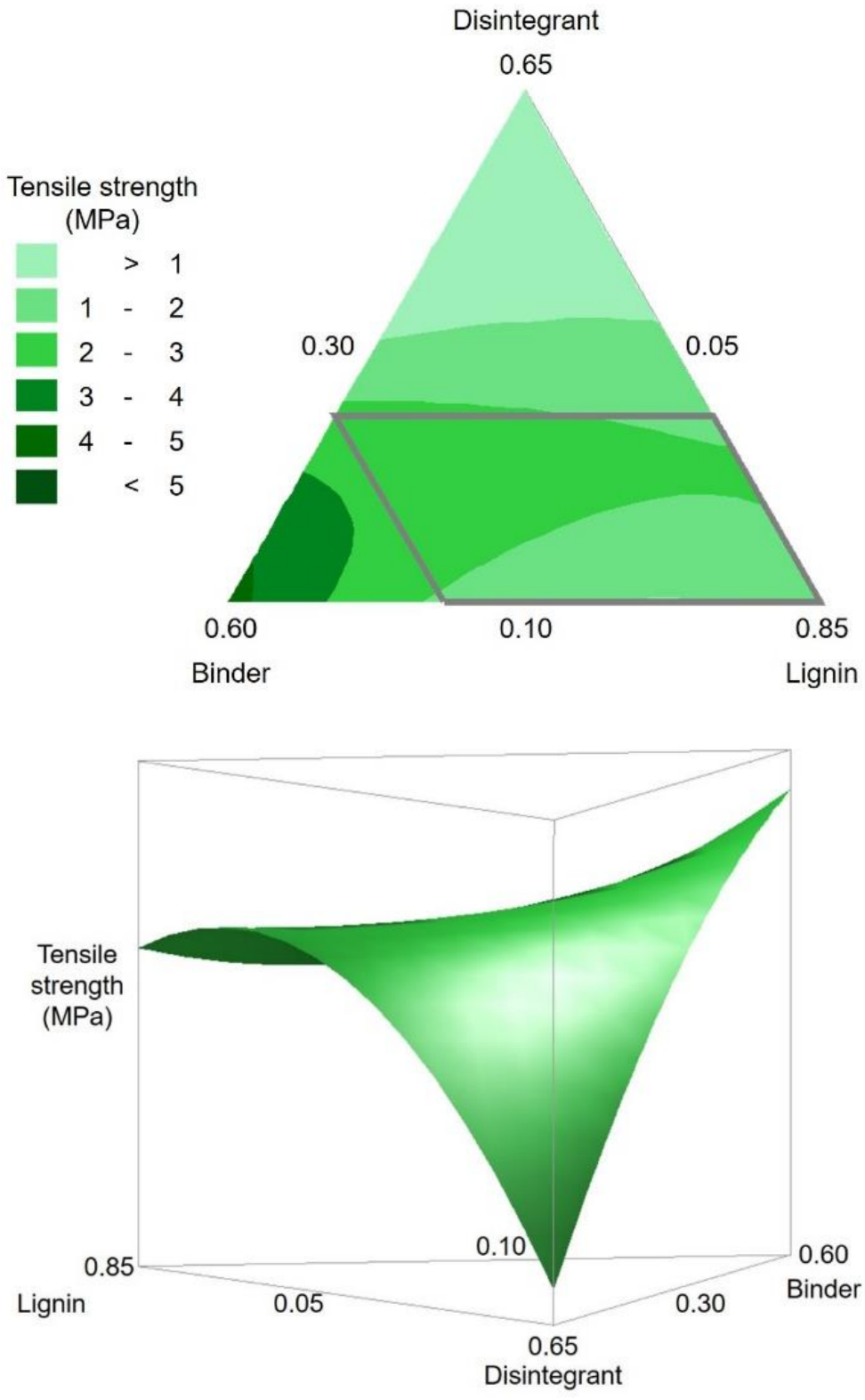

Figure 39: Contour and surface plot of tensile strength for the formulation Disintegrant Binder Lignin.

The samples with the highest mass proportion of binder (0.4 in the design: 0.2; 0.4; 0.4) yielded the highest average mass of the tablet (444.8 ± 11.8 mg). The compressibility and the flow properties are affected in this case by the particle size distribution of the formulations. The smaller particles play the void filling role between the larger particles, which increases the relative density of the tablet and reduces the starting porosity or specific tablet volume. This results in a high compressibility, highest weight and denser packaging [195]. The flow characteristics are affected due to the difference in bulk density which creates a wider variation in the mass of the tablet (11.8 mg). The tablets with the lowest friability (0.49 %) have the highest bulk density (1.231 ± 0.034 g/cm^3). The high variations in the bulk density of the formulation should be avoided and thus the choice of equal proportions of the components in the formulation is not appropriate. The bulk density and the particle size distribution are correlated terms which contribute to the tensile strength of the tablet.

Moisture content is also a factor that affects the tensile strength of the tablet. Aquasolv lignin had a moisture content of 4.6%, MCC has a residual moisture content of ≤5% and lactose monohydrate has typically 4.5–5.5% water content, as described by supplier. Moisture content in the formulation enhances the formulation of solid bridges during the compression process. On the other hand, the downside of moisture effect is also the sticking of the particles when flowing from the hopper to the die prior to compression. Particle shape is also one of the most important factors that contribute to the tensile strength of the tablet. Spherical granules have a lesser affinity to form interparticulate bonds thus affecting the overall composition of the tablet. The SEM images of MCC and lactose monohydrate in Figure 40 show that the particles are irregular shaped and have a rough surface. This creates a mechanical interlocking as the prolonged increase in the compression forces. The effects of the binder and the rough and irregular shaped lignin seen in Figure 37, this allows to create tablets with properly rearranged and mechanically interlocked compacted solid dosage form.

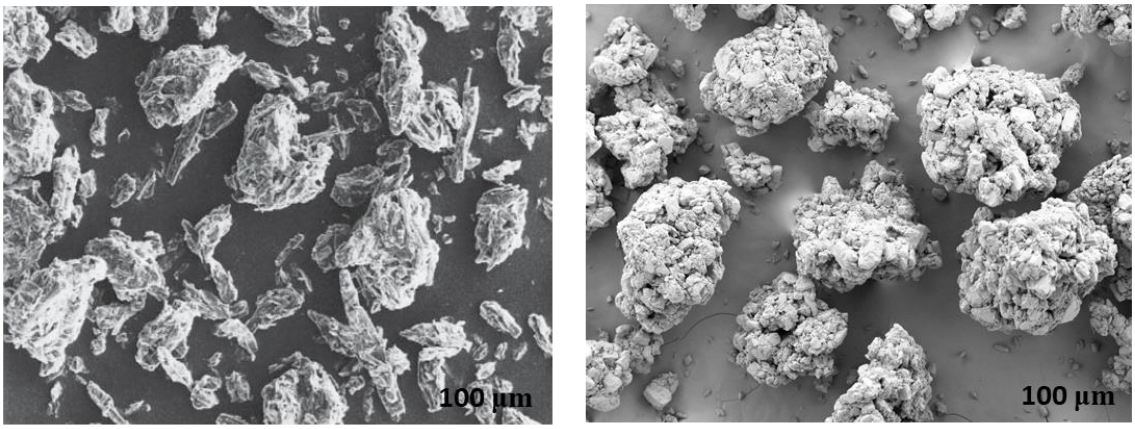

Figure 40: Excipients used in DBL formulation: microcrystalline cellulose (ACCEL – 101/ Lehmann & Voss) (left) and lactose monohydrate (Tablettose 100) (right).

5.4.5 Optimization of proportions for tensile strength and disintegration

The responses tensile strength and disintegration were optimized to target values with composite desirability. The tensile strength of the tablets was set to 1.7 MPa which is an industry standard for large production units and for scale-up. The target disintegration time is set to 180 secs for future dissolution experiments for the formulations loaded with ibuprofen. The composite desirability of the optimization was found to be 0.9812 and the individual desirability for tablet disintegration time was 0.96394 (for the value 173 seconds) and for tensile strength was 0.99885 (for the value 1.7015 MPa). The proportions in the blend were obtained to be 0.1453, 0.2657, 0.5890 for Disintegrant, Binder and Lignin proportion in the mixture.

Based on the computed optimized proportions, in the following proportion of the blend tablets were pressed at 85 kN and then analyzed for hardness (123.9 ± 7.1N), average mass (391.68 ± 6.91 mg) and mass deviation (1.45%) and dimensions of the tablet (φ = 10 ± 0.01 mm and h = 4.73 ± 0.02 mm). The tensile strength was calculated to be 1.667 ± 0.093 MPa and the disintegration time was 150 ± 16 s. The deviation of tensile strength was 2% and the disintegration time was 12% from the predicted optimized response. The values of the predicted responses are within the acceptable range due to which the proportions in the blend of $DBL_{optimized}$ are used in the preparation of formulation containing ibuprofen with 50% w/w and 70% w/w of ibuprofen.

5.4.6 Wet granulation

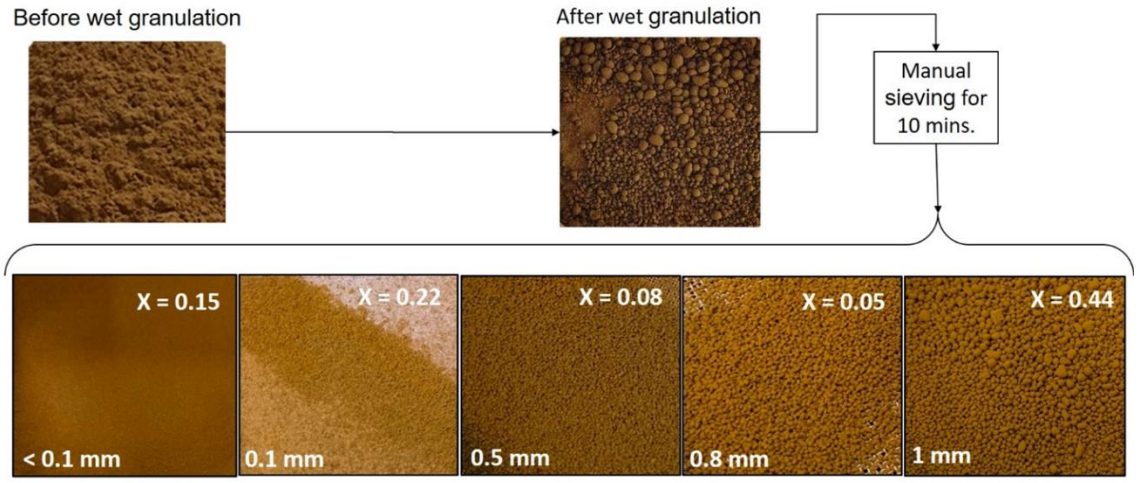

Figure 41: Granulated formulations obtained by blending AS Lignin with Lactose Monohydrate and Microcrystalline Cellulose.

Table 14: Composition of wet granulation powders

COMPOSITION	PROPORTION
DISINTEGRANT	0.2
LIGNIN	0.61
BINDER	0.19

5.4.7 Formulation of lignin-based tablets using Ibuprofen as model drug

Ibuprofen, being one of the most used non-steroidal anti-inflammatory drugs with low water solubility, was used as a model API in this study. To evaluate the effect of lignin, which is amphiphilic in nature, on the tablet disintegration of granules and compressed tablets containing Ibuprofen and assess the potential of lignin as a carrier for efficient release of API. For the dissolution studies and analysis of the release kinetics. Ibuprofen was loaded in the blend of $DBL_{optimized}$ at concentrations of 50% and 70% for the direct compression and 50% in the case of wet granulation. The samples were mixed in an ultra-mixer for 15 min prior to the process of tableting to create a well-mixed powder blend and eliminate ibuprofen hygroscopicity effects. The high tendency of sticking to the

punches and the low flowability issues of ibuprofen provide a comparison of the different techniques.

Table 15: Comparison of tensile strength and friability of formulations loaded with ibuprofen.

Formulation Components	**Ratio (Ibuprofen: Excipients)**	**Compression force (kN)**	**Tableting method**	**Tensile strength (MPa)**		**Friability loss (%)**
				Mean	Std dev	
Ibu with $DBL_{optimized}$	0.5:0.5	85	Direct compression	0.911	0.125	0.76
		90		1.785	0.236	0.79
		95		2.685	0.379	0.54
		100		2.848	0.263	0.58
IBU WITH $DBL_{WET\ GRANULATION}$	0.7:0.3	85	Wet granulation	0.618	0.207	11.18
	0.5:0.5	85		1.247	0.174	0.85

Preliminary observations of the formulation are that direct compression has and added advantage of reducing the number of steps as compared to the wet granulation techniques. The moisture sensitivity is an added issue which gives direct compression an upper hand over the wet granulation. Furthermore, the use of solvent shows a high rise in microbial levels in case of wet granulation and the unnecessary exposure of any drug to the moisture and heat can never be justified even if the compression process exerts lethal effects on the survival of microorganisms. The tablets compressed that are described in this chapter at several forces for the process of direct compression show a significant increase in the tensile strength with the gradual increase in the compression force seen in Table 16 and Figure 38. The friability of the tablets lies well within the acceptable limits with lignin performing better in case of direct compression with low friability at similar compression forces. The 70% ibuprofen was an experimental failure due to very low tensile strength of 0.611 ± 0.207 MPa and a friability loss of 11.18%. This proved that ibuprofen significantly reduces tablet integrity and has poor compaction

properties. In this regard, the WG tablets (1.247 ± 0.174 MPa) showed a higher tensile strength as compared to DC tablets (0.911 ± 0.125) at 85 kN due to the stability of the granules and the ability to form solid bridges as well as mechanical interlocking which is the only phenomenon seen in DC tablets. With the rise in the compression force in the case of DC tablets from 85 to 100 kN, the observed tensile strength value changes significantly and the loss in friability reduces as well. This is due to a more efficient particle rearrangement and a higher compression force creates a better interparticulate bonding.

The binder lactose monohydrate which has good sticking properties is extremely critical in case of the value of the tensile strength. The interaction of lignin with MCC and lactose monohydrate showed the balance of tablet to avoid capping or chipping leading to high friability. The MCC is a self-lubricating excipient with good compression properties that complement the lactose monohydrate. Lignin, as seen before, has a quadratic interaction with the binder in the blend thus creating a more stable blend even at high concentrations of 50% of ibuprofen in the tablet. The spherical and semi spherical structures of the lignin and binder provide a better flowability. This is evident from the average mass of the tablet and the mass deviation. In case of DC tablets at different forces of 85, 90, 95 and 100 kN the average mass was 384.60 ± 5.98 mg, 391.04 ± 7.24 mg, 394.16 ± 4.67 mg and 395.65 ± 3.78 mg respectively with a maximum mass deviation of a 4% (max allowed is 5%). On the other hand, WG tablets had a higher mass deviation due to a rise in moisture content.

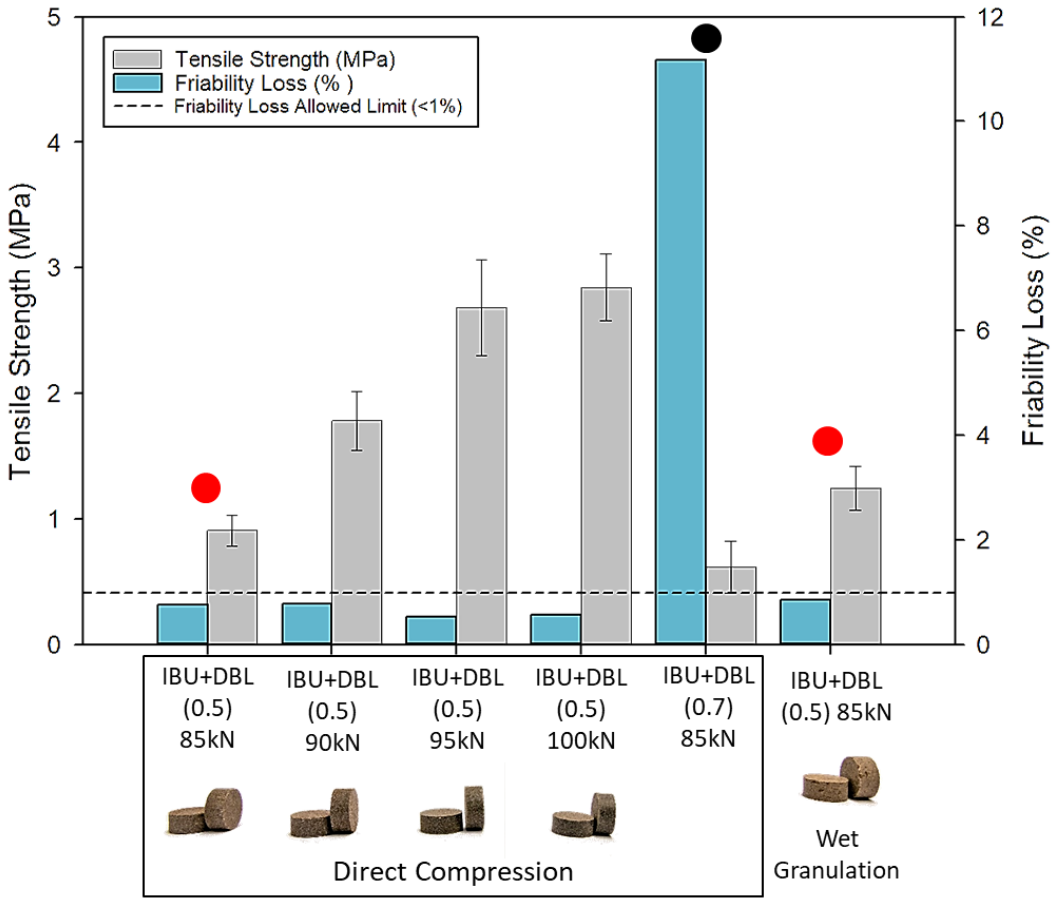

Figure 42: Tensile strength and friability loss of the formulations loaded with ibuprofen. Red dots indicate same formulations obtained via direct compression and wet granulation. Black dot indicates the highest concentration of ibuprofen used in this study.

Apart from the tensile strength, flowability, compressibility and the friability of the blends loaded with API; disintegration plays an important role in the final dissolution process and drug release studies. The tablets were tested for disintegration according to USP guidelines. The DC tablets at higher compression forces of 95 and 100 kN did not disintegrate within the specified disintegration time. The tablets which disintegrated were the tablets at forces of 85 kN for both DC and WG and 90 kN for DC tablets. The disintegration time difference between the DC and WG tablets at 85 kN is 548%. The wet granulation of the process creates granules that are hard and don't disintegrate quickly. Even with a tensile strength deviation of 43% between DC – 90kN and WG – 85kN the disintegration time difference is deviating by 15%. The disintegration time of the WG – 85kN should have been much smaller but the solid bridges in the agglomerated blend of

WG disintegrate into granules at the end of the disintegration process. These granules take longer to break into smaller fragments to finish the dissolution process.

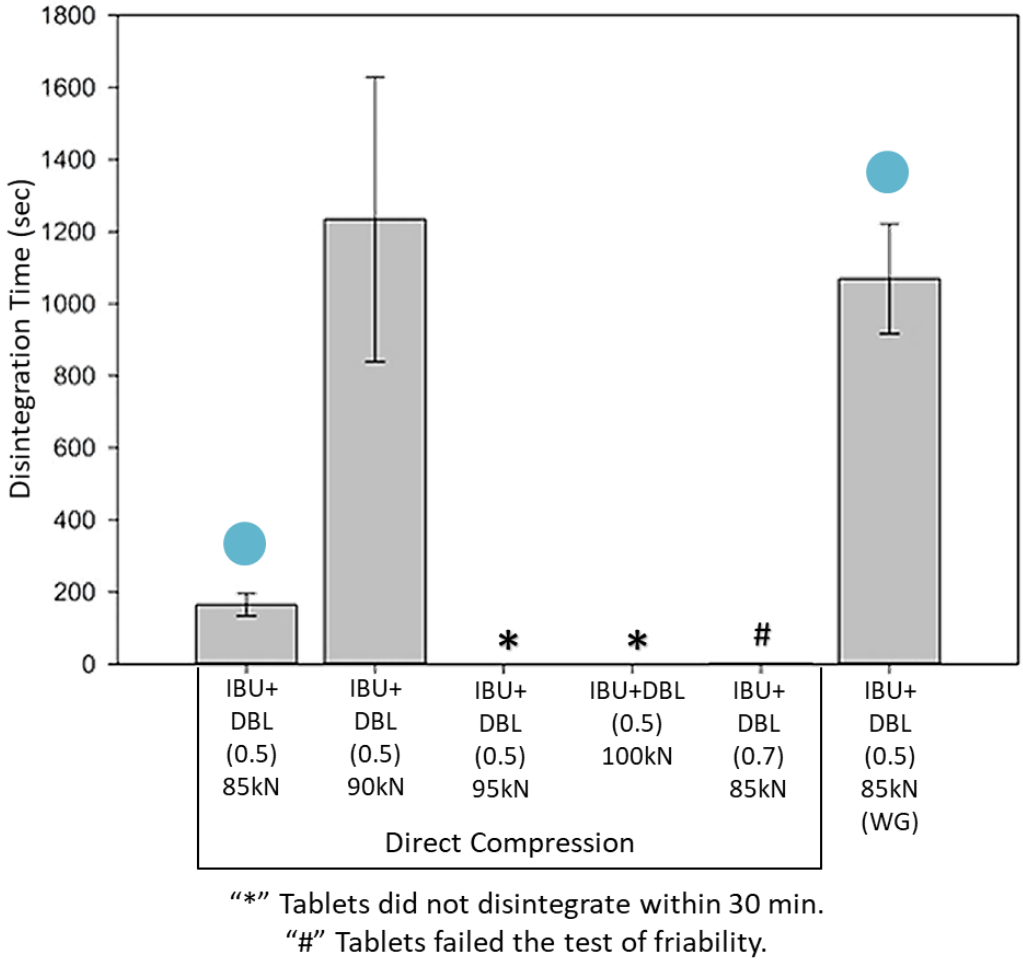

Figure 43: Comparison of the disintegration time of formulations loaded with ibuprofen. Blue dots indicate same formulations obtained via direct compression and wet granulation.

The disintegration time is affected by properties such as swelling, porosity and water sorption time. These factors were analyzed for the disintegrating tablets and it showed that the DC – 85 kN had a higher void volume and porosity thus showing agreement to lower disintegration time. The MCC is a disintegrant by creating micropores whereas the lactose monohydrate is water-soluble. The wetting properties of lignin counteract the hydrophobic effect of ibuprofen. The lignin particles have a higher degree of spreading in the case of WG – 85 kN as lignin particles are the smallest in particle size in the particle size distribution of blend containing the MCC, lactose monohydrate and lignin thus creating a covering effect on the granules (Figure 44). The tablet showed better wetting.

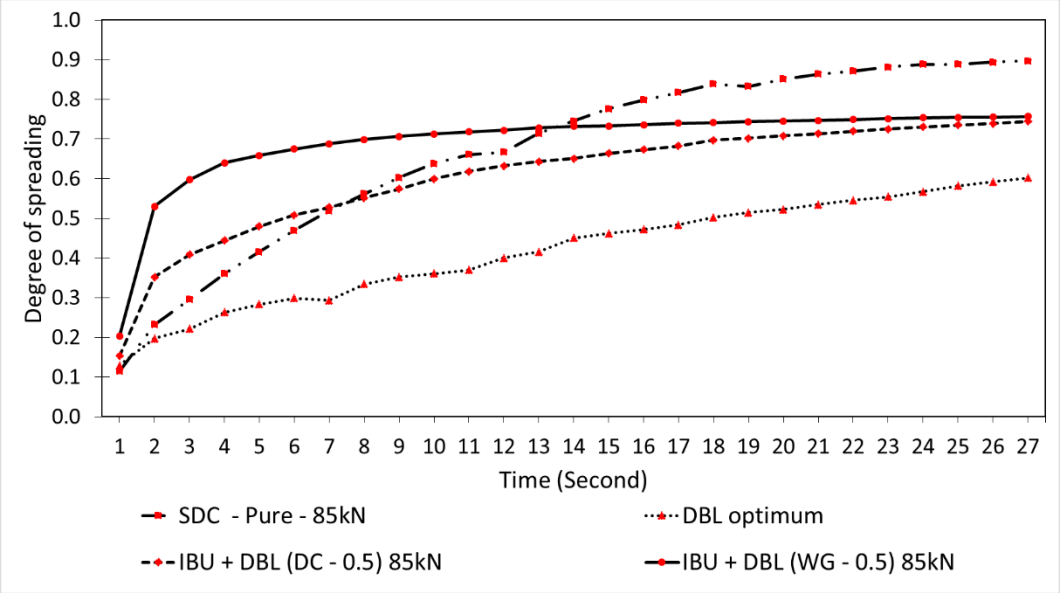

Figure 44: Comparison of the degree of spreading of pure lignin, optimized DBL and the formulation loaded with 50% ibuprofen for DC (directe compression) and WG (wet granulation) at 85 kN.

The water sorption time in case of WG – 85 kN is also lesser as compared to the DC – 85 kN due to the surface wetting phenomena. This shows the influence of lignin and the interaction effects of lignin in the blend of the formulation. The incorporation of the API reduced the tensile strength yet, the stability of the tablets validates the optimized formulation. The tablets were further analyzed in the dissolution studies. The tablets that failed the disintegration test were also analyzed in the dissolution to assess the dissolution efficiency and check for effects of sustained release of the tablets in the system. The major factors that affect the disintegration time that were observed from the mixture design and the formulation loaded with the API are water sorption, swelling, porosity and tensile strength.

5.4.8 Contact angle and wetting properties of pharmaceutical formulations

The formulation of SDC pure had the highest degree of spreading at 0.9 followed by the ibuprofen in $DBL_{optimized}$ (50 wt.%) manufactured by wet granulation (0.8) and direct compression (0.7) respectively and finally $DBL_{optimized}$ showed the least degree of spreading at 0.6 (Figure 44) among the four formulations. The variation in the degree of spreading can be attributed to the increase in the content of polymeric materials

(microcrystalline cellulose) along with lignin in the formulation that makes the surface more hydrophobic during the interaction with water [196]. This can be confirmed by the variation of the concentration of microcrystalline cellulose from 14.5 wt.% in $DBL_{optimized}$ to 7.75 wt.% in ibuprofen with $DBL_{optimized}$ and 0 wt.% in SDC pure.

The additional intermolecular and intramolecular hydrogen bonding makes it insoluble in usual aqueous solutions while the swelling properties of the microcrystalline cellulose is disadvantageous for spreading, by creating micropores for the vertical absorption of water through solvent penetration [197, 198]. The presence of part polar functional groups in the ibuprofen allows it to interact in a finite manner with the droplet of water favoring a relaxing phenomenon. Other authors working with biopolymers such as microcrystalline cellulose and their interaction with model drugs have also found the degree of spreading to remain between 0.6 – 0.7 in water systems and 0.9 in organic solvents like isopropanol and ethylene glycol [199, 200].

Apart from the degree of spreading, the dynamic measurement of the contact angle Figure 30 provides information for the absorption rate of the liquid in a dissolution medium depending on the particle characteristics of each surface [200]. In the absence of microcrystalline cellulose in the tablet matrix the absorption rate of the water is higher and absorption time is smaller as compression of the tablets influence the porous surfaces as well as the tortuosity, affecting the disintegration time and the drug release in the dissolution medium [201]. In water, there is a balance between the attractive and the repulsive interactions, where the increase in the amount of microcrystalline cellulose increases the repulsive interactions, thus affecting the surface free energies and water absorption rates substantially in the compressed matrices [196, 202]. Other authors have reported the absorption rates to be as 10 ° - 4 °/s and time up to 30 seconds [200, 201, 203].

5.4.9 Effect of process parameters on the disintegration of the formulation DBL

On the ANOVA analysis in the run order DBL Table 14, several factors affecting the process of disintegration highlighted that water sorption capacity, swelling index and the effective pore radius of the formulation had significant effects on the process. Following that, with a composite desirability of 92.98 % on the responses of tensile strength and

disintegration in this study, the predicted values were 152 s and 1.8 MPa respectively, for the water sorption capacity, swelling index and effective pore radius to be 147 secs, 33.45 % and 19.44 µm, respectively. The experimented values of the $DBL_{optimized}$ had a deviation of 1.4 %, 6.6 % and 2.9 % for water sorption time, swelling index and effective pore radius respectively. Comparing to previous studies of the commercially available excipients showed that rapid penetration of the water followed by the swelling of excipients lead to the rapid disintegration of tablets [204, 205].

Table 16: Comparison of predicted and experimental values of the powder characteristics of relevance for disintegration time.

Powder Characteristics		**Predicted**	**Experimental**	**Deviation**
Water Sorption time	WST (sec)	147	145 ± 7.1	1.4%
Swelling Index	SI (%)	33.45	35.64 ± 1.46	6.6%
Effective pore radius	Reff (µm)	19.44	18.87 ± 3.32	2.9%

5.4.10 Dissolution profiles of the different formulations

The results of the dissolution profiles for each ibuprofen with $DBL_{optimized}$ pressed at different compression forces in the dissolution media (in vitro) under simulated physiological conditions are seen in Figure 45. The dissolution profiles show that the increase in the compression force within the tablet leads to a decrease in the dissolution profile of the model drug in the dissolution media [206]. The results are consistent with those observed in the disintegration test of the formulation and the effect of surface property affecting the release of the drug [200, 206]. The comparison of the direct compression and the wet granulation indicated the dissolution efficiency at the end of the experiment (5 hrs.) to be 100 % and 98 % respectively while the 60 % release at the end of 20 minutes and 40 minutes respectively. The overall dissolution is affected by the diffusion of the drug into the dissolution media and the effect of the tablet morphology, where direct compression process showed a higher diffusion coefficient with higher rates of dissolution whereas the higher compaction in wet granulation had a more controlled release of the drug [207].

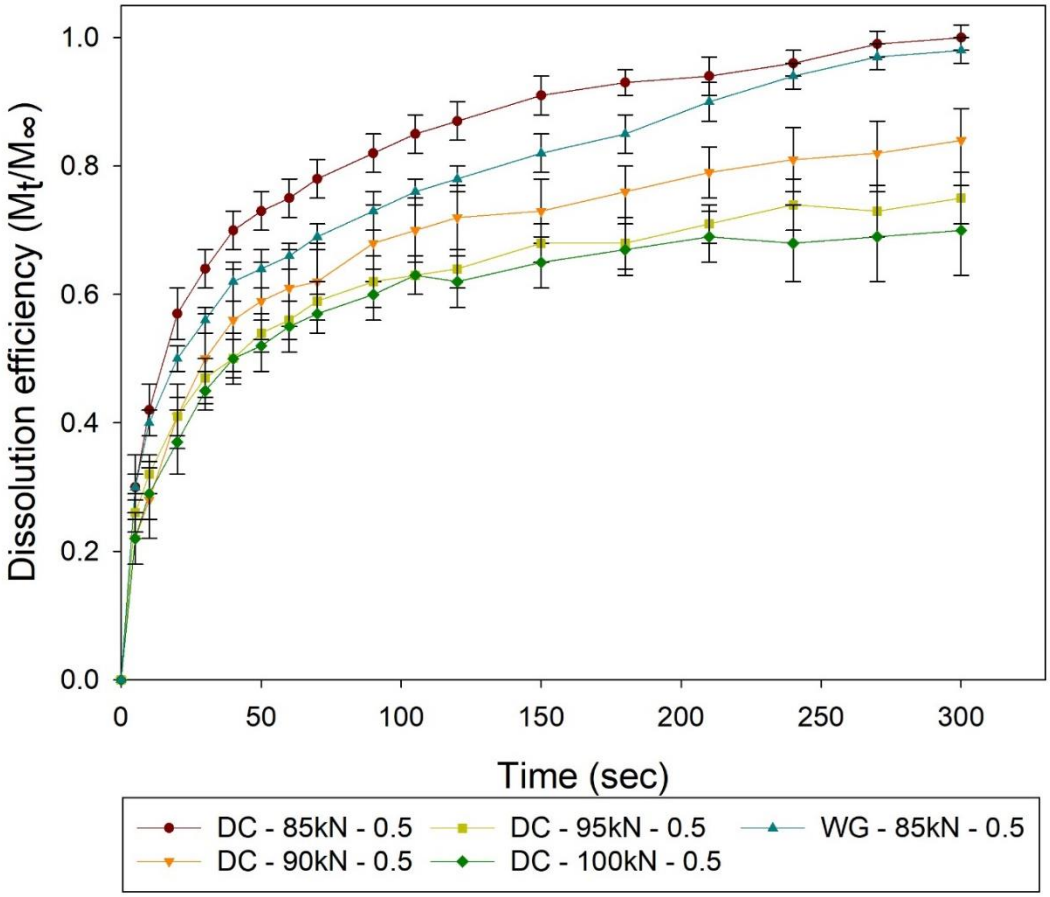

Figure 45: Drug release profile of the tablets of lignin at different forces.

It is indicated that the presence of lignin in the formulation enhances the dissolution of the API, by creating pores and facilitating swelling in the lower compression forces whereas at high compression forces through the effect of surface erosion [208]. The higher forces see a slower effect of the disintegrant due to high plastic deformation, intense reduction of the effective porosity and reduction in the equilibrium concentration of the API by reducing the surface area and surface energy for dissolution [206-208]. Other authors have worked with the process of roll compaction and milling process and have reported that an increase of compression force has a significant decrease in the release of API [207, 209] whereas using lignin as an excipient in the formulation enhances the release rates in the in vitro dissolution [206, 210].

5.4.11 Conclusion part III

AS Lignin was used to produce tablets via direct compression and wet granulation and as a potential carrier for Ibuprofen. The parameters were optimized to obtain tablet dosage forms which are in agreement with the quality established by the European Pharmacopoeia and industrial standards for tensile strength and disintegration time. Other aspects of the drug delivery such as water sorption, swelling and drug release profiles were investigated and the effects of tensile strength and disintegration time were proven. The approach showed the novelty of using lignin on one side, which enhances surface spreading and contribute to dynamic swelling that affect the disintegration time and drug release; while on the other side stabilize the tablet by providing rough surface for better mechanical interlocking, low friability and better tensile strength. This research work highlights the potential of valorizing AS lignin and the technologies and processes used should be translated to industrially available Hydrolytic lignins being obtained by second generation biorefineries.

Conclusions of the doctoral thesis

Lignins from second generation biorefineries have proven to be promising materials for various industrial applications, mostly due to its phenolic structure and multifunctionality like antioxidant and antimicrobial, along to a polymeric phenolic structure that can mimic oil-based products. Particularly, Aquasolv Lignin obtained from liquid hot water pretreatment and enzymatic hydrolysis offers an ideal candidate molecule for application in new areas like life science applications, mostly due to its free of solvent nature. However, the valorization and application of this lignin is not trivial, the processability and manufacturability of the lignin will highly depend on its particle properties like particle size, particle size distribution and morphology, to name a few. The selection of an appropriate method to obtain particles with controlled mean size appears crucial to further product development and formulation. In this regard, the process of spray drying is advantageous because it enables the integration of efficient drying and formulation of solids and these can be obtained in a controllable quality throughout the process, the process is also widely used for powder drying in pharma, food and cosmetic ingredients. Although the basic principles of the process appear as simple, the process becomes complex when the operational parameters in relation to a specific feedstock need to be chosen. In the present study, the focus was to tailor the final quality of lignin particles by using spray drying technology, a study was performed to understand the most critical process factors and the effect of those onto the quality of the obtained lignin particles. Design of experiments was used for this part of the work to establish multidimensional relationships between the factors and responses with a reasonable number of experiments.

Aquasolv lignin particles were obtained via spray drying and the desired quality was optimized by using design of experiments. It was proven that the particle size of the lignin, as well as the yield of powder are strongly dependent of the operating variables temperature, atomization pressure and feeding rate. A target particle size of less than 30 µm, moisture content of less than 4 wt%, semispherical particles as well as a yield of recovery after the cyclone of more than 50 wt% of material fed into the chamber were set for this work. From the process parameters evaluated, atomization pressure showed

the strongest effect on the particle size of the lignin obtained, followed by feeding rate and temperature. All the temperatures evaluated resulted in powders with moisture content lower than 4 wt% and no evident morphology changes were observed in the particles. SEM images showed that the produced lignin particles have a regular shape, spherical and semispherical and the particle size measurements confirmed that narrow particle sizes can be obtained in a reproducible way. These properties resulted in flowable powders that can be easily processed and applied into product formulation and existing industrial machinery, the good flowable properties exerted by the spray dried lignins are mostly due to their sphericity which causes less morphological interaction, the low moisture content has also a positive impact in preventing powder cohesiveness while flowing.

After the optimization of the process conditions to obtained spray dried particles, a thorough evaluation of the functionality of the powders was performed and a structure function relationship was established. For this, the Aquasolv lignin particles were compared to other novel lignin (Organosolv) as well as a technical lignin (Alkali) and a commercial lignin used for human consumption (hydrolytic lignin). An important aspect to consider the suitability of lignin for application in human consumption products is to confirm the non-cytotoxicity (safe to consume) of the material. The non-cytotoxicity of the spray dried AS lignin as well as the bioactive properties was thoroughly assessed in vivo and in vitro. The activities of this PhD work defined and provided the properties that AS lignin needs for its further development towards the pharmaceutical applications. The lignins tested differed in terms of water solubility (Aquasolv lignin > Organosolv > Alkali), molecular weight (Aquasolv lignin > Organosolv > Alkali) and phenolic OH content (Alkali> Organosolv > Aquasolv lignin). These molecular properties showed a clear pattern in cytotoxicity and antioxidant capacity. The lower molecular weight and higher phenolic OH content of the Organosolv and Alkali lignins resulted in higher antioxidant capacity compared to Aquasolv lignin, Organosolv 10-fold higher and Alkali 7-fold higher. However, the higher cytotoxicity in Caco-2 cells with the lowest concentrations to reduce cell viability by 50% was also found for Organosolv (5 mg/mL) and Alkali (10 mg/mL), whereas Aquasolv lignin showed no cytotoxic effect in all concentrations measured (0-20 mg/mL). With these results it can be concluded that an increase in the antioxidant capacity of lignins also increases their cytotoxicity, which should be considered considering the applicability potentials of each material. Based on

these results, the functionality of AS Lignin in targeted product prototypes can be further elaborated aiming high value applications such as cosmetics or pharmaceuticals. For the pharmaceutical applications of the spray dried particles, the oil adsorption capacity of the lignins was assessed in vitro and in vivo, using Wistar rats as model. Oil adsorption capacity can be positively correlated to lowering cholesterol and HDL levels in serum. The in vivo studies confirmed both the non-cytotoxicity of Aquasolv lignin as well as the pharmacological effect. It was shown that the Wistar rats supplemented with a high fat diet and lignin (50 mg) treatment showed similar effects than the group treated with simvastatin (a lipid-lowering allopathic medicine). Moreover, the Aquasolv lignin overperformed the conventional medicine in terms of safety for the liver, a supplementation of 100 mg of the lignin resulted in low levels of the enzyme Alanine Transaminase in Serum, which reflects low toxicity levels in the liver. The results of this work set the basis for further studies dedicated to treat hypocholesterolemia with lignin as a biobased and safer alternative, whether as a full replacement or as a coadyuvant to decrease the negative effects of allopathic medicine while delivering a similar pharmacological effect.

For a full assessment of the potential use of the spray dried particles into product formulation, an oral pharmaceutical form was produced based on both fractions of powders recovered in the spray dryer, coarse and fine. Tablets were used since they are the most common way of getting medicines and treatments and the lignin particles were tested as powder excipients where the processability with commercial excipients as well as the effect on the release of a model drug (Ibuprofen) was assessed. Wet granulation and direct compression processes were used to produce tablets and the final product was evaluated in terms of functionality -tablet swelling, drug release profiles and disintegration- as well as overall physical quality -tensile strength, breakage, and friability-. Aquasolv lignin particles contributed to the dynamic swelling of the tablet, promoting disintegration and drug release, on the other hand, the use of lignin particles as excipient yielded tablets with low friability and compliant according to international Pharmacopoeial methods.

As a conclusion of this work, it can be stated that the spray drying was successfully used to understand and control particle formation of Aquasolv Lignin. Moreover, parameters that influence particle formation are well studied and established for lignin. Now, lignin

particles can be designed by varying the spray drying conditions with the knowledge gained in this work, and the functionality of the designed particles is directly linked to the efficacy and functionality of the powders. An experimental framework and first proof of concept of the implementation of lignin particles into high value products was defined based on physical-chemical properties of the obtained powders and have the potential to be the basis for further studies of lignin utilization by using the principles of particle engineering.

Outlook

This research work proves the implementation of an easily scalable drying technology for design of lignin particles obtained from the Liquid Hot Water pretreatment and enzymatic hydrolysis process as well as strategies for valorization. The processing parameters and the conditions optimized for the Aquasolv Lignin can be transferred to industrially available lignins. These lignins differ in composition and this will have an effect in the particle formation too. Future investigations and efforts should be directed in studying multicomponent feeds and how the molecular arrangement of the different components takes place during drying. The possibility of designing particles based on placing components to the outer layer can open a whole new way of tailoring particle solubilities and functionalities and will expand the applicability of spray drying as a way for valorizing this type of materials.

Additionally, in terms of product formulation, the spray drying can be used to produce pre-formulated powders in which the lignin and other components (for example Ibuprofen) can be tailored in one single process. For this it will be important to consider the interaction between components during drying and potentially the formation of porosity in the particle shell. For pharmaceutical applications, this will be key to produce materials that are protecting the active ingredient while promoting controlled release. In terms of establishing a structure-function relationship for lignin there is room for an even better understanding of the mechanisms involved in functionality by using computational methods that predict interactions between the molecules.

References

1. Reynolds, W., C. Kirsch, and I.J.C.I.T. Smirnova, *Thermal-Enzymatic Hydrolysis of Wheat Straw in a Single High Pressure Fixed Bed.* 2015. **87**(10): p. 1305-1312.
2. Gil-Chávez, J., et al., *Optimization of the spray-drying process for developing aquasolv lignin particles using response surface methodology.* 2020.
3. Bhujbal, S.V., et al., *Qualitative and Quantitative Characterization of Composition Heterogeneity on the Surface of Spray Dried Amorphous Solid Dispersion Particles by an Advanced Surface Analysis Platform with High Surface Sensitivity and Superior Spatial Resolution.* Molecular Pharmaceutics, 2018. **15**(5): p. 2045-2053.
4. Patel, B.B., et al., *Revealing facts behind spray dried solid dispersion technology used for solubility enhancement.* Saudi Pharmaceutical Journal, 2015. **23**(4): p. 352-365.
5. Ziaee, A., et al., *Spray drying of pharmaceuticals and biopharmaceuticals: Critical parameters and experimental process optimization approaches.* European Journal of Pharmaceutical Sciences, 2019. **127**: p. 300-318.
6. Lisboa, H.M., M.E. Duarte, and M.E. Cavalcanti-Mata, *Modeling of food drying processes in industrial spray dryers.* Food and Bioproducts Processing, 2018. **107**: p. 49-60.
7. Baghel, S., H. Cathcart, and N.J.J.J.o.p.s. O'Reilly, *Polymeric amorphous solid dispersions: a review of amorphization, crystallization, stabilization, solid-state characterization, and aqueous solubilization of biopharmaceutical classification system class II drugs.* 2016. **105**(9): p. 2527-2544.
8. Albadarin, A.B., et al., *Development of stability-enhanced ternary solid dispersions via combinations of HPMCP and Soluplus® processed by hot melt extrusion.* 2017. **532**(1): p. 603-611.
9. Zhao, W., et al., *From lignin association to nano-/micro-particle preparation: extracting higher value of lignin.* 2016. **18**(21): p. 5693-5700.
10. Berlin, A. and M. Balakshin, *Industrial lignins: analysis, properties, and applications*, in *Bioenergy Research: Advances and Applications*. 2014, Elsevier. p. 315-336.
11. Lora, J., *Industrial commercial lignins: sources, properties and applications*, in *Monomers, polymers and composites from renewable resources*. 2008, Elsevier. p. 225-241.

12. Brodeur, G., et al., *Chemical and physicochemical pretreatment of lignocellulosic biomass: a review.* 2011. **2011**.
13. Prakash, A., et al., *Thermochemical valorization of lignin*, in *Recent Advances in Thermo-Chemical Conversion of Biomass*. 2015, Elsevier. p. 455-478.
14. Ekeberg, D., et al., *Characterisation of lignosulphonates and kraft lignin by hydrophobic interaction chromatography.* 2006. **565**(1): p. 121-128.
15. Gellerstedt, G., E.-L.J.H.-I.J.o.t.B. Lindfors, Chemistry, Physics, and T.o. Wood, *Structural changes in lignin during kraft pulping.* 1984. **38**(3): p. 151-158.
16. Laurichesse, S. and L. Averous, *Chemical modification of lignins: Towards biobased polymers.* Progress in Polymer Science, 2014. **39**(7): p. 1266-1290.
17. Perez-Cantu, L., et al., *Preparation of aerogels from wheat straw lignin by cross-linking with oligo (alkylene glycol)-α, ω-diglycidyl ethers.* 2014. **195**: p. 303-310.
18. Ingram, T., et al., *Comparison of different pretreatment methods for lignocellulosic materials. Part I: conversion of rye straw to valuable products.* 2011. **102**(8): p. 5221-5228.
19. Boeriu, C.G., et al., *Characterisation of structure-dependent functional properties of lignin with infrared spectroscopy.* 2004. **20**(2): p. 205-218.
20. Vanholme, R., et al., *Lignin biosynthesis and structure.* Plant physiology, 2010. **153**(3): p. 895-905.
21. Sun, Y.-C., et al., *Chemical changes of raw materials and manufactured binderless boards during hot pressing: lignin isolation and characterization.* 2014. **9**(1): p. 1055-1071.
22. El Hage, R., et al., *Characterization of milled wood lignin and ethanol organosolv lignin from miscanthus.* 2009. **94**(10): p. 1632-1638.
23. Zhao, X., et al., *Organosolv pretreatment of lignocellulosic biomass for enzymatic hydrolysis.* 2009. **82**(5): p. 815.
24. Perez-Cantu, L., et al., *Comparison of pretreatment methods for rye straw in the second generation biorefinery: Effect on cellulose, hemicellulose and lignin recovery.* Bioresource technology, 2013. **142**: p. 428-435.
25. Zhuang, X., et al., *Liquid hot water pretreatment of lignocellulosic biomass for bioethanol production accompanying with high valuable products.* 2016. **199**: p. 68-75.

26. Mosier, N., et al., *Features of promising technologies for pretreatment of lignocellulosic biomass.* 2005. **96**(6): p. 673-686.
27. Quraishi, S., et al., *Novel non-cytotoxic alginate–lignin hybrid aerogels as scaffolds for tissue engineering.* The Journal of Supercritical Fluids, 2015. **105**: p. 1-8.
28. Barapatre, A., et al., *In vitro evaluation of antioxidant and cytotoxic activities of lignin fractions extracted from Acacia nilotica.* International journal of biological macromolecules, 2016. **86**: p. 443-453.
29. Ugartondo, V., M. Mitjans, and M.P. Vinardell, *Comparative antioxidant and cytotoxic effects of lignins from different sources.* Bioresource technology, 2008. **99**(14): p. 6683-6687.
30. Dizhbite, T., et al., *Characterization of the radical scavenging activity of lignins––natural antioxidants.* Bioresource Technology, 2004. **95**(3): p. 309-317.
31. García, A., G. Spigno, and J. Labidi, *Antioxidant and biocide behaviour of lignin fractions from apple tree pruning residues.* Industrial Crops and Products, 2017. **104**: p. 242-252.
32. García, A., et al., *Lignin as natural radical scavenger. Effect of the obtaining and purification processes on the antioxidant behaviour of lignin.* Biochemical engineering journal, 2012. **67**: p. 173-185.
33. García, A., et al., *Study of the antioxidant capacity of Miscanthus sinensis lignins.* Process Biochemistry, 2010. **45**(6): p. 935-940.
34. Dong, X., et al., *Antimicrobial and antioxidant activities of lignin from residue of corn stover to ethanol production.* Industrial Crops and Products, 2011. **34**(3): p. 1629-1634.
35. Ponomarenko, J., et al., *Analytical pyrolysis–A tool for revealing of lignin structure-antioxidant activity relationship.* Journal of Analytical and Applied Pyrolysis, 2015. **113**: p. 360-369.
36. Núñez-Flores, R., et al., *Physical and functional characterization of active fish gelatin films incorporated with lignin.* Food Hydrocolloids, 2013. **30**(1): p. 163-172.
37. Lauberts, M., et al., *Fractionation of technical lignin with ionic liquids as a method for improving purity and antioxidant activity.* Industrial crops and products, 2017. **95**: p. 512-520.

38. Guo, Y., et al., *Transparent cellulose/technical lignin composite films for advanced packaging.* 2019. **11**(9): p. 1455.
39. Sadeghifar, H., D.S.J.A.S.C. Argyropoulos, and Engineering, *Correlations of the antioxidant properties of softwood kraft lignin fractions with the thermal stability of its blends with polyethylene.* 2015. **3**(2): p. 349-356.
40. Zhao, Y., et al., *The impact of lignin structural diversity on performance of cellulose nanofiber (CNF)-starch composite films.* 2019. **11**(3): p. 538.
41. Spasojević, D., et al., *Lignin model compound in alginate hydrogel: a strong antimicrobial agent with high potential in wound treatment.* International journal of antimicrobial agents, 2016. **48**(6): p. 732-735.
42. Shweta, K., et al., *Novel nanocomposites with selective antibacterial action and low cytotoxic effect on eukaryotic cells.* International journal of biological macromolecules, 2016. **92**: p. 988-997.
43. Medina, J.D.C., et al., *Biological activities and thermal behavior of lignin from oil palm empty fruit bunches as potential source of chemicals of added value.* Industrial crops and products, 2016. **94**: p. 630-637.
44. Gabov, K., et al., *Preparation, characterization and antimicrobial application of hybrid cellulose-lignin beads.* Cellulose, 2017. **24**(2): p. 641-658.
45. Yang, W., et al., *Antioxidant and antibacterial lignin nanoparticles in polyvinyl alcohol/chitosan films for active packaging.* Industrial crops and products, 2016. **94**: p. 800-811.
46. Yang, W., et al., *Effect of cellulose and lignin on disintegration, antimicrobial and antioxidant properties of PLA active films.* International journal of biological macromolecules, 2016. **89**: p. 360-368.
47. Gordobil, O., et al., *Potential use of kraft and organosolv lignins as a natural additive for healthcare products.* 2018. **8**(43): p. 24525-24533.
48. Chastre, J. and J.-L. Trouillet. *Problem pathogens (Pseudomonas aeruginosa and Acinetobacter)*. in *Seminars in respiratory infections*. 2000.
49. Balasundram, N., K. Sundram, and S. Samman, *Phenolic compounds in plants and agri-industrial by-products: Antioxidant activity, occurrence, and potential uses.* Food Chem, 2006. **99**(1): p. 191-203.
50. Dong, X., et al., *Antimicrobial and antioxidant activities of lignin from residue of corn stover to ethanol production.* Ind. Crop Prod., 2011. **34**(3): p. 1629-1634.

51. Vazquez-Olivo, G., et al., *Antioxidant Capacity of Lignin and Phenolic Compounds from Corn Stover.* Waste Biomass Valori, 2019. **10**(1): p. 95-102.
52. Espinoza-Acosta, J.L., et al., *Antioxidant, antimicrobial, and antimutagenic properties of technical lignins and their applications.* BioResources, 2016. **11**(2): p. 5452-5481.
53. Arshanitsa, A., et al., *Fractionation of technical lignins as a tool for improvement of their antioxidant properties.* J. Anal. Appl. Pyrolysis, 2013. **103**: p. 78-85.
54. Rowell, R.M. and F.M. Keany, *Fiberboards made from acetylated bagasse fiber.* Wood Fiber Sci., 1991. **23**(1): p. 15-22.
55. Freudenberg, K., *Lignin: Its constitution and formation from p-hydroxycinnamyl alcohols.* Science, 1965. **148**(3670): p. 595-600.
56. Nada, A.-A.M.A., et al., *Infrared spectroscopy of some treated lignins.* Polymer Degradation and Stability, 1998. **62**(1): p. 157-163.
57. Levy, P., et al., *Biorefining of biomass to liquid fuels and organic chemicals.* 1981. **3**(3): p. 207-215.
58. Davin, L.B. and N.G. Lewis, *Lignin primary structures and dirigent sites.* Curr Opin Biotechnol, 2005. **16**(4): p. 407-15.
59. Al-Kaidy, H., et al., *Biotechnology and Bioprocess Engineering – From the First Ullmann's Article to Recent Trends.* ChemBioEng Reviews, 2015. **2**(3): p. 175-184.
60. Kumar, A.K. and S. Sharma, *Recent updates on different methods of pretreatment of lignocellulosic feedstocks: a review.* Bioresources and Bioprocessing, 2017. **4**(1): p. 7.
61. Yakubova, M.R., et al., *Sorption properties of lignins and prospects of their use as medicinal agents.* 1995. **31**(4): p. 534-535.
62. Mielenz, J.R.A., William S.; Klasson, K. Thomas; McMillan, James D., *Applied Biochemistry and Biotecnology*. ABAB Symposium. 2007, Totowa, NJ: Humana Press. 16.
63. Chowdhury, M.A., *The controlled release of bioactive compounds from lignin and lignin-based biopolymer matrices.* International Journal of Biological Macromolecules, 2014. **65**: p. 136-147.
64. Pishnamazi, M., et al., *Microcrystalline cellulose, lactose and lignin blends: Process mapping of dry granulation via roll compaction.* Powder Technology, 2018.

65. Hill, D.J.T., et al. *Water diffusion in methacrylate based copolymer hydrogels of 2-hydroxyethyl methacrylate*. in *Macromolecular Symposia*. 2004.

66. Cotterill, J.V., R.M. Wilkins, and F.T. da Silva, *Controlled release of diuron from granules based on a lignin matrix system.* Journal of Controlled Release, 1996. **40**(1): p. 133-142.

67. Vishtal, A. and A. Kraslawski, *Challenges in industrial applications of technical lignins.* BioResources, 2011. **6**(3): p. 3547-3568.

68. Penkina, A., et al., *Direct compression of cellulose and lignin isolated by a new catalytic treatment.* AAPS PharmSciTech, 2013. **14**(3): p. 1129-36.

69. Wang, H., M. Tucker, and Y. Ji, *Recent Development in Chemical Depolymerization of Lignin: A Review %J Journal of Applied Chemistry.* 2013. **2013**: p. 9.

70. Osamura, T., et al., *Characterization of tableting properties measured with a multi-functional compaction instrument for several pharmaceutical excipients and actual tablet formulations.* International Journal of Pharmaceutics, 2016. **510**(1): p. 195-202.

71. McAuliffe, M.A.P., et al., *The Use of PAT and Off-line Methods for Monitoring of Roller Compacted Ribbon and Granule Properties with a View to Continuous Processing.* Organic Process Research & Development, 2015. **19**(1): p. 158-166.

72. Souihi, N., et al., *Roll compaction process modeling: Transfer between equipment and impact of process parameters.* International Journal of Pharmaceutics, 2015. **484**(1): p. 192-206.

73. Rai, S., P. Dutta, and G. Mehrotra, *Lignin Incorporated Antimicrobial Chitosan Film for Food Packaging Application.* Journal of Polymer Materials, 2017. **34**(1): p. 171.

74. Nadif, A., D. Hunkeler, and P. Käuper, *Sulfur-free lignins from alkaline pulping tested in mortar for use as mortar additives.* Bioresource technology, 2002. **84**(1): p. 49-55.

75. Gundersen, S. and J. Sjöblom, *High-and low-molecular-weight lignosulfonates and Kraft lignins as oil/water-emulsion stabilizers studied by means of electrical conductivity.* Colloid and polymer science, 1999. **277**(5): p. 462-468.

76. Calvo-Flores, F.G. and J.A. Dobado, *Lignin as renewable raw material.* ChemSusChem, 2010. **3**(11): p. 1227-1235.

77. Gargulak, J. and S. Lebo, *Commercial use of lignin-based materials*. 2000, ACS Publications.

78. Lora, J.H. and W.G. Glasser, *Recent industrial applications of lignin: a sustainable alternative to nonrenewable materials.* Journal of Polymers and the Environment, 2002. **10**(1-2): p. 39-48.

79. Pye, E.K., *Industrial lignin production and applications.* Biorefineries-industrial processes and products: status quo and future directions, 2008: p. 165-200.

80. Mathiasson, A. and D. Kubat, *Lignin as binder in particle boards using high frequency heating.* Holz als Roh-und Werkstoff, 1994. **52**(1): p. 9.

81. Gellerstedt, G. and G. Henriksson, *Chapter 9 - Lignins: Major Sources, Structure and Properties A2 - Belgacem, Mohamed Naceur*, in *Monomers, Polymers and Composites from Renewable Resources*, A. Gandini, Editor. 2008, Elsevier: Amsterdam. p. 201-224.

82. Ohra-aho, T., et al., *Structure of Brewer's spent grain lignin and its interactions with gut microbiota in vitro.* Journal of agricultural and food chemistry, 2016. **64**(4): p. 812-820.

83. Maukonen, J., et al., *Interactions of insoluble residue from enzymatic hydrolysis of brewer's spent grain with intestinal microbiota in mice.* Journal of agricultural and food chemistry, 2017. **65**(18): p. 3748-3756.

84. Hasegawa, Y., et al., *Lignosulfonic acid-induced inhibition of intestinal glucose absorption.* Journal of nutritional science and vitaminology, 2015. **61**(6): p. 449-454.

85. Hillman, L., et al., *Effects of the fibre components pectin, cellulose, and lignin on bile salt metabolism and biliary lipid composition in man.* Gut, 1986. **27**(1): p. 29-36.

86. Calvert, G. and R.A. Yeates, *Adsorption of bile salts by soya-bean flour, wheat bran, lucerne (Medicago sativa), sawdust and lignin; the effect of saponins and other plant constituents.* British Journal of Nutrition, 1982. **47**(1): p. 45-52.

87. Iqbal, J. and M.M. Hussain, *Intestinal lipid absorption.* American Journal of Physiology-Endocrinology and Metabolism, 2009. **296**(6): p. E1183-E1194.

88. Carr, T.P. and E.D. Jesch, *Food components that reduce cholesterol absorption.* Advances in food and nutrition research, 2006. **51**: p. 165-204.

89. Story, J.A. and D. Kritchevsky, *Bile acid metabolism and fiber.* The American journal of clinical nutrition, 1978. **31**(10): p. S199-S202.

90. Eastwood, M. and D. Hamilton, *Studies on the adsorption of bile salts to non-absorbed components of diet.* Biochimica et Biophysica Acta (BBA)-Lipids and Lipid Metabolism, 1968. **152**(1): p. 165-173.

91. Gallaher, D. and B.O. Schneeman, *Intestinal interaction of bile acids, phospholipids, dietary fibers, and cholestyramine.* American journal of physiology-Gastrointestinal and liver physiology, 1986. **250**(4): p. G420-G426.

92. Singh, H., A. Ye, and D. Horne, *Structuring food emulsions in the gastrointestinal tract to modify lipid digestion.* Progress in lipid research, 2009. **48**(2): p. 92-100.

93. Kay, R., *Dietary fiber.* Journal of lipid research, 1982. **23**(2): p. 221-242.

94. Kay, R.M., et al., *Differential adsorption of bile acids by lignins.* Dietary Fibers: Chemistry and Nutrition, 2012: p. 57.

95. Rodríguez-Gutiérrez, G., et al., *Properties of lignin, cellulose, and hemicelluloses isolated from olive cake and olive stones: binding of water, oil, bile acids, and glucose.* Journal of agricultural and food chemistry, 2014. **62**(36): p. 8973-8981.

96. Rotstein, O.D., et al., *Prevention of cholesterol gallstones by lignin and lactulose in the hamster.* Gastroenterology, 1981. **81**(6): p. 1098-1103.

97. Carter, J.W., et al., *Type and amount of individual dietary fibers on: serum lipid profiles, serum glucose concentration and energy intake in rats.* Nutrition research, 1998. **18**(10): p. 1743-1756.

98. Tolba, R., G. Wu, and A. Chen, *Adsorption of dietary oils onto lignin for promising pharmaceutical and nutritional applications.* BioResources, 2011. **6**(2): p. 1322-1335.

99. Joana Gil-Chávez, G., et al., *Technologies for extraction and production of bioactive compounds to be used as nutraceuticals and food ingredients: an overview.* Comprehensive Reviews in Food Science and Food Safety, 2013. **12**(1): p. 5-23.

100. Siro, I., et al., *Functional food. Product development, marketing and consumer acceptance—A review.* Appetite, 2008. **51**(3): p. 456-467.

101. Chiewchan, N., *Microstructure, constituents, and their relationship with quality and functionality of dietary fibers*, in *Food Microstructure and Its Relationship with Quality and Stability*. 2017, Elsevier. p. 193-216.

102. Redgwell, R.J. and M. Fischer, *Dietary fiber as a versatile food component: an industrial perspective.* Molecular Nutrition & Food Research, 2005. **49**(6): p. 521-535.

103. Ainsworth, P., et al., *Effect of brewers spent grain addition and screw speed on the selected physical and nutritional properties of an extruded snack.* Journal of Food Engineering, 2007. **81**(4): p. 702-709.
104. Elleuch, M., et al., *Dietary fibre and fibre-rich by-products of food processing: Characterisation, technological functionality and commercial applications: A review.* Food chemistry, 2011. **124**(2): p. 411-421.
105. Aura, A.-M.L.M. *Wood components to boos the quality of food products*. Wood components to boost the quality of food products [Media] 2016 01.06.2016 [cited 2018 13.04.2018]; Wood components to boost the quality of food products]. Available from: http://www.vttresearch.com/media/news/wood-components-to-boost-the-quality-of-food-products.
106. Thiel, A., et al., *Calcium lignosulphonate: Re-evaluation of relevant endpoints to re-confirm validity and NOAEL of a 90-day feeding study in rats.* Regulatory Toxicology and Pharmacology, 2013. **66**(3): p. 286-299.
107. BBI, J. *Bio-Based Industries, Public-Private Partnerships*. 2018; Available from: https://www.bbi-europe.eu/projects.
108. Yu, W., et al., *What is the "typical" particle shape of active pharmaceutical ingredients?* 2017. **313**: p. 1-8.
109. Jaeda, H.J.H.-H.-U.D., *The Use of a Ring Shear Tester to Evaluate the Flowability of Pharmaceutical Bulk Solids.* 2009.
110. Hao, T.J.R.A., *Understanding empirical powder flowability criteria scaled by Hausner ratio or Carr index with the analogous viscosity concept.* 2015. **5**(70): p. 57212-57215.
111. Kaerger, J.S., S. Edge, and R.J.E.J.o.P.S. Price, *Influence of particle size and shape on flowability and compactibility of binary mixtures of paracetamol and microcrystalline cellulose.* 2004. **22**(2-3): p. 173-179.
112. Fu, X., et al., *Effect of particle shape and size on flow properties of lactose powders.* 2012. **10**(2): p. 203-208.
113. Fassihi, A., I.J.D.d. Kanfer, and i. pharmacy, *Effect of compressibility and powder flow properties on tablet weight variation.* 1986. **12**(11-13): p. 1947-1966.
114. Ilić, I., et al., *The compressibility and compactibility of different types of lactose.* 2009. **35**(10): p. 1271-1280.

115. Leturia, M., et al., *Characterization of flow properties of cohesive powders: A comparative study of traditional and new testing methods.* 2014. **253**: p. 406-423.

116. Boel, E., et al., *Unraveling particle formation: from single droplet drying to spray drying and electrospraying.* 2020. **12**(7): p. 625.

117. Schiffter, H. and G.J.J.o.p.s. Lee, *Single-droplet evaporation kinetics and particle formation in an acoustic levitator. Part 1: Evaporation of water microdroplets assessed using boundary-layer and acoustic levitation theories.* 2007. **96**(9): p. 2274-2283.

118. Nuzzo, M., et al., *Surface Composition and Morphology of Particles Dried Individually and by Spray Drying.* Drying Technology, 2015. **33**(6): p. 757-767.

119. Cotabarren, I.M., et al., *Modelling of the spray drying process for particle design.* Chemical Engineering Research and Design, 2018. **132**: p. 1091-1104.

120. Broadhead, J., et al., *The spray drying of pharmaceuticals.* 1992. **18**(11-12): p. 1169-1206.

121. Singh, A. and G. Van den Mooter, *Spray drying formulation of amorphous solid dispersions.* Advanced Drug Delivery Reviews, 2016. **100**: p. 27-50.

122. Huang, D. *Modeling of particle formation during spray drying*. in *Palma, Spain: Eur. Dry. Conf*. 2011.

123. Poozesh, S., et al., *Understanding the process-product-performance interplay of spray dried drug-polymer systems through complete structural and chemical characterization of single spray dried particles.* Powder Technology, 2017. **320**: p. 685-695.

124. Poozesh, S. and E.J.I.J.o.P. Bilgili, *Scale-up of pharmaceutical spray drying using scale-up rules: A review.* 2019. **562**: p. 271-292.

125. Beisl, S., A. Miltner, and A.J.I.j.o.m.s. Friedl, *Lignin from micro-to nanosize: production methods.* 2017. **18**(6): p. 1244.

126. Chauhan, P.S.J.B.T.R., *Lignin nanoparticles: Eco-friendly and versatile tool for new era.* 2019: p. 100374.

127. Yearla, S.R. and K.J.J.o.E.N. Padmasree, *Preparation and characterisation of lignin nanoparticles: evaluation of their potential as antioxidants and UV protectants.* 2016. **11**(4): p. 289-302.

128. Li, H., et al., *Preparation of nanocapsules via the self-assembly of kraft lignin: A totally green process with renewable resources.* 2016. **4**(4): p. 1946-1953.

129. Lievonen, M., et al., *A simple process for lignin nanoparticle preparation.* 2016. **18**(5): p. 1416-1422.
130. Frangville, C., et al., *Fabrication of environmentally biodegradable lignin nanoparticles.* 2012. **13**(18): p. 4235-4243.
131. Gilca, I.A., et al., *Preparation of lignin nanoparticles by chemical modification.* 2014. **23**(5): p. 355-363.
132. Schulze, P., et al., *Continuous Separation of Lignin from Organosolv Pulping Liquors: Combined Lignin Particle Formation and Solvent Recovery.* 2019. **58**(9): p. 3797-3810.
133. Myint, A.A., et al., *One pot synthesis of environmentally friendly lignin nanoparticles with compressed liquid carbon dioxide as an antisolvent.* 2016. **18**(7): p. 2129-2146.
134. Lu, Q., et al., *Comparative antioxidant activity of nanoscale lignin prepared by a supercritical antisolvent (SAS) process with non-nanoscale lignin.* 2012. **135**(1): p. 63-67.
135. Hirleman, E.D., *Modeling of multiple scattering effects in Fraunhofer diffraction particle size analysis*, in *Optical Particle Sizing*. 1988, Springer. p. 159-175.
136. Hausner, H.H., *Friction conditions in a mass of metal powder*. 1967, Polytechnic Inst. of Brooklyn. Univ. of California, Los Angeles.
137. Molyneux, P., *The use of the stable free radical diphenylpicrylhydrazyl (DPPH) for estimating antioxidant activity.* Songklanakarin J. Sci. Technol., 2004. **26**(2): p. 211-219.
138. Cao, G., H.M. Alessio, and R.G. Cutler, *Oxygen-radical absorbance capacity assay for antioxidants.* Free Radic Biol Med, 1993. **14**(3): p. 303-311.
139. Wolfe, K.L., et al., *Cellular antioxidant activity of common fruits.* J Agric Food Chem, 2008. **56**(18): p. 8418-8426.
140. Serra, A.T., et al., *Characterization of traditional and exotic apple varieties from Portugal. Part 2–Antioxidant and antiproliferative activities.* J Funct Foods, 2010. **2**(1): p. 46-53.
141. Wang, H. and J.A. Joseph, *Quantifying cellular oxidative stress by dichlorofluorescein assay using microplate reader.* Free Radic Biol Med, 1999. **27**(5-6): p. 612-616.
142. Mai, T.T. and N.V. Chuyen, *Anti-hyperglycemic activity of an aqueous extract from flower buds of Cleistocalyx operculatus (Roxb.) Merr and Perry.* Biosci. Biotechnol. Biochem., 2007. **71**(1): p. 69-76.

143. Al-Dabbas, M.M., et al., *Antioxidant and α-amylase inhibitory compounds from aerial parts of Varthemia iphionoides Boiss.* 2006. **70**(9): p. 2178-2184.

144. Sambuy, Y., et al., *The Caco-2 cell line as a model of the intestinal barrier: influence of cell and culture-related factors on Caco-2 cell functional characteristics.* Cell Biol Toxicol, 2005. **21**(1): p. 1-26.

145. L C Hillman, et al., *Effects of the fibre components pectin, cellulose, and lignin on bile salt metabolism and biliary lipid composition in man.* Gut, 1986. **27**.

146. Saad A Noeman, Hala E Hamooda, and A.A. Baalash, *Biochemical Study of Oxidative Stress Markers in the Liver, Kidney and Heart of High Fat Diet Induced Obesity in Rats.* Diabetology & Metabolic Syndrome, 2011.

147. Gloria A. Otunola, et al., *Effects of diet-induced hypercholesterolemia on the lipid profile and some enzyme activities in female Wistar rats.* African Journal of Biochemistry Research, 2010. **4** (6).

148. Sanaa R. Galaly, et al., *Effects of Orlistat and herbal mixture extract on brain, testes functions and oxidative stress biomarkers in a rat model of high fat diet.* Beni-Suef University Journal of Basic and Applied Sciences, 2014. **3**(2): p. 93-105.

149. J. Wang , et al., *Selection of potential probiotic lactobacilli for cholesterol-lowering properties and their effect on cholesterol metabolism in rats fed a high-lipid diet.* J Dairy Sci, 2012. **95**(4): p. 1645-54.

150. Jordi Folch, M. Lees, and G.H.S. Stanley, *A Simple Method For The Isolation and Purification of Total Lipids From Animal Tissues.* 1953.

151. He, W., et al., *Optimization of supercritical carbon dioxide extraction of Gardenia fruit oil and the analysis of functional components.* 2010. **87**(9): p. 1071-1079.

152. Zarena, A., N. Sachindra, and K.U.J.F.c. Sankar, *Optimisation of ethanol modified supercritical carbon dioxide on the extract yield and antioxidant activity from Garcinia mangostana L.* 2012. **130**(1): p. 203-208.

153. Ferrari, C.C., S.P.M. Germer, and J.M.J.D.T. de Aguirre, *Effects of spray-drying conditions on the physicochemical properties of blackberry powder.* 2012. **30**(2): p. 154-163.

154. Tonon, R.V., C. Brabet, and M.D.J.J.o.F.E. Hubinger, *Influence of process conditions on the physicochemical properties of açai (Euterpe oleraceae Mart.) powder produced by spray drying.* 2008. **88**(3): p. 411-418.

155. Quek, S.Y., et al., *The physicochemical properties of spray-dried watermelon powders.* 2007. **46**(5): p. 386-392.
156. Maa, Y.-F., et al., *The effect of operating and formulation variables on the morphology of spray-dried protein particles.* 1997. **2**(3): p. 213-223.
157. Walzel, P.J.C.E. and Technology, *Influence of the spray method on product quality and morphology in spray drying.* 2011. **34**(7): p. 1039-1048.
158. Ludwig, W., et al., *Analysis of pneumatic nozzle operation with the stochastic Euler-Lagrange model.* Chemical Engineering Science, 2019. **197**: p. 386-403.
159. Schmitz-Schug, I., U. Kulozik, and P. Foerst, *Modeling spray drying of dairy products – Impact of drying kinetics, reaction kinetics and spray drying conditions on lysine loss.* Chemical Engineering Science, 2016. **141**: p. 315-329.
160. Shishir, M.R.I. and W. Chen, *Trends of spray drying: A critical review on drying of fruit and vegetable juices.* Trends in Food Science & Technology, 2017. **65**: p. 49-67.
161. Sabarez, H.T., *Thermal Drying of Foods*, in *Fruit Preservation: Novel and Conventional Technologies*, A. Rosenthal, et al., Editors. 2018, Springer New York: New York, NY. p. 181-210.
162. Gaytan, I., et al., *Effect of working pressure, fluid temperature, nozzle type and nozzle orifice size, on spray characteristics using viscous feed additive DL-2-hydroxy-4-(methylthio)-butanoic-acid.* Powder Technology, 2018. **336**: p. 383-392.
163. Maenpuen, S., et al., *Production of Valuable Phenolic Compounds from Lignin by Biocatalysis: State-of-the-Art Perspective*, ed. H.N. Chang. 2018.
164. Baesch, S., et al., *Influence of the drying conditions on the particle distribution in particle filled polymer films: Experimental validation of predictive drying regime maps.* Chemical Engineering and Processing - Process Intensification, 2018. **123**: p. 138-147.
165. Ivey, J.W., et al., *Experimental investigations of particle formation from propellant and solvent droplets using a monodisperse spray dryer.* Aerosol Science and Technology, 2018. **52**(6): p. 702-716.
166. Sablania, V. and S.J.D. Bosco, *Optimization of spray drying parameters for Murraya koenigii (Linn) leaves extract using response surface methodology.* Powder Technology, 2018. **335**: p. 35-41.

167. Francia, V., et al., *Agglomeration during spray drying: Airborne clusters or breakage at the walls?* Chemical Engineering Science, 2017. **162**: p. 284-299.

168. Al-Khattawi, A., et al., *The design and scale-up of spray dried particle delivery systems.* Expert Opinion on Drug Delivery, 2018. **15**(1): p. 47-63.

169. Démuth, B., et al., *Downstream processing of polymer-based amorphous solid dispersions to generate tablet formulations.* International Journal of Pharmaceutics, 2015. **486**(1): p. 268-286.

170. Mezhericher, M., A. Levy, and I. Borde, *Spray drying modelling based on advanced droplet drying kinetics.* Chemical Engineering and Processing: Process Intensification, 2010. **49**(11): p. 1205-1213.

171. Muzaffar, K. and P. Kumar, *Parameter optimization for spray drying of tamarind pulp using response surface methodology.* Powder Technology, 2015. **279**: p. 179-184.

172. Krishnaiah, D., et al., *Optimisation of spray drying operating conditions of Morinda citrifolia L. fruit extract using response surface methodology.* Journal of King Saud University - Engineering Sciences, 2015. **27**(1): p. 26-36.

173. Littringer, E., et al., *The morphology of spray dried mannitol particles—The vital importance of droplet size.* 2013. **239**: p. 162-174.

174. Dizhbite, T., et al., *Characterization of the radical scavenging activity of lignins––natural antioxidants.* Bioresour. Technol., 2004. **95**(3): p. 309-317.

175. Dienaitė, L., et al., *Valorization of six Nepeta species by assessing the antioxidant potential, phytochemical composition and bioactivity of their extracts in cell cultures.* J Funct Foods, 2018. **45**: p. 512-522.

176. Wan, H., et al., *A Caco-2 cell-based quantitative antioxidant activity assay for antioxidants.* Food Chem, 2015. **175**: p. 601-608.

177. Tundis, R., M. Loizzo, and F. Menichini, *Natural products as α-amylase and α-glucosidase inhibitors and their hypoglycaemic potential in the treatment of diabetes: an update.* Mini-Rev Med Chem, 2010. **10**(4): p. 315-331.

178. López-Alarcón, C. and A. Denicola, *Evaluating the antioxidant capacity of natural products: A review on chemical and cellular-based assays.* Anal. Chim. Acta, 2013. **763**: p. 1-10.

179. Xiao, J., et al., *Interaction of natural polyphenols with α-amylase in vitro: molecular property–affinity relationship aspect.* Mol BioSyst, 2011. **7**(6): p. 1883-1890.

180. Zajácz, Á., et al., *Aleppo tannin: structural analysis and salivary amylase inhibition.* Carbohydr. Res., 2007. **342**(5): p. 717-723.
181. Ugartondo, V., M. Mitjans, and M.P.J.B.t. Vinardell, *Comparative antioxidant and cytotoxic effects of lignins from different sources.* 2008. **99**(14): p. 6683-6687.
182. Tewari-Singh, N., et al., *Biological and molecular mechanisms of sulfur mustard analogue-induced toxicity in JB6 and HaCaT cells: possible role of ataxia telangiectasia-mutated/ataxia telangiectasia-Rad3-related cell cycle checkpoint pathway.* 2010. **23**(6): p. 1034-1044.
183. Perlamutrov, Y.N., et al., *Double-blind controlled randomised study of lactulose and lignin hydrolysed combination in complex therapy of atopic dermatitis.* 2016. **27**(1): p. 30418.
184. Heaton, K., S. Heaton, and R.J.S.j.o.g. Barry, *An in vivo comparison of two bile salt binding agents, cholestyramine and lignin.* 1971. **6**(3): p. 281-286.
185. Pishnamazi, M., et al., *Effect of lignin on the release rate of acetylsalicylic acid tablets.* 2019. **124**: p. 354-359.
186. Gabbott, I.P., et al., *The combined effect of wet granulation process parameters and dried granule moisture content on tablet quality attributes.* 2016. **106**: p. 70-78.
187. Late, S.G., Y.Y. Yu, and A.K. Banga, *Effects of disintegration-promoting agent, lubricants and moisture treatment on optimized fast disintegrating tablets.* Int J Pharm, 2009. **365**(1-2): p. 4-11.
188. Patel, S., A.M. Kaushal, and A.K.J.P.r. Bansal, *Effect of particle size and compression force on compaction behavior and derived mathematical parameters of compressibility.* 2007. **24**(1): p. 111-124.
189. Adolfsson, Å., et al., *Effect of particle size and compaction load on interparticulate bonding structure for some pharmaceutical materials studied by compaction and strength characterisation in butanol.* 1997. **44**(3): p. 243-251.
190. Adolfsson, Å., et al., *Use of tablet tensile strength adjusted for surface area and mean interparticulate distance to evaluate dominating bonding mechanisms.* 1999. **25**(6): p. 753-764.
191. Lindberg, N.O., et al., *Flowability measurements of pharmaceutical powder mixtures with poor flow using five different techniques.* 2004. **30**(7): p. 785-791.

192. Schulze, D. *Flow properties of powders and bulk solids and silo design for flow*. in *Produktbroschüre, Internationaler Kongress für Partikeltechnologie Powtech/Partec Nürnberg,(27.-29.03. 2001)*. 2001.

193. Saw, H.Y., et al., *Correlation between Powder Flow Properties Measured by Shear Testing and Hausner Ratio.* Procedia Engineering, 2015. **102**: p. 218-225.

194. Wang, Y., et al., *A method to analyze shear cell data of powders measured under different initial consolidation stresses.* Powder Technology, 2016. **294**: p. 105-112.

195. Hamad, I., *The Effect of Particle Size on Compressibility of Cinnamon Granules*. Vol. 2015, 3 (4): 150-153, ISSN: 2328-4595 (PRINT), ISSN: 2328-4609 (ONLINE). 2015.

196. Xie, Y., et al., *Surface Hydrophobic Modification of Microcrystalline Cellulose by Poly(methylhydro)siloxane Using Response Surface Methodology.* Polymers, 2018. **10**(12): p. 1335.

197. Lindh, E.L., et al., *Non-exchanging hydroxyl groups on the surface of cellulose fibrils: the role of interaction with water.* 2016. **434**: p. 136-142.

198. Tukaram, B.N., I.V. Rajagopalan, and P.S.I.J.I.j.o.p.r.I. Shartchandra, *The effects of lactose, microcrystalline cellulose and dicalcium phosphate on swelling and erosion of compressed HPMC matrix tablets: texture analyzer.* 2010. **9**(4): p. 349.

199. Hapgood, K.P., et al., *Drop Penetration into Porous Powder Beds.* Journal of Colloid and Interface Science, 2002. **253**(2): p. 353-366.

200. Yarce, C.J., et al., *Relationship between Surface Properties and In Vitro Drug Release from a Compressed Matrix Containing an Amphiphilic Polymer Material.* Pharmaceuticals (Basel, Switzerland), 2016. **9**(3): p. 34.

201. Fredenberg, S., et al., *The mechanisms of drug release in poly(lactic-co-glycolic acid)-based drug delivery systems—A review.* International Journal of Pharmaceutics, 2011. **415**(1): p. 34-52.

202. Nsor-Atindana, J., et al., *Functionality and nutritional aspects of microcrystalline cellulose in food.* 2017. **172**: p. 159-174.

203. Siepmann, J. and N.A. Peppas, *Modeling of drug release from delivery systems based on hydroxypropyl methylcellulose (HPMC).* Advanced Drug Delivery Reviews, 2001. **48**(2): p. 139-157.

204. Yang, B., et al., *Evaluation about wettability, water absorption or swelling of excipients through various methods and the correlation between these parameters*

and tablet disintegration. Drug Development and Industrial Pharmacy, 2018. **44**(9): p. 1417-1425.

205. Yassin, S., et al., *The Disintegration Process in Microcrystalline Cellulose Based Tablets I.: Influence of Temperature, Porosity and Superdisintegrants.* 2015.
206. Pishnamazi, M., et al., *Application of lignin in controlled release: development of predictive model based on artificial neural network for API release.* Cellulose, 2019. **26**(10): p. 6165-6178.
207. Van Snick, B., et al., *Continuous direct compression as manufacturing platform for sustained release tablets.* International Journal of Pharmaceutics, 2017. **519**(1): p. 390-407.
208. Shipar, M.A.H., et al., *Affect of granule sizes, types and concentrations of lubricants and compression forces on tablet properties.* 2014. **5**(11): p. 4893.
209. Lindman, B., G. Karlström, and L.J.J.o.M.L. Stigsson, *On the mechanism of dissolution of cellulose.* 2010. **156**(1): p. 76-81.
210. Pishnamazi, M., et al., *Effect of lignin on the release rate of acetylsalicylic acid tablets.* International Journal of Biological Macromolecules, 2019. **124**: p. 354-359.

List of figures

FIGURE 1: PROPOSED MECHANISM OF LIGNIN FOR RADICAL SCAVENGING VIA ELECTRON DONATION..... 9
FIGURE 2: STRUCTURE-RELATIONSHIP OF LIGNIN AS ANTIMICROBIAL AGENT. EXAMPLE IS SHOWN FOR STAPHYLOCOCCUS AUREUS, SPHERICAL GRAM-POSITIVE BACTERIA CAUSING A WIDE RANGE OF MAJOR INFECTIONS IN MAN AND ANIMALS.....11
FIGURE 3: SCHEMATIC MECHANISM PROPOSED FOR LIGNIN ACTIVITY ON BINDING BILE ACIDS IN THE SMALL INTESTINE AND LOWERING CHOLESTEROL LEVELS IN BLOOD. 17
FIGURE 4: FRICTION ON A HORIZONTAL PLANE (A), AND FRICTION ON AN INCLINED PLANE (B). 22
FIGURE 5: YIELD LOCUS OF TWO TYPES OF POWDER A) AND ILLUSTRATION OF THE MEASUREMENT IN THE JENIKE´S SHEAR CELL.....23
FIGURE 6: EXAMPLE OF HOW COHESIVENESS IN THE POWDERS AFFECTS COMPRESSION. NON-COHESIVE POWDERS ARE LESS SENSITIVE TO CHANGES IN THE FLOW/CHANGE OF VOLUME AND THE VOIDS BETWEEN PARTICLES ALMOST REMAIN INTACT UNLESS HIGH STRESS IS APPLIED. FOR COHESIVE POWDERS, THE PARTICLES FLOW WITH THE STRESS/CHANGE IN VOLUME, ACCOMODATING WITHIN THE EXISTING AGGLOMERATES [115]. 26
FIGURE 7. SCHEMATIC OF A TYPICAL SPRAY DRYER 27
FIGURE 8. EVOLUTION OF PARTICLE AND CRUST FORMATION DURING SPRAY DRYING. 29
FIGURE 9 TWO FLUID NOZZLES WITH MECHANISMS OF EXTERNAL (A) AND INTERNAL (B) MIXING. THE FEED AND THE ATOMIZING GAS ARE FED INTO THE SYSTEM IN CO-CURRENT FLOW AND SPRAYED AT THE TIME OF CONTACT.....31
FIGURE 10 LABORATORY SCALE APPROACHES TO PRODUCE LIGNIN MACRO AND NOPARTICLES FOR HIGH VALUE APPLICATIONS 36
FIGURE 11 OVERVIEW OF THE EXPERIMENTS, PROCESS PARAMATERS AND PRODUCT FORMULATION DESIGNED FROM THE AS LIGNIN PARTICLES OBTAINED VIA SPRAY DRYING. 40
FIGURE 12: SCHEMATIC OF THE BIOREFINING PROCESS EXISTING AT TUHH. 41
FIGURE 13: SCHEMATIC DIAGRAM OF THE SPRAY DRYING PROCESS. THE X_1, X_2, X_3 CORRESPOND TO THE VARIED PROCESS PARAMETERS INLET TEMPERATURE, ATOMIZATION PRESSURE AND FEED RATE RESPECTIVELY. Y_1 AND Y_2 CORRESPOND TO THE PROCESS RESPONSES OF PARTICLE SIZE AND MASS YIELD OF FINE POWDER. 45
FIGURE 14: SIMPLIFIED SCHEME OF THE EXPERIMENTS USED FOR THE SIMULATED GASTROINTESTINAL CONDITIONS FOR THE OIL ADSORPTION CAPACITY OF AS SPRAZ DRIED PARTICLES AND LIGNIN-BASED FORMULATIONS. 54
FIGURE 15: CONTACT ANGLE MEASUREMENT THROUGH SESSILE DROP MEASUREMENT TECHNIQUE..65
FIGURE 16: SURFACE AND COUNTOUR PLOTS PRESENTING THE EFFECT OF TEMPERATURE AND ATOMIZATION PRESSURE ON THE RESPONSES "MASS YIELD OF FINES" AND "PARTICLE SIZE (D50)" 72
FIGURE 17: SURFACE AND CONTOUR PLOTS PRESENTING THE EFFECT OF TEMPERATURE AND FEEDING RATE ON THE RESPONSES "MASS YIELD FINE" AND "PARTICLE SIZE (D50)".....74
FIGURE 18: SURFACE AND CONTOUR PLOTS ON THE EFFECT OF ATOMIZATION PRESSURE AND FEEDING RATE ON THE RESPONSES "MASS YIELD FINE" AND "PARTICLE SIZE (D50)". 76
FIGURE 19: DESIRABILITY PLOTS SHOWING THE PREDICTED VALUES. 78
FIGURE 20 SEM IMAGE OF AS LIGNIN PARTICLES AT DRYING CONDITIONS OF 173°C, 1.8 BAR AND 62 ML MIN-1. 81
FIGURE 21 DIFFERENT MORPHOLOGIES OF SPRAY DRIED AS LIGNIN A) SOLID POROUS, B) COLLAPSED HOLLOW PARTICLE, C) SOLID HOLLOW AND D) SOLID PARTICLE.....81

Figure 22: ORAC antioxidant capacity evaluation of four lignin types. Results are expressed as µmol TEg-1. 84
Figure 23: DPPH antioxidant capacity of four different lignins in five free radical concentrations. Results are reported as percentage of DPPH radical scavenging. 85
Figure 24: Efficient concentration (EC50) to scavenge half of the amount of DPPH free radical present for four different lignins. Results are presented in EC50 (mg/mL). 85
Figure 25: Cellular antioxidant activity (CAA) of four different lignins. Effective concentrations (EC50) are presented in mg/mL. 87
Figure 26: Half maximal inhibitory concentration (IC50) values represent the concentrations that inhibits 50% of enzymatic activity. IC50 values (mg/mL) of four different lignins for (a) a-amylase and b) a-glucosidase assays....89
Figure 27: Cytotoxic effect of lignins on Caco-2 cells after 4h of incubation. Results were expressed as mean ± SD of at least three independent experiments performed in triplicate. Aquasolv 1 corresponds to the fine fraction obtained during spray drying and Aquasolv 2 to the coarse fraction. 91
Figure 28 Adsorption capacities of the biopolymer samples according to ISO 787/5. SW lignin (softwood lignin), SW-CO2 lignin (softwood, supercritically dried lignin), AS Lignin (spray dried lignin), AS-CO2 lignin (AS lignin obtained via LHW pretreatment and supercritically dried), AL-Lignin (alkali lignin), OS Lignin (organosolv lignin). 93
Figure 29 Oil adsorption capacity under simulated gastrointestinal conditions. 96
Figure 30 Effect of supercritical CO2/ethanol treatment on adsorption capacity of SW and AL-lignin. 96
Figure 31 Contact angle (oil) on the different materials used for oil adsorption. 97
Figure 32 Gained Body weight (bars) and the heart fat weight (circles) of all groups. HFD is the high fat diet, ND is the normal diet. SV is the simvastatin, Lig is lignin. 100
Figure 33 Rate of total cholesterol in the serum (pink) and in the feces (brown) for all groups. The rate was calculated as the differences between cholesterol concentration in day 14 and day 21 for serum and feces divided by number of days. 102
Figure 34 Rate of triglycerides in the serum (pink) and in the feces (brown) for all groups. The rate was calculated as the differences between cholesterol concentration in day 14 and day 21 for serum, and feces divided by number of days. 103
Figure 35 Rate of HDL in the serum (yellow) and in the feces (blue) for all groups. The rate was calculated as the differences between cholesterol concentration in day 14 and day 21 for serum, and feces divided by number of days. 104
Figure 36 Ratio of Alanine Transaminase measured in serum analysis. ALT concentration in serum U/L., C1: control 1 receive normal diet only, n=4, C2: control 2 receive high fat diet only, n=4, Lig: lignin, SV: simvastatin, ND+100 Lig: Normal Diet + 100 mg lignin, n=4, HFD+50, 100 and 500 Lig: High Fat Diet + 50, 100 & 500 mg lignin, respectively, n=7 each group, HFD+SV: High Fat Deit +simvastatin 40 mg, n=4, HFD+100 Lig+SV: High Fat Diet + 100 lignin + simvastatin 40 mg, n=7. 105

FIGURE 37 SEM IMAGES OF AS LIGNIN POWDER USED FOR TABLET FORMULATION..... 108
FIGURE 38: TABLET HARDNESS AND DISINTEGRATION TIME OF PURE LIGNIN TABLETS AT DIFFERENT COMPRESSION FORCES. 112
FIGURE 39 CONTOUR AND SURFACE PLOT OF TENSILE STRENGTH FOR THE FORMULATION DISINTEGRANT BINDER LIGNIN. 115
FIGURE 40: EXCIPIENTS USED IN DBL FORMULATION: MICROCRYSTALLINE CELLULOSE (ACCEL – 101/ LEHMANN & VOSS) (LEFT) AND LACTOSE MONOHYDRATE (TABLETTOSE 100) (RIGHT). 117
FIGURE 41: GRANULATED FORMULATIONS OBTAINED BY BLENDING AS LIGNIN WITH LACTOSE MONOHYDRATE AND MICROCRYSTALLINE CELLULOSE. 118
FIGURE 42: TENSILE STRENGTH AND FRIABILITY LOSS OF THE FORMULATIONS LOADED WITH IBUPROFEN. RED DOTS INDICATE SAME FORMULATIONS OBTAINED VIA DIRECT COMPRESSION AND WET GRANULATION. BLACK DOT INDICATES THE HIGHEST CONCENTRATION OF IBUPROFEN USED IN THIS STUDY. 121
FIGURE 43: COMPARISON OF THE DISINTEGRATION TIME OF FORMULATIONS LOADED WITH IBUPROFEN. BLUE DOTS INDICATE SAME FORMULATIONS OBTAINED VIA DIRECT COMPRESSION AND WET GRANULATION. 122
FIGURE 44: COMPARISON OF THE DEGREE OF SPREADING OF PURE LIGNIN, OPTIMIZED DBL AND THE FORMULATION LOADED WITH 50% IBUPROFEN FOR DC (DIRECTE COMPRESSION) AND WG (WET GRANULATION) AT 85 KN. 123
FIGURE 45 DRUG RELEASE PROFILE OF THE TABLETS OF LIGNIN AT DIFFERENT FORCES. 126
FIGURE 46 SOLVENT EXCHANGE PROCESS FOR LIGNIN PARTICLES SUSPENDED IN WATER 157
FIGURE 47 ANTIOXIDANT CAPACITY OF THE SOLVENT REMOVED AFTER SOLVENT EXCHANGE OF AS LIGNIN WITH ETHANOL, ACETONE AND ACETONITRILE 158
FIGURE 48 EXTRACTABLES FROM THE ORIGINAL AS LIGNIN WET CAKE, SEPARATED DURING THE STEPS OF SOLVENT EXCHANGE (SE) WITH ACETONE (A), ACETONITRILE (B) AND ETHANOL (C). 159
FIGURE 49 SURFACE AREA, PORE VOLUME AND AVERAGE PORE SIZE OF THE POROUS PARTICLE OBTAINED VIA SOLVENT EXCHANGE AND SUPERCRITICAL CO2 DRYING 160
FIGURE 50 SCHEMATIC OF THE SPRAY DRYING EQUIPMENT USED IN THIS WORK 160
FIGURE 51 EXAMPLE OF A MEASUREMENT OF TABLET DISINTEGRATION ACCORDING TO PHARMACOPOEIAL METHODS 161
FIGURE 52 EFFECT OF THE NOZZLE SIZE ON THE PARTICLE SIZE OF AS LIGNIN PRODUCED WITH ATOMIZATION PRESSURE OF 3 AND 4 BAR 163
FIGURE 53 COUNTOUR PLOTS FOR THE COMBINED EFFECTS OF THE PROCESSING CONDITIONS FEEDING RATE, ATOMIZATION PRESSURE AND DRYING TEMPERATURE ON THE ANTIOXIDANT CAPACITY OF LIGNIN SPRAY DRIED POWDERS. 164
FIGURE 54 INTERACTION PLOTS FOR ANTIOXIDANT CAPACITY, FITTED MEANS 165
FIGURE 55 MAIN EFFECTS PLOTS FOR ANTIOXIDANT CAPACITY 165
FIGURE 56 COUNTOUR PLOTS ON THE COMBINED EFFECT OF PROCESS PARAMETERS ON MASS YIELD OF FINES 166
FIGURE 57 TENSILE STRENGHT OF THE LIGNIN BASED TABLETS 175
FIGURE 58 RESULTS ON DISINTEGRATION OF THE LIGNIN BASED TABLETS EVALUATED 176

List of tables

TABLE 1: MAJOR USES AND MOLECULAR PROPERTIES OF LIGNINS OBTAINED FROM DIFFERENT BIOREFINING PROCESSES 5
TABLE 2: COMPOSITION OF THE AS LIGNIN WHEN SUBMITTED TO ONE AND TWO STEPS ENZYMATIC HYDROLYSIS WITH CTEC2® ENZYMES 42
TABLE 3: CODED AND REAL LEVELS OF THE INDEPENDENT VARIABLE USED IN THE EXPERIMENTAL DESIGN TO ESTIMATE PARTICLE SIZE OF THE AQUASOLV LIGNIN POWDERS OBTAINED BY SPRAY DRYING. 46
TABLE 4: DESIGN OF EXPERIMENTS SHOWING THE UNCODED UNITS FOR COMPONENT – DBL. 60
TABLE 5: CENTRAL COMPOSITE ROTATABLE DESIGN 67
TABLE 6: ACTUAL VALUES IN THE DESIGN OF EXPERIMENTS AND RESPONSES 68
TABLE 7: ANOVA DATA SHOWING THE P-VALUE OF THE MODEL TERMS AND THE R2 OF THE MODEL. 69
TABLE 8: REGRESSION COEFFICIENTS FOR THE RESPONSES. 70
TABLE 9: PREDICTED AND EXPERIMENTAL VALUE OF THE RESPONSES AT OPTIMIZED CONDITIONS. 78
TABLE 10: CONTACT ANGLE OF ALL THE SAMPLES TESTED FOR OIL ADSORPTION CAPACITY WITH WATER AND OIL (CORN OIL). 98
TABLE 11: FLOW PROPERTY MEASUREMENT USING THE JENIKE SHEAR CELL. 109
TABLE 12: BREAKAGE FORCE AND TABLET DISINTEGRATION TIME OF PURE LIGNIN SAMPLES. 110
TABLE 13: ANOVA OF TENSILE STRENGTH FOR THE FORMULATION OF DBL. 113
TABLE 14: COMPOSITION OF WET GRANULATION POWDERS 118
TABLE 15: COMPARISON OF TENSILE STRENGTH AND FRIABILITY OF FORMULATIONS LOADED WITH IBUPROFEN 119
TABLE 16: COMPARISON OF PREDICTED AND EXPERIMENTAL VALUES OF THE POWDER CHARACTERISTICS OF RELEVANCE FOR DISINTEGRATION TIME. 125
TABLE 17: ADSORPTION CAPACITY OF BIOPOLYMERS UNDER GASTRIC AND GASTROINTESTINAL ENVIRONMENTS AGAINST TWO TYPES OF OIL. 167
TABLE 18 OIL ADSORPTION CAPACITIES OF THE LIGNINS OBTAINED VIA SOLVENT EXCHANGE AND SUPERCRITICAL DRYING COMPARED TO THEIR STANDARD POWDERS 167
TABLE 19 OIL ADSORPTION CAPACITY FOR BIOPOLYMERS ACCORDING TO ISO787/5 167
TABLE 20: BODY AND HEART FAT WEIGHT OF ALL THE TESTED GROUPS 168
TABLE 2:1 RATE AND THE AVERAGE OF TOTAL CHOLESTEROL CONCENTRATION IN SERUM AND FECES ANALYSIS OF ALL THE TESTED GROUPS 168
TABLE 22: RATE AND THE AVERAGE OF TRIACILGLYCERIDES CONCENTRATION IN SERUM AND FECES ANALYSIS OF ALL THE TESTED GROUPS 169
TABLE 23: RATE AND AVERAGE OF HDL CHOLESTEROL CONCENTRATION IN SERUM AND FECES ANALYSIS FOR ALL THE GROUPS 170

Symbols and abbreviations

Latin symbol	Meaning
H	Viscosity
M	Molecular Weight
K	Factor in polymer solvent systems
T_g	Glass Transition Temperature
a_w	Water activity
P	Vapour pressure of water
p_w	Equillibrium Vapour Pressure of Water
Pe_i	Peclet Number
K	Evaporation Rate
D_i	Diffusion Rate
D	Diameter of the Particle
d_o	Initial Diameter of the Particle
t	Time
τ_D	Drying time
E_i	Surface Enrichment
$C_{s,i}$	Surface Concentration
$C_{m,i}$	Average Concentration in Droplet
β_i	Function of Peclet Number in Surface Enrichment
Y	Response
X	Input Variable
N	Levels in the dimesional design space

Greek symbol	Unit	Meaning
α	-	Relative distance of the star points from the factorial part in a Central Composite Design (CCD)
β	-	Polynomial regression coefficient
ε	-	Statistical error
σ	-	Standard deviation

Abbreviations

Abbreviation	Meaning
LHW	Liquid Hot water
LSR	Liquid to Solid Ratio
HEPA	High efficiency particulate air
DoE	Design of Experiments
RSM	Response Surface Methodology
ANOVA	Analysis of Variance
CCD	Central Composite Design
CCRD	Central Composite Rotatable Design
DPPH	2,2-diphenyl-1-picrylhydrazyl
IUPAC	International Union of Pure and Applied Chemistry
DF	Degrees of Freedom

Appendix

A1: Powder flowability property depending on angle of repose value

Flow Property	Angle of Repose (degrees)
Excellent	25–30
Good	31–35
Fair—aid not needed	36–40
Passable—may hang up	41–45
Poor—must agitate, vibrate	46–55
Very poor	56–65
Very, very poor	> 66

A2: Gas Antisolvent Precipitation (GAS) of AS Lignin for the production of porous particles: solvent exchange and supercritical drying

To produce lignin porous particles, wet lignin 63 wt.% TS was used for the solvent exchange before GAS process. The Antisolvent precipitation with supercritical CO2 is well known process to produce narrow and homogeneous particles with increased porosity and surface area. In this process, supercritical CO_2 causes the precipitation of the solids by selectively solubilizing the solvent but not the solute that is dissolved/suspended in the liquid, thus decreasing the solvating power of the liquid mixture. However, in order to use this process, the initial solvent (usually water) needs to be replaced by a solvent that is well miscible in CO_2. Afterwards, this solvent is extracted with CO_2 at pressures above the critical point of that mixture. The solvents evaluated for solvent exchange were ethanol, acetone and acetonitrile.

To prepare the lignin for GAS process, the solvent exchange (SE) from water to ethanol / acetone / acetonitrile was done removing the water by centrifugation, and gradually adding 25 wt%, 50 wt% and 100 wt% of the solvent to the particles. Centrifugation was done after 2 hours of solvent-particle contact, every time before adding a solution with higher solvent concentration (Figure 46). This procedure was repeated at least three times until a solvent concentration of 97 wt % was achieved. Afterwards, the solvents

were extracted from the particles at operating conditions of 45 °C, 120 bar and experiments were carried out over 4 hours.

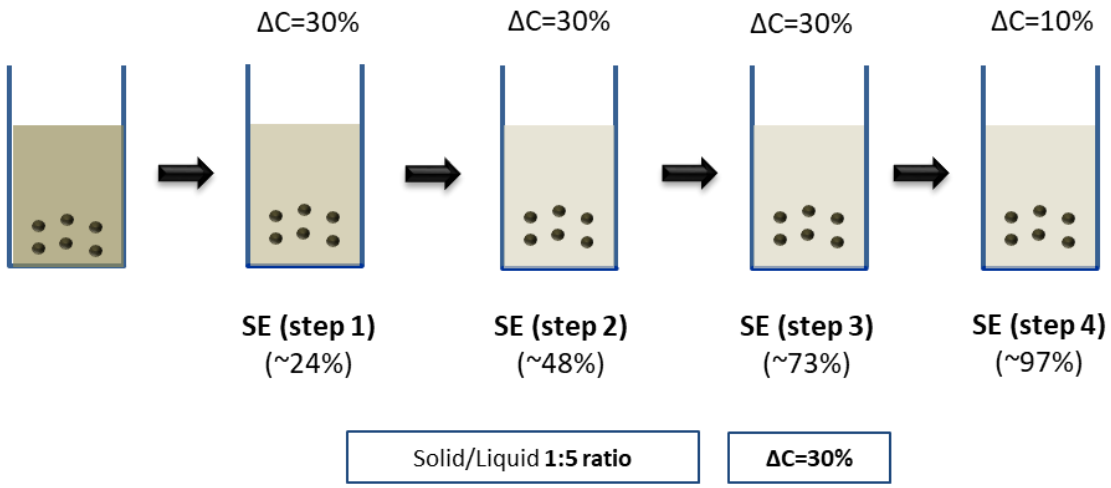

Figure 46 Solvent exchange process for lignin particles suspended in water

During the solvent exchange process, it was observed that there was extraction of the lignin components into the solvent, and this was confirmed by measuring the antioxidant activity of the solvent recovered in every step. The antioxidant activity is given by the amount of simple phenolic compounds that were easily extracted from the lignin macromolecular structure and the amount of -OH groups from such phenolics is directly related with the % of scavenging of the free radical DPPH (2,2-diphenyl-1picrylhydrazyl).

In the figure 47, it can be seen that AOX capacity of the extracts increases with the concentration of the solvent, no effect of the type of solvent was found.

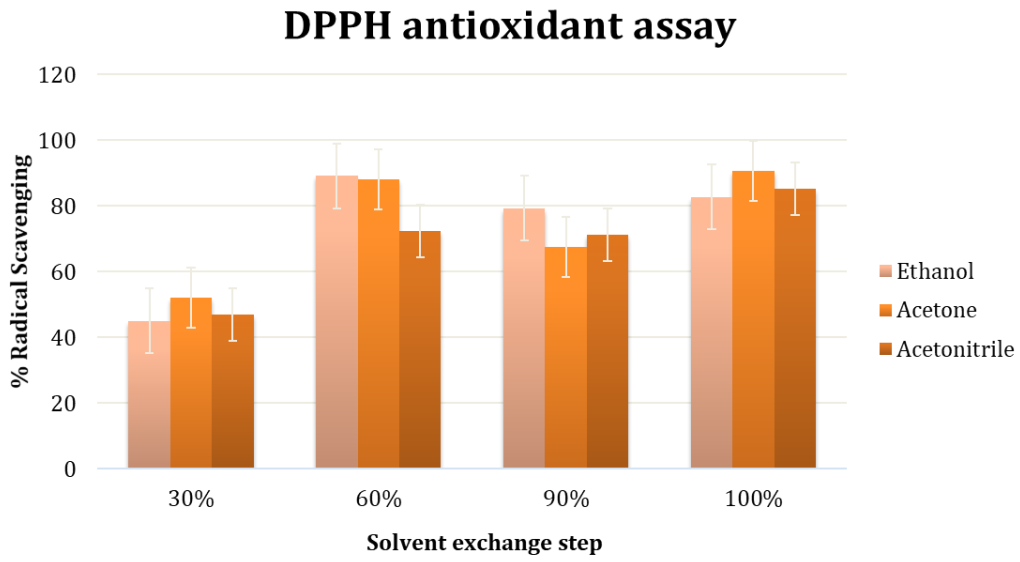

Figure 47 Antioxidant capacity of the solvent removed after solvent exchange of AS lignin with ethanol, acetone and acetonitrile

The particles obtained via SC-CO2, showed a slight reduction on the composition (due to the extractives removed during solvent exchange) compared with the lignin without solvent exchange which has a composition of 85% hydrolysis residue. The quality of these particles remains present and potential application in high value markets, i.e. cosmetics where a minimum purity of approximately 70 % is required.

	Lignin Particles Composition (%)		
	Lignin	**Acid Soluble Lignin**	**Sugars**
Ethanol	79.5	1.3	19.99
Acetonitrile	81.7	1.6	17.61
Acetone	80	1.3	19.03

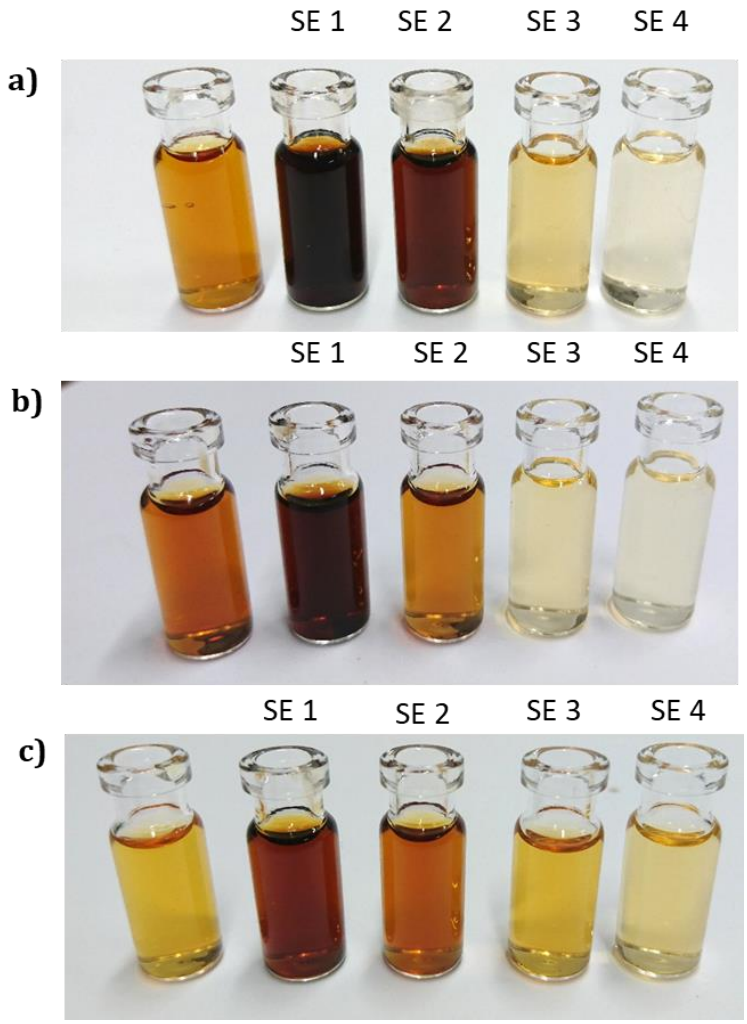

Figure 48 Extractables from the original AS lignin wet cake, separated during the steps of solvent exchange (SE) with Acetone (a), Acetonitrile (b) and Ethanol (c).

The post particle formation process from lignin obtained via Liquid Hot Water was assessed by means of high-pressure technologies. The effect of liquid/lignin mixture on porosity, surface area and particle size of the final particles was evaluated. Particles suspended in ethanol showed the highest surface area (90 m2/g), particle size (d50) of 20 µm and pore size of the particles was 160.5 Å. Similar results were found for acetone. However, the particles suspended in acetonitrile showed reduced surface area (15 m2/g) and high pore size (371.8 Å).

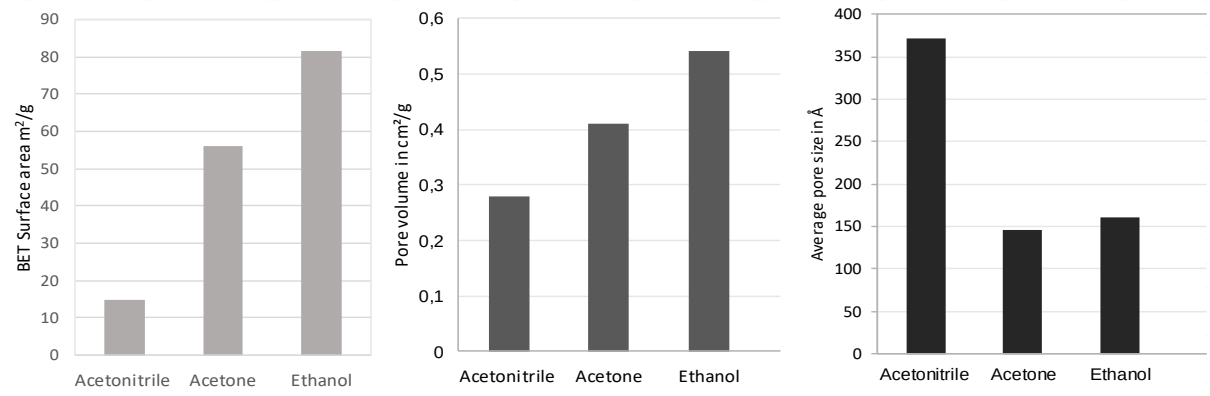

Figure 49 Surface area, pore volume and average pore size of the porous particle obtained via solvent exchange and supercritical CO2 drying

A3: Flow chart of the spray dryer Mobile Minor ®

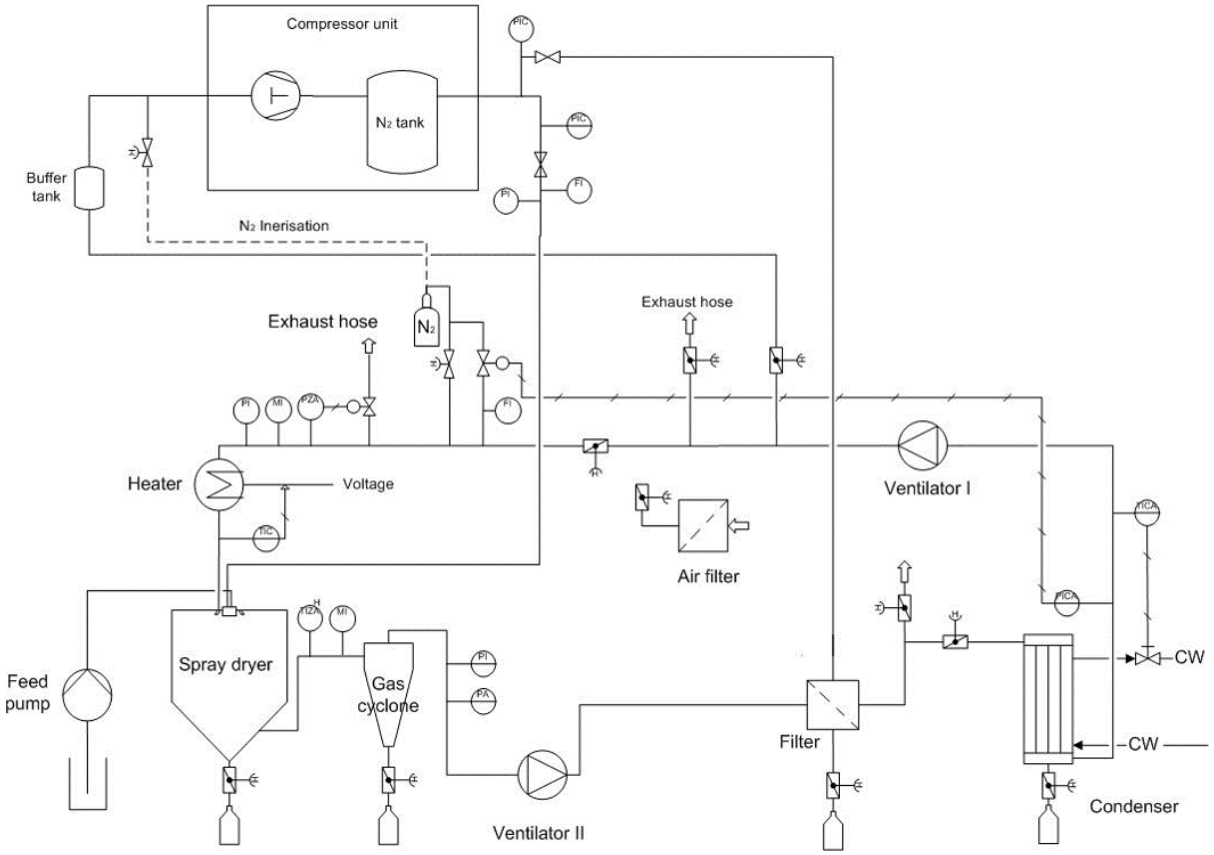

Figure 50 Schematic of the spray drying equipment used in this work

A4: Tablet disintegration test according to Pharmacopeia

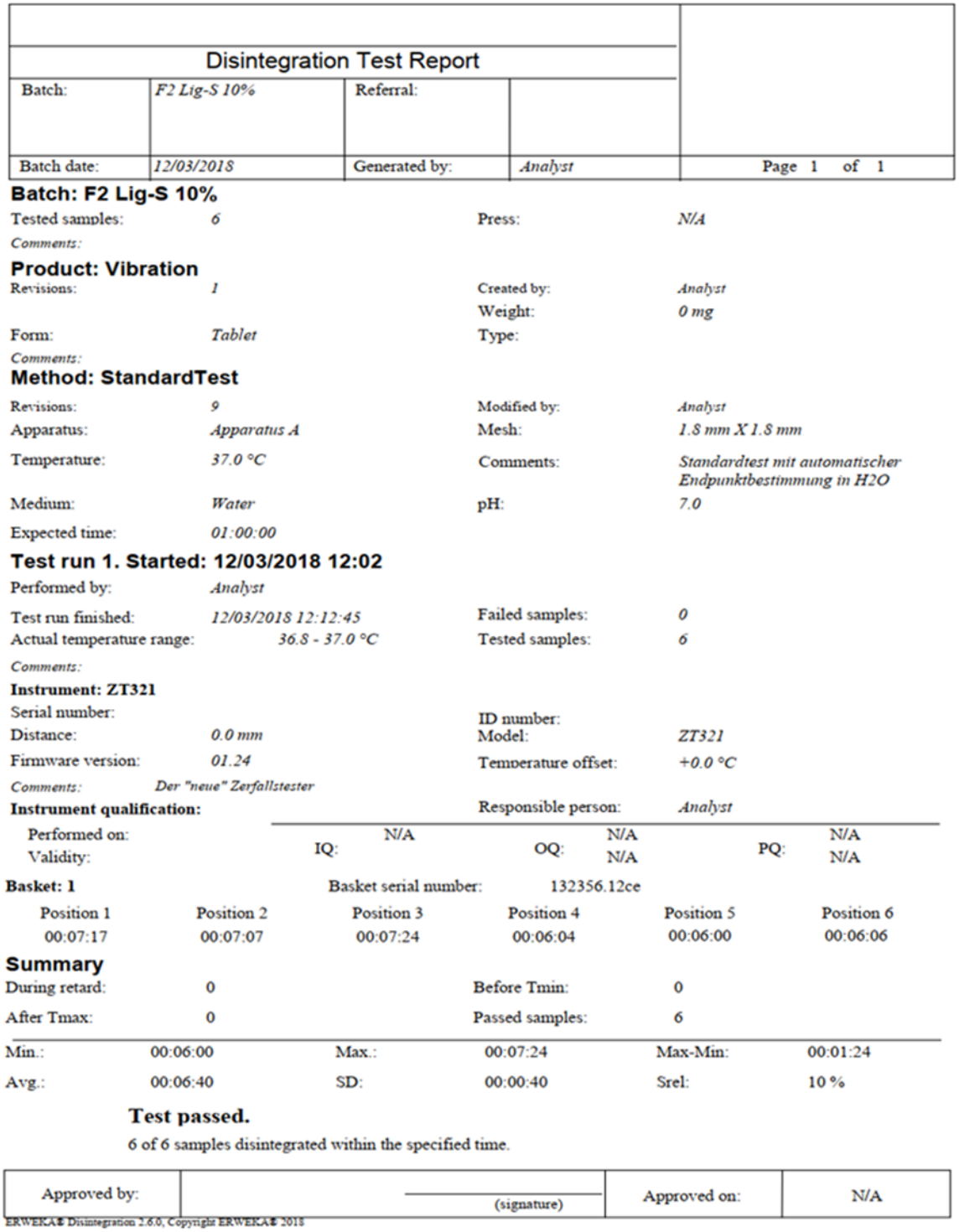

Disintegration Test Report

Batch:	*F2 Lig-S 10%*	Referral:		
Batch date:	*12/03/2018*	Generated by:	*Analyst*	Page 1 of 1

Batch: F2 Lig-S 10%

Tested samples: *6* Press: *N/A*

Comments:

Product: Vibration

Revisions: *1* Created by: *Analyst*

Weight: *0 mg*

Form: *Tablet* Type:

Comments:

Method: StandardTest

Revisions: *9* Modified by: *Analyst*

Apparatus: *Apparatus A* Mesh: *1.8 mm X 1.8 mm*

Temperature: *37.0 °C* Comments: *Standardtest mit automatischer Endpunktbestimmung in H2O*

Medium: *Water* pH: *7.0*

Expected time: *01:00:00*

Test run 1. Started: 12/03/2018 12:02

Performed by: *Analyst*

Test run finished: *12/03/2018 12:12:45* Failed samples: *0*

Actual temperature range: *36.8 - 37.0 °C* Tested samples: *6*

Comments:

Instrument: ZT321

Serial number: ID number:

Distance: *0.0 mm* Model: *ZT321*

Firmware version: *01.24* Temperature offset: *+0.0 °C*

Comments: *Der "neue" Zerfallstester*

Instrument qualification: Responsible person: *Analyst*

Performed on:					
Validity:	IQ: N/A	OQ: N/A	N/A	PQ: N/A	N/A

Basket: 1 Basket serial number: 132356.12ce

Position 1	Position 2	Position 3	Position 4	Position 5	Position 6
00:07:17	00:07:07	00:07:24	00:06:04	00:06:00	00:06:06

Summary

During retard: 0 Before Tmin: 0

After Tmax: 0 Passed samples: 6

Min.:	00:06:00	Max.:	00:07:24	Max-Min:	00:01:24
Avg.:	00:06:40	SD:	00:00:40	Srel:	10 %

Test passed.

6 of 6 samples disintegrated within the specified time.

Approved by:	(signature)	Approved on:	N/A

ERWEKA® Disintegration 2.6.0, Copyright ERWEKA® 2018

Figure 51 Example of a measurement of tablet disintegration according to pharmacopoeial methods

A5: Design of experiments showing uncoded units

Std Order	Run Order	Pt Type	Blocks	Temp (°C)	Atomization Pressure (bar)	Feed Rate (ml/min)
10	1	-1	1	206.8	1.5	70
7	2	1	1	180	1.7	75
2	3	1	1	200	1.3	65
4	4	1	1	200	1.7	65
17	5	0	1	190	1.5	70
1	6	1	1	180	1.3	65
18	7	0	1	190	1.5	70
16	8	0	1	190	1.5	70
14	9	-1	1	190	1.5	78.4
19	10	0	1	190	1.5	70
13	11	-1	1	190	1.5	61.6
3	12	1	1	180	1.7	65
6	13	1	1	200	1.3	75
15	14	0	1	190	1.5	70
20	15	0	1	190	1.5	70
9	16	-1	1	173.2	1.5	70
5	17	1	1	180	1.3	75
12	18	-1	1	190	1.8	70
8	19	1	1	200	1.7	75
11	20	-1	1	190	1.1	70

A6: Nozzle effect on spray dried particles produced with atomization pressure of 3-4 bar

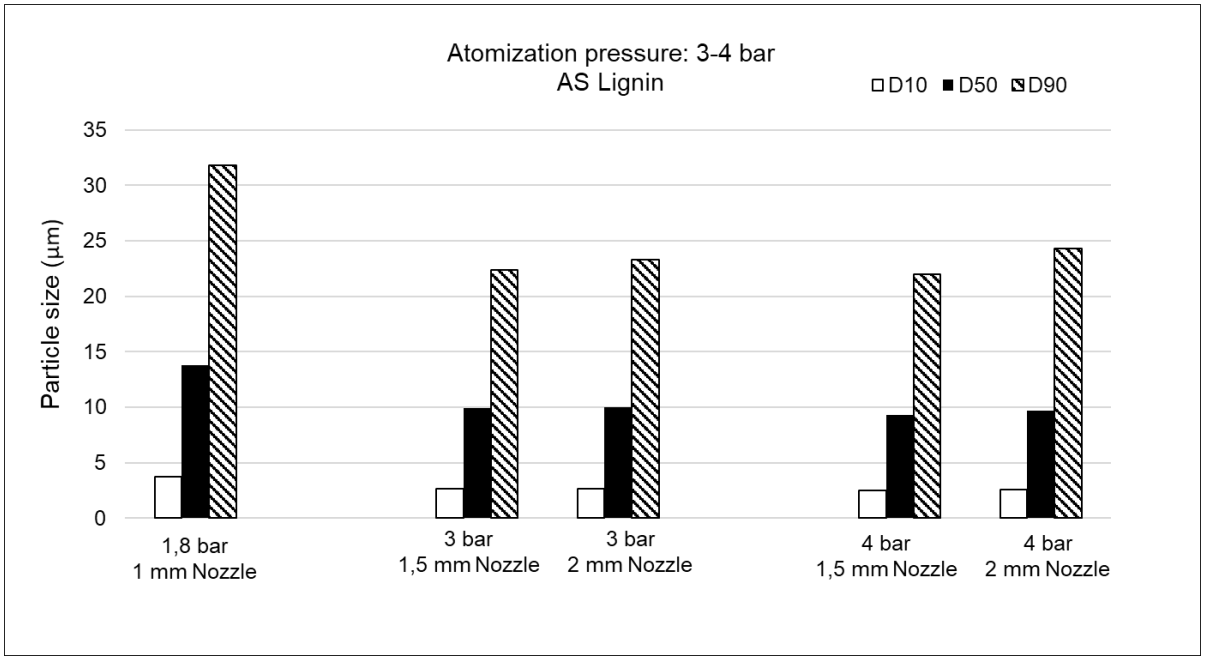

Figure 52 Effect of the nozzle size on the particle size of AS lignin produced with atomization pressure of 3 and 4 bar

A7: Plots for combined effect of process parameters on antioxidant capacity

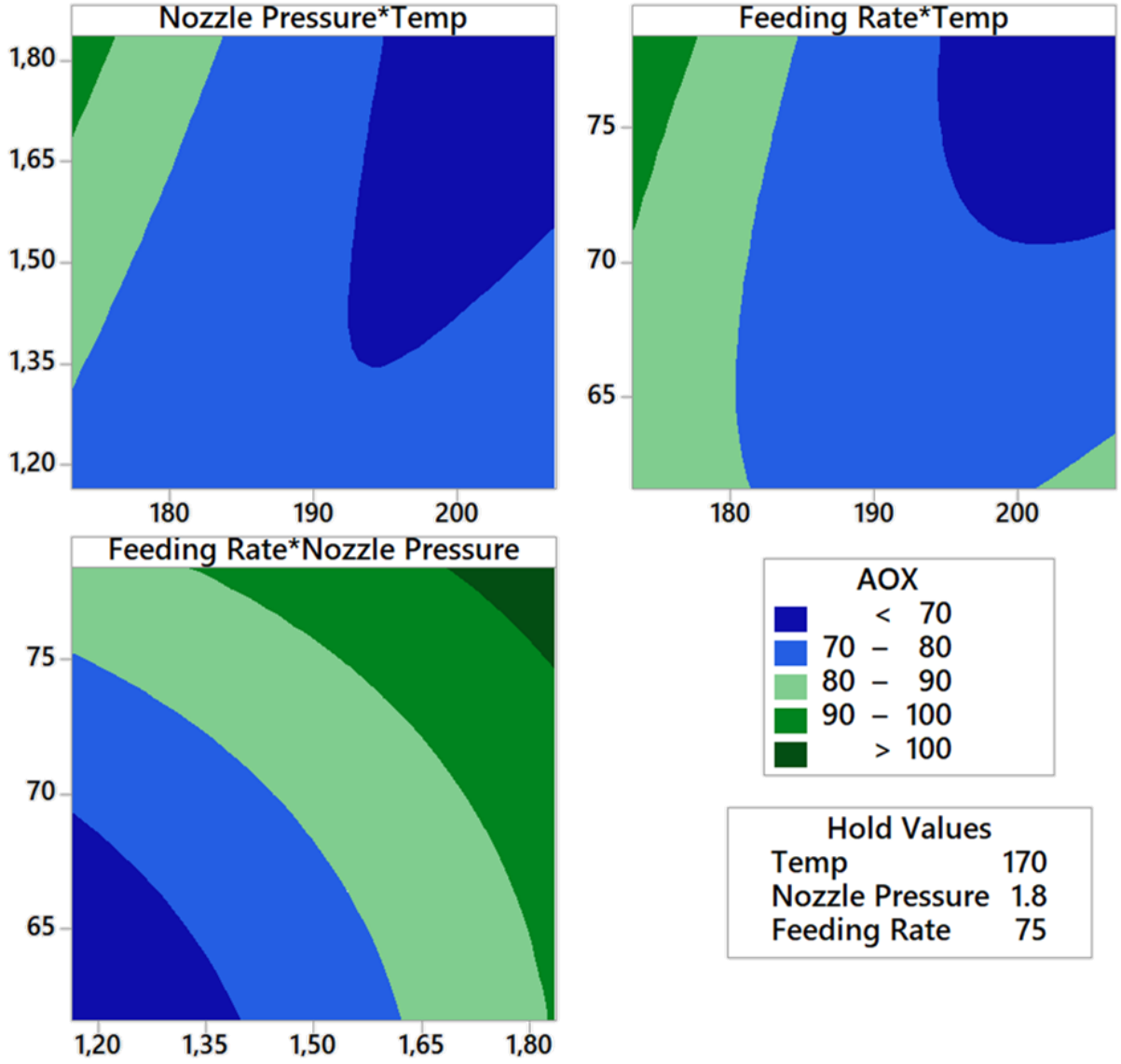

Figure 53 Countour plots for the combined effects of the processing conditions Feeding rate, atomization pressure and drying temperature on the antioxidant capacity of lignin spray dried powders.

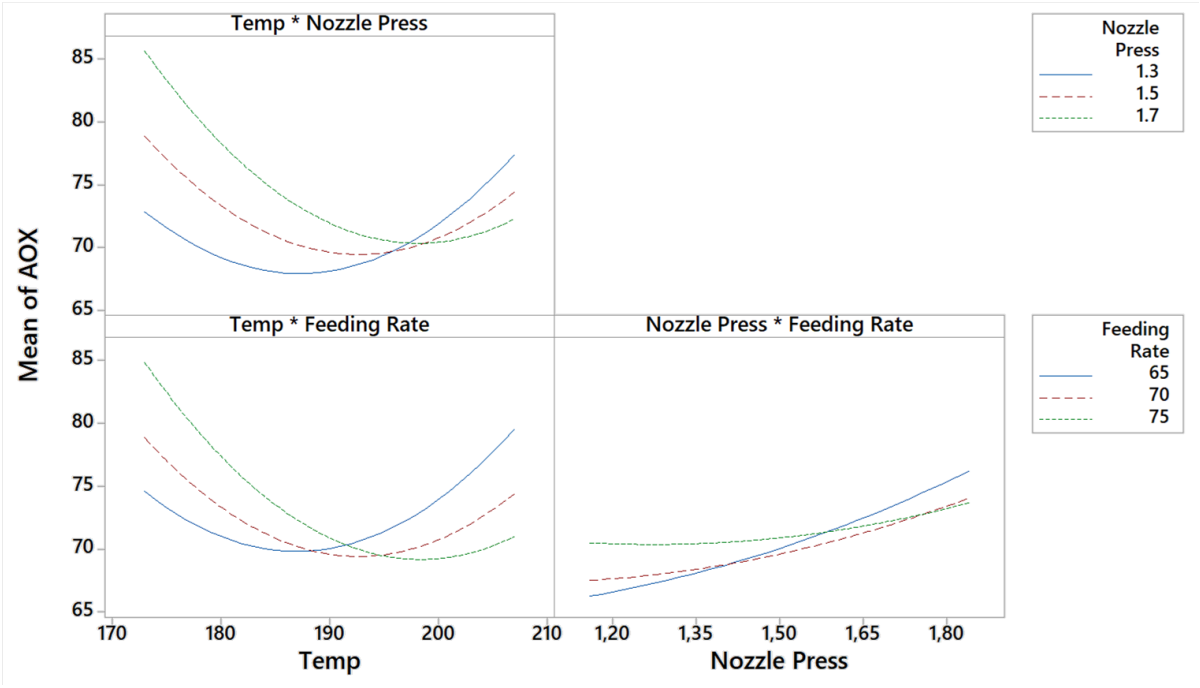

Figure 54 Interaction plots for antioxidant capacity, fitted means

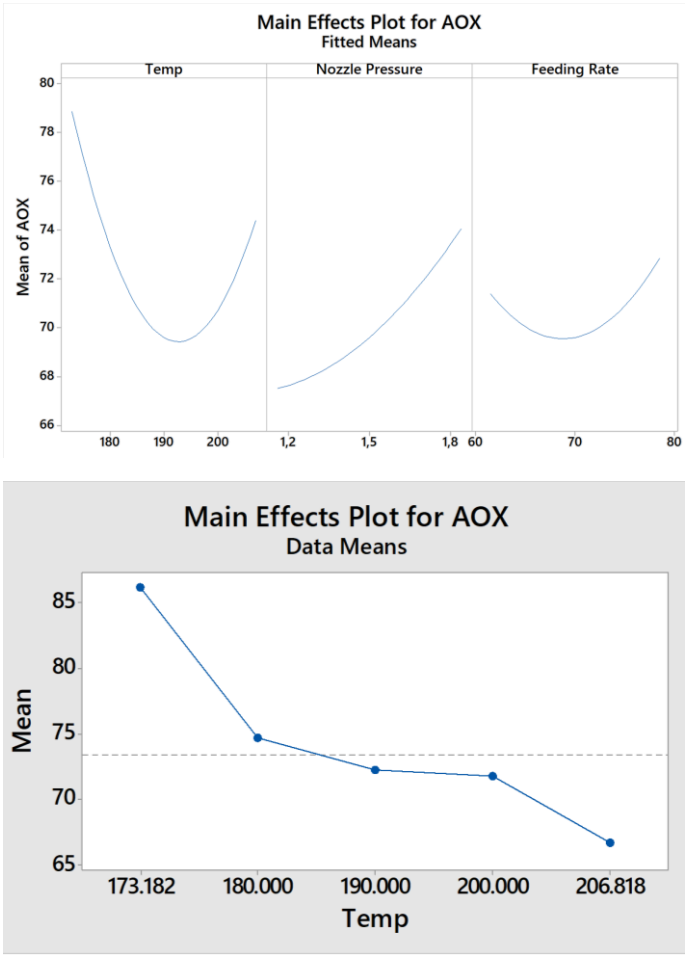

Figure 55 Main effects plots for antioxidant capacity

A8: Contour plots for combined effect of process parameters on the responses mass yield of fines and particle size D50 of spray dried lignin

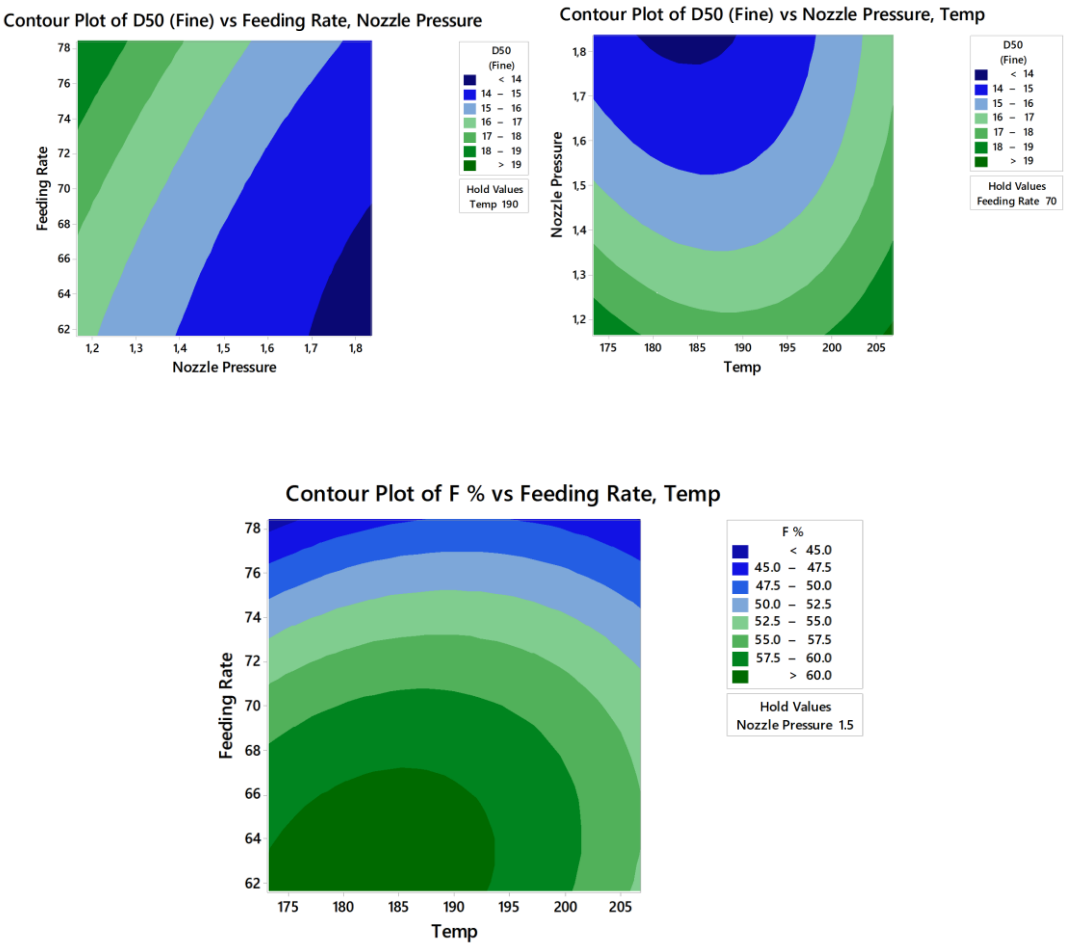

Figure 56 Countour plots on the combined effect of process parameters on mass yield of fines

A9: Results on the oil adsorption capacity of AS Lignin powders and comparable biopolymers

Table 17 Adsorption capacity of biopolymers under gastric and gastrointestinal environments against two types of oil.

Sample	**Gastric adsorption [g/g]**	**Intestinal adsorption [g/g]**	
	Corn oil	**Corn oil**	**Olive oil**
Softwood lignin	1.97 ± 0.27	2.51 ± 0.09	2.42 ± 0.09
AS-lignin	1.51 ± 0.10	2.53 ± 0.10	2.67 ± 0.02
Alkali lignin	1.46 ± 0.05	1.06 ± 0.18	0.99 ± 0.16
OS-lignin	2.01 ± 0.14	1.99 ± 0.10	2.19 ± 0.13
Chitosan	Full dissolution	2.87 ± 0.06	2.80 ± 0.01
Pectin	Full dissolution	Full dissolution	Full dissolution
Alginate	2.18 ± 0.05	Full dissolution	Full dissolution

Table 18 Oil adsorption capacities of the lignins obtained via solvent exchange and supercritical drying compared to their standard powders.

Sample	**Gastric adsorption [g/g]**	**Intestinal adsorption [g/g]**		**Ölzahl [g/g]**	
	Corn oil	**Corn oil**	**Olive oil**	**Corn oil**	**Olive oil**
Softwood lignin	1.97 ± 0.27	2.51 ± 0.09	2.42 ± 0.09	1.13 ± 0.04	1.13 ± 0.04
SC-dried SW-lignin	2.30 ± 0.02	2.52 ± 0.04	2.39 ± 0.02	4.15 ± 0.58	4.15 ± 0.58
AS -lignin	1.51 ± 0.10	2.53 ± 0.10	2.67 ± 0.02	1.59 ± 0.19	1.59 ± 0.19
SC-dried AS-lignin	1.60 ± 0.12	2.01 ± 0.02	2.98 ± 0.08	2.03 ± 0.04	2.03 ± 0.04

Table 19 Oil adsorption capacity for biopolymers according to ISO787/5

Sample	Standard adsorption capacities [Oil count number] [g/g]	
	Corn oil	**Olive oil**
Softwood lignin	1.13 ± 0.01	0.86 ± 0.04
Aquasolv lignin	1.19 ± 0.02	1.59 ± 0.19
Alkali Lignin	0.58 ± 0.06	0.24 ± 0.03
OS-Lignin	0.73 ± 0.02	0.70 ± 0.00
Chitosan	0.84 ± 0.01	1.12 ± 0.05
Pectin	0.26 ± 0.02	0.36 ± 0.04
Alginate	0.41 ± 0.03	0.41 ± 0.01

A10: Results of the in vivo test of lignin as hypocholesterolemic agent in Wistar rats

Table 20 Body and heart fat weight of all the tested groups

Parameter	C1	C2	ND+100Lig	HFD+50Lig	HFD+100Lig	HFD+500Lig	HFD+SV	HFD+100Lig+SV
Rate of body weight gain (g/d)	2.41 ± 0.08	2.41 ± 0.15	2.17 ± 0.07	1.43 ± 0.05	2.49 ± 0.32	2.02 ± 0.52	1.37 ± 0.21	1.88 ± 0.08
Average Heart fat weight (g)	0.186 ± 0.08	0.263 ± 0.10	0.079 ± 0.09	0.021 ± 0.041	0.177 ± 0.139	0.126 ± 0.180	0.011 ± 0.023	0.064 ± 0.074

Standard Deviation ±

C1: control 1 receive normal diet only, n=4

C2: control 2 receive high fat diet only, n=4.

Lig: lignin

SV: simvastatin

ND+100 Lig: Normal Diet + 100 mg lignin, n=4.

HFD+50, 100 and 500 Lig: High Fat Diet + 50, 100 & 500 mg lignin, respectively, n=7 each group.

HFD+SV: High Fat Deit +simvastatin 40 mg, n=4.

HFD+100 Lig+SV: High Fat Diet + 100 lignin + simvastatin 40 mg, n=7.

Table 21 Rate and the average of total cholesterol concentration in serum and feces analysis of all the tested groups

Parameter	C1	C2	ND+100Lig	HFD+50Lig	HFD+100Lig	HFD+500Lig	HFD+SV	HFD+100Lig+SV
Serum mg/dl/d	↓ 3.19 ± 0.83	↓ 9.97 ± 0.90	↓ 0.03 ± 0.74	↓ 4.88 ± 0.91	↓ 1.97 ± 1.78	↓ 5.2 ± 0.92	↓ 6.69 ± 1.63	↓ 4.87 ± 0.96
Feces mg/ml/g/d	↓ 21 ± 3.94	↓ 3.86 ± 1.36	↑ 2.32 ± 0.52	↑ 3.93 ± 1.96	↓ 10.7 ± 2.58	↓ 0.93 ± 0.28	↑ 2.88 ± 1.03	↑ 1.41 ± 1.39

Times	T7		T14		T21		T28	
Groups	Serum mg/dl	Feces mg/ml/g feces	Serum mg/dl	Feces mg/ml/g feces	Serum mg/dl	Feces mg/ml/g feces	Serum mg/dl	Feces mg/ml/g feces
C1	83.7 ± 24.2	186 ± 70	105 ± 41	39.4 ± 14	82.7 ± 19.5	19 ± 13.8	81.7 ± 12.3	42.3 ± 16.9
C2	267.2 ± 81.1	96.2 ± 46.6	242.8 ± 14.6	69.2 ± 21.6	173 ± 29.7	112.3 ± 76.8	147 ± 32.1	91 ± 35.7
ND+100Lig	95.8 ± 6.8	18 ± 10.6	101.5 ± 30.2	35.2 ± 19	101.3 ± 24.4	23 ± 17.7	75.3 ± 8.8	31.5 ± 6.4
HFD+50Lig	166.6 ± 38.8	67.8 ± 76.5	176.6 ± 39.8	95.3 ± 47	142.4 ± 28	80 ± 49.7	154.2 ± 34.2	21.4 ± 10.7
HFD+100Lig	130.5 ± 36.5	133 ± 71.3	176 ± 15.4	57.9 ± 24.3	162.2 ± 30.5	52.2 ± 31.4	131 ± 17.6	90.9 ± 34.7
HFD+500Lig	145.4 ± 30.7	64.5 ± 24	158 ± 15.3	57.9 ± 31.1	121 ± 40.8	63.7 ± 43.6	124.9 ± 36.8	68.5 ± 34.6
HFD+SV	131.3 ± 46	63 ± 36.9	169.3 ± 76.5	83.3 ± 55	122.5 ± 28.3	76.2 ± 66.5	113 ± 32.2	50.6 ± 27.2
HFD+100Lig+SV	142.5 ± 38.2	38.2 ± 19.5	157.9 ± 14	48 ± 34.7	123.8 ± 14.2	83.7 ± 49.5	110 ± 14.8	49.3 ± 34.4

Standard Deviation ±

T7: after ND or HFD.

T14, T21 and T28: after treatment.

C1: control 1 receive normal diet only, n=4

C2: control 2 receive high fat diet only, n=4.

Lig: lignin

SV: simvastatin

ND+100 Lig: Normal Diet + 100 mg lignin, n=4.

HFD+50, 100 and 500 Lig: High Fat Diet + 50, 100 & 500 mg lignin, respectively, n=7 each group.

HFD+SV: High Fat Deit +simvastatin 40 mg, n=4.

HFD+100 Lig+SV: High Fat Diet + 100 lignin + simvastatin 40 mg, n=7.

Table 22 Rate and the average of Triacilglycerides concentration in serum and feces analysis of all the tested groups

Parameter	C1	C2	ND+100Lig	HFD+50Lig	HFD+100Lig	HFD+500Lig	HFD+SV	HFD+100Lig+SV
Serum mg/dl/d	↑ 7.13 ± 1.44	↑ 6.93 ± 0.93	↑1.21 ± 1.71	↓ 1.41 ± 2	↑ 2.21 ± 3.94	↓ 4.66 ± 3.99	↓ 7.01 ± 3.32	↑ 11.5 ± 3.73
Feces mg/ml/g/d	↓ 35.4 ± 7	↑2.97 ± 2.79	↑3.46 ± 2.91	↑ 6.83 ± 6.25	↑ 4.43 ± 1.29	↑ 5.98 ± 2.02	↑ 24.6 ± 4.30	↑ 9.74 ± 2.27

Times	T7		T14		T21		T28	
Groups	Serum mg/dl	Feces mg/ml/g feces	Serum mg/dl	Feces mg/ml/g feces	Serum mg/dl	Feces mg/ml/g feces	Serum mg/dl	Feces mg/ml/g feces
C1	61.5 ± 44	373.2 ± 134	72.2 ± 12	124.8 ± 7.4	122.2 ± 15.9	223 ± 93.4	95.4 ± 25.8	206.2 ± 66.6
C2	88.9 ± 47	178.4 ± 33	89 ± 27.7	199.2 ± 92.2	137.5 ± 23.7	201.9 ± 80.5	164.4 ± 60.2	329 ± 83.9
ND+100Lig	27.2 ± 18	65.5 ± 18.5	92.7 ± 33.7	89.8 ± 15.2	101.3 ± 54.3	206 ± 31.8	105.3 ± 56.2	165 ± 48
HFD+50Lig	20.7 ± 14	88.6 ± 28.2	108 ± 61.8	136.4 ± 27	98 ± 16.2	293 ± 122.9	116.2 ± 29.9	137.4 ± 73.2
HFD+100Lig	41.2 ± 21	105 ± 30	179.3 ± 79.9	136 ± 44.6	194.8 ± 51.7	128.9 ± 61.4	177.6 ± 64.4	191 ± 147.2
HFD+500Lig	65.2 ± 20.3	69 ± 18.2	194.6 ± 76.5	111 ± 27	162 ± 93	94.5 ± 20	130.4 ± 81.3	186.2 ± 149.2
HFD+SV	54 ± 5.7	117.6 ± 17.5	164.4 ± 22.9	290.3 ± 97.7	115.3 ± 36.7	262.9 ± 95	109.3 ± 19.4	279.3 ± 143.3
HFD+100Lig+SV	68.9 ± 45.3	104 ± 32.7	131.8 ± 53.4	172.8 ± 59.3	212.3 ± 97.2	171.9 ± 51.7	130.6 ± 44	140.8 ± 52.2

Standard Deviation ±

T7: after ND or HFD.

T14, T21 and T28: after treatment.

C1: control 1 receive normal diet only, n=4

C2: control 2 receive high fat diet only, n=4.

Lig: lignin

SV: simvastatin

ND+100 Lig: Normal Diet + 100 mg lignin, n=4.

HFD+50, 100 and 500 Lig: High Fat Diet + 50, 100 & 500 mg lignin, respectively, n=7 each group.

HFD+SV: High Fat Deit +simvastatin 40 mg, n=4.

HFD+100 Lig+SV: High Fat Diet + 100 lignin + simvastatin 40 mg, n=7.

Table 23 Rate and average of HDL cholesterol concentration in serum and feces analysis for all the groups

Parameter	C1	C2	ND+100Lig	HFD+50Lig	HFD+100Lig	HFD+500Lig	HFD+SV	HFD+100Lig+SV
Serum mg/dl/d	↑ 0.66 ± 0.21	↑ 0.34 ± 0.12	↑0.81 ± 0.21	↑0.84 ± 0.38	↑ 1.04 ± 0.30	↑ 0.73 ± 0.25	↑ 0.65 ± 0.28	↑ 0.54 ± 0.17
Feces mg/ml/g/d	↑ 0.75 ± 0.17	↓ 1.01 ± 0.27	↓ 0.4 ± 0.04	↑ 0.22 ± 0.25	↓0.48 ± 0.08	↓ 0.32 ± 0.22	↑ 1.23 ± 0.42	↑ 0.37 ± 0.15

Times	T7		T14		T21		T28	
Groups	Serum mg/dl	Feces mg/ml/g feces	Serum mg/dl	Feces mg/ml/g feces	Serum mg/dl	Feces mg/ml/g feces	Serum mg/dl	Feces mg/ml/g feces
C1	10 ± 8.8	8.2 ± 2.3	3.1 ± 0.4	13.5 ± 3	7.7 ± 0.9	14.8 ± 12.3	3.6 ± 0.2	12.6 ± 4.8
C2	8.5 ± 1.8	19.6 ± 4.5	4.5 ± 2.2	12.5 ± 8.5	6.9 ± 3	13.4 ± 4.2	3.3 ± 0.02	18.5 ± 12
ND+100Lig	7.3 ± 5.6	12.4 ± 3.6	2.8 ± 0.3	9.6 ± 1.8	8.5 ± 0.3	9.4 ± 1.6	3.4 ± 0.02	7 ± 0.8
HFD+50Lig	17.7 ± 4.1	11.9 ± 3.5	3.2 ± 0.7	13.4 ± 4.9	9 ± 1.5	16.3 ± 9	3.3 ± 1.5	8 ± 4.3
HFD+100Lig	11.5 ± 4.6	12.5 ± 5	2.8 ± 0.2	9.1 ± 2	10 ± 2.5	9.4 ± 3.7	3.4 ± 0.05	5 ± 1.1
HFD+500Lig	11.9 ± 3.3	9.4 ± 3.5	3.4 ± 1.6	7 ± 2.7	8.5 ± 1.9	5.6 ± 2.9	3.4 ± 0.05	12.6 ± 9.4
HFD+SV	13.8 ± 8.6	12.2 ± 2.8	2.9 ± 0.3	20.9 ± 3.8	7.5 ± 0.5	23.2 ± 13.5	3.3 ± 0.03	6.5 ± 0.5
HFD+100Lig+SV	4 ± 2.2	9.4 ± 3.2	2.9 ± 0.5	12 ± 6	7.9 ± 1.4	10 ± 5.3	3.4 ± 0.05	5.9 ±1.4

Standard Deviation ±

T7: after ND or HFD.

T14, T21 and T28: after treatment.

C1: control 1 receive normal diet only, n=4

C2: control 2 receive high fat diet only, n=4.

Lig: lignin

SV: simvastatin

ND+100 Lig: Normal Diet + 100 mg lignin, n=4.

HFD+50, 100 and 500 Lig: High Fat Diet + 50, 100 & 500 mg lignin, respectively, n=7 each group.

HFD+SV: High Fat Deit +simvastatin 40 mg, n=4.

HFD+100 Lig+SV: High Fat Diet + 100 lignin + simvastatin 40 mg, n=7.

A11: Plots of cytotoxicity for measured AS lignin and lignin-based formulations

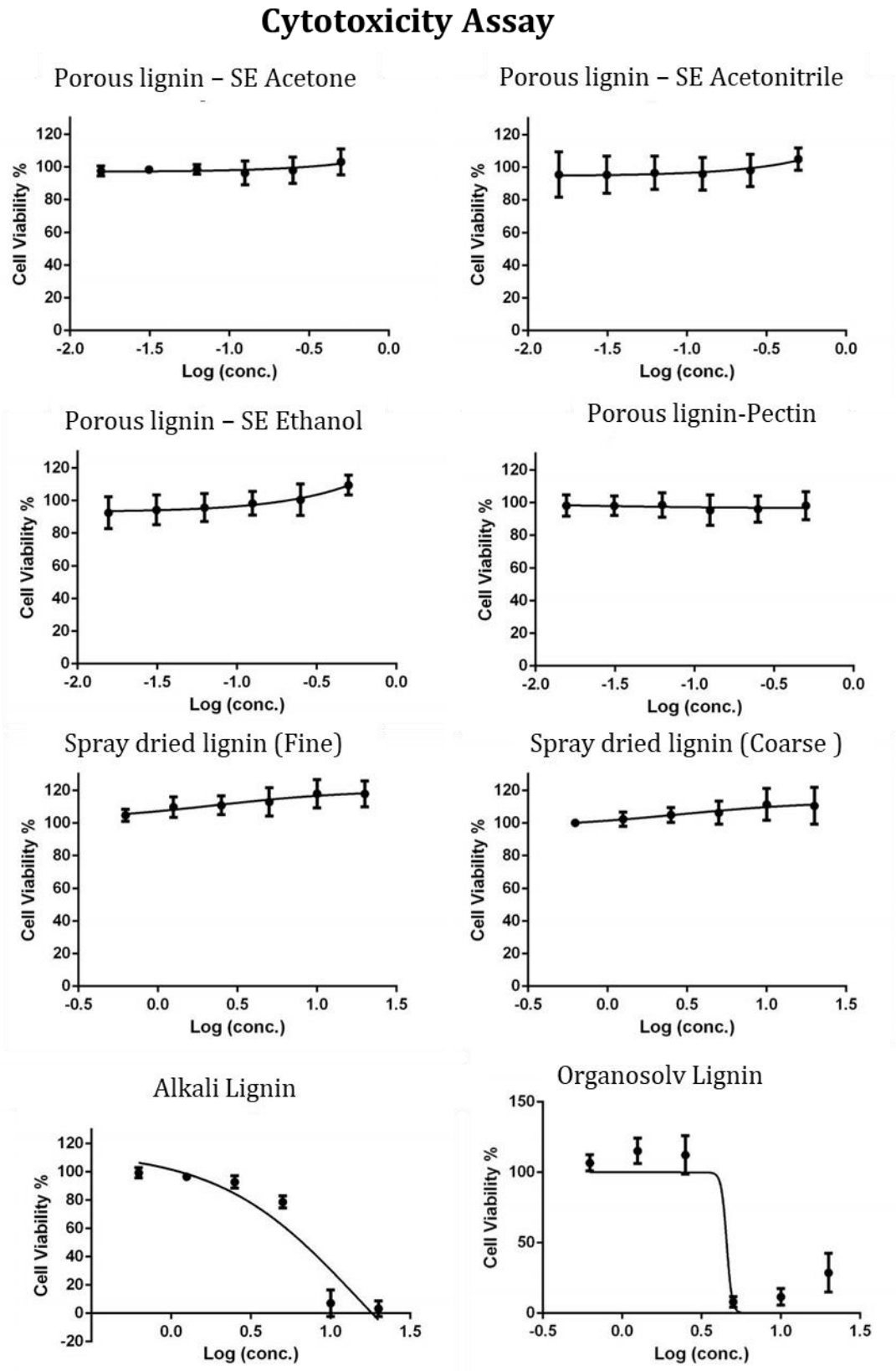

A12: Plots of alpha-glucosidase enzyme inhibition by addition of AS lignin and lignin-based formulations

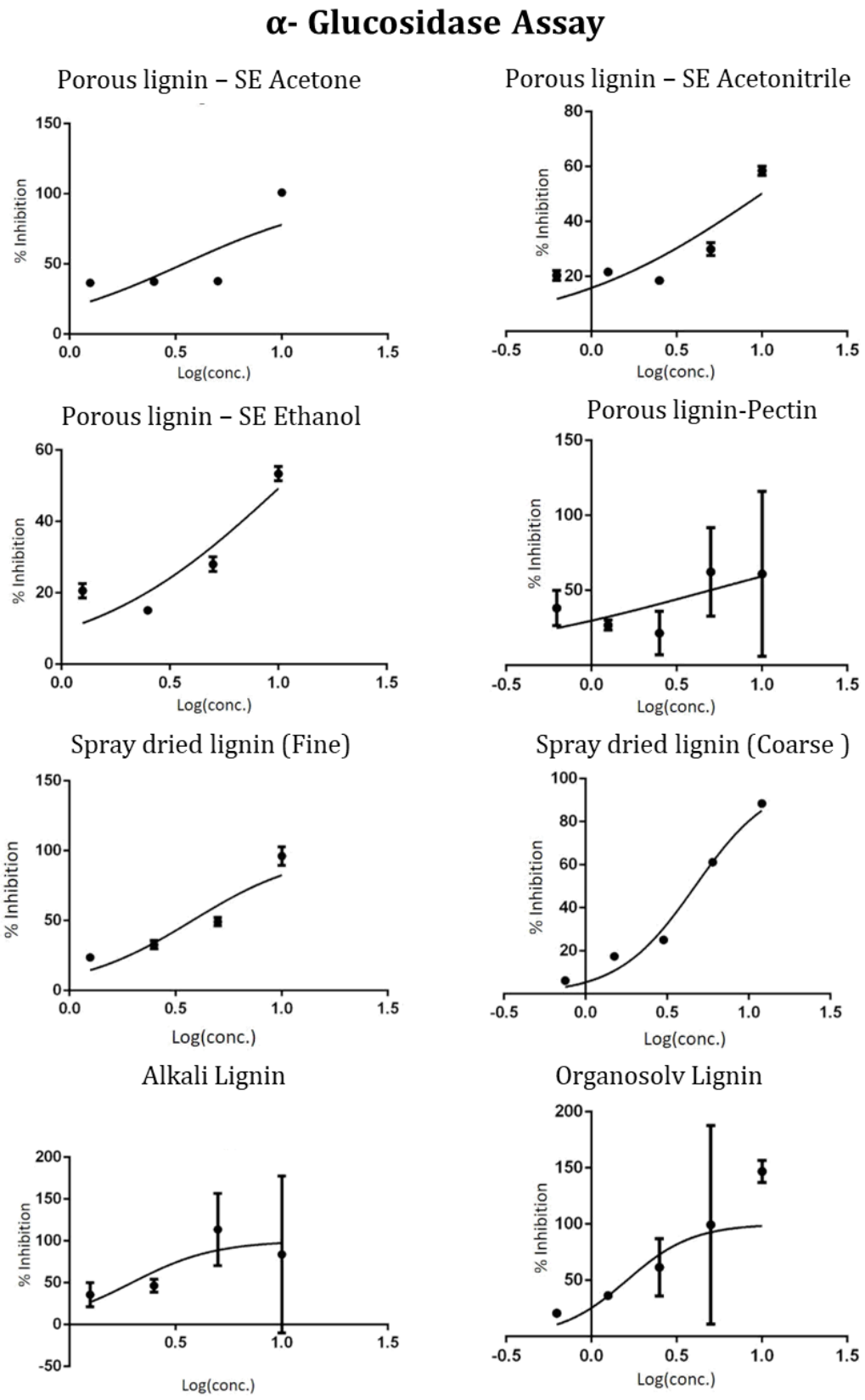

A13: Plots of alpha-amylase enzyme inhibition by addition of AS lignin and lignin-based formulations

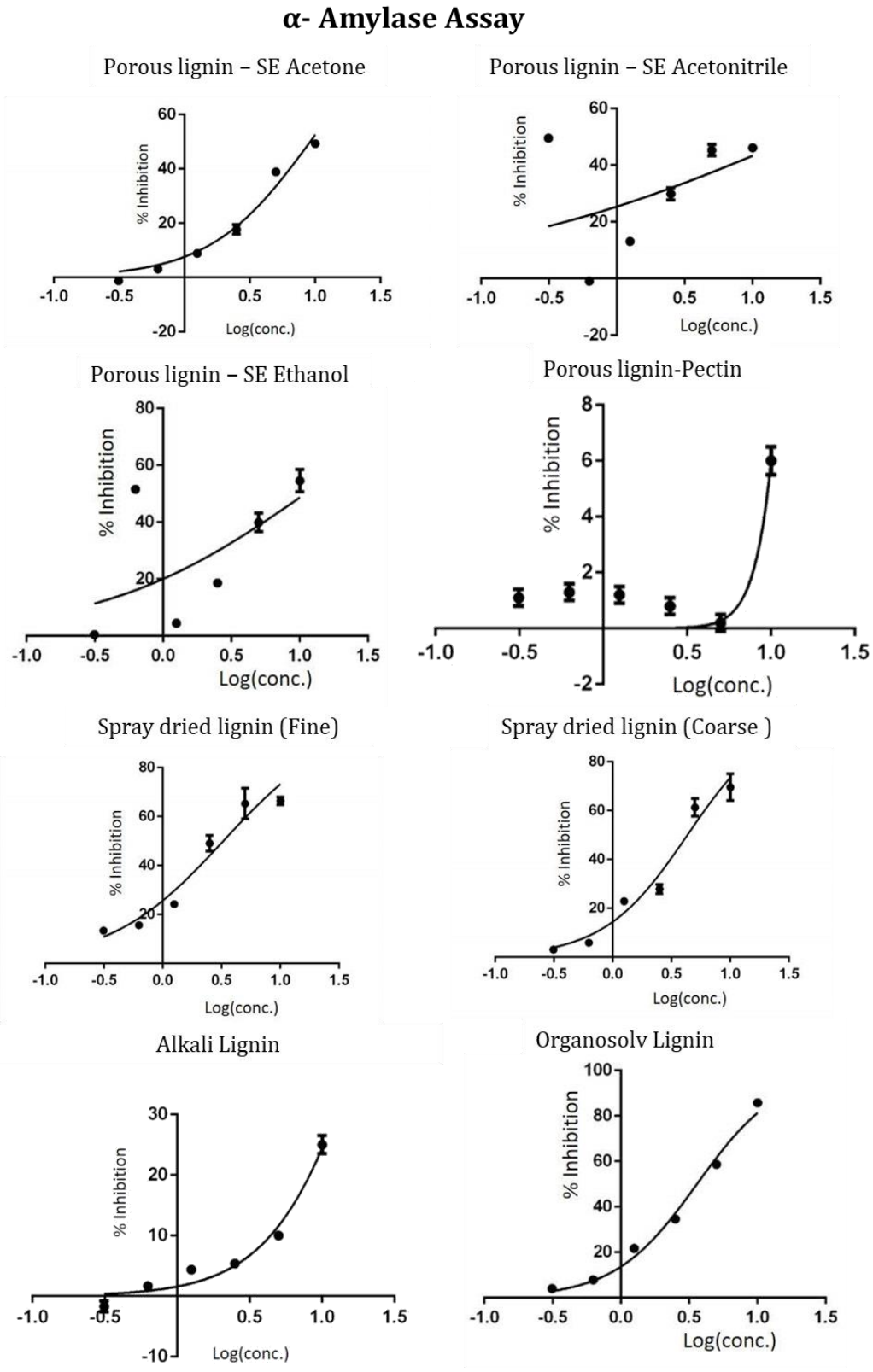

A14: In vitro oil adsorption capacity measured by DIN NOM

Sample 1: Start	
Sample 1: 2 mL	
Sample 1: End	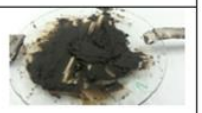
Sample 3: Start	
Sample 3: End	
Sample 4: Start	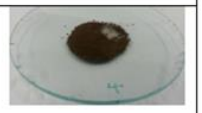
Sample 4: 0.6 mL (4-5 droplets)	

Sample 4: 1.2 mL (1-2 droplets)	
Sample 4: End	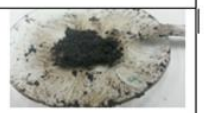
Sample 5: After start	
Sample 5: 1.2 mL	
Sample 5: End	
Sample 6: Start	
Sample 6: End	

Sample 7: 5 mL	
Sample 7: 10 mL	
Sample 7: Ende	
Sample 8: 5 mL	
Sample 8: 10 mL	
Sample 8: End	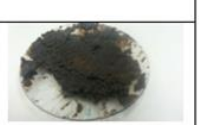
Sample 9: Start	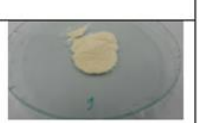

Sample 9: 0.6 mL	
Sample 9: End	
Sample 10: After 5 droplets	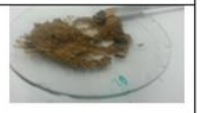
Sample 10: End	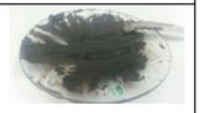
Sample 11: After Start	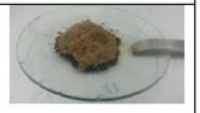
Sample 11: End	
Sample 12: Start	

Sample 12: 2. 50	
Sample 12: End	

A15: Results on the disintegration and tensile strength of the tablets from the mixture design of Disintegrant Binder Lignin

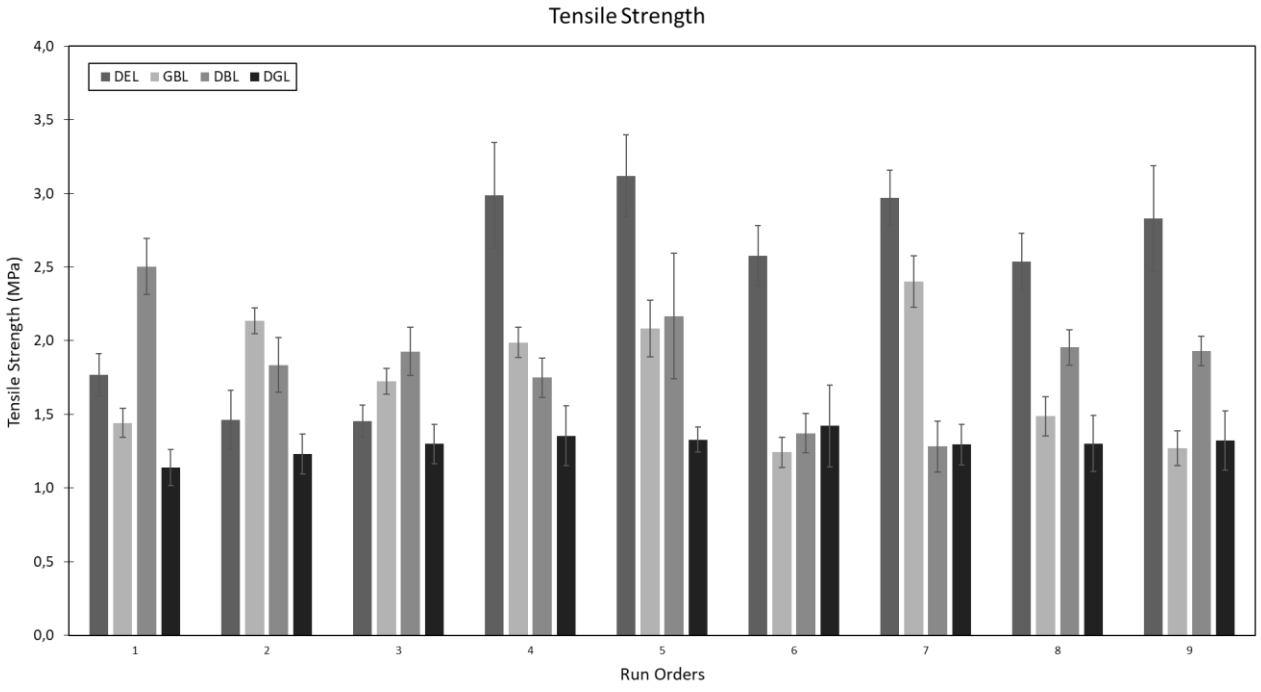

Figure 57 Tensile strenght of the lignin based tablets

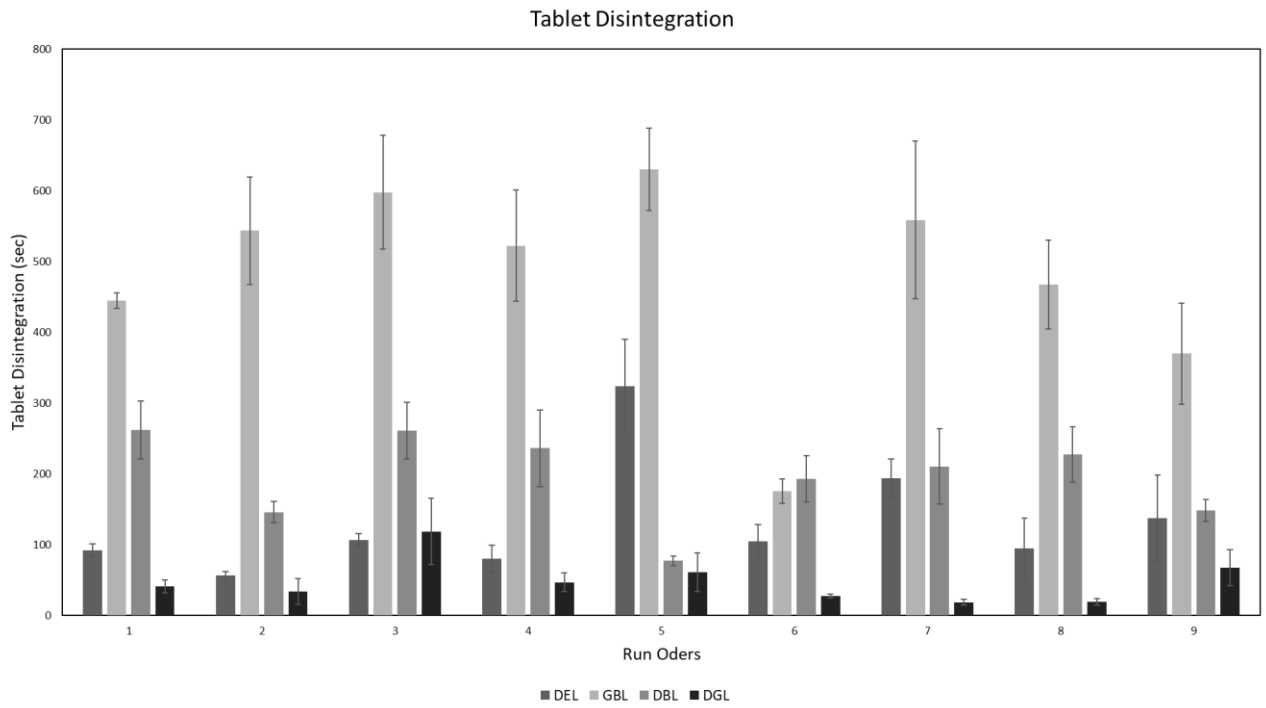

Figure 58 Results on disintegration of the lignin based tablets evaluated

Publication list

Journal articles

1. **Gil-Chávez, J**., Gurikov, P., Hu, X. et al. Application of novel and technical lignins in food and pharmaceutical industries: structure-function relationship and current challenges. Biomass Conv. Bioref. (2019).
2. **G. Joana Gil-Chávez**, Sidhant Satya Prakash Padhi, Carolina V. Pereira, Joana N. Guerreiro, Ana A. Matias, Irina Smirnova (2019): Cytotoxicity and biological capacity of sulfur-free lignins obtained in novel biorefining process, *International Journal of Biological Macromolecules*. Volume 136, (697-703).
3. Xihua Hu, **Joana Gil-Chavez**, Aleksa Hadzi-Ristic, Christian Kreft, Cai Rong Lim, Carsten Zetzl & Irina Smirnova (2019). Lignin from second-generation biorefinery for pressure-sensitive adhesive tapes. *Biomass Conversion and Biorefinery.*
4. **Joana Gil-Chávez**, Sidhant Satya Prakash Padhi, Ulrich Hartge, Stefan Heinrich, Irina Smirnova (2020). Optimization of the spray-drying process for developing aquasolv lignin particles using response surface methodology, Advanced Powder Technology. Vol 31, (2348-2356).
5. **Joana Gil-Chávez,** Sidhant Satya Prakash Padhi, Claudia S. Leopold and Irina Smirnova (2020). Application of Aquasolv Lignin in Ibuprofen-loaded pharmaceutical formulations obtained via Direct Compression and Wet Granulation. International Journal of Biological Macromolecules Volume 174: (229-239)
6. Razan Altarabeen, **G. Joana Gil-Chávez**, Wienke Reynolds, Sonja Schmidt and Irina Smirnova (2020). Lignin-based polyurethane foams. *In revision.*

Patent

1. **Gilda Joana Gil Chavez,** Irina Smirnova, Stefan Heinrich, Ernst-Ulrich Hartge (PCT/EP2019/057892). [EN] Method for producing ultrafine lignin particles [DE] Verfahren zur herstellung ultrafeiner Lignin-partikel, (WO/2020/192929). Published on 01.10.2020.

Student theses

In the context of this Ph.D. thesis and related research projects at the Institute of Thermal Separation Processes, Project and Master Theses were supervised. The results of the following theses were partially or completely used in the present Ph.D. thesis or further evaluated if necessary.

1. Altarabeen, Razan (2019): Lignin-based PU foams. **Project work**, TUHH (TVT).
2. Dicke, Erik (2020) Development and optimization of Lignin-PU Aerogels aiming their use as insulating material. **Master thesis**, TUHH (TVT).
3. Gnana, Charles (2016) Experimental comparison of lignin quality obtained with Hot Liquid Water (HLW) followed by enzymatic hydrolysis and Ionic Liquids methods for lignocellulosic materials. **Master Thesis**, Collaboration between Durban University of Technology and TUHH (TVT).
4. Masinde, Daudi (2018) Post Treatment Of Wheat Straw And Softwood Biomass From Liquid Hot Water Pretreatment Towards Enhanced Lignin Extraction. **Project work**, TUHH (TVT).
5. Padhi, Sidhant Satya Prakash (2017) Lignin spray drying: influence of main process variables on lignin particle size using response surface methodology. **Project work**, TUHH (TVT).
6. Padhi, Sidhant Satya Prakash (2018) Evaluation of Bioactive Properties of Lignin and Lignin-based formulations and comparison with EFSA approved products. **Erasmus internship**, collaboration between iBET Portugal and TUHH (TVT).
7. Padhi, Sidhant Satya Prakash (2019). Use of Lignin in Pharmaceutical Dosage Forms, Performance during Direct Compression and Wet Granulation. **Master Thesis**, TUHH (TVT)
8. Saadat, Seyed Sahand (2019) Evaluation of oil adsorption capacity of novel and technical Lignins under simulated gastrointestinal conditions. **Project work**, TUHH (TVT).
9. Zimmer, Christin (2020) Lignin Polylactic Acid Foams: material and process development. **Master thesis**, Hochschule Bremerhaven in collaboration with TUHH (TVT).